Numerical Optimization for Cutting Process in Glass Fiber Reinforced Plastic Using Conventional and Non-Conventional Methods

Hussein Mohammad Ali Ibraheem

Submitted to the
Institute of Graduate Studies and Research
in partial fulfillment of the requirements for the Degree of

Doctor of Philosophy
in
Mechanical Engineering

Eastern Mediterranean University
July 2013
Gazimağusa, North Cyprus

Approval of the Institute of Graduate Studies and Research

Prof. Dr. Elvan Yılmaz
Director

I certify that this thesis satisfies the requirements as a thesis for the degree of Doctorate of Philosophy in Mechanical Engineering.

Assoc. Prof. Dr. Uğur Atikol
Chair, Department of Mechanical Engineering

We certify that we have read this thesis and that in our opinion it is fully adequate in scope and quality as a thesis for the degree of Doctorate of Philosophy in Mechanical Engineering.

Prof. Dr. Majid Hashemipour
Supervisor

Examining Committee

1. Prof. Dr. Majid Hashemipour

2. Prof. Dr. Murat Bengisu

3. Assoc. Prof. Dr. İbrahim Etem Saklakoğlu

4. Assist. Prof. Dr. Ghulam Hussain

5. Assist. Prof. Dr. Hasan Hacışevki

ABSTRACT

Glass fiber reinforced polymer (GFRP) composites are used in many industrial applications due to the advantages they offer compared to other materials. These advantages are the light weight with the high strength, good toughness, high corrosion resistance, high thermal resistance and relative ease of manufacture of components using GFRPs, makes these materials candidates for more and more applications. Joining GFRP composite laminate to other metal material structure could not be avoided; the bolt joining efficiency depend critically on the quality of machined holes in all the industrial applications. There are many cutting processes which are used for producing riveted and bolted joints during the assembly operation of composite laminates with other parts. For riveted and bolted joints, precise holes must be made in the components to ensure high joint strength and precision. Conventional machining such as drilling and milling of hole making in composite materials face many challenges due to the properties of the matrix, diverse fiber , fiber orientation and the inhomogeneous nature of the composite. Non conventional machining like abrasive water jet machining (AWJM) & laser beam machining (LBM) processes have been used for processing composite materials because of the advantages they offered as compared to the traditional techniques.

The objective of the current work is to evaluate the effect of drilling, milling, abrasive water jet and laser beam machining parameters on hole making process of GFRP. Statistical approach is used to know the effects of the predictor parameters on the response variables. Analysis of variance (ANOVA) was used to isolate the effects of the predictor parameters affecting the hole making in both abrasive water jet and laser processes. The result shows that abrasive water jet cutting promises a better

cutting, less cost of operation and high production compared to the other cutting technologies.

Keywords: CO_2 laser, AWJM, Cutting Parameters, Laminated GFRP, Cut quality, Cost, Productivity and Optimization.

ÖZ

Cam elyaf ile güçlendirilmiş polimer (CTP) Kompozit çünkü bunlar diğer geleneksel ve geleneksel olmayan malzemeler ile karşılaştırıldığında üstün avantajları sunar uygulamaları bir çok sayıdaki kullanılmaktadır. Bu avantajlar ağırlık oranı yüksek mukavemetli, yüksek modüllü, yüksek kırılma tokluğu, yüksek korozyon ve ısıl direnci vardır. Dolayısıyla üretim maliyeti düşük sunan GFRPs ile komponent imalatı göreceli olarak kolay, daha fazla uygulama için bu malzemeler aday hale getirlir. Yapısal malzeme olarak diğer metal malzeme yapısı kompozit laminate katılmadan kaçınılması olamazdı; verimliliği ve kaliteyi birleştiren cıvata tüm endüstriyel uygulamalarda işlenmiş delik kalitesine eleştirel bağlıdır. Çeşitli kesme işlemleri yaygın olarak diğer bileşenler ile kompozit laminatların montaj işlemi sırasında perçinli ve cıvatalarını üretmek için kullanılır. Perçinli ve cıvatalı eklem için, hasarlı ücretsiz ve hassas delikler yüksek ortak gücü ve hassasiyeti sağlamak için bileşenleri olarak yapılmalıdır. Delik delme ve frezeleme fiber takviyeli kompozit yapma gibi Konvansiyonel işleme çeşitli lif ve matriks özellikleri, elyaf oryantasyonu, malzemenin homojen olmayan yapısı nedeniyle zordur. Aşındırıcı su jeti ile işleme (AWJM) & Lazer ışını işleme (LBM) işlemleri nedeniyle geleneksel tekniklerle karşılaştırıldığında bu teknolojilerin sağladığı avantajlardan kompozit malzemelerin işlenmesi için kullanılmaktadır.

Mevcut çalışmanın amacı delik GFRP verme sürecinde üzerinde delme, frezeleme, aşındırıcı su jeti ve lazer ışını işleme parametrelerinin etkisini değerlendirmek için. İstatistiksel yaklaşım yanıt değişkenler kontrol parametrelerinin etkisini anlamak için kullanılır. Varyans analizi (ANOVA) analiz aşındırıcı su püskürtme ve lazer işlemleri hem de alma deliği etkileyen parametrelerin etkilerinin izole etmek için

yapıldı. Bunun sonucu aşındırıcı su jeti kesim, lazer ışını kesme teknolojisi ile karşılaştırıldığında çalışma ve yüksek üretim daha iyi bir kesim, daha az maliyet vaad edir gösterir.

Anahtar Kelimeler: CO2 lazer, AWJM, delme, frezeleme, Parametreler, Lamine GFK, Kesme kalitesi, Maliyet, Verimlilik ve Optimizasyon Kesme.

To

My Wife and Children's for their patience and encouragement

ACKNOWLEDGMENT

I would like to introduce my great thank to Assoc. Prof. Dr. Asif Iqbal for his support and guidance in the preparation of this work. The author would like to thank also, Assoc. Prof. Dr. Uğur Atikol , Chairman of the Department of Mechanical Engineering, Eastern Mediterranean University, for his help with various issues during doing the work. I am also obliged to Prof. Dr. Majid Hashemipour for his continuous support and help during my thesis.

The authors would like to acknowledge the help and support provided by the staff of College of Mechanical and Electrical Engineering / Nanjing University of Aeronautic and Astronautic in performing experimental work there.

I owe quit a lot to my family for their support and patient during my study and absent to them.

TABLE OF CONTENTS

LIST OF TABLES

LIST OF FIGURES

LIST OF ABBREVIATIONS

GFRP	Glass fiber reinforced plastic
AWJM	Abrasive water jet machining
LBM	Laser beam machining
D	Nominal hole diameter (mm)
t	Material thickness (mm)
f_z	Feed rate in drilling (mm/rev)
f_z	Feed rate in milling (mm/z)
F_z	Thrust force (N)
F_w	Machining force (N)
z	Number of teeth in end mill.
Vc	Cutting feed (m/min)
P	Jet pressure (MPa)
AF	Abrasive flow rate (gm/min)
Sod	Stand-off distance (mm)
LP	Laser beam power (KW)
V	Assist.gas flow rate (Lit/hr)
R_a	Arithmetic surface roughness (μm)

O.O.R	Out of roundness (mm)
D_{U-} D_L	Difference between upper and lower surface diameter (mm)
UDF	Upper delamination factor
LDF	Lower delamination factor
T.S	Tensile strength (MPa)
C	Cost (USD)
Pr	Productivity (No. of holes per min)
HAZ	Heat affected zone

Chapter 1

INTRODUCTION

1.1 Composite Materials

Composite materials are constructed from two materials; one material is called the reinforcement or discrete phase. The other is called a matrix or continuous phase. The fiber and the matrix have two different properties but when combined together they form a material with significantly different properties that are not found in either of the individual materials, such as high strength per weight ratio, high corrosion and thermal resistance and high stiffness, which are markedly superior to those of comparable metallic alloys. The duty of the matrix phase is to hold the reinforcement in order to form the desired shape; while the function of the reinforced is to carry the major external load thus improves the overall mechanical properties of the matrix. When the two phases are mixed properly, the new combined material present better strength than would each individual material [1]. The simplest explanation of a composite material is shown in figure 1.

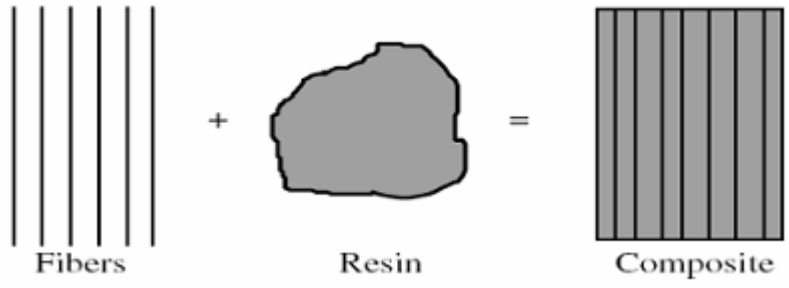

Figure 1: Formation of composite material using fibers and resins [2].

1.2 Advantages of Composite Materials

Composite materials are used in various fields compared to other materials due to the following advantages [2]:

1. They have high strength per weight ratio. The use of light weight materials result in the increase of the fuel efficiency of automobiles and airplanes.
2. High fracture toughness,
3. Composites show better impact properties compared to metals; they are a good dampers and they reduce the noise and vibration high damping, which makes these materials candidates in more applications like in automobiles, aircrafts, tennis rackets and golf clubs.
4. Composites have a low thermal expansion coefficient, which can lead to provide a good dimensional stability.
5. Most composites materials are made of plastics or resin and hence provide a high level of corrosion resistance compared to other traditional materials which need a special treatments to protect them from corrosion
6. Manufacturing composite materials take less time, and the part can be made to be a particular shape or size not requiring further more. Complex parts with special shapes and contours can be directly machined. The fabrication of complex parts means, a fewer number of parts is required to assemble and more production time saved.
7. The pressure and temperature required in the processing of composite is much less than that required for metals, thereby providing aflexibility in the way of processing the composites, in turn providing flexibility in production.

1.3 Disadvantages of Composite Materials

Although there are many advantages in using the composite materials, some drawbacks need to be taken into consideration [2]. Some of these drawbacks are:

1. Composite materials are more costly than other materials like steel and aluminum.
2. The temperature resistance for composite is dependent upon the matrix material used for binding the fibers. Most matrix materials are polymer based; hence, the maximum working temperature is less than in metals do.
3. Composites absorb moisture, which affect the way they behave.
4. Recycling of composite is difficult.

In spite of all the above drawbacks mentioned previously, the composite materials have more advantages than metals to use. The weight reduction that composite bring about is of a great advantages. Composites are replacing metals in most parts, as they are much lighter than metals. Most of the drawbacks can be controlled or composites can be used in places or environments, which do not affect them. Thus offering low cost of production, makes these materials candidates for more and more applications [3]. An indication of the increased usage of composites is shown in figure2 [4].

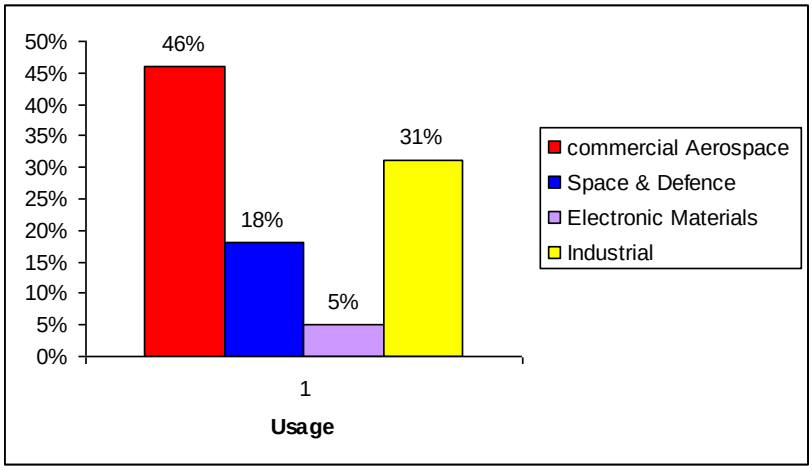

Figure2: Percentage use of composites by various industries [4].

Joining composite laminate to other metal material structure could not be avoided; the bolt joining efficiency depends critically on the quality of machined holes in many industrial applications as in the assembly of aerospace components [5]. Many machining processes are used for producing riveted and bolted joints during the assembly operation of composite laminates with other components. Hole making is one of these operations. As an example, there are over 100,000 holes made for a small single engine aircraft, while a million of holes are made in a large transport aircraft for fasteners such as rivets, bolts and nuts [6]**.** For riveted and bolted joints, precise holes must be made in the components to obtain high strength and reliable joints [7, 8].

1.4 Classification of Composite Materials

Composite materials can be available for the use in the following two forms [9]:

1. Natural Composites

There are many natural materials, which can be grouped under the natural composites such as bones, shells, wood, pearlier (steel which is a mixture of a phase and Fe_3C) etc.

2. Man-Made Composites

Man-made composites can be obtained by combining two or more materials in definite proportions under controlled conditions. For example Mud mixed with the straw to produce stronger mud mortar and bricks, decorative laminates, fiber reinforced plastic (FRP), Composites, concrete and RCC, reinforced Glass etc.

Man-made Composites can be classified in the following manner:

1.4.1 According to the Type of Matrix Material

Composite materials can be classified according to the type of the matrix material used in their fabrication [9]:

1. Metal Matrix Composites.

2. Ceramic Matrix Composites.

3. Polymer Matrix Composites

1.4.1.1 Metal Matrix Composites (MMC)

This type of Composites has many advantages over other metals such as higher specific strength, better properties at elevated temperatures, and lower coefficient of thermal expansion. Because of these characteristics, metal matrix composites are used for applications requiring higher operating temperatures than are possible with polymer matrix composites materials. Most of these composites are developed for the aerospace industry, but there are also anew applications are found in the automotive industry, like in the automobile engine parts. For example, the combustion chamber nozzle of the rockets and the space shuttle, housing, heat exchangers, structural members etc.

1.4.1.2 Ceramic Matrix Composites (CMC)

The main purpose in producing ceramic matrix composites is to increase the toughness.

1.4.1.3 Polymer Matrix Composites (PMC)

Polymer matrix composites are the commonly used matrix materials in the industrial applications. The reason for this is twofold. First, the mechanical properties of polymers are inadequate (low strength and stiffness compared to the metals and ceramics) for many structural purposes. This problem can be overcome by reinforcing other materials with polymers. Secondly, there is no needing for high

pressure and temperature in the processing of polymer matrix composites. In addition, simpler equipments are used for producing the polymer matrix composites. For these reasons the polymer matrix composites are rapidly became a popular for structural applications. There are two main types of polymer composites, these are: fiber reinforced polymer (FRP) and particle reinforced polymer (PRP).

1.4.2 According to the Geometry of Reinforcement

Composite materials can be classified according to the geometry of reinforcement. The strengthening mechanism is strongly dependent on the geometry of reinforcement. Figure 3 shows a commonly accepted classification scheme for composite materials.

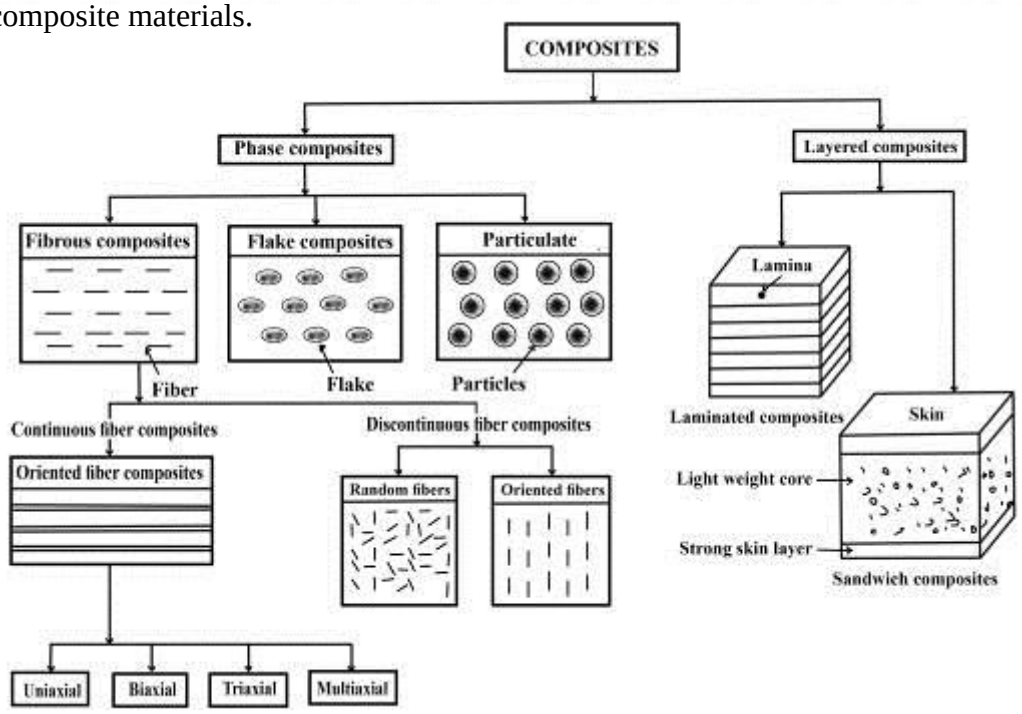

Figure3: Classification of composite materials [9].

It is clear from Figure 3 that there are three main configurations of composites according to the geometry of reinforcement, and a brief description for each type is available in the following subsections.

1.4.2.1 Fibrous Composite

A fiber is characterized by its length greater than its cross-sectional dimensions. The dimensions of the reinforcement determine the properties of the composite. Fibers are very active in improving the failure resistance of the matrix, since a reinforcement having a long dimension prevent the growth of incipient cracks normal to the reinforcement that might happen, otherwise lead to failure, especially with brittle matrices. Fibers of non polymeric materials exhibit much higher strength along their length since large flaws, which may be present in the bulk material, are minimized because of the small cross-sectional dimensions of the fiber. In the case of polymeric materials, orientation of the molecular structure is responsible for high strength and stiffness. Fibrous composites can be widely classified as single layer and multi layer composites. Single layer composites may actually be made from several layers with each layer having the same orientation and properties and thus the entire laminate may be considered as a single layer composite. Most composites used in the structural applications are multilayered. Each layer is a single layer composite and its orientation is varied according to the requirement. Several identical or different layers are bonded together to form a multilayered composites applicable for engineering applications. When the constituent materials in each layer are the same, they are called simply laminates. While the hybrid laminates refer to the multilayered composites consisting of layers made up of different constituent materials. Fibers in a single layer composite may be short or long compared to its overall dimensions. Composites with long fibers are called continuous fiber reinforced composites and those with short fibers, discontinuous fiber reinforced composites. The continuous fibers in single layer composites can be all in one direction to form a unidirectional composite. These composites are produce by laying

the fibers parallel and mixed them with resinous material. While the bidirectional reinforcement is fabricate in a single layer with mutually perpendicular directions as in a woven fabric. The strength of the two perpendicular directions is approximately equal in the bidirectional reinforcement. The direction distribution of discontinuous fibers in the composite material cannot be easily controlled. Therefore, fibers can be either randomly distributed or preferred distributed. In most cases, the fibers are assumed to be randomly distributed in the composites. But, in the injection moulding of a fiber reinforced polymer, the orientation of fibers may be occur in the flow direction of preferred oriented fibers in the composites.

1.4.2.2 Particulate Composites

In this type of composites, the reinforcement is of particle nature. It can be spherical, cubic, tetragonal, a platelet, or of other regular or irregular shape. In general, particles are not very active in improving fracture resistance but they improve the stiffness of the composite to a limited extent. Particle fillers can be used to improve the properties of composite materials such as to modify the thermal and electrical conductivities, improve performance at elevated temperatures, reduce friction, increase wear and abrasion resistance, improve machinability, increase surface hardness and reduce shrinkage.

1.4.2.3 Flake Composite

A flake composite consists of thin, flat flakes held together by a binder or placed in a matrix. Almost all flake composite matrixes are plastic resins. The most important flake materials are aluminum, mica and glass [10].

Flakes will provide:

1. Uniform mechanical properties in the plane of the flakes
2. Higher strength
3. Higher flexural modulus

4. Higher dielectric strength and heat resistance

5. Better resistance to penetration by liquids and vapor

6. Lower cost

1.5 Types of Fiber Reinforced Polymer (FRP)

According to the type of fiber material, the fiber reinforced composite materials can be classified to three types; these are: Carbon fiber reinforced plastic (CFRP), glass fiber reinforced plastic (GFRP) and aramid fiber reinforced plastic (AFRP) [5]. The following is a brief description for the three types:

1.5.1 Carbon Fiber Reinforced Polymer (CFRP)

This type of reinforced polymer contains thin fibers of about 0.005–0.010 mm in diameter and composed mostly of carbon atoms. The carbon atoms are mixed together in microscopic crystals that are more or less aligned parallel to the long axis of the fiber.

1.5.2 Glass Fiber Reinforced Polymer (GFRP)

Glass fiber reinforced plastic is commonly known as fiberglass, developed commercially after the Second World War. It was the first lightweight, high-strength, and relatively inexpensive engineering composite. The use of fiberglass has grown rapidly since that time. The term ‘Fiberglass’ is referred to as a thermoset plastic resin which is reinforced with glass fibers. Through the GFRP composite, the glass fibers are surrounded by polymers matrix. Each of the glass fiber and the matrix keep its own chemical, physical and mechanical properties [1]. There are two common types of glass fibers. These are the E-glass (electrical) and the S-glass (high strength). E-glass can be considered as the most commonly used fiber

reinforcement. This type of glass has a good heat resistance, and high electrical properties. For more critical requirements, S-Glass offers higher heat resistance and about one-third higher tensile strength (at a higher cost) than that of E-glass. GFRP composites has been used in many engineering applications such as aircraft structures, boats, automobiles, machines tools and sports equipments, due to the advantages they offer compared to other conventional and non-conventional materials [1]. The level of composite strength can be determine during the moulded of FRP/Composite by control the arrangement of the glass fibers (How the individual strands are positioned). The three basic configuration of glass fiber reinforcement are unidirectional, bidirectional and multidirectional. The former provide the maximum strength in the direction of the fibers. It can be continuous or intermittent, depending on the specific needs depending on the part shape and process used. This configuration allows a very high reinforcement loading for maximum strengths. The fibers in a bidirectional configuration are in two directions perpendicular to each other, thus providing the highest strength in those directions. The same number of fibers need not necessarily be used in both directions. High fiber loading can be obtained in woven bidirectional reinforcements. Multidirectional or random configuration provides essentially equal strength in all directions of the finished part [11]. The glass fibers are made from silicon oxide with addition of some amounts of other oxides [9]. They have a high strength, good temperature and corrosion resistance, and low price. Glass Fiber Reinforced Plastics (GFRP's) are widely used in the mechanical joints of components and structures in various applications [12].

Glass fiber is available in the following forms [10]. Figure 4 shows these forms

1. Continuous Fiber

2. Chopped strands

3. Woven

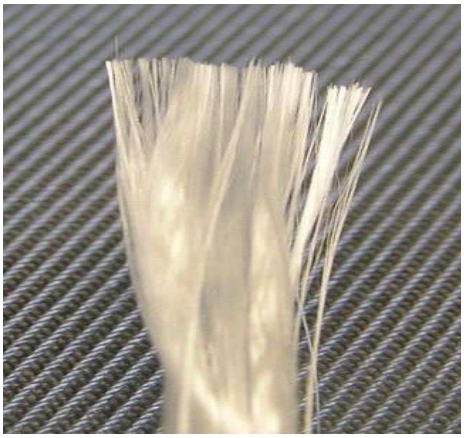

(a) Continuous Fiber

(b) Chopped Strands

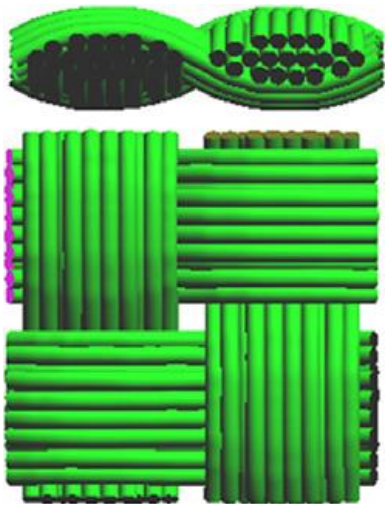

(c) Woven Fabric

Figure 4: Forms of Glass Fiber: (a) Continuous Fiber (b) Chopped Strands (c) Woven Fabric [5, 10].

1.5.3 Aramid (Kevlar) Fiber

Aramid is the universal name for aromatic polyamide. It is presented in 1972 by du Pont under the trade name Kevlar. There are two commercial types: Kevlar-29 and Kevlar-49. The former has a low-density, high strength, low modulus fiber and it is designed for some applications like ropes, cables, armor shield, etc. while the second one has low density, high strength, and high modulus. It is used in aerospace, space shuttle, ships and boats, automotive, and other industrial applications [1]. The present work focuses on glass fiber reinforced plastics.

1.6 Machining of Glass Fiber Reinforced Plastic

Machining process in general is one of the basic operations required to cut the materials into the required size and dimensions. Machining include removal of material from the work piece by means of certain processes in order to get the desired size and shape as per the specifications. Machining of GFRP composite materials differs in many aspects from the machining of traditional materials [7]. Machining of composites is difficult. This is because, the material behavior is non-homogeneous and anisotropic and also depends on the diverse reinforcement and matrix properties, and the volume fraction of matrix and reinforcement. The tool which is used in the machining process is subjected to alternatively the matrix and reinforcement materials, whose response to the machining process can be entirely different. For that reason, a number of problems may be follow the machining of fiber reinforced composite materials [13]. The differences in the material properties and the degree of anisotropy, cause difficulty in the predicting of the material behavior while being machined. This can result in specific problems of FRP machining which can be listed as follows:

(a) Delamination due to local dynamic loading caused by different stiffness's of the fiber and matrix, illustrating for the delamination can be shown in Figure 5.

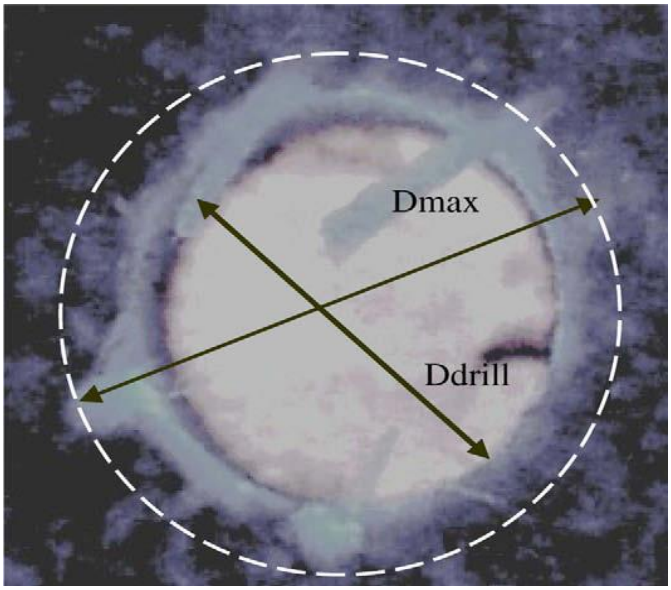

Figure 5: The delamination around the drilled hole [14].

(b) Spalling, chipping and delamination of the material.

(c) Fuzzing due to pulled out and crushed fibers;

(d) Burning due to poor thermal conductivity;

(e) Dimensional accuracy during machining of composite is very hard to predict since the reinforcement and matrix have different coefficient of thermal expansion.

Cutting tools may also be damaged by abrasive fibers rounding the cutting edges prematurely. The difference in hardness between the fiber and matrix may lead to edge chipping of the tool. In addition, the tool may be clogged by melted matrix material. Some of the most common conventional machining processes used are drilling, turning, and milling. Earlier composites were machined like metals, but due to the bad cut quality which resulted from such type of machining processes and the

tool wear problems led to the further study of composite machining [13]. These types of conventional machining techniques were adapted to machine glass fiber-reinforced composites because of the availability of equipment and experience, although the response of GFRP composites to the machining is completely different from the machining of other materials. In some cases, conventional machining with a cutting tool harder than the work material may not be an economical proposition. Therefore, the need arises for alternate material removal processes or nonconventional machining processes, like laser machining, water jet machining (WJM) and abrasive water jet machining (AWJM) processes, electrical discharge machining, etc. [1]. When the GFRP became more popular and widely used in the civilian sector, such as in auto and other consumer industries, material and machining costs became the driving factors and a high level of automation for the mass manufacturing of composite parts will be required to bring the costs down and compete with other materials. The progress in the nonconventional machining processes offer an a chance to process these materials economically, therefore realizing the full potential of the composite materials.

Machining can be classified into the following two types.

1) Conventional machining

2) Non-conventional machining

The following is the description for the two types of machining processes of GFRP composite materials.

1.6.1 Conventional Machining

Conventional machining processes are those processes, which involve cutting action by physical contact between tool and work piece having relative motion between the same. They are (i) drilling, (ii) milling, (iii) turning, (iv) shaping, (v) grinding, etc. [15].

1.6.1.1 Drilling Process

It is one of the popular cutting processes which is used a drill bit in a drill to make holes in solid materials. When the drill is rotated and moved on the work piece, the material is removed in the form of chips and moves along the fluted shank of the drill. Figure 6 shows the schematic of drilling process. There are various types of tools used in drilling process depending on the type of material to be machine, the size and number of the holes required, and the time required to complete the machining. The holes created are used primarily for fastening one component to another, passing coolants, and for wiring purposes. Drilling has been widely used to make holes in metals, but due to its availability and because it is more cost effective than the non-conventional cutting processes, it is now being used to remove materials from composites as well. However, composites machining by drilling process result in some problems. One of the major problems caused by drilling process is delamination. It was mentioned in the literature that, in aircraft industry for example, the rejection of parts made from the composite laminates due to drilling- induced delamination damages in final assembly was 60% [16]. Therefore, any drilling-induced delamination that results in reject of the component represents an expensive loss since the drilling process is a final machining operation in the assembly of the component that is made from the composite laminates. Thus, and in order to increase the drilling efficiency of the composite laminates with the minimum waste and

damages, it is necessary to understand the behavior of the available drilling processes [16].

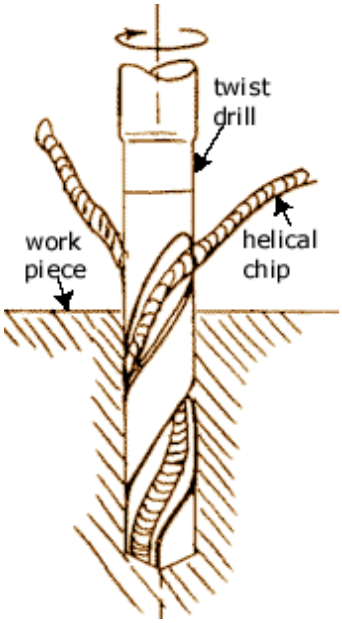

Figure 6: Schematic illustrating the drilling process [17].

1.6.1.1.1Advantages of Drilling Process of Composite Materials

1. It is a simple process.
2. It is economical and efficient machining processes for the assembly of components in the aerospace and automotive industries [18].
3. It can produce deep circular holes [19].

1.6.1.1.2 Disadvantages of Drilling Process on Composite Materials

There are many problems encountered when drilling of composite materials. These problems include [18].

1. Rapid tool wear due to material abrasiveness
2. The delamination, debonding and fiber pullout resulted by the thrust of the tool.

1.6.1.2 Milling Process

It can be consider as a corrective operation for removing the excess material by using a milling cutter to make a high cut quality surface [20]. The rotation axis of the tool is perpendicular to the feed direction [21]. Figure 7 shows, the schematic of milling process. Using the milling process to machine the composite materials may be affected by the ability of these materials to delaminate and the fiber/resin of the composite is pullout due to the action of machining forces. Therefore, in order to improve the quality of the machined surface, such problems must be addressed [22].

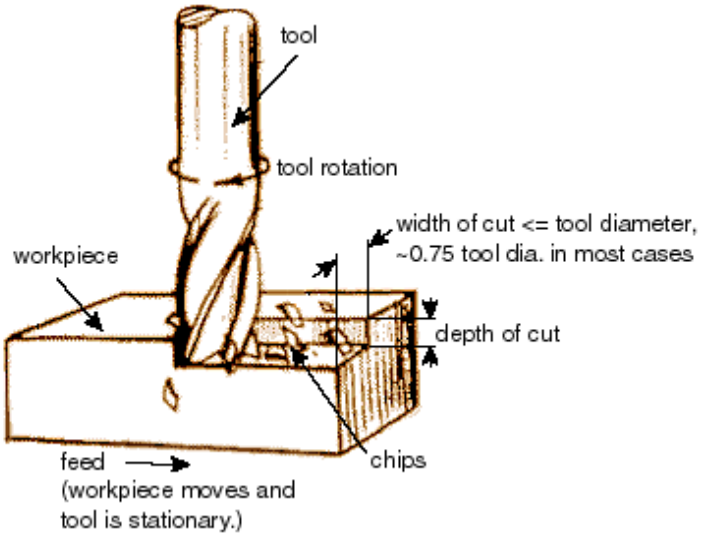

Figure 7: Schematic illustrate the milling process [22].

1.6.1.2.1 Advantages of Milling Process of Composite Materials

This type of machining process can be considered as a good completely operation in order to produce a well-defined and high cut quality surfaces [23].

1.6.1.2.2 Disadvantages of Milling Process of Composite Materials

1. Surface delamination associated with the characteristics of the material and the cutting parameters used is the major problem in milling of composites.
2. Chatter or vibration can occur resulting in low quality of surface finish and quite often accelerated tool wear [24].

1.6.2 Non-Conventional Machining

There are a numbers of unconventional machining processes used in manufacturing industries. These are: (i) Chemical, (ii) Electrochemical (iii) Thermoelectric (iv) Electro-discharge machining (v) LBM (vi) Ultrasonic Machining (vii) WJM (viii) AWJM [25].

1.6.2.1 Abrasive Water Jet Machining (AWJM)

AWJM is a process applicable to all the types of the materials [26]. It is used in various industrial processes especially in the cutting of complex shapes, mining and demolition, industrial machining and impulse fragmenting. The mechanism of machining by AWJ can be described as follows: a jet of water at a high pressure and velocity is mixed with a stream of fine-grained abrasive particles like silicon carbide or aluminum oxide in a suitable ratio, and focused on a work piece surface through a nozzle. The material removal process happens due to the erosion resulted by the impact of abrasive particles on the workpiece surface [27]. Figure 8 shows, the schematic of an abrasive water jet cutting system. When the water pressure is increased, the increase in the jet kinetic energy results in a high momentum which is transfered to the abrasive particles such that the impact and change in momentum of the abrasive material leads to cut the target [28].

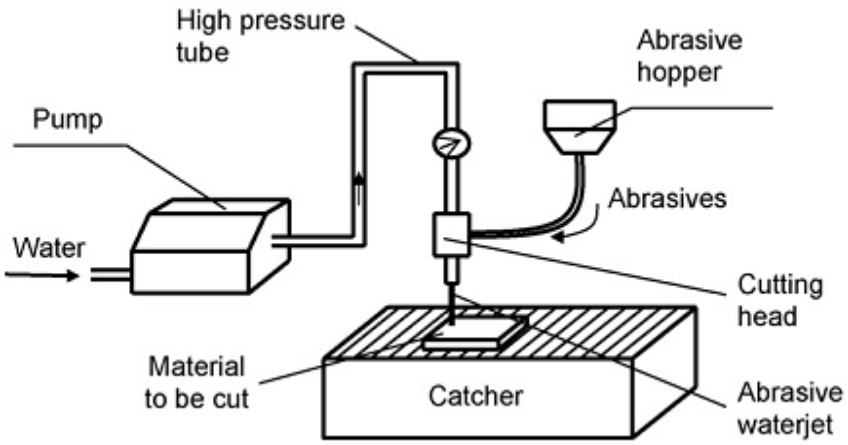

Figure 8: Schematic of abrasive water jet cutting system [29].

Figure 9 shows, a sample of cut surface generated by abrasive water jets. It is shown from the figure that the kerf is wider at the top than at the bottom, this is due to the decrease in water pressure, produced the taper.

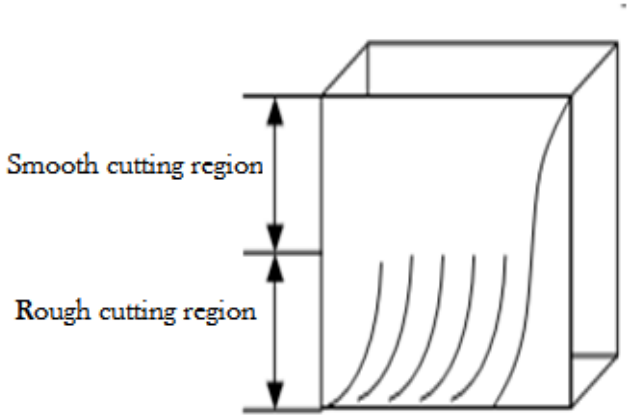

Figure 9: Kerf geometry image example [30].

Probably the most important aspect in kerf geometry is the taper angle, as shown in Figure 10. According to Shanmugam, D. K. [31] , kerf taper angle is an undesirable geometrical feature inherent to abrasive water jet machining.

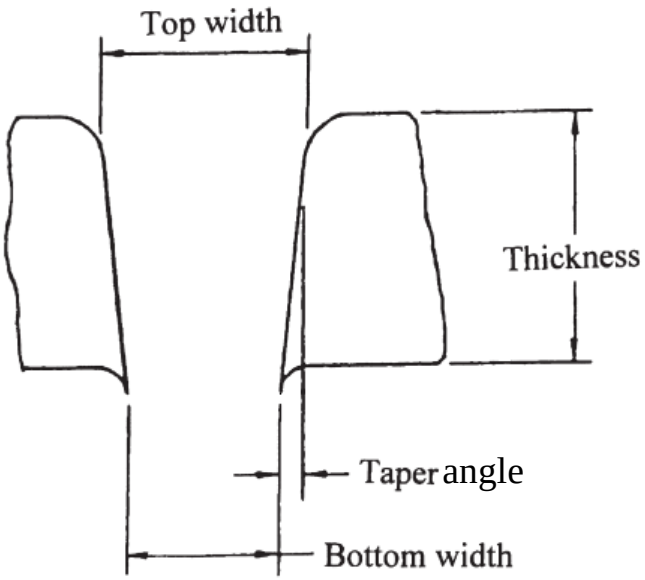

Figure10: Kerf width and kerfs taper illustration [31].

Striations are formed due to the change in the distribution of the particles with respect to the cut surface [32]. Chao and Geskin [33] used spectral analysis and found in their study that the machine vibration is the main cause of striation in AWJ cutting. The general cut surface produced by the abrasive water jet (AWJ) cutting consists of an upper smooth zone, which is free of any striations, and a lower rough zone where the wavy striations are the dominant characteristic features [33].

1.6.2.1.1 Advantages of AWJM Process

The following are the advantages offers by using the abrasive water jet machining process [29].

1. Extremely versatile process;

2. No heat affected zones;

3. Localizes structural changes;

4. Easy to program;

5. Maximum cutting thickness can be up to 25 mm;

6. Minimum material waste due to cutting;

7. Minimum cutting forces;

8. One jet setup can be used for nearly all abrasive jet jobs;

9. Eliminates thermal distortion.

1.6.2.1.2 Disadvantages of AWJM Process

Despite all the characteristics they posses, abrasive water jet cutting holds some disadvantages, as described below [29]:

1. An inappropriate selection of the cutting velocity may produce surface roughness values and kerf taper angles out of normal. It may also cause the burr, which would require secondary finishing. The existence of a material gap may produce cut surface defects. Each material has its own set of characteristics. The short life of some parts, like nozzle and orifice, add replacement costs and overheads to AWJ operation.
2. Another disadvantage is the fact that the cutting material is placed on top of support bars. The support bars may represent a problem in the final presentation of the work pieces, due to jet deflection.
3. The capital cost is high.
4. High noise levels during operation.

1.6.2.2 Laser Beam Machining (LBM)

It is a thermal material-removal process which uses a high-energy, coherent light beam to melt or vaporize particles on the surface of material work pieces. In LBM process, the work piece material is locally melted by the focused laser beam. The melt is then blown away with the help of assist gas like oxygen and nitrogen, which flows coaxially with the laser beam. Lasers have been used in many industrial applications on various types of materials. It is used for different types of machining

such as micromachining and macro machining. LBM has been applied also in the three dimensions machining, namely, threading, turning, grooving etc. [26]. Figure 11shows a schematic of laser beam machining.

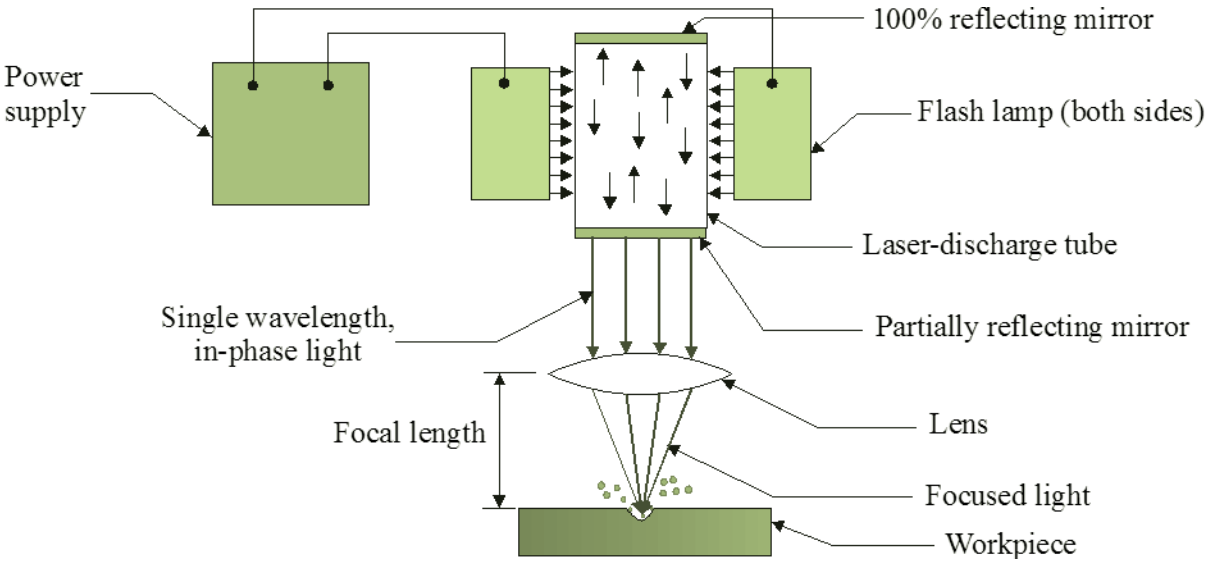

Figure11: Schematic of laser beam machining [35].

The three essential components of a laser-cutting machine are laser medium, excitation source and the optical resonator. The excitation source drives the atom, ions or molecules of the laser medium to a position where there is an excess of those at high energy level over those at a low level. This inversion in the normal thermodynamic population distribution result the laser action.

Each laser beam has its own power and, thus, has a defined heat input into the workpiece. However, because of the different properties of the fiber and matrix, the two components react very differently due to the thermal input. In general, the fibers needed higher energy for the vaporization than that required for the matrix. When a CO_2 laser is used to machine composites materials of higher conductive fibers, a large volume of resin is vaporized in the process, this lead to the delamination and

matrix recession of the composite. There is a limitation in using laser machining, that is the heat-affected zone (HAZ). This zone results from the matrix recession, matrix decomposition and delamination. Matrix recession occurs when the matrix and fibers are removed at different rates owing to their different thermo physical properties. Matrix recession leaves a zone of fibers free from the matrix material.

1.6.2.2.1 Types of Lasers

The main types of the lasers applied in the industries nowadays are carbon dioxide (CO_2) laser, neodymium yttria-alumina garnet (Nd: YAG) ($Y_3Al_5O_{12}$), and excimer lasers. The range of power for the CO_2 lasers can be up to 15 kW and there is possibility to use it in continuous-wave or pulsed mode. The YAG lasers are used in pulsed mode and the power range can be of 7-10 kW [36]. CO_2 laser has a wavelength of 10.6 μm while the YAG laser has a wavelength of 1.06 μm [37]. Because CO_2 lasers have higher average powers with cheaper cost-per-watt and they have an early history of success in industrial laser cutting, today the majority of cutting operations are carried out by CO2 lasers, especially for nonmetals, which have better absorption at far infrared wavelength. Nd: YAG laser has shorter wavelength, smaller focused spot size, and is better absorbed by metals than CO2 lasers. Multikilowatts Nd: YAG lasers are commercially available and they usually are delivered by fibers. All these factors lead to the increasing popularity of Nd: YAG lasers in industrial laser cutting, especially for metals. Q-switched Nd: YAG lasers are dominant in pulsed laser cutting. Excimer lasers have UV wavelengths that are strongly absorbed by both metals and nonmetals, the spatial resolution are higher than visible and infrared lasers, and thus they are mainly used for high-precision laser cutting, especially for polymers and semiconductors. Recently, conventional lasers using diode pumping and direct diode lasers are reducing their size and

increasing their average power quickly, which may change the dominant role of bulky conventional lasers in industrial laser cutting [37].

1.6.2.2.2 Advantages of LBM Process

There are many advantages offered by laser machining, these are including the following: [37, 38].

1. Minimum waste of material;
2. Minimum required time for the set-up ;
3. Parallel-sided cuts is possible;
4. Low overall distortion of part ;
5. The lasers can be used to cut a plastic of varying thickness by simply change in the intensity of the beam;
6. Lasers are used to cut through plastics and to engrave on it;
7. There is no tool wear because the method is a non- contact approach. Thus, preventing the product from any damage and deformation.

1.6.2.2.3 Disadvantages of LBM Process

There are some limitations combined the use of LBM process [37] .These are as follow:

1. A composite material is one, which contains two distinct phases that are not in thermodynamic equilibrium. The property of the two phases used in the composite are usually significantly different, which makes the machining of them is difficult;
2. Limitations on the material thickness due to the taper problem;
3. The capital cost is high;
4. Maintenance need high cost.

1.7 Problem Statement

With the upcoming usage of the GFRP composites in many areas of applications, machining of these materials has become a major concern in the manufacturing fields. The present knowledge about machining of GFRP composites, unfortunately, is seemed inadequate for the optimal economic utilization.

There is some areas in the machining of composites is still need to be enlightened more clearly. It was shown from the literature survey that: One of the areas where there is still much scope of work is necessary to be done is the hole making of woven glass fiber reinforced polyester composite materials as there is little work has been done on this material among all the fiber reinforced composite materials. Concerning the quality of machined hole, the main problem is related to the delamination, fiber/resin pullout, out of roundness, dimensional accuracy, the surface roughness and the reduction in tensile strength. In order to get over these problems, it is necessary to go on various types of cutting process in order to estimate the optimum values of the above drawbacks because the unsuitable choice may lead to unwanted work material degradation. Also, it is necessary to decide which type of the machining process is the optimal process.

Chapter 2

LITERATURE REVIEW

The objective of studding the literature is to provide information on the issues to be considered in this thesis and to emphasize the relevance of the present work. Composite materials play an important role in a wide range of application fields in many switches from the traditional engineering materials. Glass fiber reinforced composite materials are such type of materials which is used in various types of products like aerospace, automobile, sporting chattels, marine components, pipes, containers, etc. Machining of polymers/ composites is used when the quantity of the required items does not excuse the cost for moulds, or when a product needs an accurate dimension and better surface finish. As a high performance polymers have been increasingly used in a large number of industrial applications. Therefore, the machining quality becomes a predominant factor in the development of a new processes and materials [39]. However, the knowledge about the polymer behavior under machining is still insufficient.

The following subsections provide a review on the diverse research activities accomplished in drilling, milling, AWJM and LBM processes of composite materials.

2.1 Previous Works Related to the Drilling and Milling Processes

Many researchers carried the consideration in drilling and milling of composite materials separately. E. Kilickap [40] investigates the effect of cutting parameters in drilling process of composites, like cutting speed and feed rate, and point angle on the delamination. The generated lesion associated with the drilling of GFRP composites were observed, at the upper and lower surface. He used the Taguchi method for the analyses in his study. The conclusion revealed that feed rate and cutting speed were the most influential factors on the delamination. He assigned that minimum delamination were obtained using lower cutting speeds and feed rates. El-Sonbaty, et al. [41] studied the effect of some variables upon the thrust force, and surface roughness in drilling machining of fiber-reinforced composite materials. The cutting parameters included in this study are cutting speed, feed rate, drill diameter and fiber content in the composite. Drills with diameters of 8, 9, 10, 11, 12, and 13mm to are used to machine GFRP at a constant rotational speed. The composite material used in their work was manufactured from randomly oriented glass fiber-reinforced epoxy, with different values of fiber volume fractions (Vf), using hand-lay-up technology. They found that the thrust force and torque increases with the increase of drill diameter and feed rate, due to the increase in the shear area. They also, concluded that in composite with volume fraction equal to 9:8–23.7%, the thrust force and torque decreased as the cutting speed is increased. The drilled holes of GFRP with lower Vf ratio at lower feed have higher surface roughness than that drilled at higher feed. N.S. Mohana, et al. [42] studied the effects of machining parameters upon the delamination in drilling process of high strength E-glass chopped fiber composite material. The evaluated parameters in their study were speed, feed rate, drill diameter and specimen thickness. They used the Taguchi and

response surface methodology to select the factors and the combination of factors that affect the delamination. They concluded that the specimen thickness, feed rate and cutting speed are reckoned to be the most significant factors contributing to the delamination. M.B. Lazar, et al. [43] defined experimentally, the distribution of the loads (axial and tangential) along the thickness of the carbon-fiber and glass-fiber reinforced composite plates. They found that the highest loads at the tool tip near the chisel edge for all cases. They also concluded that the maximum load per ply varies mainly with the axial feed rate and tool geometry, while the spindle speed has small or no effect. M. Adam Khan, et al. [44] studied the machinibility of E-glass composite material. They have been used two different alumina-cutting tools, these are a mixed alumina cutting tool (CC650) and a Sic whisker reinforced alumina-cutting tool (CC670). The machining was performed at different cutting speeds with constant feed rate and depth of cut. The execution of the alumina cutting tools has been evaluated by measuring the flank wear and surface roughness of the machined composite. It was found that the mixed alumina cutting tool fails after 8 min of machining at 250 m/min as it crosses the failure criterion for flank wear (i.e. 0.4 mm wear for finish machining). While the failure in the same cutting tool occurs after 6 min of machining at 300 m/min; however, the Sic whisker reinforced alumina cutting tool approaches tool failure after 9 min of machining. V. Krishnaraj, et al. [45] evaluated the generated damage through the use of drilling in GFRP material, which was prejudicial to the mechanical behavior of the composite structure. Their study is concentrated on the analyzing of the effect of spindle speed and feed rate upon the strength of the woven fabric laminates composite and they have been studied also, the residual stress distribution around the hole. The holes have been made at the centre of the specimens by a CNC machining centre using 6 mm diameter micrograin

carbide drill for two spindle speeds (1000, 4000 rpm) and different feed rates (0.02, 0.06, 0.10 and 0.20 mm/rev). The results assigned that the failure strength and the stress concentration depends on the drilling parameters. Better mechanical strength is obtained by using a spindle speed of 3000 rpm and feed rate of 0.02 mm/rev. E.S. Lee [46] investigated experimentally the drilling of GFRP using a tools made from different types of materials with various geometries. He found that the excellent machining of the work piece is achieved by the proper selection of the cutting tool material and geometry. The results indicated also, that the surface quality is related closely to the feed rate and cutting tool. S.A. Hussain, et al. [47] studied and developed a model for the surface roughness in machining of GFRP pipes using Response Surface Methodology (RSM). Experiments were conducted through the established Taguchi's Design of Experiments (DOE). The studied cutting parameters were cutting speed, feed rate, depth of cut, and fiber orientation of the workpiece. The result shows that the developed model is a suitable for the prediction of surface roughness in the machining of GFRP composites. V. Schulze, et al. [48] presented two strategies for making a hole by milling process using standard tools. The two strategies included the guide of the process forces toward the center of the work piece when machining the outer layers. The experiments have been accomplished upon a short glass fiber reinforced polyester. The experimental results support the idea that the machining damage can be significantly reduced by machining strategies which direct the process forces inwards as compared to the reference process of circular milling. The results also assigned that the failure decreases with the increase of the process forces that is directed toward the center of the work piece. R. Rusinek [49] studied the milling process of the epoxide-polymetrxi composite reinforced carbon fiber. He investigated the influence of the feed rate and rotational speed upon

the cutting forces. The experiments have been done using a CNC machine with feed rate ranging from 200 to 720 mm/min and rotational speed from 2000 to 8000-rpm .The researcher analyzed the experimental time series using the delay coordinates method in order to find the stable cutting regions. He used this information to predict a new model for the cutting forces that can be used to build a new regenerative vibration model for milling of the material used in his study. The analysis demonstrate that oscillations of cutting force are more regular, with larger amplitude, in case of unstable cutting, while cutting is stable (with less amplitude) the signal has stochastic component that is visible in Poincare maps and recurrence plots. . V. Schulze, et al. [20] examined the effect of cutting velocity and feed rate upon the machining force (Fw), delamination factor (Fd), surface roughness (Ra) and international dimensional precision (IT) using two types of GFRP composite materials, these are Viapal VUP 9731 and ATLAC 382-05. Analysis of variance is executed to evaluate the cutting characteristics of GFRP composite materials using a cemented carbide end mill. The results show that the end mill produces less damage on the Viapal VUP 9731 composite material than the ATLAC 382-05.

2.2 Previous Works Related to the AWJM and LBM Processes

The related studies on AWJM & LBM of composite materials have been carried out by many researchers. M. A. Azmir, et al. [50] assessed experimentally the effect of Abrasive Water Jet Machining parameters upon the surface roughness and kerf taper ratio of aramid fiber reinforced plastics composite. The approach was based on Taguchi's method and Analysis of Variance to optimize the AWJM parameters for effective machining. They found that the traverse rate was considered to be the most significant factor followed by the hydraulic pressure upon the roughness quality

criteria. While in the case of the kerf taper, traverse rate showed that the greatest influence is by the standoff distance. They were also confirmed that the optimal combination of AWJM parameters satisfy the real need for machining of composites in practice. E. Lemma, et al. [3] studied experimentally the performance of cutting the GFRP composite between using the oscillation and normal (without head oscillation) cutting process. A comparison of the results has been made and it has been shown that there is valuable improvement in the quality of the cut surfaces produced by the head oscillation technique than normal AWJ technique. D.A. Axinte, et al. [51] studied the ability of the AWJM to cut the polycrystalline diamond (PCD) using abrasive media with different hardness, like aluminum oxide (Al2O3), silicon carbide (SiC) and diamond. While they keep some other operating parameters constant like pump pressure, standoff distance and size of abrasives. The feed speed has been adjusted to enable full jet penetration for each type of the abrasives. It was found that the material removal rates and the nozzle wear ratios vary significantly with the employment of different types of abrasives. D.K. Shanmugam, et al. [28] used the abrasive water jet technique to machine two types of composites: epoxy pre-impregnated graphite woven fabric and glass epoxy. They studied the cutting performance measure and the kerf taper angle. The results indicate that, within the selected ranges of the machining parameters, the increase in the jet pressure results in decrease of the kerf taper angles and increased within the standoff distance range of 2–5mm. While, the kerf taper angle seems to decrease insignificantly with increases the abrasive mass flow rate. A. A. E1-Domiaty, et al. [52] proposed a model for predicting the maximum depth of cut for different types of materials using various machining parameters. The predicted model is able to predict the maximum depth of cut that can be obtained in a given material for a given set of process parameters

without the need for many experimental constants. The only hypothesis used in this model is the shape of the kerf. This hypothesis requires a definition for the kerf contour over which the abrasive water jet is acting. L.M. Hlava, et al. [53] measured the slop angle between the tangent to the striation and the tangent to the axis of the water jet. Then, the slop angle is used to predict the model. The obtained model is included into the algorithm of the program to authorize the quality control through the abrasive water jet cutting. J. Wang [54] studied experimentally the abrasive Water jet cutting of polymer matrix composites. It has been shown that the abrasive water jet cutting technology is a good alternative method for machining the polymer matrix composite, with a good productivity and kerf quality. A.A. Cenna, et al. [55] improved a model to predicts some parameters in the laser cutting of composite like the kerf width, material removal rate and the energy transmitted through the cut kerf. Many experiments were carried out using different laser to compare the experimental result with the predicted results. The results show very good agreement. I.A. Choudhury, et al. [38] used a CO_2 laser to machine three polymeric materials namely: polypropylene, polycarbonate and polymethyl methacrylate. The response variables measured in this study are the heat affected zone (HAZ), surface roughness and dimensional accuracy. Predictive models have been developed by the response surface methodology (RSM) and their adequacy was tested using the analysis of variance. It was found that the response is well modeled by a linear function of the input parameters. The dimensional accuracy were examined by measuring the deviation of the actual value from the nominal value. It was found that polymethyl methacrylate has less HAZ, followed by polycarbonate and polypropylene. For the surface roughness, polymethyl methacrylate has better cut edge quality than polypropylene and polycarbonate. Z.L. Li, et al. [56] studied the quality characteristics

in machining the carbon fiber reinforced plastic using the diode pumped solid-state (DPSS) UV laser. The results show that the minimum HAZ is achievable using the short-pulsed UV laser. F. Caiazzo, et al. [57] used the CO_2 laser to machine three thermoplastic polymers, namely: polyethylene (PE), polypropylene (PP), polycarbonate (PC) with various thicknesses ranging from 2 to 10 mm. The examined response variables were laser power, range of cutting speed, type of focusing lens, pressure and flow of the covering gas, thickness of the samples. As a result, the authors determined the "degree" of laser cutting machinibility for the three polymers as follows: PC high, PP medium-high, and PE lower. Ming-Fei Chen, et al. [58] studied the effects of various process parameters, such as, assisted gas-flow rate, pulse repetition frequency, cutting speed, and focus position to achieve the optimum characteristics of transmittance ratio and work-piece surface roughness in composite material. Nine experiments were performed based on the orthogonal array. The results assigned that the optimal process parameters as 20 L/min for assisted-gas flow rate, 5 kHz for pulse repetition frequency, 2 mm/s for cutting speed, and 0 mm for laser focusing position. It was also found that the assisted-gas flow rate has more effect than any other single parameter. H.A. Eltawahni, et al. [59] introduced a method for selecting the process parameters in laser cutting of MDF based on the design of experiments (DOE) approach. ACO_2 laser was used to cut three thicknesses of MDF panels, these are: 4, 6 and 9 mm, of MDF. The process factors studied are: laser power, cutting speed, gas pressure and focal point position. The response variables are the upper kerf width, the lower kerf width, the ratio between the upper kerf width to the lower kerf width, the cut section roughness and the operating cost. D.K. Shanmugam, et al. [60] studied the kerf characteristics and surface roughness of two different materials, carbon composite and fiber-reinforced plastic, using abrasive

water jet, plain water jet and laser cutting. The results show the potential possibility of using those methods. Though using all the methods seemed to be quite possible, Abrasive water jet cutting promises a better cutting compared to the other two.

2.3 The Goal of the Present Work

The optimization of the process parameters for multiple performance characteristics of the material included in the present research is still not reported in the literature and as the optimal machining process parameters is more efficient it was applied in the present study than the “trial and error” method. The current research presents a comprehensive approach to select optimal cutting parameters for high cut quality, productivity and low cost, minimum reduction in tensile strength of hole making using conventional machining technologies (drilling and milling machining processes) and non conventional machining technologies (AWJM and LBM processes) in glass fiber reinforced epoxy composite material sheets type 3240, using a statistical approach. Analysis of variance (ANOVA) was performed to select the optimal cutting parameters. A numerical optimization was also completed in order to simultaneously maximize/minimize different combinations of performance measures.

Chapter 3

EXPERIMENTAL WORK

The experimentations which have done in the present work specifies the machining of glass fiber specimens on drilling, milling, abrasive water jet and laser beam machines for the purpose of optimization the process parameters using statistical computing package Design-Expert 8.

The following sub-sections describe the cutting mechanism by drilling and milling processes, cutting mechanism by AWJM and LBM process, material used, design of experiment and experimental setup.

3.1 Cutting Mechanism by Drilling and Milling Processes

The mechanism following the operation of hole making using drilling and milling machining processes at both exit and entry surface of glass fiber specimens is described as follow: Machining of composite laminates is difficult to perform due to their non-homogeneous, anisotropic, and the highly abrasive of their reinforced fibers render them difficult to machine [7, 61]. Several undesirable problems like delamination, and fiber pullout produced by drilling and milling, drastically reduce the strength against fatigue, thus sitting the long-term performance of composite laminates [62]. Among the problems caused by drilling and milling of composites, delamination is considered as a major damage. To minimize these problems, and to achieve the acceptable range of quality upon the machined surface, it is required to

understand the cutting mechanisms of material removal. Delamination occurs at the entry and exit sides of the hole. Delamination by drill tool on either side follows different mechanisms. This type of damage occurs as a result of the peeling effect of the drill tool as it approaches the surface of the laminate during drilling [63]. This mechanism is called as "peeling-up". Similarly as the tool approaches the exit side, the last ply called sub-laminate which is under the pressure of drill tool gets delaminated. This trend of delamination is refer to as Push-out mechanism. When the drill bit approaches the entrance, it has to machine a relatively thick laminate, because of this higher resistance would be faced by the drill bit. When the drill bit approaches the exit it has to machine a relatively thin laminate, because of this lower resistance would be applied on the drill bit. This particular reason makes peel up delamination as minimum one compared to the push out delamination [63]. The delamination due to peel up and push out action can be decreased to a minimum extent by supplying a pad support at the inlet and outlet side of the hole through the drilling process [64]. The chip formation process depends upon either fracture or shear or upon the combination of both, based on the fiber orientation and tool geometry. The high volume fraction of abrasive fibers can cause rapid tool wear [13].

3.2 Cutting Mechanism by LBM and AWJM Processes

Alternative machining processes have been adopted to conquer the rapid tool wear in conventional machining of some composites. LBM and AWJM processes are two types of these alternative processes. These two types of machining are noncontact machining operations. Thus, no cutting tools, and consequently, no cutting forces accompanied these types of machining. In the following text, some of the issues

involved in the cutting mechanism of composites using the two cutting processes are outlined.

As it is mentioned previously, the GFRP composites are blend of two materials, glass fiber and polymer matrix, that have significantly different characteristics. Since each of these materials oxidizes at a different temperature, the laser beam process used to cut the glass fibers would cause the epoxy resin to decompose and melt resulting in a flow of the fibers within the resin causes charring and tearing of the resin layer [65]. There are three mechanisms in laser cutting, these are: laser fusion cutting, laser oxygen cutting, and laser sublimation/vaporization cutting. In the first mechanism, the material is melted by the laser beam, and a jet of gas is used to blow out the slushy material or a vacuum device is used to suck away the molten material. A cutting front is formed at one end of the cutting kerf. The laser supplies the energy for melting and thermal diffusion while the gas jet provides the momentum to remove the molten material. In order to block the oxidation, it is necessary to use assistant gases like argon, nitrogen, and helium. Laser oxygen cutting applies to reactive materials such as low carbon steel and titanium. In laser oxygen cutting, the laser is used to heat the material until the exothermic reaction with oxygen begins. The material is burnt through by the chemical reaction mainly. In this process the oxygen gas jet is used. This will reduce the requirements in the laser power. Under the same power level, higher cutting speed and thicker section cutting can be achieved using laser oxygen cutting than laser fusion cutting. Laser sublimation/vaporization cutting generally applies to materials having low conductivity and low latent heat of vaporization, like the organic materials. Chemical reaction with oxygen may be uncontrollable for these materials. In the laser

micromachining, however, this mechanism applies to a wide range of materials, comprising metals and ceramics. For this mechanism, no oxygen is used and the material is vaporized or sublimated by the laser energy only. This mechanism requires the highest laser power and laser intensity among the three mechanisms [37].

The Abrasive water jet cutting technology uses a jet of water under high pressure, and high velocity mixed with abrasive slurry to cut the target material by means of erosion.

GFRPs, like most other composites, are inhomogeneous materials that contain both ductile and brittle behaving materials, which interact differently with the forces exerted by the incoming abrasive jets [1]. The closely accepted explanation concerning the physics of the material removal process and the striation formation mechanisms in ductile and homogenous materials is that of Hashish [66] who performed an implementation of the AWJ cutting process using a high-speed camera to record the material removal process in a Plexiglas sample. He concluded that the material removal process is a cyclic penetration process which consists two cutting regimes. He termed these two regimes as ‘‘cutting wear zone’’ and ‘‘deformation wear zone’’. Figure 12 shows these two zones and the abrasive particle trajectory path in these two zones. Hashish also suggested that the cutting process include three stages, these are: the entry stage, the cyclic cutting stage and the exit stage as shown in Figure 13. In the cutting wear zone, material removal occurs by the striking of the abrasive particles with the work piece at shallow angles of attack while the material removal in the deformation wear zone is achieved by the impinging of the abrasive particles at large angles of attack. The general erosion process starts in a periodic

state with a steady material removal up to a critical depth (hc) followed by the construction and removal of steps as the cutting depth increases. Under the critical depth, the material removal process is starting to be unsteady, resulting in the construction of striations or waviness on the wall of the cut surface [67]. Thus, the change of material removal process from one style to another is suggested to be the reason of striation or waviness [68]. The material removal process in ductile materials is regarded to be mainly as a result of the erosion process at shallow angles and the plastic deformation at large angles [69]. However, in contrast, the material removal process in the brittle materials is viewed as a brittle fracture process i.e. material removal occurs by mainly chipping [70]. El-Domiaty and Abdel-Rahman [70] proposed elastic–plastic erosion models based on fracture mechanics to calculate the maximum depth of cut and the surface roughness. The models were constructed to predict the maximum depth as a function of the fracture toughness, hardness and process parameters. The erosion process of the brittle materials is controlled by the formation of cracks and their progress. The fracture toughness of the material is a measure of the materials resistance to the crack propagation [70].

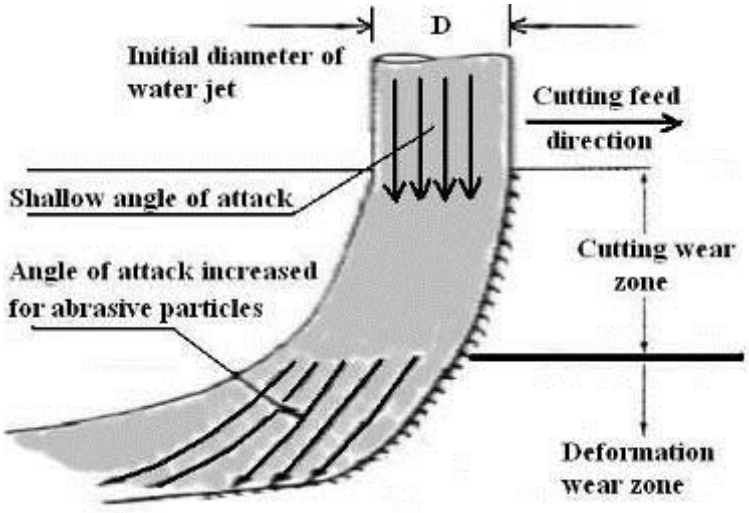

Figure 12: Cutting and deformation wear zones in AWJ cutting [69].

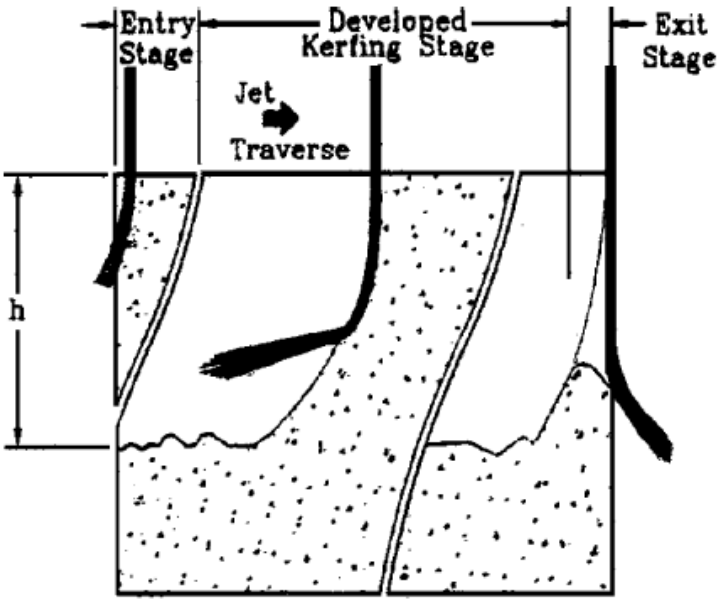

Figure 13: Stages in the AWJ cutting process [69].

3.3 Material

The experiments have been carried out in a sheet of woven laminated glass fiber reinforced plastic (GFRP), type 3240 produced by Jinhao Material Co. / China. The glass fiber was E-glass and the matrix polymer was epoxy resin. Two fiber densities (gram of fiber per cubic centimeter in GFRP): 0.82 gm /cm^3 and 1.32 gm /cm^3, which are equal to fiber volume fractions of 45% and 70%, respectively, of GFRP, with 8 mm and 16 mm thickness for each material density, were selected for the present work as shown in figure 14.

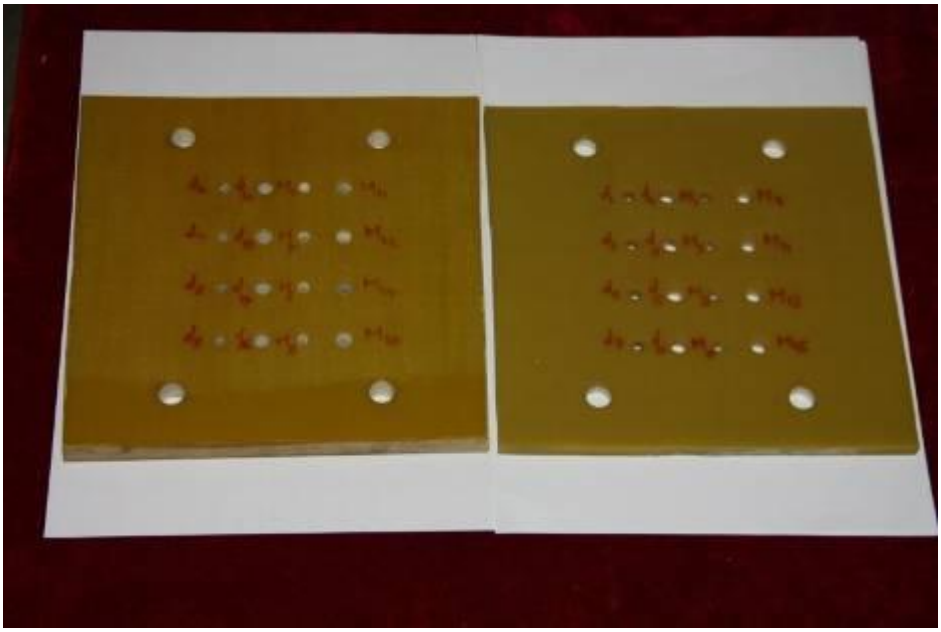

(a)

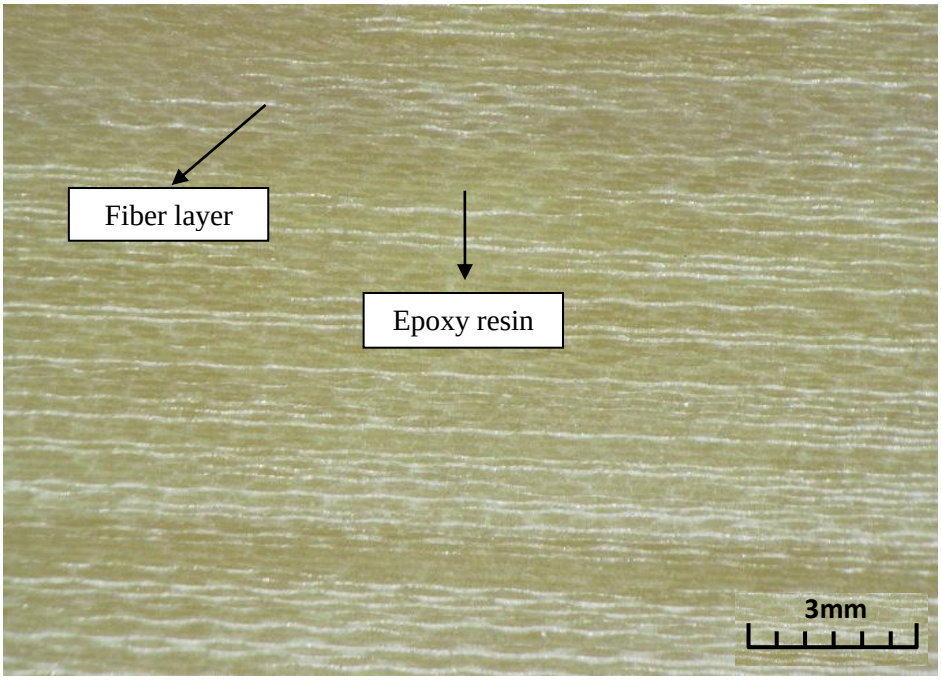

(b)

Figure 14: (a) Laminated GFRP with the two thickness. (b) Cross-sectional view

The main properties of the laminated GFRP material are listed in Table 1.

Table 1: Main properties of the Laminated GFRP Type 3240

No.	Property	Value /unit
1	Fiber density in GFRP	0.82 gm/cm^3
2	Fiber volume fraction	45%
3	Max. working temperature	200 ^{o}C
4	Average tensile strength	295.45 MPa
5	Layer thickness	0.5 mm

This type of GFRP is mainly used in aerospace, transportation tools, building panels, portable buildings, floor grating, doors, boats, ship structures, car panels, decorative art, sporting components, insulation boards and circuit boards, etc.

3.4 Design of Experiments

In general, factorial design is considered to be the most efficient way of conducting the experiments. Factorial design signifies that, in each complete trial or replication of the experiment all possible combinations of the levels of the factors are examined. For all the experiments in drilling, milling, AWJM and LBM processes, some of the predicted variables were chosen depending upon the available literature, availability of the machine specifications, and the experience of the authors and the others are selected based on the preliminary trial runs.

3.4.1 Design of Experiments for Drilling and Milling Process

A four factors, two-levels, full-factorial design of experiments (2^4 = 16 tests) was developed for each of the two cutting processes to select the effective factors upon

the cutting quality and the reduction in tensile strength. High and low, setting of the input parameters is shown in table 2.

Table 2: High and low levels of the input factors in drilling and milling process

Code	Input factor	Unit	Level 1	Level 2
A	Specimen thickness	mm	8	16
B	Cutting speed	m/min	24	48
C	Feed rate (Drilling)	mm/rev	0.06	0.09
	Feed rate (Milling)	mm/tooth	0.06	0.09
D	Nominal hole diameter	mm	6	8

3.4.2 Design of Experiments for AWJM and LBM Process

Two groups of the control parameters in each type of the cutting processes were developed to study the effects of more factors affecting the response variables. Some of the control parameters, which are the parameters related to the machining process are determined by trial runs. Preliminary trial runs were carried out using abrasive water jet for determining the minimum or maximum values of jet pressure, cutting feed and standoff distance that is required for the GFRP material to cut through. With those trial runs it was determined that the jet pressure should be not less than 150 MPa, standoff distance should be not more than 3mm and cutting feed not less than 0.2 m/min. Using laser beam cutting process, preliminary tests were conducted to determine the range of laser power, cutting feed and standoff distance. In this study, it was determined that the GFRP material was cut through with laser power not less than 1.5 KW, standoff distance not more than 2 mm and cutting feed not less than 0.1 m/min. The control parameters ranges are carefully provided between the levels for comparison purpose. A five factors, two-levels, full-factorial design of experiments (2^5= 32 tests) were developed in each group of each cutting technologies (AWJM

and LBM). High and low levels of the control parameters for the AWJM and LBM are shown in tables 3 and 4 respectively.

Table 3: High and Low levels of the input factors in (AWJM)

code	Input factor	Unit	Group 1		Group 2	
			Level 1	Level 2	Level 1	Level 2
A	Nominal hole diameter (D)	mm	6	8	6	8
B	Material thickness (t)	mm	8	16	8	16
C	Cutting feed (Vc)	m/min	0.2	0.3	0.2	0.3
D	Fiber density(ρ)	gm/cm^3	0.82	1.32	Fixed(0.82)	Fixed(0.82)
E	Abrasive flow rate (AF)	gm/min	100	130	Fixed(100)	Fixed(100)
F	Jet pressure (P)	MPa	Fixed(150)	Fixed(150)	150	200
G	Standoff distance (Sod)	mm	Fixed(1)	Fixed(1)	2	3

Table 4: High and Low levels of the input factors in (LBM)

code	Input factor	Unit	Group 1		Group 2	
			Level 1	Level 2	Level 1	Level 2
A	Nominal hole diameter (D)	mm	6	8	6	8
B	Material thickness (t)	mm	8	16	8	16
C	Cutting feed (V_C)	m/min	0.2	0.3	0.2	0.3
D	Fiber density (ρ)	gm/cm3	0.82	1.32	Fixed(0.82)	Fixed(0.82)
E	Assist. Gas flow rate (V)	Lit/min	25	45	Fixed(25)	Fixed(25)
F	Laser beam power (LP)	KW	Fixed(1.5)	Fixed(1.5)	1.5	2
G	Standoff distance (Sod)	mm	Fixed(1)	Fixed(1)	1	2

3.5 Response Variables

The response variables (performance measures) to be measured in 32 tests for each group can be described as follows:

1. Arithmetic surface roughness: The goodness of a manufactured part is describe by its geometry and surface roughness. The surface roughness is influenced by the fatigue life, friction, wear, and tear of the parts [38]. The arithmetic mean surface roughness (R_a), is a commonly used parameter in the industries. In the present work, it was measured using a contact-type stylus Mahr Perth meter. The readings were taken at four different locations along the cut hole depth surface– measured in microns. The mean values is reported for the analysis.
2. Delamination can be defined as the ratio between the expanded diameter (D_{max}) of the damage zone around the hole to the actual diameter of the hole (D). Delamination can be quantified by a ratio known as delamination factor (DF) [63]. Figure 4 illustrates the above description.

   $D_F = D_{max} / D$ …… (1)

   If delamination factor is 1, then there is no delamination, but if it is more than 1, then delamination exists. In the present work, both upper & lower maximum diameters (D_{max}) in the damage around each hole for each specimen were measured by using optical microscope type Leica DVM500. Higher values of delamination factor represent high surface damage. Delamination factor was measured at the upper and lower surfaces around the hole.
3. Thrust force (F_z) and Machining force (F_w): The former is the force acting along the hole depth during the drilling process. In the present work, the thrust force is measured by a piezoelectric dynamometer fixed on the table of the drilling machine and the force is recorded through a charge-amplifier on a data-recorder.

While in the case of milling process, Machining force (F_w) is determined from the following equation:

$$F_w = \sqrt{Fx^2 + Fy^2 + Fz^2} \quad \ldots\ldots\ldots\ldots\ldots\ldots \quad (2)$$

Where:

F_x, F_y and F_z are the three perpendicular components of the machining force. The three components of the machining force were measured using a piezoelectric dynamometer.

4. Dimensional accuracy. The dimensional accuracy of an item is of a crucial importance in the industrial applications, especially for the discipline assembly operation. In the manufacturing process, the designed part will be introduced in a drawing with all the measurements given within a certain range of allowances. The allowance determines the limits of the induced deviations for which the tolerance should be made in the design, and within which actual size is permissible. In the present work, the dimensional accuracy was taken in terms of out of roundness (O.O.R) and the difference between the upper & lower diameter (D_u-D_L). High values of these terms represent low dimensional accuracy.

$$O.O.R = (L_1+L_2+L_3) / 3 \ldots\ldots\ldots\ldots\ldots (3)$$

Where:

L_1, L_2 and L_3 are the deviation distances at three different points measured from the optical microscope image for each hole.

5. Tensile strength, measured in MPa. 64 tensile tests of hole specimens (32 hole specimens cut each by AWJM and LBM) according to ASTM D5766 [13] were carried using Universal Tensile Testing Machine, Type WDW-300, made by Changchun Kexin Com. / China. Figure 15 shows this setup.

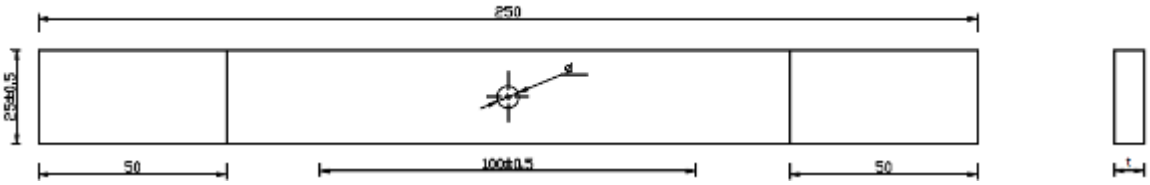

(a)

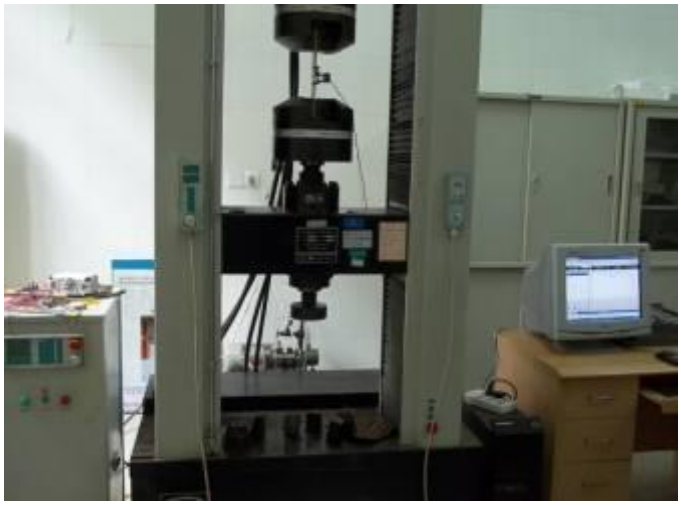

(b)

Figure 15: (a) Standard hole specimen for tensile test. (b) Universal Tensile Testing Machine

6. Cost (C), which includes the machining cost and tool cost.

a. Cost for drilling process is given by:

Cost = Tool cost per hole + Machining cost

Where:

- Machining cost = cost of labor/hr + electrical power consuming + tool change cost = 11.2 USD/hour
- Tool cost is as follows :

  - Cost of HSS drill, 6mm diameter = 1.92 USD

- Cost of HSS drill, 8mm diameter = 2.56 USD

- Life of HSS drill is 100 holes based on the operator's experience.
- Total cutting time (T) through the total life of the HSS drill is

  = 100 holes × cutting time (t)

  = 100 × thickness/feed rate

- Tool cost = (cost of drill / total cutting time) × cutting time per hole

  = cost of drill / 100

- Cost = cost of drill / 100 + 11.2 (USD/ hour) × cutting time (hour)

b. Cost for milling process is given by:

Cost = tool cost + machining cost

Where:

- Machining cost including cost of labor/hr + electrical power consuming + tool change cost = 11.2 USD/hour
- Tool cost is as follow :
  - Mill 5mm diameter (cemented carbide) = 8.01 USD
  - Mill 6mm diameter (cemented carbide) = 9.61 USD
- Life of cemented carbide mill is 600 holes based on the operator's experience.
- Total cutting time (T) through the total life of the cemented carbide mill is

  = 600 holes × cutting time per hole (t)

  = 600 × thickness/feed rate

- Tool cost = (price of the tool / total cutting time) × cutting time per hole = price of tool / 600
- Cost = price of tool / 600 + 11.2 (USD/ hour) × cutting time (hour)

c. Cost for abrasive water jet machining (AWJM) is given by:

Cost = tool cost + machining cost

Where:

Abrasive water jet cutting cost = Hourly equipment cost + cost of consumables (cost of electricity + cost of abrasive + cost of water + cost of tips) + cost of service and maintenance.

Where:

Hourly equipment cost = 8 .012 USD / hr

Cost of consumables + cost of service & maintenance = 8.012 USD / hr

Total cost = 8,012+8.012 = 16.024 USD / hr × cutting time (hr)

d. Cost for laser cutting is given by:

Cost = tool cost / hr + cost of consumables (cost of electricity + cost of the laser & assistance gasses + cost of lenses) / hr + cost of service and maintenance / hr

= 16.025 USD / hr (tool cost) + 11.217 USD / hr (electricity) + 20.833 USD / hr (machining, service & maintenance)

= 48.07 USD / hr

7. Productivity (Pr) that represents the number of holes cut per minute.

a. Productivity calculation for drilling cutting:

No. of holes per minute = 1/ [material thickness to be cut (mm)/feed (mm/min)] + (tool positioning+ retraction time)

b. Productivity calculation for milling cutting:

No. of holes per minute = 1/ feed (mm/min) [material thickness to be cut (mm) + (1+ 3.14) (D- D_m)] + (Tool positioning & Retraction time)

Where:

D = Nominal hole diameter

D_m = Tool diameter

Tool positioning + Retraction time in both drilling and milling processes = 2 sec

c. Productivity calculation for AWJM and LBM cutting:

Time (min) per hole = $t_R+t_P+t_C$

No. of holes per minute= 1/ $t_R+t_P+t_C$

No. of holes per minute = 1/ [Retraction and positioning time + piercing time + cutting time]

Retraction and positioning time for AWJM = 2 sec

Piercing time for AWJM = 1 sec

Retraction and positioning time for LBM = 1.5 sec

Piercing time for LBM = 1.5 sec

Cutting time for AWJM and LBM = $[(1 + 2\pi) (D – D_n /2)] / V_C$

Where:

D = hole diameter (mm)

D_n = diameter of water jet or laser beam (mm) = 1.5mm

V_C = cutting feed (mm/min)

3.6 Experimental Setup

3.6.1 Experimental Setup for Drilling and Milling Process

Drilling & milling experiments have been conducted on CNC Vertical Machining Center, type TH5 660 A in Nanjing university of aeronautic and astronautic/China . The spindle power is 7.5 kW and the maximum speed is 5300 rpm. In all the tests, the cutting tool used for drilling process is high speed steel (HSS) twist drill of 6 and 8 mm diameters. The geometry of the twist drills is a straight shank length of 38 mm for 6 mm diameter, and the shank length of 42 mm for 8 mm, helix angle for the drill tool of 6 mm is 25 º, while the helix angle for the drill tool of 8 mm is 30º. The number of flutes for both twist drills is equal to 3. The twist drill is hardened. The tool used for cutting the holes by milling process is made of cemented carbide with diameters of 5 mm and 6 mm. The geometry for both mill cutters can be summarized as: a rake angle of 7 º, a straight shank length of 26 and no. of flutes is two. Figure 16 shows the twist drill and end mill cutter used in these experiments.

The advantage of using cemented carbide drills over HSS is its strength to withstand cutting forces. From the tool life point of view, HSS performs very well in discontinuous cutting applications. The dimensions of the work piece material used in the present works are 200mm × 200mm × 8mm and 200mm × 200mm × 16mm. A multi component piezoelectric dynamometer Kistler type 9256 C, together with a load amplifier was used to obtain the three perpendicular components of the machining forces on the work pieces. Arithmetic surface roughness (R_a) was

measured along the depth of the cutting hole at four points using Mahr Perth meter M1 according to ISO 4287. Optical Microscope type Leica DVM500, having accuracy 0.001 mm has been used to measure the cut profile. The experimental setup for drilling and milling processes is presented in figure17.

Figure 16: Twist drill (left) and end mill (right) used in the experiments.

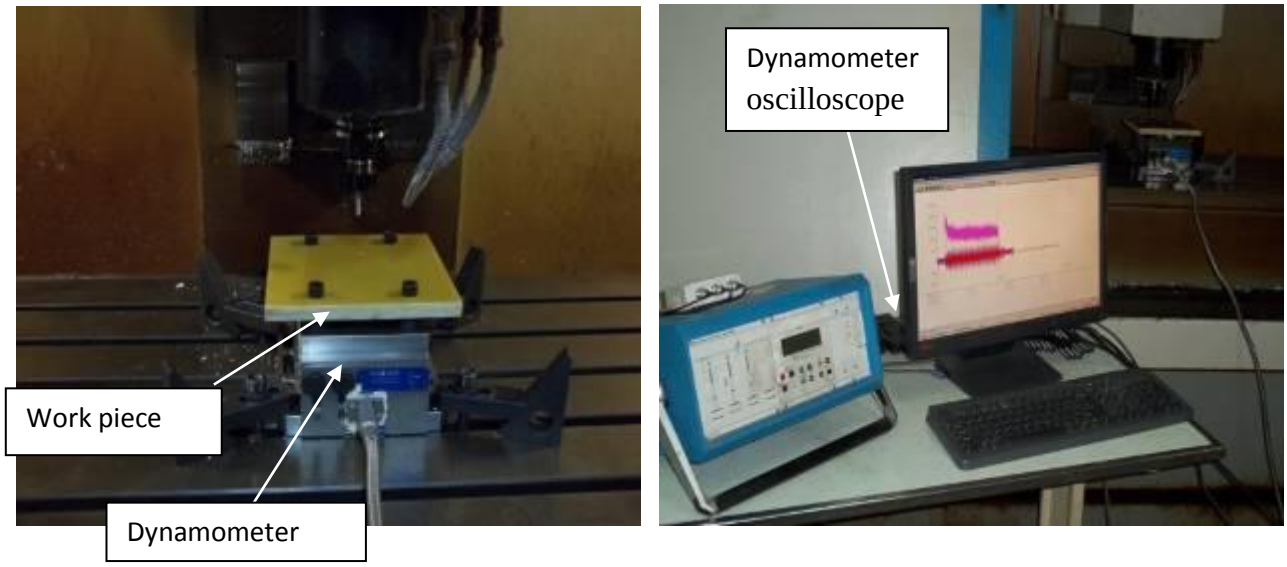

(a)

(b) (c)

Figure 17 Experimental Setup: (a) Fixation of work piece on the vertical machining center with kistler dynamometer and its oscilloscope (b) Surface measurement setup (c) Optical microscope measurement setup.

3.6.2 Experimental Setup for AWJM and LBM Process

AWJM experiments were conducted on ultra high pressure water cutting machine produced by Nanjing Hezhan Microtechnic Co. Ltd., China with a maximum pressure of 220-230 MPa, abrasive flow rate 3.7 gm/min and water flow rate 3.5-3.7

lit/hr. The type of abrasive used was garnet. In all the AWJM experiments, the nozzle diameter was 1 mm. LBM experiments were conducted on Rw – 6015 X cantilevered flight optical path laser cutter produced by Nanjing Nanchuan Laser Equipment Ltd., China. CO_2 continuous beam laser using nitrogen as assistant gas, has been used. The laser equipment has a power range of 2-4 KW; maximum speed 50m/min and table size 2500/1250mm. In all the laser experiments, the nozzle (orifice) diameter was 1.5 mm. The dimensions of the work piece material used in the present work are 200mm × 200mm × 8mm and 200mm × 200mm ×16mm. Arithmetic surface roughness (R_a) was measured along the depth of the cutting hole at four points using Mahr Perth meter M1. Optical Microscope of type Leica DVM500, having accuracy 0.001 mm was used to measure the cut profile. The experimental setup for AWJM and LBM processes is presented in figure18.

(a) AWJM setup

(b) LBM setup

(c) Optical microscope setup

Figure 18 Experimental setup : (a) Fixation of the work piece on the AWJM; (b) Fixation of the work piece on the LBM; (c) Optical microscope setup

Chapter 4

EXPERIMENTAL RESULTS

The quality of cutting hole using drilling, milling, AWJM and LBM processes is evaluated by the response parameters: surface roughness, delamination factor, difference between upper & lower diameter, and out of roundness. Thrust and machining forces in drilling and milling processes were also evaluated. The reduction in tensile strength of all the cutting specimens for all the types of cutting processes was also evaluated in this work. The experimental data has been analyzed using the analysis of variance.

4.1 ANOVA (Analysis of Variance)

It is a computational procedure used to select the effect of various design factors and to observe the degree of sensitivity of the result to various factors that affect the quality characteristics [73]. It can be defined also as a statistical technique used to locate the rate of the effect of an input parameter or group of an input parameter on the total variation of response parameter(s) [78]. ANOVA provides a statistical inspection of whether or not the means of several groups are all equal. As there are many predictor and response variables included in the present work, it means a large number of ANOVA tables will take a big space. For that reason, only F and P values were included in the ANOVA tables. F-value can be defined as the ratio between the square mean of the input parameter to the square mean of the error (mean square of any factor is a ratio between the sum of squares to the degree of freedom). While P-

value is minimum level of a significance that would result in reject of the null hypothesis, (In Null hypothesis, there is no difference between the mean of all predictor variables, i.e. there is no effect of each or all the predictor variables on the response variable). The bold numbers of p- values represent the parameters having significant effects. ANOVA analyses were completed using a version 8 of commercial statistical software called Design-Expert®. More details concerning the analyses are given in the upcoming sub-sections.

4.2 Experimental Results for Drilling and Milling Processes

Tables 5 & 6 present the results obtained from 16 tests each by drilling & milling processes.

Table 5: Experimental results for drilling process

Exp. No	Control Variables				Response Variables								
	t (mm)	Vc (m/min)	f_z (mm/rev)	D (mm)	F_z (N)	R_a (μ_m)	DF		C (USD)	D_u-D_L (mm)	O.O.R. (mm)	T.S. (MPa)	Pr (holes/min)
	A	B	C	D			UDF	LDF					
1	8	24	0.06	6	60.84	1.380	0.616	0.689	0.0681	+0.093	0.248	265.46	7.24
2	16	24	0.06	6	64.56	1.572	0.684	0.75	0.0901	+0.051	0.270	262.89	4.11
3	8	48	0.06	6	63.59	1.146	0.813	0.843	0.0461	+0.070	0.341	265.99	11.66
4	16	48	0.06	6	57.8	1.208	0.796	0.85	0.0591	+0.043	0.376	250.33	7.24
5	8	24	0.09	6	85.15	1.853	1.189	1.158	0.0521	+0.145	0.546	246.51	9.69
6	16	24	0.09	6	80.43	2.004	1.116	1.118	0.0681	+0.053	0.350	256.81	5.78
7	8	48	0.09	6	88.93	1.488	1.27	1.254	0.0431	+0.12	0.487	266.32	14.65
8	16	48	0.09	6	89.18	1.786	1.215	1.248	0.0521	+0.025	0.297	253.95	9.69
9	8	24	0.06	8	84.46	1.762	0.683	0.719	0.0802	+0.029	0.459	260.96	5.78
10	16	24	0.06	8	95.45	1.602	0.69	0.784	0.1082	+0.086	0.453	250.48	3.19
11	8	48	0.06	8	89.89	1.321	0.77	0.881	0.0492	+0.16	0.580	244.41	9.69
12	16	48	0.06	8	101.61	1.4	0.823	0.864	0.0652	+0.167	0.475	250.96	5.78
13	8	24	0.09	8	93.15	1.95	1.124	1.092	0.0592	+0.177	0.485	253.31	7.91
14	16	24	0.09	8	98.15	1.863	1.118	1.192	0.0772	+0.123	0.491	253.35	4.55
15	8	48	0.09	8	104.49	1.632	1.31	1.284	0.0462	+0.138	0.483	248.01	12.51
16	16	48	0.09	8	108.66	1.59	1.27	1.31	0.0562	+0.131	0.450	249.96	7.91

Table 6: Experimental results for milling process

Exp. No	Control Variables				Response variables								
	t (mm)	Vc (m/min)	f_z (mm/z)	D (mm)	F_w (N)	R_a (μ_m)	DF		C (USD)	Du-Dl (mm)	O.O.R. (mm)	T.S. (MPa)	Pr (holes /min)
	A	B	C	D			UDF	LDF					
1	8	24	0.06	6	65.869	1.462	1.012	0.94	0.0625	-0.001	0.335	267.76	10.04
2	16	24	0.06	6	63.461	1.35	0.81	0.968	0.0775	+0.01	0.252	268.13	6.98
3	8	48	0.06	6	70.122	0.885	0.88	0.91	0.0405	+0.02	0.239	258.62	15.05
4	16	48	0.06	6	67.880	0.936	0.924	0.986	0.0495	+0.018	0.338	259.21	11.33
5	8	24	0.09	6	79.459	1.631	1.163	1.151	0.0465	+0.04	0.523	248.16	12.90
6	16	24	0.09	6	133.62	1.582	1.083	1.050	0.0595	+0.034	0.225	258.36	9.38
7	8	48	0.09	6	88.939	1.194	1.112	1.068	0.0405	+0.085	0.356	247.43	18.04
8	16	48	0.09	6	81.209	1.28	1.142	1.228	0.0465	+0.052	0.333	248.16	14.29
9	8	24	0.06	8	34.120	1.246	0.684	0.724	0.1086	+0.017	0.354	247.43	6.90
10	16	24	0.06	8	38.84	1.320	0.771	0.801	0.0966	+0.012	0.408	289.67	5.30
11	8	48	0.06	8	34.511	1.248	0.843	0.876	0.0686	+0.116	0.349	269.78	11.23
12	16	48	0.06	8	42.944	1.140	0.794	0.85	0.0596	-0.04	0.445	251.99	9.02
13	8	24	0.09	8	39.407	1.382	1.111	1.057	0.0806	+0.03	0.487	254.19	9.29
14	16	24	0.09	8	46.746	1.283	1.100	1.155	0.0716	-0.03	0.408	255.44	7.31
15	8	48	0.09	8	41.795	1.25	1.072	1.056	0.0596	-0.046	0.302	261.32	14.19
16	16	48	0.09	8	47.564	1.294	1.111	1.126	0.0526	-0.027	0.404	263.24	11.76

4.3 Experimental Results for AWJM and LBM Processes

The experimental results for the two groups in each of the AWJM and LBM processes are listed in Tables 7- 10 respectively.

Table 7: Experimental results for group 1 of AWJM process , P=150 MPa , Sod= 2mm

N.	Predictor Variables					Response Variables					
	D (mm) **A**	t (mm) **B**	V_C (m/min) **C**	ρ (gm/cm3) **D**	AF (gm/min) **E**	(R_a) μm	O.O.R (mm)	D_u-D_F (mm)	T.S. (MPa)	C (USD)	Pr (holes/min)
1	6	8	0.2	0.82	100	0.402	0.111	-0.133	283.95	0.062	7.51
2	8	8	0.2	0.82	100	1.968	0.141	-0.265	283.53	0.053	5.90
3	6	16	0.2	0.82	100	0.475	0.145	-0.021	285.23	0.062	7.51
4	8	16	0.2	0.82	100	1.415	0.114	+0.097	246.76	0.075	5.90
5	6	8	0.3	0.82	100	0.727	0.161	+0.164	294.74	0.053	9.74
6	8	8	0.3	0.82	100	0.849	0.135	+0.174	269.12	0.062	7.87
7	6	16	0.3	0.82	100	0.427	0.062	+0.133	249.67	0.053	9.74
8	8	16	0.3	0.82	100	1.523	0.094	+0.13	291.32	0.062	7.87
9	6	8	0.2	1.32	100	1.887	0.110	+0.205	341.57	0.062	9.74
10	8	8	0.2	1.32	100	2.049	0.196	+0.311	346.27	0.075	7.87
11	6	16	0.2	1.32	100	2.121	0.061	+0.077	347.02	0.062	7.51
12	6	8	0.3	1.32	100	1.666	0.070	+0.166	360.17	0.053	9.74
13	8	16	0.2	1.32	100	2.764	0.162	+0.071	338.29	0.075	5.90
14	8	8	0.3	1.32	100	1.936	0.108	+0.335	371.74	0.053	7.87
15	6	16	0.3	1.32	100	1.996	0.088	+0.151	350.31	0.053	9.74
16	8	16	0.3	1.32	100	1.988	0.133	-0.103	348.10	0.062	7.87
17	6	8	0.2	0.82	130	0.763	0.129	+0.259	97.43	0.048	7.51
18	8	8	0.2	0.82	130	1.091	0.136	+0.25	122.79	0.071	5.90
19	6	16	0.2	0.82	130	1.660	0.21	+0.659	235.36	0.062	7.51
20	6	8	0.3	0.82	130	0.623	0.123	+0.101	91.25	0.066	9.74
21	6	8	0.2	1.32	130	1.522	0.135	+0.131	349.23	0.062	7.51
22	8	16	0.2	0.82	130	2.107	3.05	Defect	284.67	0.062	5.90
23	8	8	0.3	0.82	130	1.488	0.121	+0.352	280.22	0.057	7.87
24	8	8	0.2	1.32	130	1.769	0.159	+0.455	320.56	0.075	5.90
25	6	16	0.3	0.82	130	1.276	0.202	+0.786	301.45	0.053	9.74
26	6	16	0.2	1.32	130	2.805	0.110	-0.119	360.71	0.066	7.51
27	6	8	0.3	1.32	130	1.781	0.094	+0.18	359.09	0.053	9.74
28	8	8	0.3	1.32	130	1.997	0.263	+0.486	347.48	0.075	7.87
29	8	16	0.3	0.82	130	2.197	0.219	+0.503	281.51	0.053	7.87
30	8	16	0.2	1.32	130	2.325	0.168	+0.208	345.65	0.075	5.90
31	6	16	0.3	1.32	130	2.187	0.331	+0.241	358.50	0.053	9.74
32	8	16	0.3	1.32	130	2.668	0.194	+0.178	359.09	0.062	7.87

Table 8: Experimental results for group 2 of AWJM process,ρ= 0.82 gm/cm^{3}AF=100 g/min

N.	Predictor Variables					Response Variables					
	D (mm) **A**	t (mm) **B**	V_C (m/min) **C**	P MPa **D**	Sod **(mm)** **E**	R_a (μm)	O.O.R (mm)	Du-DF (mm)	T.S (MPa)	C (USD)	Pr (holes/min)
1	6	8	0.2	150	2	0.402	0.111	-0.133	283.95	0.062	7.51
2	8	8	0.2	150	2	1.968	0.141	-0.265	283.53	0.053	5.90
3	6	16	0.2	150	2	0.475	0.145	-0.021	285.23	0.062	7.51
4	8	16	0.2	150	2	1.415	0.114	+0.097	246.76	0.075	5.90
5	6	8	0.3	150	2	0.727	0.161	+0.164	294.74	0.053	9.74
6	8	8	0.3	150	2	0.849	0.135	+0.174	269.12	0.062	7.87
7	6	16	0.3	150	2	0.427	0.062	+0.133	249.67	0.053	9.74
8	8	16	0.3	150	2	1.523	0.094	+0.13	291.32	0.062	7.87
9	6	8	0.2	200	2	0.578	0.16	+0.277	115.20	0.062	7.51
10	8	8	0.2	200	2	1.368	0.131	+0.305	115.51	0.075	5.90
11	6	16	0.2	200	2	0.483	0.071	+0.142	299.6	0.057	7.51
12	6	8	0.3	200	2	0.876	0.154	+0.069	274.61	0.053	9.74
13	8	16	0.2	200	2	1.635	0.105	+0.143	274.60	0.075	5.90
14	8	8	0.3	200	2	1.964	0.133	+0.316	98.01	0.053	7.87
15	6	16	0.3	200	2	0.417	0.084	+0.086	291.78	0.062	9.74
16	8	16	0.3	200	2	1.335	0.174	+0.474	224.71	0.053	7.87
17	6	8	0.2	150	3	0.760	0.222	+0.225	280.39	0.080	7.51
18	8	8	0.2	150	3	1.802	0.229	+0.309	263.97	0.075	5.90
19	6	16	0.2	150	3	0.6	0.088	+0.086	235.36	0.071	7.51
20	6	8	0.3	150	3	0.639	0.102	+0.234	98.95	0.057	9.74
21	6	8	0.2	200	3	0.970	0.275	+0.286	281.71	0.062	7.51
22	8	16	0.2	150	3	1.852	0.069	+0.015	284.67	0.075	5.90
23	8	8	0.3	150	3	2.146	0.122	+0.269	114.78	0.062	7.87
24	8	8	0.2	200	3	1.789	0.167	+0.378	119.34	0.075	5.90
25	6	16	0.3	150	3	1.649	0.122	+0.385	294.8	0.057	9.74
26	6	16	0.2	200	3	0.847	0.138	+0.288	291.45	0.057	7.51
27	6	8	0.3	200	3	0.513	0.153	+0.343	71.97	0.053	9.74
28	8	8	0.3	200	3	1.938	0.198	+0.389	119.56	0.062	7.87
29	8	16	0.3	150	3	1.509	0.124	+0.074	279.34	0.057	7.87
30	8	16	0.2	200	3	1.97	0.125	+0.216	287.21	0.075	5.90
31	6	16	0.3	200	3	1.315	0.128	+0.479	288.22	0.062	9.74
32	8	16	0.3	200	3	1.593	0.196	+0.237	281.73	0.075	7.87

Table 9: Experimental results for group1 of LBM process, LP = 1.5 kW, Sod=1mm

N.	Predictor Variables					Response Variables					
	D (mm) **A**	t (mm) **B**	V_C (m/min) **C**	ρ (gm/cm^3) **D**	V Lit/hr **E**	R_a (μm)	O.O.R (mm)	Du-DF (mm)	T.S (MPa)	C/hole (USD)	Pr (holes/min)
1	6	8	0.1	0.82	25	4.343	0.251	-0.158	159.08	0.160	4.31
2	8	8	0.1	0.82	25	2.730	0.163	+0.045	246.99	0.186	3.28
3	6	16	0.1	0.82	25	4.164	0.251	+0.039	160.53	0.186	4.31
4	8	16	0.1	0.82	25	3.834	0.260	+0.206	169.93	0.227	3.28
5	6	8	0.2	0.82	25	4.587	0.166	+0.448	108.42	0.106	7.09
6	8	8	0.2	0.82	25	4.609	0.134	+0.061	104.41	0.133	5.63
7	6	16	0.2	0.82	25	5.57	0.393	+0.001	159.54	0.133	7.09
8	8	16	0.2	0.82	25	5.13	0.303	-0.109	138.27	0.146	5.63
9	6	8	0.1	1.32	25	5.362	0.076	-0.237	182.41	0.160	4.31
10	8	8	0.1	1.32	25	4.444	0.164	-0.119	152.252	0.186	3.28
11	6	16	0.1	1.32	25	3.555	0.103	-0.361	232.067	0.173	4.31
12	6	8	0.2	1.32	25	3.981	0.064	-0.121	185.657	0.106	7.09
13	8	16	0.1	1.32	25	4.141	0.167	-0.455	221.935	0.227	3.28
14	8	8	0.2	1.32	25	5.176	0.160	-0.053	155.244	0.133	5.63
15	6	16	0.2	1.32	25	5.02	0.121	-0.284	288.83	0.106	7.09
16	8	16	0.2	1.32	25	4.543	0.206	-0.34	230.809	0.133	5.63
17	6	8	0.1	0.82	45	2.951	0.134	-0.116	88.82	0.186	4.31
18	8	8	0.1	0.82	45	2.78	0.191	-0.076	228.90	0.227	3.28
19	6	16	0.1	0.82	45	3.216	0.113	-0.007	175.53	0.173	4.31
20	6	8	0.2	0.82	45	3.331	0.087	-0.089	267.04	0.106	7.09
21	6	8	0.1	1.32	45	3.108	0.037	-0.191	153.34	0.160	4.31
22	8	16	0.1	0.82	45	3.649	0.182	-0.072	164.78	0.227	3.28
23	8	8	0.2	0.82	45	3.45	0.186	-0.055	91.18	0.133	5.63
24	8	8	0.1	1.32	45	2.871	0.112	-0.052	375.4	0.227	3.28
25	6	16	0.2	0.82	45	5.13	0.095	-0.026	183.82	0.106	7.09
26	6	16	0.1	1.32	45	4.48	0.119	-0.435	235.093	0.160	4.31
27	6	8	0.2	1.32	45	3.837	0.067	-0.12	184.994	0.106	7.09
28	8	8	0.2	1.32	45	3.616	0.112	-0.024	149.379	0.133	5.63
29	8	16	0.2	0.82	45	4.36	0.187	-0.208	175.96	0.133	5.63
30	8	16	0.1	1.32	45	4.03	0.147	-0.629	259.692	0.213	3.28
31	6	16	0.2	1.32	45	4.14	0.125	-0.277	230.571	0.106	7.09
32	8	16	0.2	1.32	45	3.913	0.175	-0.343	247.435	0.133	5.63

Table 10: Experimental results for group 2 of LBM , ρ= 0.82 gm/cm^3, V= 25 Lit/hr

N.	Predictor Variables					Response Variables					
	D (mm) **A**	t (mm) **B**	V_C (m/min) **C**	LP (kW) **D**	Sod (mm) **E**	(R_a) (μm)	O.O.R (mm)	Du-DF (mm)	T.S. (MPa)	C/hole (USD)	Pr (holes/min)
1	6	8	0.1	1.5	1	4.343	0.251	-0.158	159.08	0.160	4.31
2	8	8	0.1	1.5	1	2.730	0.163	+0.045	246.99	0.186	3.28
3	6	16	0.1	1.5	1	4.164	0.251	-0.039	160.53	0.186	4.31
4	8	16	0.1	1.5	1	3.834	0.260	-0.206	169.93	0.227	3.28
5	6	8	0.2	1.5	1	4.587	0.166	+0.448	108.42	0.106	7.09
6	8	8	0.2	1.5	1	4.609	0.134	+0.061	104.41	0.133	5.63
7	6	16	0.2	1.5	1	5.57	0.393	+0.001	159.54	0.133	7.09
8	8	16	0.2	1.5	1	5.13	0.303	-0.109	138.27	0.146	5.63
9	6	8	0.1	2	1	4.426	0.188	-0.022	71.51	0.200	4.31
10	8	8	0.1	2	1	4.444	0.092	-0.053	70.37	0.227	3.28
11	6	16	0.1	2	1	4.06	0.081	-0.102	65.89	0.173	4.31
12	6	8	0.2	2	1	3.555	0.19	-0.09	77.11	0.160	7.09
13	8	16	0.1	2	1	3.884	0.290	-0.402	65.73	0.227	3.28
14	8	8	0.2	2	1	5.302	0.136	+0.06	79.26	0.133	5.63
15	6	16	0.2	2	1	5.16	0.110	-0.207	70.07	0.146	7.09
16	8	16	0.2	2	1	5.03	0.393	-0.106	69.69	0.160	5.63
17	6	8	0.1	1.5	2	5.44	0.219	-0.316	88.49	0.186	4.31
18	8	8	0.1	1.5	2	5.19	0.292	-0.053	84.19	0.227	3.28
19	6	16	0.1	1.5	2	5.84	0.21	-0.178	136.51	0.186	4.31
20	6	8	0.2	1.5	2	5.55	0.195	-0.009	262.24	0.106	7.09
21	6	8	0.1	2	2	4.73	0.201	-0.022	68.49	0.160	4.31
22	8	16	0.1	1.5	2	5.67	0.220	-0.156	130.18	0.213	3.28
23	8	8	0.2	1.5	2	6.27	0.25	+0.003	94.56	0.133	5.63
24	8	8	0.1	2	2	4.945	0.093	-0.058	73.75	0.227	3.28
25	6	16	0.2	1.5	2	6.92	0.277	-0.256	172.01	0.133	7.09
26	6	16	0.1	2	2	5.73	0.192	-0.256	62.56	0.173	4.31
27	6	8	0.2	2	2	5.69	0.28	+0.09	75.99	0.186	7.09
28	8	8	0.2	2	2	5.41	0.147	-0.015	78.09	0.133	5.63
29	8	16	0.2	1.5	2	6.49	0.459	-0.022	131.32	0.213	5.63
30	8	16	0.1	2	2	5.23	0.325	-0.363	65.84	0.227	3.28
31	6	16	0.2	2	2	6.34	0.185	-0.032	70.18	0.133	7.09
32	8	16	0.2	2	2	6.18	0.333	-0.048	69.88	0.227	5.63

ANOVA tables accomplished on the data concerning the response variables of hole making by drilling, milling, AWJM and LBM processes were listed in the upcoming subsections. Influence of all the individual predicted variables have been shown in these tables. The influence of the possible interactions between the predicted variables was analyzed and only the significant variables and interactions have been shown in the plots. The influence of any parameter is considered in ANOVA tables to be significant if p-value≤0.05; marginally significant if 0.05≤p-value and insignificant otherwise.

4.3.1 Results Analysis for Drilling Process

Tables 11-12 present ANOVA results accomplished on the data concerning the response variables for drilling process.

Table 11: ANOVA for Ra; Fz; and T.S. in drilling process

Source	**R_a**		**F_z**		**T.S.**	
	F-value	**P- value**	**F-value**	**P- value**	**F-value**	**P- value**
Model	22.14	**0.0016**	50.06	**0.0002**	0.99	0.5398
A-(t)	3.37	0.1258	5.29	0.0699	0.59	0.4777
B-(V)	80.90	**0.0003**	14.49	**0.0125**	0.47	0.5243
C-(f_z)	106.82	**0.0001**	138.98	**0.0001**	0.64	0.4589
D-(D)	6.47	0.0517	282.86	**0.0001**	3.84	0.1074
A×B	0.3132	0.3132	0.18	0.6913	0.5870	0.5870
A×C	0.6076	0.6076	2.09	0.2078	0.4807	0.4807
A×D	0.0192	**0.0192**	12.15	**0.0176**	0.5545	0.5545
B×C	0.8129	0.8129	5.91	0.0593	0.2653	0.2653
B×D	0.8513	0.8513	5.11	0.0733	0.3530	0.3530
C×D	0.0225	**0.0225**	33.57	**0.0022**	0.5433	0.5433

Table 12: ANOVA for UDF; LDF; and (D_u - D_L) in drilling process

Source	UDF		LDF		D_u - D_L	
	F-value	**P- value**	**F-value**	**P- value**	**F-value**	**P- value**
Model	69.44	**0.0001**	74.48	**0.0001**	4.86	0.0475
A-(t)	0.15	0.7161	2.40	0.1824	4.85	0.0789
B-(V)	50.56	**0.0009**	66.40	**0.0005**	0.35	0.5808
C-(f_z)	638.88	**0.0001**	669.16	**0.0001**	2.84	0.1530
D-(D)	0.41	0.5494	2.91	0.1488	10.69	**0.0222**
A×B	0.11	0.7541	1.93	0.2233	0.78	0.4182
A×C	3.55	0.1183	0.081	0.7876	5.13	0.0729
A×D	0.43	0.5414	1.44	0.2838	10.68	**0.0222**
B×C	1.140	0.9744	0.100	0.7649	5.16	0.0722
B×D	0.26	0.6341	0.32	0.5943	7.15	**0.0441**
C×D	0.016	0.9029	0.016	0.9044	0.94	0.3774

The columns F-value and p-value in tables 11 and 12 suggest that cutting speed & feed rate are significant factors upon surface roughness while the machining force is significantly affected by feed rate, hole diameter and by the interaction between material thickness & hole diameter and the interaction between feed rate & hole diameter. The upper and lower delamination factors are significantly affected by feed rate, while the difference between upper and lower diameter is affected by feed rate and the interaction between the feed rate and the hole diameter. The table also shows that there is no significant factor on the tensile strength.

Figures 19 - 23 shows, in a graphical form, the effects of influential variables upon the surface roughness, thrust force, delamination factor at upper & lower surface and the difference between upper & lower diameter respectively.

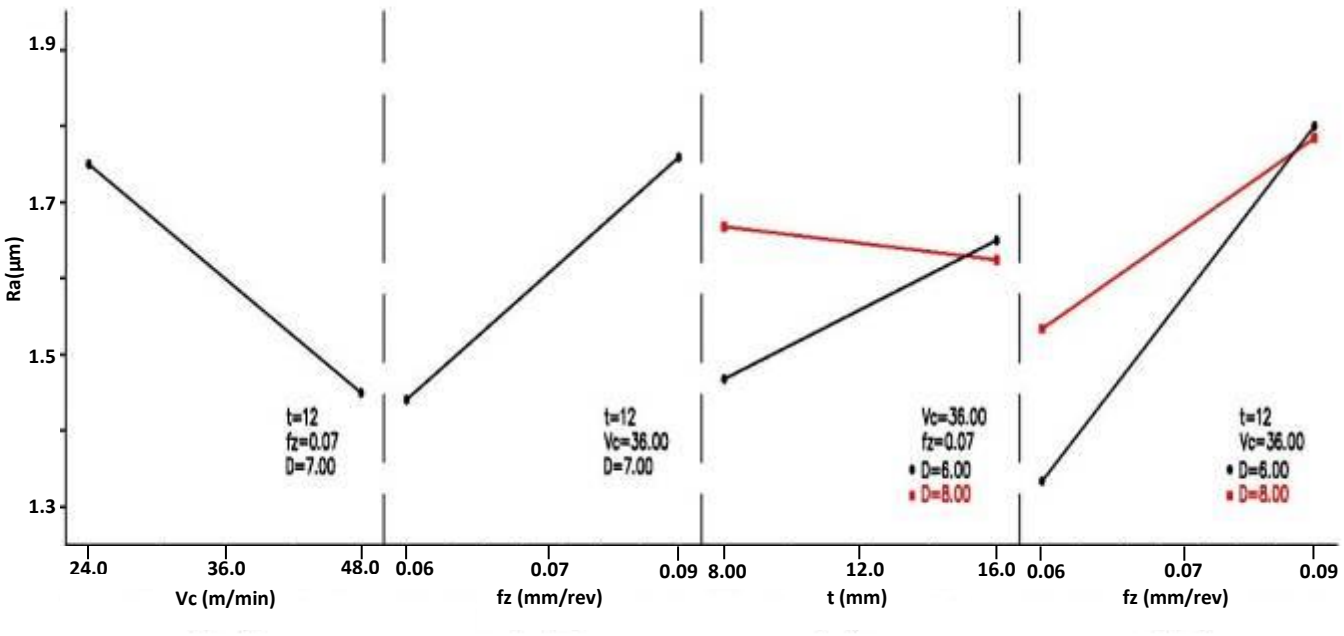

(a) (b) (c) (d)

Figure 19: Factorial plots showing the effects of: (a) cutting speed; (b) feed rate; (c) interaction between material thickness and nominal hole diameter; and (d) interaction between feed rate and nominal hole diameter upon arithmetic surface roughness (Ra) in drilling process.

It is clear from figure19 (a & b) that surface roughness is a minimum at the high value of cutting speed and the low value of feed rate . Figure19 (c & d) show the effects of interaction between 1. material thickness and nominal hole diameter 2.feed rate and nominal hole diameter. It can be noticed that at the high level of material thickness & feed rate, the surface roughness acquired is nearly the same value for the two diameters, but at the low level of the material thickness & feed rate, the surface roughness increses as the hole diameter increased. The results show that the increase in the feed rate cause the surface roughness of the hole surface increase upto 1.75 µm. The increase in feed rate increased the heat generation and hence, tool wear.

The increase in the feed rate also cause increases in chatter and produces incomplete machining at a faster traverse, resulting in a higher surface roughness [15].

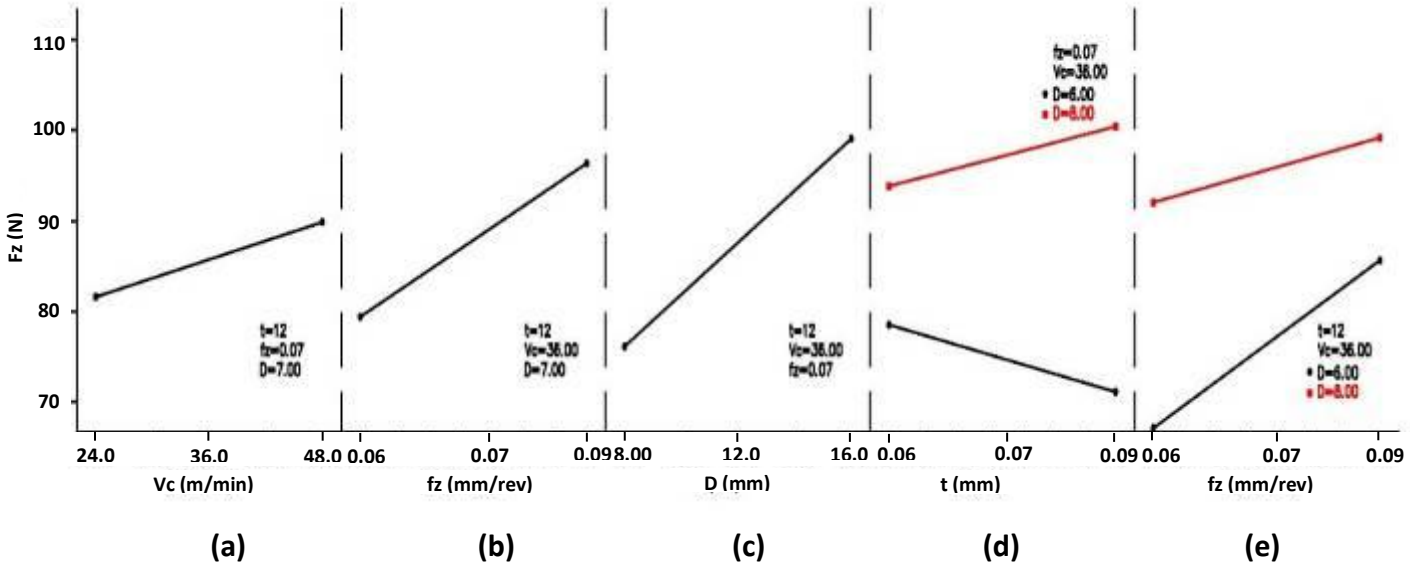

Figure 20: Factorial plots showing the effects of: (a) cutting speed; (b) feed rate; (c) nominal hole diameter; (d) interaction between material thickness and nominal hole diameter; and (e) interaction between feed rate and nominal hole diameter upon average thrust force (F_z) in drilling process

Figure 20 (a) indicates that the increase in the thrust force with the increase in the cutting speed is not too significant because of the higher temperatures generated from the increase in heat generation associated with the minimum coefficient of thermal conduction together with the minimum transition temperature of plastics [8]. From figure 20 (b & c) it is clear that the thrust force is maximum at high levels of feed rate & hole diameter. The increase in the feed rate causes an increase in the load upon the drill, which results in an increase of the thrust force in drilling of composites. The interaction plots in figure 20 (d & e) show that the effect of hole diameter is significant but it is more significant at the high level of material thickness. The same behavior was observed in the case of interaction between feed rate & hole diameter.

Figures 21 & 22 present the effects of the significant parameters upon the delamination factor at upper & lower surface. It is clear from the graphs (a & b) in figures 21 & 22 that the influence of the feed rate is more significant than the cutting speed upon the delamination. The delamination is increased more as the feed rate increased than in the case of increasing the cutting speed. The increase of the feed rate cause increases in the thrust force and delamination. Thrust force and delamination are the inter-connected phenomenon, in which the increase in the thrust force cause increases in the delamination factor and vice versa. As the cutting speed increases, the thrust force causes decreases in the delamination at both upper and lower surface. It is perhaps due to the fact that the temperature of the cutting area is elevated at high speed, thus promoting softening of matrix (epoxy resin) and inducing less delamination. At higher speed drilling behaves like a piercing operation and lesser entangled fiber pull out takes place within a minimum time. This justifies the importance of high speed drilling [63].

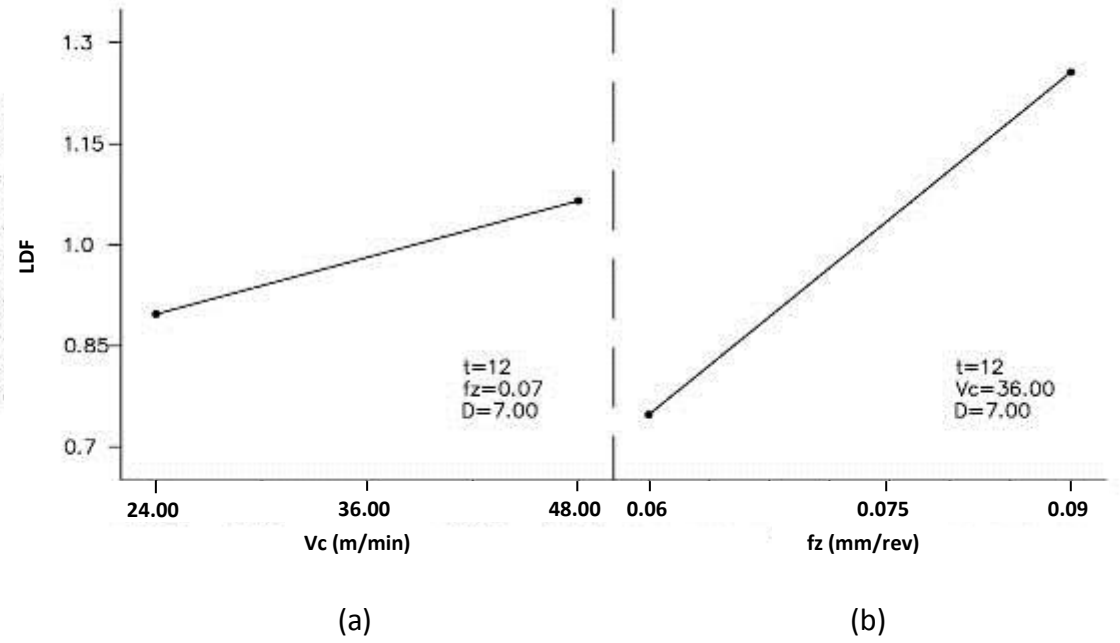

Figure 21: Factorial plots showing the effects of: (a) cutting speed; and (b) feed rate upon delamination factor at the upper surface in drilling process

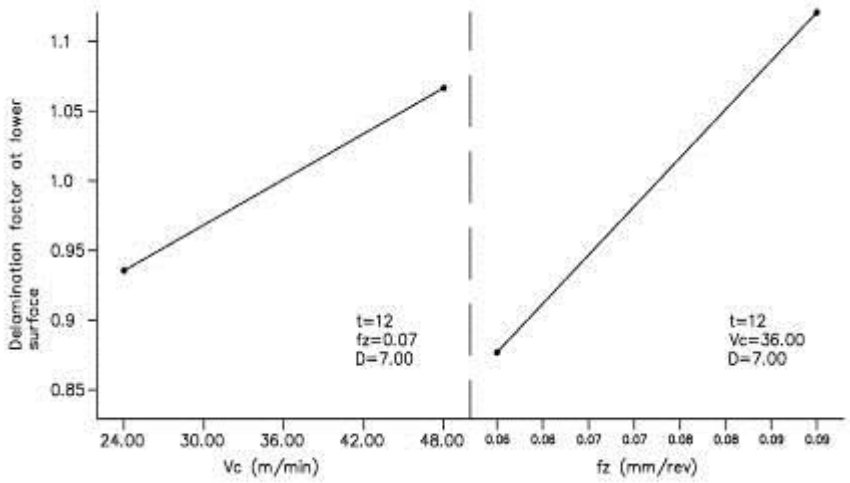

(a) (b)

Figure 22: Factorial plots showing the effects of: (a) cutting speed; and (b) feed rate upon delamination factor at the lower surface in drilling process.

Figure 23 shows in graphical form, the effects of the significant parameters upon the difference between upper & lower diameter. Graphs (a, b) in figure 23 show that the difference between upper & lower diameter increases as the hole diameter increases. The difference is a relevant term. By increase in hole diameter, the absolute value of the difference also increases.

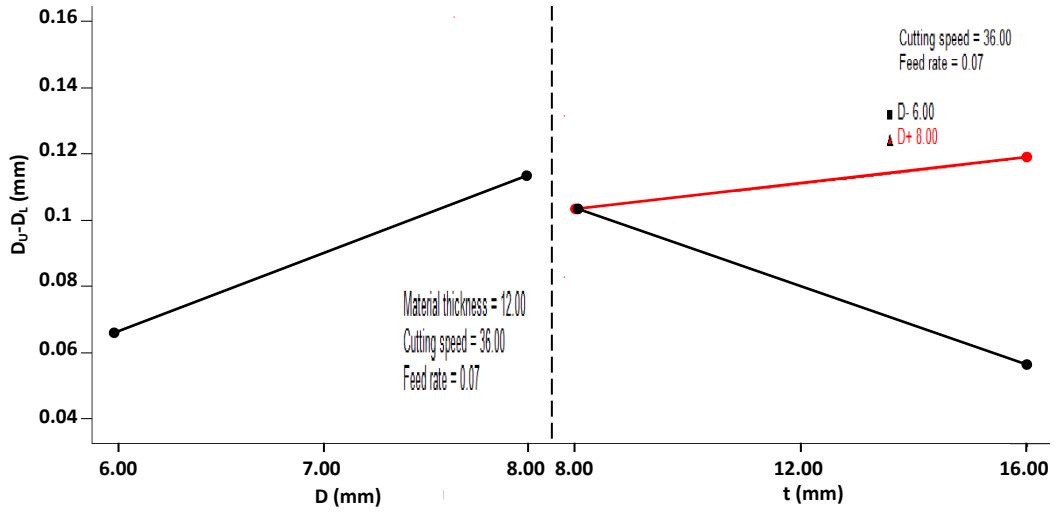

(a) (b)

Figure 23: Factorial plots showing the effects of: (a) nominal hole diameter; and (b) interaction between material thickness and nominal hole diameter upon the difference between upper & lower diameter in drilling process.

4.3.2 Results Analysis for the Milling Process

Tables 13- 14 present ANOVA results accomplished on the data concerning surface roughness, machining force and tensile strength for milling process.

Table 13: ANOVA for Ra; F_w; and T.S. in milling process.

Source	R_a		F_w		T.S.	
	F-value	P- value	F-value	P- value	F-value	P- value
Model	11.53	**0.0073**	70.71	**0.0001**	0.76	0.666
A-(T)	0.17	0.6983	2.90	0.1491	0.67	0.449
B-(Vc)	54.37	**0.0007**	4.03	0.1010	0.37	0.568
C-(f_z)	22.63	**0.0051**	67.73	**0.0004**	2.51	0.173
D-(D)	0.33	0.5930	608.01	**0.0001**	0.60	0.474
A×B	0.89	0.3898	0.90	0.3870	2.03	0.213
A×C	0.078	0.7908	0.033	0.8621	0.055	0.823
A×D	0.056	0.8226	8.97	**0.0303**	0.11	0.757
B×C	1.26	0.3125	0.12	0.7414	0.60	0.472
B×D	27.05	0.0035	0.40	0.5569	0.35	0.578
C×D	8.43	**0.0336**	13.99	**0.0134**	0.31	0.599

Table 14: ANOVA for UDF; LDF; and DU-DL in milling process.

Source	UDF		LDF		Du-D_L	
	F-value	**P- value**	**F-value**	**P- value**	**F-value**	**P- value**
Model	7.53	**0.019**	4.90	**0.046**	5.07	**0.043**
A-(T)	0.27	0.624	1.67	0.252	0.032	0.864
B-(Vc)	0.28	0.619	0.74	0.429	13.47	0.014
C-(f_z)	63.78	**0.0005**	38.65	**0.001**	11.51	**0.019**
D-(D)	5.52	0.065	4.93	0.077	3.03	0.142
A×B	0.98	0.367	0.36	0.573	3.18	0.134
A×C	0.13	0.733	0.059	0.817	0.78	0.418
A×D	1.01	0.360	0.036	0.857	2.43	0.179
B×C	0.46	0.529	0.18	0.692	5.42	0.067
B×D	0.36	0.573	0.089	0.777	0.35	0.581
C×D	2.47	0.177	2.32	0.188	10.52	**0.022**

Tables 13 and 14 show that the influence of the cutting speed and feed rate are significant upon the surface roughness while, the machining force is significantly affected by the feed rate, hole diameter and by the interaction between the material thickness and the hole diameter and also, the interaction between the feed rate & hole diameter. The upper and lower delamination factors are significantly affected by feed rate, while the difference between upper and lower diameter is affected by feed rate and interaction between feed rate and hole diameter. The table also shows that effect of non of the input parameters is significant on the tensile strength.

Figures 24 - 27show in graphical form, the effects of influential parameters upon surface roughness, machining force, delamination factor at upper & lower surface and the difference between upper & lower diameter respectively.

Figure 24 indicates that the surface roughness of the wall of hole is increased as the feed rate is increased and decreased as the cutting speed is increased. The effect of

altering the feed rate on the surface roughness has been more dominant than that of the cutting speed as indicated in the previous statistical analyses. This is expected, since the feed rate influences the mechanisms of chip formation is largely determines the value of surface roughness. Moreover, the deterioration in the surface roughness at higher feed rate could be attributed to the increased strain rate on the composite material, which promotes excessive fractures on glass fibers and epoxy matrix. Actually, the values of surface roughness during milling process can also be influenced by many factors. These are the range of tool wear, tool geometry like tool concavity and relief angles as well as the vibrations or chatter [77]. While the increase in the cutting speed resulting in improving the surface roughness. This is due to the reduction in the material deformation at the tool-chip interface through the cutting process. In summary, in order to obtain a best surface finishing, it is required to used a high cutting speed and low feed rate [20].

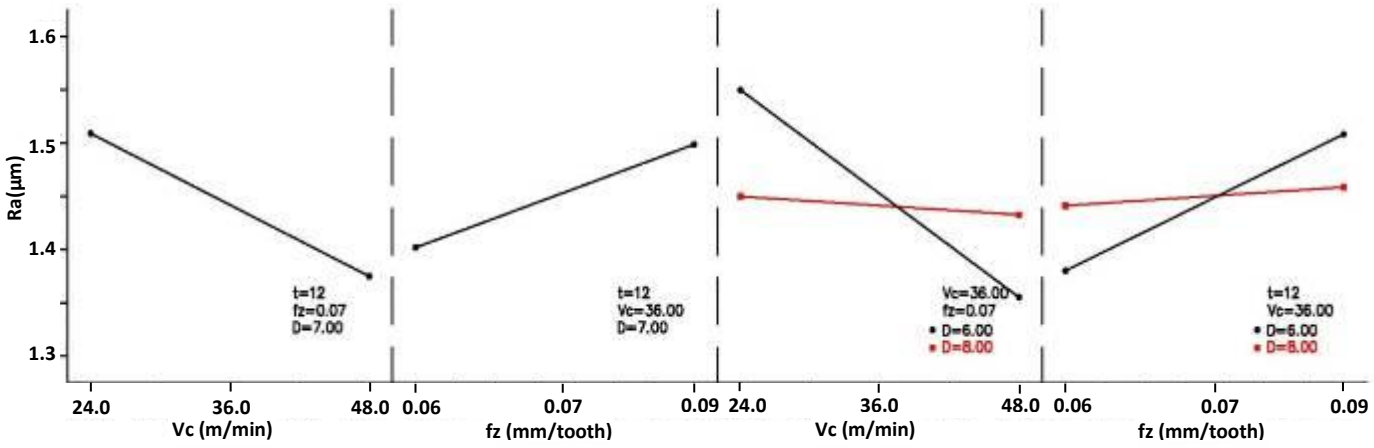

(a) (b) (c) (d)

Figure 24: Factorial plots showing the effects of: (a) cutting speed; (b) feed rate; (c) interaction between cutting speed and nominal hole diameter; and (d) interaction between feed rate and nominal hole diameter upon surface roughness in milling process.

Figure 25, indicates that the machining force in the work piece decreases with the increase of cutting speed and when the feed rate is raised, the cutting resistance grows as well [24]. The increase in the feed rate will cause increase in the load upon the drill, leading to an increase in the machining force upon the work piece [18].

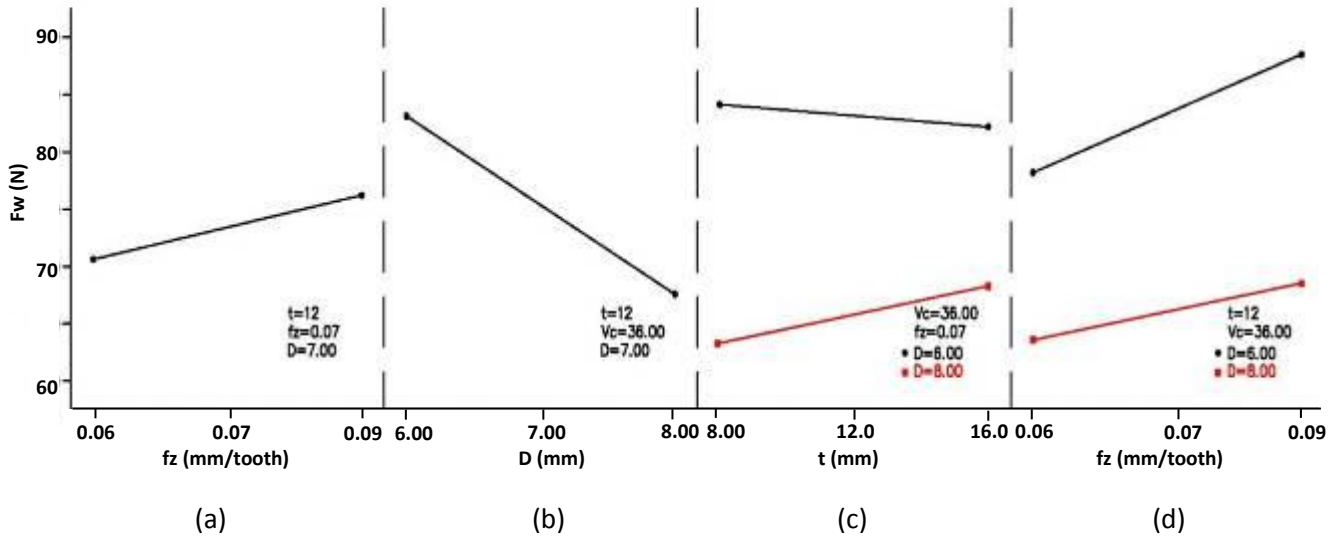

Figure 25: Factorial plots showing the effects of: (a) feed rate; (b) nominal hole diameter; (c) interaction between material thickness and nominal hole diameter; and (d) interaction between feed rate and nominal hole diameter upon machining force in milling process.

Graphs (a & b) in figure 26 show that the delamination is increased at the upper & lower surfaces as the feed rate is increased. This is due to the debonding and fiber breakage that takes place at high feed rate.

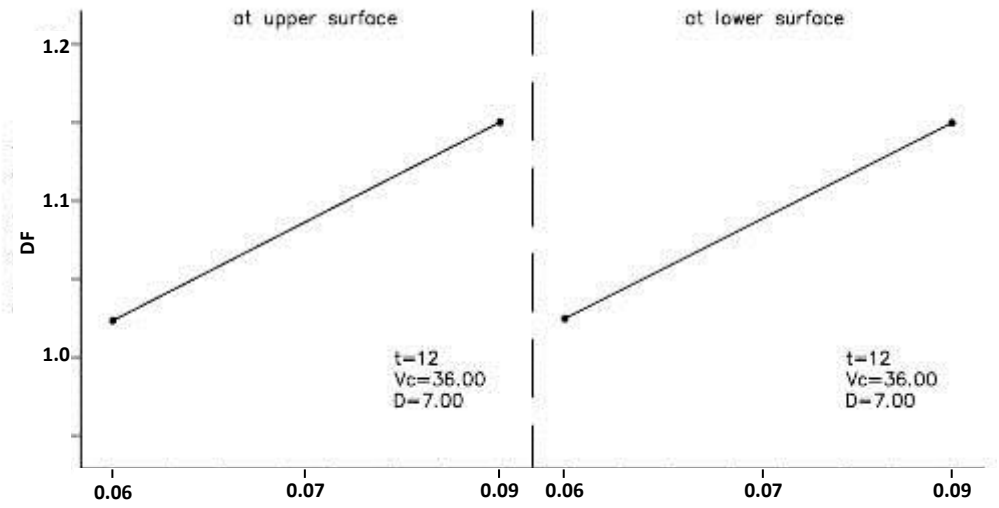

(a) (b)

Figure 26: Factorial plots showing the effects of: (a) feed rate at upper surface; and (b) feed rate at lower surface upon delamination factor at upper & lower surfaces in milling process.

It is clear from figure 27 (a, b & c) that the difference between the upper and lower diameter is increased as the feed rate and nominal hole diameter increased. The increase in the feed rate result in the increase of the upper and lower surface delamination around the hole and consequently increase in the dimensions of the hole diameter [79]. By increasing feed rate, the chip load is increased, which in turn increases vibration and/or chatter. The induced vibrations cause increase in the difference.

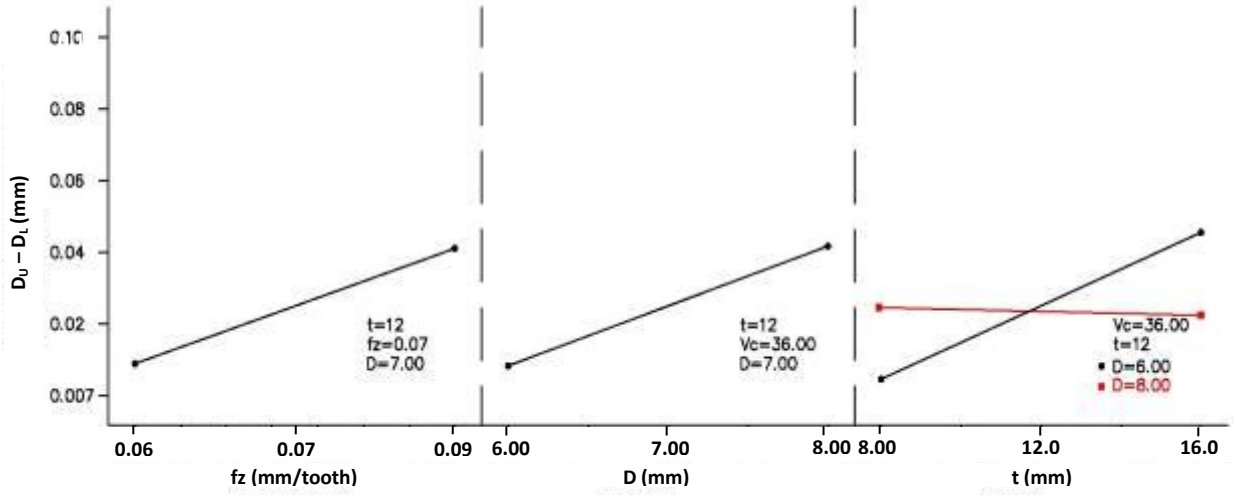

(a) (b) (c)

Figure 27: Factorial plots showing the effects of: (a) feed rate; (b) nominal hole diameter; (c) interaction between material thickness and nominal hole diameter upon difference between upper & lower diameter in milling process.

4.3.3 Analysis of the Results for AWJM Process

Tables 15 and 16 offer the results of ANOVA accomplished upon the data

concerning the response variables for group 1 and 2 of AWJM process respectively.

Table 15: ANOVA for Ra; O.O.R; D_U-D_L; and T.S for group 1 of AWJM process

Source	R_a		O.O.R		D_U-D_L		T.S	
	F-value	**P- value**	**F-value**	**P- value**	**F-value**	**P- value**	**F-value**	**P- value**
Model	9.90	**0.0001**	1.74	0.1417	3.88	**0.0053**	6.12	0.0004
A-(D)	22.12	**0.0002**	1.50	0.2391	4.51	0.0497	0.58	0.4580
B-(t)	19.91	**0.0004**	0.75	0.3991	3.22	0.0918	4.25	0.0558
C-(V_C)	1.17	0.2964	0.36	0.5553	1.73	0.2067	2.08	0.1685
D-(ρ)	75.81	**0.0001**	0.24	0.6319	0.38	0.5447	57.44	**0.0001**
E- (AF)	5.99	**0.0264**	9.08	**0.0083**	19.15	**0.0005**	5.22	**0.0364**
A×B	0.025	0.8758	1.21	0.2869	3.36	0.0855	0.49	0.4926
A×C	4.381×10^{-3}	0.9480	0.064	0.8034	0.56	0.4651	0.75	0.3987
A×D	8.18	**0.0113**	2.30	0.1492	0.048	0.8295	1.45	0.2463
A×E	1.13	0.3037	0.54	0.4712	1.769×10^{-3}	0.9670	0.84	0.3739
B×C	0.38	0.5457	0.81	0.3804	3.01	0.1019	0.35	0.5625
B×D	0.42	0.5258	4.58×10^{-3}	0.9468	4.68	**0.0459**	3.87	0.0669
B×E	8.93	**0.0087**	4.41	0.0520	12.06	**0.0031**	8.43	**0.0104**
C×D	0.023	0.8814	0.46	0.506	2.944×10^{-3}	0.9574	0.26	0.6168
C×E	1.68	0.2154	3.80	0.0689	0.63	0.4392	0.78	0.3896
D×E	2.78	0.1148	0.54	0.4712	4.89	**0.0419**	5.06	**0.0390**

The columns F-value and p-value in table 15, propose that the influences of the hole diameter, thickness of material, fiber density, abrasive flow rate and the interaction between material thickness and abrasive flow rate are significant factors upon the arithmetic surface roughness. The table shows also that the abrasive flow rate is a significant factor on out of roundness. Moreover, it is also clear from table 15 that abrasive flow rate, interaction between the material thickness and cutting feed, interaction between material thickness and fiber density, and interaction between fiber density and abrasive flow rate are influential factors upon the difference between the upper and lower diameter. Finally, the analysis shows also that the fiber density; abrasive flow rate, interaction between material thickness and abrasive flow rate, interaction between fiber density and abrasive flow rate have significant effects on the structure's tensile strength.

Table 16: ANOVA for Ra, O.O.R, D_U-D_L; and T.S for group 2 of AWJM process

Source	R_a		O.O.R		D_U-D_L		T.S	
	F-value	**P- value**	**F-value**	**P- value**	**F-value**	**P- value**	**F-value**	**P- value**
Model	4.62	**0.0021**	2.03	0.0863	4.12	**0.0038**	2.75	**0.0263**
A-(D)	55.81	**0.0001**	0.13	0.7208	0.51	0.4871	1.02	0.3282
B-(t)	5.979	0.9393	11.5	**0.0037**	11.07	**0.0043**	17.73	**0.0007**
C-(V_C)	0.11	0.7476	0.45	0.5129	3.07	0.0990	2.24	0.1543
D-(P)	0.38	0.5449	2.48	0.1345	12.41	**0.0028**	3.59	0.0763
E- (Sod)	8.32	**0.0108**	4.71	**0.0455**	3.89	0.0663	1.33	0.2657
A×B	0.10	0.7540	1.21	0.2875	2.30	0.1492	0.24	0.6295
A×C	1.29	0.2728	2.32	0.1474	0.010	0.9210	0.079	0.7825
A×D	0.010	0.9215	0.052	0.8217	1.40	0.2543	1.29	0.2720
A×E	1.18	0.2943	0.12	0.7340	9.88	**0.0063**	0.65	0.4320
B×C	0.13	0.7270	3.34	0.0863	7.59	**0.0141**	1.61	0.2231
B×D	0.13	0.7186	0.061	0.8080	5.21	**0.0365**	5.69	**0.0297**
B×E	1.50	0.2389	0.81	0.3801	0.21	0.6496	1.63	0.2197
C×D	0.050	0.8253	1.21	0.2875	2.71	0.1195	0.073	0.7906
C×E	0.030	0.8643	0.71	0.4134	0.77	0.3944	3.24	0.0907
D×E	0.21	0.6504	1.29	0.2726	0.86	0.3675	0.88	0.3610

The columns F-value and p-value in table 16, which show the identification of significant input parameters in-group 2 of AWJM process, suggest that the effects of material thickness and standoff distance are significant upon out of roundness. Whereas the influential factors for the difference in hole diameter are thickness , jet pressure , interaction between hole diameter and stand- off distance, interaction between thickness and feed and interaction between thickness and jet pressure.

Figures 28 - 31 show, in graphical forms, the effects of influential parameters upon surface roughness for group 1 of AWJM process.

It is clear from graphs a, b and c of figure28 that surface roughness increases with increasing hole diameter, thickness of GFRP material and fiber density. Increasing the fiber density means there is a larger quantity of the fiber in GFRP material that could be pulled out, which in turn, lead to higher roughness on the cut surface. As the

material thickness increases, the speed of the jet along the thickness decreases, which, results in the gradual decrease in the average kinetic energy of the abrasive particles result in lessening of the capability of material removal [71]. This also lead to greater disruption in the plies and the fibers to be pulled out, which in turn, produces higher surface roughness [72]. It was also found that increase the fiber density of the material result in a rougher surface. This is due to the effect of compression load that has been used through the production of glass/epoxy laminates. When the compression load increases, the amount of voids are easily squeezed out along with the flow of matrix [73]. Thus, machining of the composite laminate which has a higher fiber density look forward to produce a better surface finish due to the lack of void areas and uneven surfaces but in the present study, different results were obtained and this may be due to the insufficient pressing loads used in the production of the utilized material. Graph (d) shows that the roughness is increased with the increase of the abrasive flow rate. The increase in the abrasive flow rate means increase the amount of the particles involved in the mixing lead to the increase the inter-collision of the particles among themselves, causing a loss of kinetic energy and hence, the roughness increases consequentially. The interaction between thickness of GFRP material and the flow rate of the abrasives, also the interaction between the hole diameter and the fiber density indicated that these factors have significant effects upon the surface roughness as shown in graphs (e and f) of figure 28.

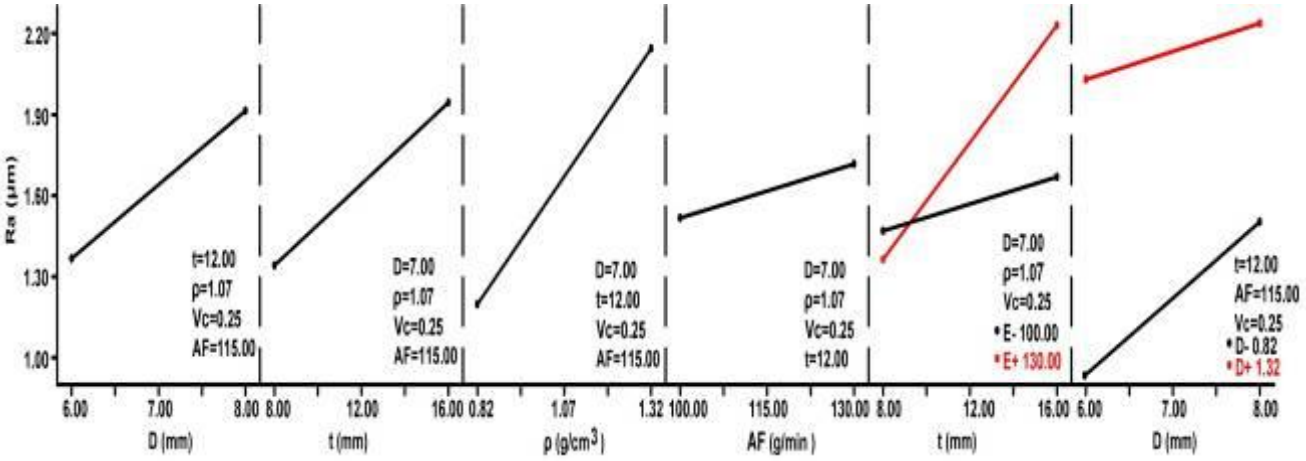

(a) (b) (c) (d) (e) (f)

Figure 28: Factorial plots showing the effects of: (a) Hole diameter; (b) Material thickness; (c) Fiber density; (d) Abrasive flow rate; (e) interaction between material thickness and abrasive flow rate; and (f) interaction between hole diameter and fiber density upon arithmetic surface roughness (Ra) for group 1 of AWJM process.

It is obvious from figure 29 that the increase in the flow rate of the abrasives causes increases in the out of roundness of hole diameter. This is because the increase in the count of the abrasive particles results in the increase of the inter-collision of particles among themselves and hence causes a loss of kinetic energy. The lack of the jet kinetic energy result in a greater waviness in the cut profile and. This phenomenon leads to increase in the O.O.R. [72].

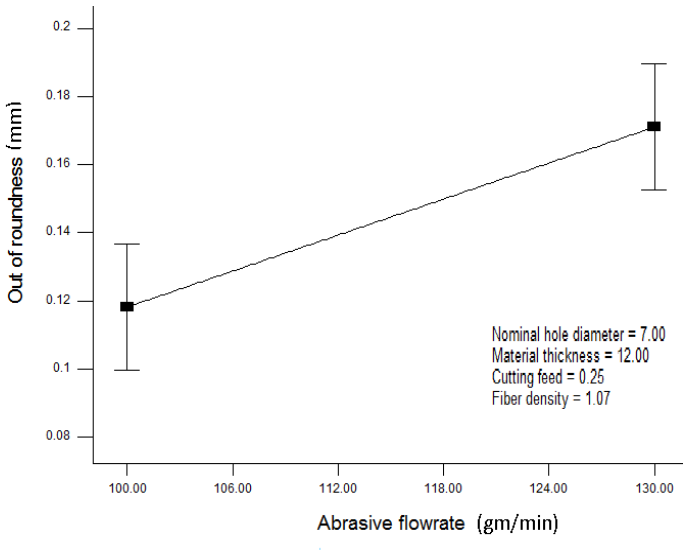

Figure 29: Factorial plot showing the effect of abrasive flow rate upon out of roundness (O.O.R) for group1 of AWJM process.

Graphs a & b of figure 30, show that the difference between the upper and lower diameter is increased as the hole diameter is increased while, it decreases with the increased of the of GFRP thickness. It was noticed after a through cut, a nearly tapered hole is produced at the top surface being wider than the bottom surface. This is in agreement with the results obtained by Khan and Haque [74]. As it was explained by Khan and Haque [74], in their study concerning the effect of various abrasive materials during the AWJM of glass fiber reinforced, the use of harder abrasive material such as silicon carbide and aluminum oxide resulted in retaining its cutting capability. Consequently, the surface of cuts became smoother. It is realized from graphs (c, d & e) that the abrasive flow rate has strong effect on the difference between upper and lower diameter.

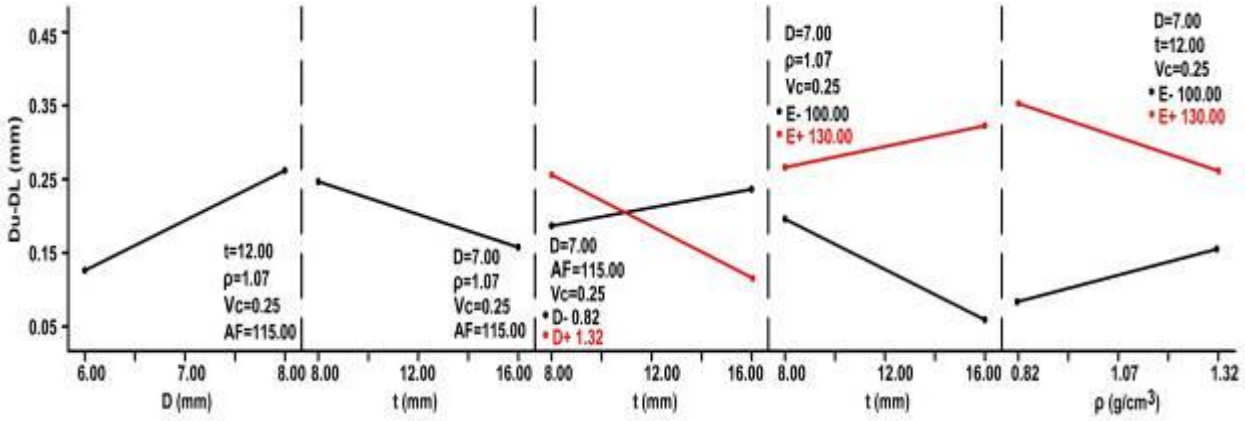

(a) **(b)** **(c)** **(d)** **(e)**

Figure 30: Factorial plots showing the effects of: (a) Hole diameter; (b) Material thickness; (c) interaction between material thickness and abrasive flow rate; (d) interaction between material thickness and abrasive flow rate; and (f) interaction between fiber density and abrasive flow rate upon difference between upper and lower diameter (Du-D_F) for group 1 of AWJM process.

Graphs a and b in figure 31 show that strength of GFRP material increase as the fiber density is increased. The increase in fiber density of GFRP material means increase the amount of fiber per cubic centimeter of GFRP, which result in increase the strength of material. Graph (b) shows that when the abrasive flow rate is increased, the jet can cut through the laminate easily. As a result, a large amount of fiber material will be removed. This phenomenon increased the reduction in the tensile strength of the GFRP composite.

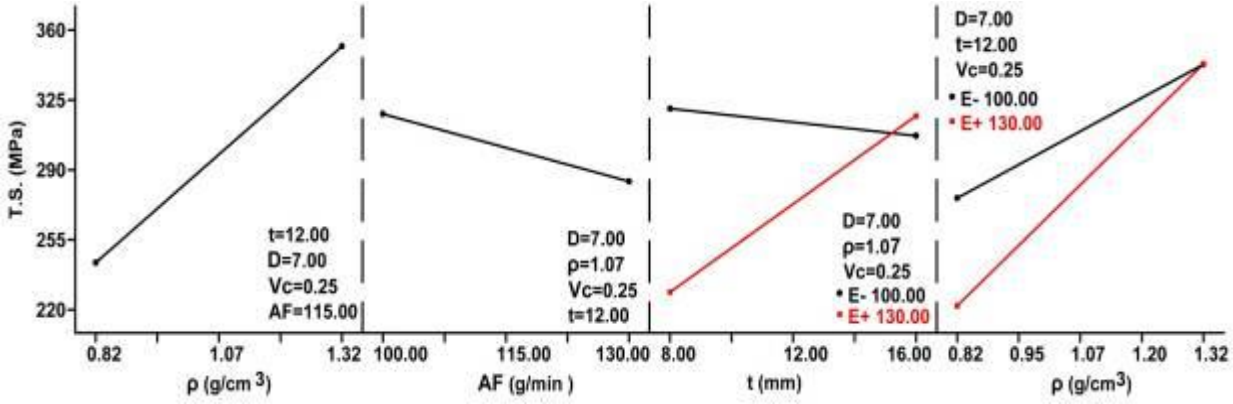

(a) **(b)** **(c)** **(d)**

Figure 31: Factorial plots showing the effects of: (a) Fiber density; (b) Abrasive flow rate; (c) interaction between material thickness and abrasive flow rate; and (d) interaction between fiber density and abrasive flow rate upon the tensile strength for group 1 of AWJM process.

Figures 32, 33, 34 and 35 show, in graphical form, the effects of influential parameters upon surface roughness, out of roundness, difference between upper and lower diameter and tensile strength, respectively, for group 2 of AWJM process.

Graph (a) in figure 32 has the same explanation as in graph (a) of figure 28 graph (b) shows that when the standoff distance(The distance from the tope surface of the work piece to the tip of the nozzle) is increased, it gives more chance for the jet to expand before impingement which may increase vulnerability to external drag from the surrounding environment. Thus, the increase in the standoff distance result in the increased of jet diameter as the cutting is initiated and in turn, reduces the kinetic energy density of the jet at impingement. Consequently, the surface roughness will be increased as illustrated in figure 32(b). Therefore, it is eligible to use a lower standoff distance to produce a smooth surface.

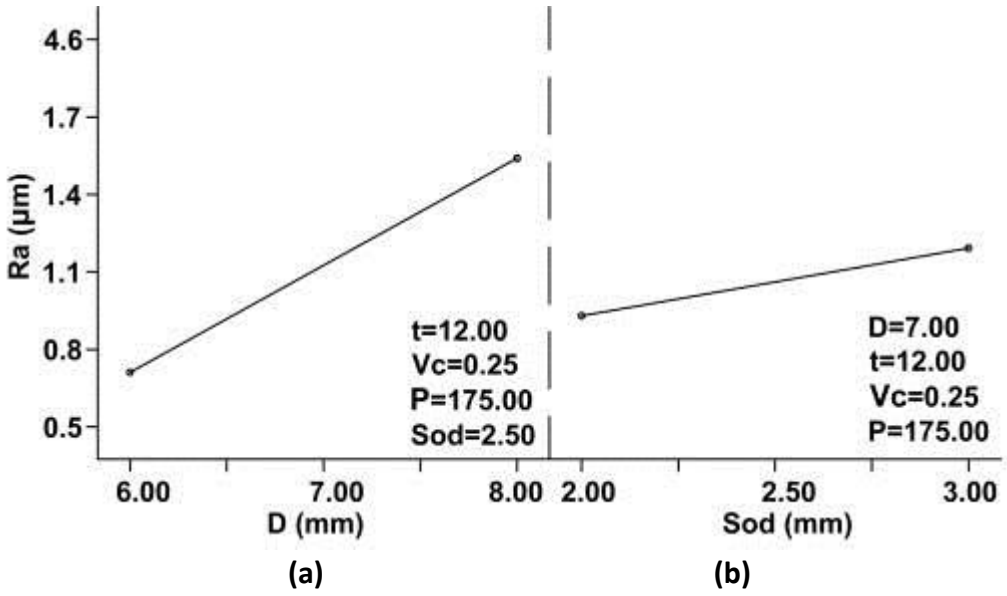

Figure 32 Factorial plots showing the effects of: (a) hole diameter; and (b) standoff distance upon surface roughness for group 2 of AWJM process.

It is clear from graph (a) of figure 33 that as cutting feed of abrasive water jet is increased the dimensional accuracy in term of out of roundness of the cutting surface is improved. This is dependent on the amount of the kinetic energy absorbed by the work piece due to the hydrodynamic friction of abrasive water jet [33]. The theory of fluid mechanics indicates that the prime factor in the hydro abrasive cutting process is the water stream velocity. The stream velocity strongly depends on: the jet pressure, diameter of the diamond orifice and the diameter of the focusing tube. Therefore, the surface quality gets better as the jet pressure is increased and the orifice diameter is decreased. This is because, the abrasive water jet disposes with higher energy concentrated to smaller area of the workpiece [33]. While graph (b) shows that by increasing the standoff distance the out of roundness is increased. This is because the surface of the material is subjected to the downstream of the jet. At the downstream, the jet starts to diverge losing its coherence herewith reducing the effective cutting area will directly affects the kerfs taper profile [28].

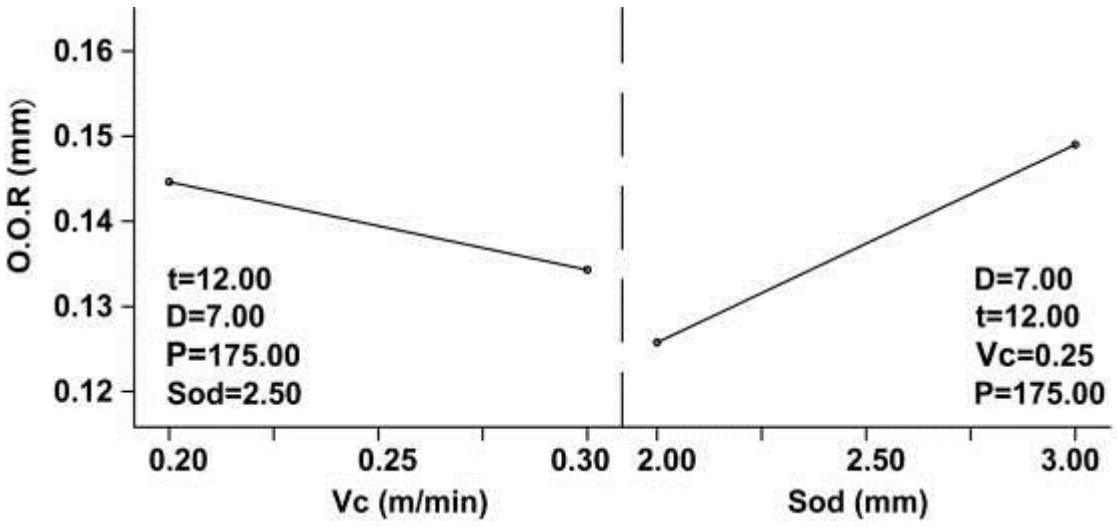

(a) **(b)**

Figure 33: Factorial plots showing the effects of: (a) cutting feed; and (b) standoff distance upon out of roundness for group 2 of AWJM process.

Graphs (a , b, c, d and e) in figure 34 show that the difference between the upper and lower diameters is increased as the material thickness to be cut decreases or water jet pressure increases. This is because the geometry of the taper is depending upon the shape of the jet, which is not similar to the shape of a fixed geometry tool. In fact, due to the hydrodynamic characteristics of the jet, its geometry is significantly influenced by the jet pressure, cutting feed and the standoff distance. In AWJ cutting process, the water jet hits the work piece at the upper erosion base, where erosion process begins [33]. Moreover, when the jet pressure is increased, the kinetic energy of the jet is increased which result in a high momentum of the abrasive particles, generating a wider-bottom kerf, leading to the decrease in the kerf taper angle [28]. And as a result the difference between upper and lower hole diameter is increased.

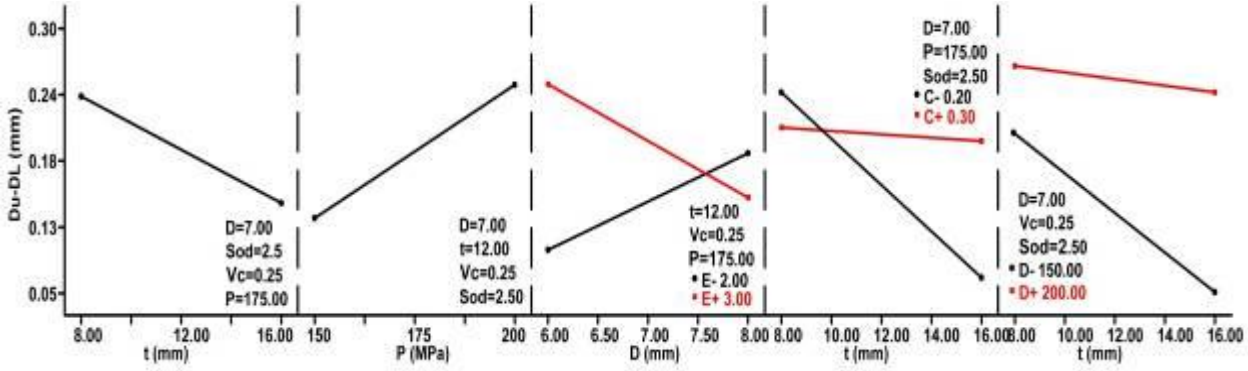

(a) **(b)** **(c)** **(d)** **(e)**

Figure 34: Factorial plots showing the effects of: (a) material thickness; (b) water jet pressure; (c) interaction between nominal hole diameter and standoff distance; (d) interaction between material thickness and cutting feed; and (e) interaction between material thickness and water jet pressure upon difference between upper and lower diameter for group 2 of AWJM process.

Graph (a) in figure 35 shows that the specimen thickness and the interaction between specimen thickness and jet pressure are significant factors upon the strength of the composite material.

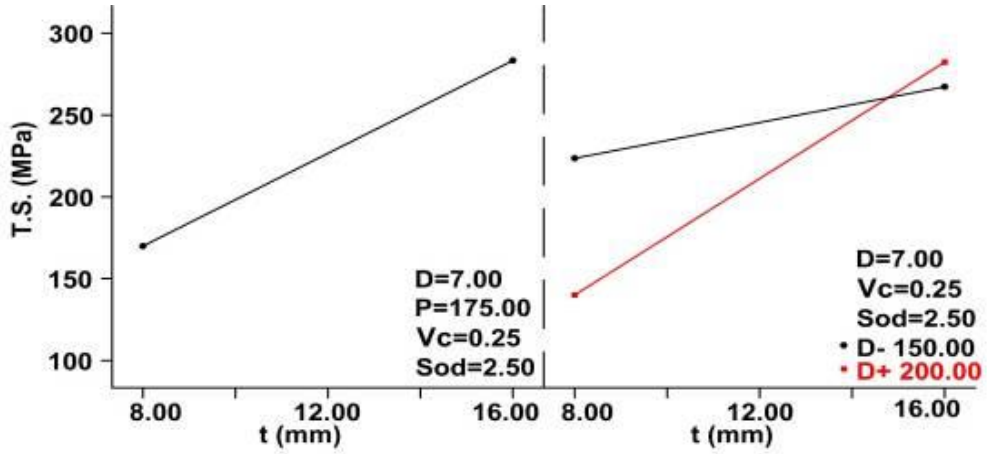

(a) **(b)**

Figure 35: Factorial plots showing the effects of: (a) material thickness; and (b) interaction between material thickness and water jet pressure on tensile strength for group 2 of AWJM process.

4.3.4 Results Analysis for LBM Process

Tables 17 and 18 offer ANOVA results accomplished on the data concerning the experiments for the group 1 and 2 respectively using LBM process.

Table 17: ANOVA for Ra; O.O.R; D_U-D_L; and T.S for group 1 of LBM process

Source	R_a		O.O.R		D_U-D_L		T.S	
	F-value	**P- value**	**F-value**	**P- value**	**F-value**	**P- value**	**F-value**	**P- value**
Model	3.35	**0.0108**	4.63	**0.0021**	3.8	**0.0079**	1.31	0.2974
A-(D)	1.33	0.2659	14.24	**0.0017**	0.40	0.5344	0.21	0.6521
B-(t)	6.43	**0.0220**	11.95	**0.0032**	0.39	0.5419	1.30	0.2705
C-(V_C)	12.51	**0.0027**	0.052	0.8224	1.20	0.2904	1.00	0.3323
D- ρ)	0.62	0.4438	19.88	**0.0004**	13.62	**0.0020**	6.74	**0.0195**
E- (V)	16.50	**0.0009**	10.46	**0.0052**	0.12	0.7359	1.06	0.3186
A×B	2.410	0.9615	0.60	0.4510	16.49	**0.0009**	0.62	0.4426
A×C	0.39	0.5399	0.024	0.8796	0.070	0.7943	5.17	**0.0371**
A×D	0.43	0.5191	4.37	0.0529	4.02	0.0622	0.13	0.7249
A×E	0.022	0.8837	2.46	0.1360	0.027	0.8713	0.62	0.4441
B×C	0.81	0.3802	1.07	0.3206	0.096	0.7602	1.45	0.2459
B×D	2.55	0.1300	1.05	0.3158	15.08	**0.0013**	0.90	0.3567
B×E	4.24	0.0562	0.34	0.5667	0.99	0.3351	0.39	0.5425
C×D	4.26	0.0556	0.93	0.3484	0.39	0.5397	2.29×10^{-3}	0.9624
C×E	0.20	0.6622	7.67×10^{-4}	0.9786	0.79	0.3870	0.013	0.9089
D×E	1.751	0.9671	1.95	0.1817	0.038	0.8472	0.084	0.7754

The columns F-value and p-value in table 17, which show the identification of significant input parameters of group 1 of LBM process, suggest that the effects of material thickness, cutting feed, assist gas flow rate are significant on arithmetic surface roughness. The table shows also that hole diameter, thickness of GFRP, fiber density, and assist gas flow rate are influential factors on out of roundness. Moreover, the effects of fiber density, interaction between hole diameter and thickness of GFRP, and also interaction between material thickness and fiber density are significant on the difference between upper and lower diameter. Finally, the analysis shows also that the fiber density, interaction between hole diameter and cutting feed are significant on tensile strength.

Table 18: ANOVA for Ra; O.O.R; D_U-D_L; and T.S for group 2 of LBM process

Source	R_a		O.O.R		D_U-D_L		T.S	
	F-value	**P- value**	**F-value**	**P- value**	**F-value**	**P- value**	**F-value**	**P- value**
Model	8.09	**0.0001**	1.76	0.1371	1.22	0.3498	5.14	**0.0012**
A-(D)	0.49	0.4921	0.46	0.5088	0.028	0.8689	0.46	0.5081
B-(t)	10.28	**0.0055**	6.18	**0.0244**	1.72	0.2079	0.052	0.8228
C-(V_C)	27.62	**0.0001**	1.45	0.2464	3.56	0.0776	0.22	0.6462
D-(LP)	0.79	0.3873	4.76	**0.0445**	0.40	0.5346	63.54	**0.0001**
E- (Sod)	69.27	**0.0001**	1.82	0.1962	0.29	0.5991	1.00	0.3333
A×B	1.36	0.2605	9.81	0.0064	2.45	0.1373	0.020	0.8904
A×C	2.38	0.1424	0.19	0.6707	0.52	0.4829	2.02	0.1742
A×D	1.67	0.2152	0.22	0.6457	0.22	0.6490	0.81	0.3814
A×E	3.538×10^{-4}	0.9852	5.666×10^{-4}	0.9409	1.72	0.2081	1.32	0.2680
B×C	2.17	0.1599	0.82	0.3777	0.91	0.3551	3.859×10^{-4}	0.9951
B×D	0.51	0.4848	0.028	0.8699	1.42	0.2500	1.85	0.1927
B×E	0.88	0.3632	0.12	0.7345	2.04	0.1720	0.11	0.7428
C×D	1.16	0.2965	0.25	0.6215	1.10	0.3105	0.24	0.6314
C×E	0.15	0.6992	0.060	0.8093	1.79	0.1992	4.62	**0.0472**
D×E	2.57	0.1282	0.19	0.6654	0.091	0.7667	0.80	0.3855

The columns F-value and p-value in table 18, which show the identification of significant input parameters of group 2 of LBM process, suggest that the effect of material thickness, cutting feed, stand- off distance are significant on surface roughness of the hole. Whereas the significant factors on the out of roundness are the thickness of the material and the power of laser beam. The table shows also that there are no significant factors on the difference between upper and lower diameter. Finally, the analysis shows that the significant factors on the tensile strength are the laser power and the interaction between cutting feed and standoff distance.

Figures 36, 37, 38 and 39 show, in graphical form, the effects of influential parameters on surface roughness, out of roundness, and tensile strength respectively, for group (1) of LBM process. It is clear from the graphs (a, b and c) in Fig.36 that each of the factors has a valuable effect on the roughness of the hole surface. It was

found that the roughness is proportionate to the specimen thickness and cutting speed. This is because, as the thickness of the specimen is increased; the depth of the cut is increased and there will be a large amount of material burn through cut that in turn results in high roughness, this in agreement together with the result reported by [82]. While, with increasing cutting speed, there is not enough time available for an adequate melt and flow of molten plastic, this phenomenon causes generation of a rough cut hole surface, which is in a good agreement for the result reported by [75].While graph (c) shows improvement in the surface roughness with the increases in the assist gas flow rate. This is because the assistant gas supply a force to dismiss the melt from the cut zone and cools the cut zone by forced convection. The ineffectual removal of the molten layer can result in deterioration of the cut quality. The main task of the assist gas in the laser cutting of composites is mechanical removal of the byproducts from the cutting zone [36]. When the gas is reactive, it also transmit an additional exothermic energy to assist in machining. Hence, the efficiency and overall quality of the laser machining is highly dependent upon the interaction of the gas jet with the specimen material [80].

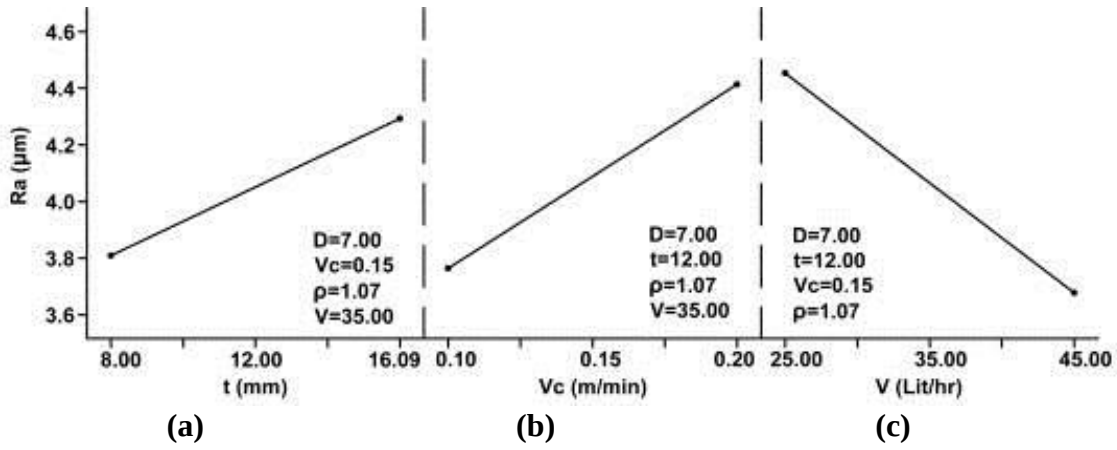

Figure 36: Factorial plots showing the effects of: (a) thickness of GFRP; (b) cutting feed; and (c) assist.gas flow rate upon surface roughness for group 1 of LBM process.

The deviation in hole diameter (out of roundness) is increased with increase in the hole diameter and material thickness as shown in graphs a and b of figure 37. This is because during cutting process, the temperature of the laser beam is very high and vaporizes more material by widening the kerf width as the hole diameter increase. Increasing the specimen thickness owing to longer interaction time and more heat is conducted into the material with deterioration of the achievable cut quality [36]. In graphs c and d, out of roundness of hole diameter is decreases as the fiber density and gas flow rate increased. This is due to the large differences between the thermal properties of resin matrix and glass fibers. The energy required to evaporate the glass is also very high compared to the matrix. Therefore, the laser power requirements is highly dependent on the fibers used, their volume fraction, and not on the matrix. However, too high a laser power may vaporize or chemically degrade the polymer matrix, which is, reflects on the cut surface profile [36].

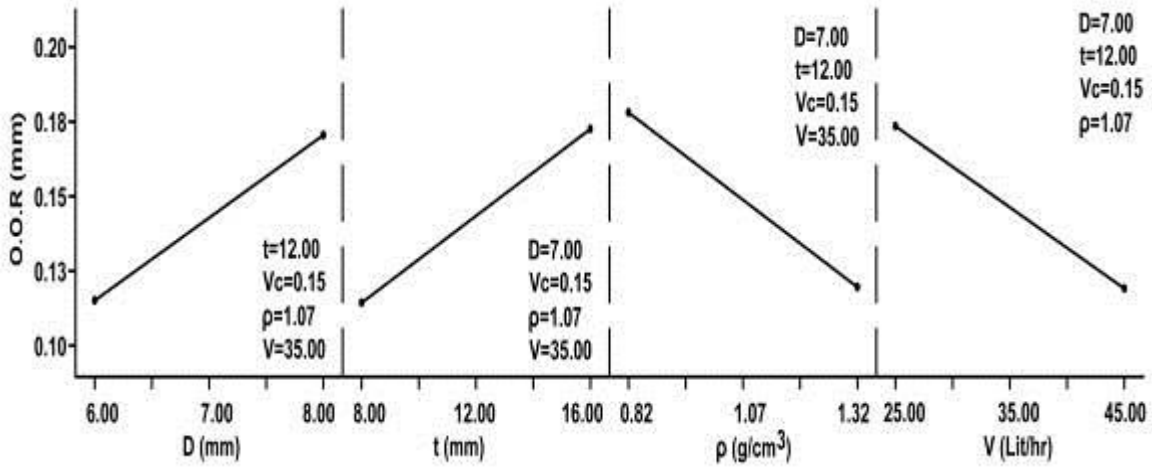

(a) **(b)** **(c)** **(d)**

Figure 37: Factorial plots showing the effects of: (a) hole diameter; (b) thickness of GFRP; (c) fiber density; and (d) assist.gas flow rate upon out of roundness for group 1 of LBM process.

Figure 38 shows that the difference between upper and lower diameter of the hole is increased as the fiber density in GFRP material (graph a) increases. The laser beam process used to cut the glass fibers would cause the epoxy resin to decompose and

melt resulting in a flow of the fibers within the resin causing charring and tearing in the resin layer. Then, the slope of the cut surface tends to decrease resulting in the difference between upper and lower diameter [1].

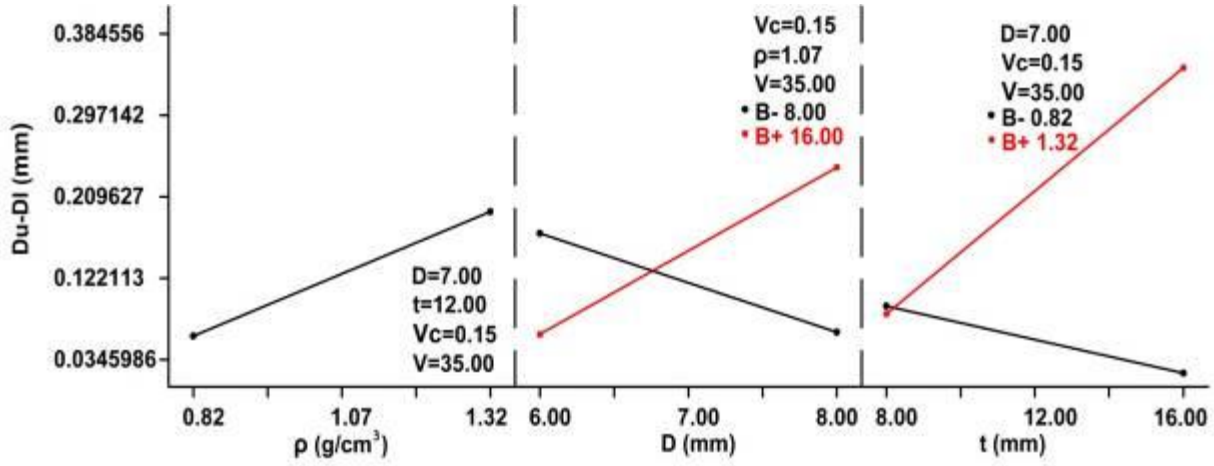

(a) **(b)** **(c)**

Figure 38: Factorial plots showing the effects of: (a) fiber density; (b) interaction between hole diameter and material thickness; and (c) interaction between material thickness and fiber density upon the difference between upper and lower diameter for group 1 of LBM process.

Figure 39 (a and b) shows that the strength of the hole sample of the GFRP material increases at high level of fiber density and hole diameter. Glass fibers are stronger than the epoxy, so if a composite contains higher content of glass, it is understandably expected to possess higher strength.

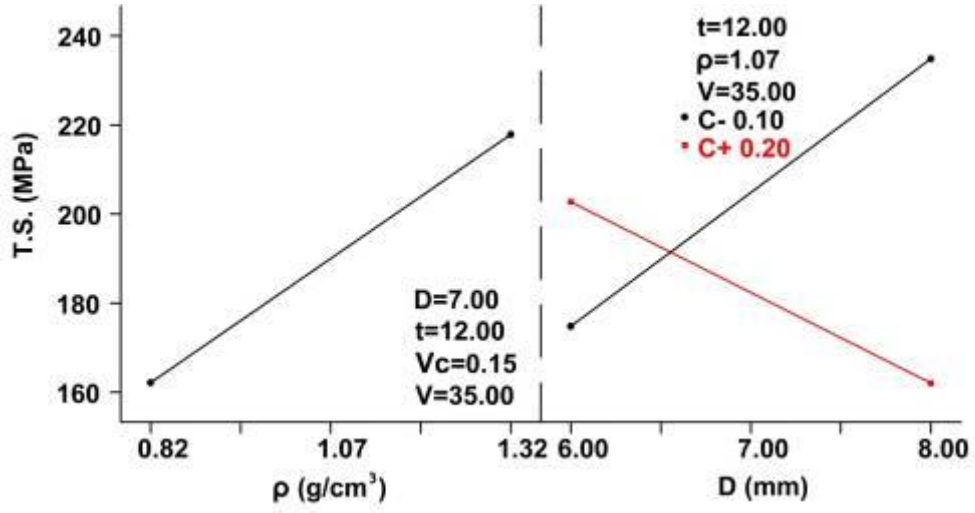

(a) **(b)**

Figure 39: Factorial plots showing the effects of (a) fiber density; and (b) interaction between hole diameter and cutting feed upon the tensile strength for group 1 of LBM process.

Figures. 40 - 42 show, in graphical form, the effects of influential parameters upon surface roughness, out of roundness, and tensile strength, respectively, for group (2) of LBM process.

As it was indicated in figure 36, it is again clear from graphs a and b of figure 40 that the roughness of the hole surface is increased as thickness of the specimen and the cutting speed is increased. It can be noticed from graph (c) in figure 40 that the standoff distance has significant effect on surface roughness. Increasing the standoff distance means the surface of the specimen will expose to the down flame of the laser beam. At the down flame, the beam starts to splay losing its cohesive herewith reducing the energy intensity of the beam that directly minimize the removal capability of the gas jet and lead to a poor surface finish [81].

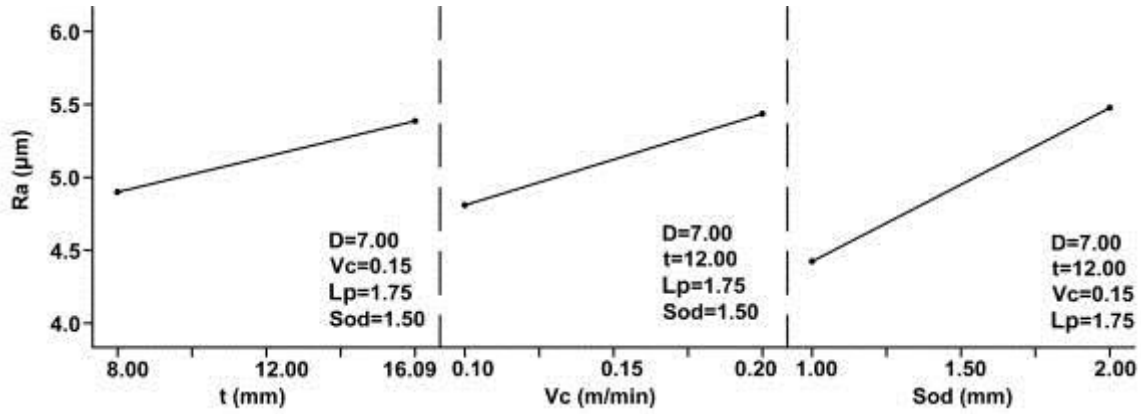

(a) **(b)** **(c)**

Figure 40: Factorial plots showing the effects of: (a) material thickness; (b) cutting feed; and (c) Standoff distance upon the surface roughness for group 2 of LBM process.

It is clear from figure 41 (a and b), that increase in material thickness and laser power leads to increase in cut path deviation around the hole diameter. The quality of cut surface depends upon the interaction time between the laser beam and the material. The value of damage depends upon the thickness of the sample. Therefore, the thinner sample has minimum damage value and the thicker sample lead to longer interaction time and result in more surface damage.

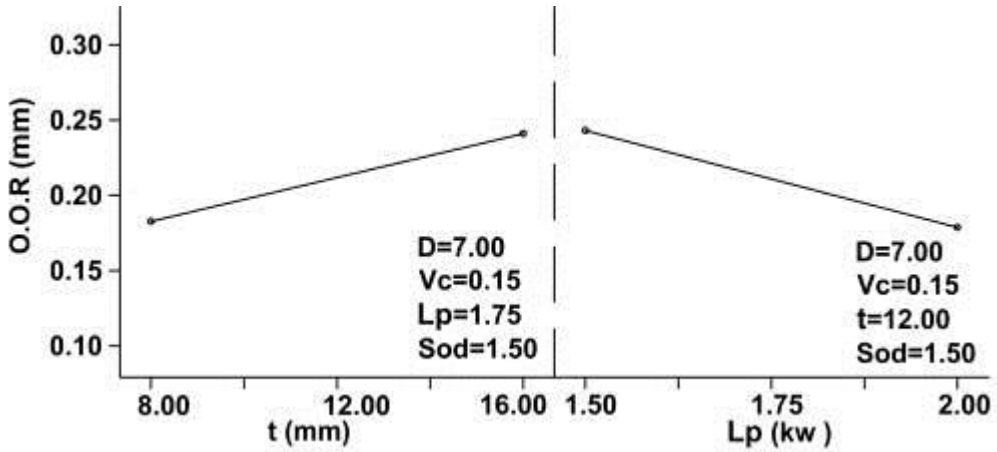

(a) **(b)**

Figure 41: Factorial plots showing the effects of: (a) material thickness; and (b) laser power upon out of roundness for group 2 of LBM process.

Finally, graph (a) in figure 42 shows that the strength of the composite decreased as the laser power is increased. When the laser power is increase, the heat affected zone (HAZ) is increased and a large volume of fibers in the composite is vaporized, causing a change in the thermal properties of the material lead to the reduction in the strength of the composite [36].

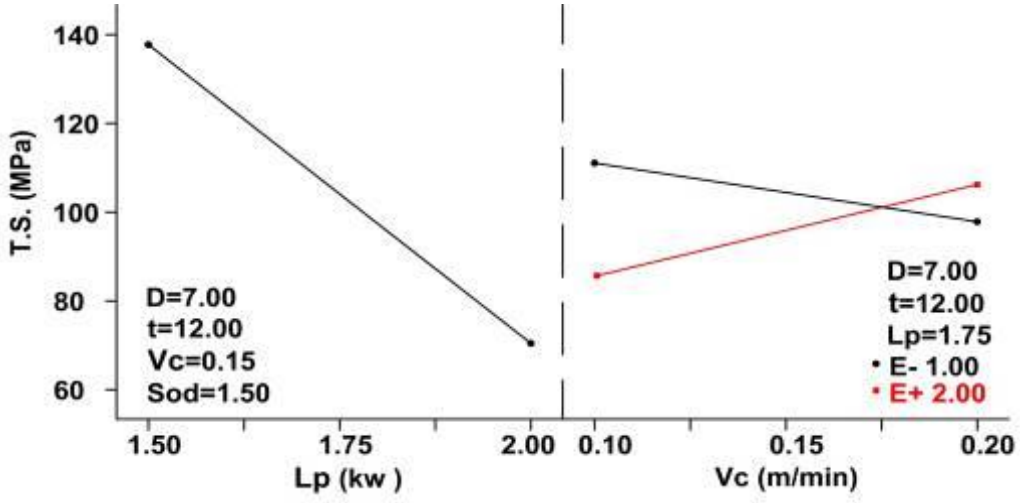

(a) **(b)**

Figure 42: Factorial plots showing the effects of: (a) laser power; and (b) interaction between cutting feed and standoff distance on tensile strength for group 2 of LBM process.

Chapter 5

OPTIMIZATION OF THE PROCESSES

Drilling, milling, AWJM and LBM cutting processes are widely used in various manufacturing industries. These technologies have many overlapping applications. Thus, it is useful for the industry to know these processes in order to select the optimum settings in different conditions. The comprehensive knowledge on the cut quality, dimensional accuracy, cost and productivity will help the users of these operations on the choice of the best machining process. Therefore, it is better to find the best cutting conditions through which then the desirable quality, productivity and cost saving of cutting can be obtained. The numerical optimization has been performed using Derringer-Suich multi-criteria decision modeling approach. In Derringer-Suich, multi-criteria optimization technique different desirability functions are assigned to maximization / minimization of different response parameters (variables). Commercial statistical software called Design-Expert® is used for this purpose [76].

5.1 Numerical Optimization of Drilling and Milling Processes

The goal of the numerical optimization in a hole making by drilling & milling can be any of the following targets:

1. Minimize the average arithmetic surface roughness along the depth of cutting hole (R_a).

2. Minimize the average arithmetic surface roughness (R_a) and minimize the cost per hole, simultaneously.
3. Minimize the average arithmetic surface roughness (R_a) and maximize productivity (Pr), simultaneously.
4. Minimize the average arithmetic surface roughness (R_a) and minimize the thrust force (F_z) or the machining force (F_w), simultaneously.
5. Minimize the difference between upper and lower diameter (DU-DL).
6. Minimize the thrust force (F_z) or the machining force(F_w).
7. Minimize delamination at upper & lower surfaces;
8. Minimize the cost (C) and Maximize productivity (Pr).

Tables 19 & 20 present the optimized values (within the tested ranges) of the control variables for various objectives. The last pillar in the tables shows the real results of the confirmation tests accomplished against each optimized parameters. The two tables show also that low surface roughness can be obtained using high levels of cutting speed and low levels of feed rate because, the high level of feed rate causes increase in the chatter and produces incomplete machining which lead to a higher surface roughness. The tables show also that the minimum values of the difference between upper and lower diameter and the minimum values of damage at the upper and lower surface of the hole can be obtained using the low levels of the cutting speed and feed rate. Finally, minimum cost and maximum production of holes per minutes can be obtained if the high levels of cutting speed and feed rate are employed. Confirmatory experiments were carried out with the optimum cutting parameters. It was shown that the experimental values are close to the predicted values of the objectives and thus the optimization method is reliable and valuable.

Table 19: Predictions and Experimental results against each set of objective in drilling process

No	Objectives	Fixed Parameters		Optimized Parameters		Comparison	
		t (mm)	D (mm)	Vc (m/min)	f_z (mm/rev)	Predicted values	Experimental values
1	Minimize (R_a)	12	7	48	0.06	1.26 μm	1.21 μm
2	Minimize(R_a) & Minimize (C)					1.26 μm 0.075 USD	1.21 μm 0.07 USD
3	Minimize (R_a) & Minimize (F_z)					1.26 μ_m 78.22N	1.21 μm 86.4N
4	Minimum (R_a)& Maximize (Pr)	12	7	48	0.07	1.38 μm 14.5 hole/min	1.32 μm 14.5 hole/min
5	Minimize (Du-D_L)	12	7	24	0.06	0.058 mm	0.045 mm
6	Minimize (F_z)					76.32 N	81.2 N
7	Minimize (DFu & DF_L)					0.66 0.76	0.62 0.78
8	Minimize (C) & Maximize (Pr)	12	7	48	0.09	0.075 USD 14.5 hole/min	Not applicable

Table 20: Predictions and Experimental results against each set of objective in milling process

No	Objectives	Fixed Parameters		Optimized Parameters		Comparison	
		t (mm)	D (mm)	Vc (m/min)	f_z (mm/tooth)	Predicted values	Experimental values
1	Minimum (R_a)	12	7	48	0.06	1.05 μm	1.16 μm
2	Minimum (R_a) & Minimize (C)					1.05 μm 0.07 USD	1.16 μm 0.07 USD
3	Minimum (R_a) & Minimize (F_w)					1.05 μm 53.86 N	1.16 μm 53.86 N
4	Minimum (R_a)& Maximize (Pr)	12	7	48	0.07	1.12 μm 12.6 hole/min	1.18 μm 12.6 hole/min
5	Minimize (D_U-D_L)	12	7	24	0.06	0.006 mm	0.01 mm
6	Minimize (F_w)	12	7	48	0.06	53.86 N	68.5 N
7	Minimize(DF u&DF_L)	12	7	24	0.06	0.81 0.85	0.77 0.86
8	Minimize C & maximize (Pr)	12	7	48	0.08	0.07 USD 13.42 hole/min	Not applicable

5.2 Numerical Optimization of AWJM and LBM Processes

The AWJM and LBM processes are commonly used in the manufacturing industry. Using these two cutting technologies, the quality of the cut surfaces is highly dependent on the appropriate choice of machining parameters. Surface roughness, out of roundness, difference between upper and lower diameter, cost, tensile strength and the productivity play a predominant role in determining the machining accuracy. Therefore, it is better to find the best cutting conditions which then the desirable quality, productivity or cost saving of the cutting can be obtained. Optimization criteria can be assigned to find the optimum cutting conditions. Hence, six optimization criteria have been introduced for each of the two cutting technologies (AWJM and LBM) as in tables 21 and 22, namely:

1. Minimize the average arithmetic surface roughness along the depth of cutting hole (R_a).
2. Minimize the average arithmetic surface roughness (R_a) and minimize the cost per hole, simultaneously.
3. Minimize the average arithmetic surface roughness (R_a) and Maximize the productivity (Pr) (Maximize Number of holes/min), simultaneously.
4. Minimize average arithmetic surface roughness (R_a) and Maximize tensile strength (T.S), simultaneously.
5. Minimize the difference between upper & lower diameter (DU-DL) and Minimize out of roundness (O.O.R), simultaneously.
6. Minimize Cost(C) and Maximize Productivity (Pr) , simultaneously.

Tables 21 and 22 present the optimized values (within the tested ranges) of the predictor variables for various objectives in AWJM and LBM technologies. Last columns of the tables show the actual results of the confirmation experiments performed against each optimized combination.

Table 21 shows that minimum values of surface roughness, cost of operation, out of roundness, difference between upper and lower diameters, and maximum values of productivity and structural strength, in AWJM, can be achieved by cutting at high levels of cutting feed and low setting of jet pressure and stand-off distance. Table 22 shows that minimum values of surface roughness in LBM can be achieved by cutting at low levels of cutting feed, stand of distance and laser power. Moreover, cutting at high levels of cutting feed, assist gas flow rate and low levels of stand of distance, laser power can be used to obtain simultaneously, minimum surface roughness with minimum cost of operation, minimum surface roughness with maximum productivity. In addition, the table shows that minimum of surface roughness with maximum of strength can be obtained using low levels of cutting feed, standoff distance, laser power and high levels of assist gas flow rate. Minimum value of difference between upper and lower diameter simultaneously with minimum value in out of roundness can be obtained using high levels of cutting feed, assist gas flow rate, laser power and low levels of standoff distance. Finally, minimum operation cost together with maximum productivity in LBM can be obtained using high values of cutting feed, assist gas flow rate and low levels of laser power and standoff distance.

Table 21: Predictions and Experimental results against each set of objective in AWJ process

No	Objectives	Fixed parameters		Optimized Parameters					Predicted values	Experimental values
		D (mm)	t (mm)	V_C (m/min)	ρ (gm/cm3)	AF (gm/min)	P (MPa)	Sod (mm)		
1	Min.(R_a)	7	12	0.3	0.82	100	150	2	0.85 μm	0.97 μm
2	Min.(R_a) & Min. C/hole								0.85 μm 0.05 USD	1.16 μm 0.05 USD
3	Min.(R_a)&Max. holes/min								0.85 μm 8.67 holes/min	1.16 μm 8.67 holes/min
4	Min.(R_a) & Max.T.S.								0.85 μm 283.04 MPa	1.16 μm 299 MPa
5	Min. Du-D_F and Min. O.O.R			0.2					0.11 mm 0.12 mm	0.13 mm 0.1 mm
6	Min. C/hole & Max.holes/min			0.3					0.05 USD 8.67 holes/min	Not applicable

Table 22: Predictions and Experimental results against each set of objective in LBM process

No	Objectives	Fixed parameters		Optimized Parameters					Predicted values	Experimental values
		D (mm)	t (mm)	V_C (m/min)	ρ (gm/cm3)	V (Lit/hr)	L.P (kW)	Sod (mm)		
1	Min.(R_a)	7	12	0.1	0.82 1.32	45	1.5	1	3.1 μm 3.6 μm	2.836 μm
2	Min.(R_a) & Min. C/hole			0.2	1.32				3.8 μm 0.11USD	3.39 μm 0.11USD
3	Min.(R_a)&Max. holes/min								3.84 μm 6.3 holes/min	4.32 μm 6.3 holes/min
4	Min.(R_a) & Max.T.S.			0.1					3.6 μm 247.58 MPa	3.88 μm 262.4 MPa
5	Min. Du-D_F and Min. O.O.R			0.2	0.88		2		0.06 mm 0.13mm	0.08 mm 0.11 mm
6	Min. C/hole & Max.holes/min				1.32		1.5		0.11 USD 6.3 holes/min	Not applicable

Abrasive water jet and lasers processes are widely used machining processes especially for those difficult-to-cut materials such as composite materials, in various industrial applications, due to their advantages over the conventional cutting processes. The main advantages of laser cutting are: no tool wear or vibration as it is a non-contact process, low heat input, which results in less distortion and its capability to be numerically controlled [86].

The experimental results show that, better quality of final cutting wall (minimum surface roughness and out of roundness), higher tensile strength, minimum cost operation per hole, higher productivity (No. of holes per min.) and a little bit higher difference between upper and lower diameter, were achieved by the use of AWJ technology over LBM for comparable working conditions.

AWJM can produce clean and good quality cut surfaces. Consequently, AWJ cutting process is a viable and alternative technology for polymer matrix composite processing with good cut quality and productivity.

Chapter 6

DISCUSSIONS AND CONCLUSIONS

As mentioned previously, woven laminated GFRP composite, which is used in many industrial applications was machined by drilling, milling, AWJM and LBM processes. The aim was to investigate the effects and select the optimal values of predicted variables to obtain high quality of the cut holes surface (minimum wall roughness, minimum deviation in the cutting profile (out of roundness), minimum difference between the upper and lower diameter, high tensile strength, low operation cost and high productivity. The quality of the cut holes is characterized by its dimensional accuracy and surface texture such as surface roughness. The dimensional accuracy of a part is of critical importance in the manufacturing industry, especially for precision assembly operation. In the manufacturing process, the designed part will be presented in a drawing with all dimensions normally given within a certain range of tolerances. The tolerance defines the limits of induced deviation for which allowance should be made in the design, and within which actual size is acceptable. Surface roughness affects corrosion, fatigue life, friction and wear and tear of manufacturing parts [38]. The quality of the cut holes can be critical to the life of the riveted joints for which the holes are used. Aspects of the hole such as waviness/roughness of its wall surface, axial straightness and roundness of the hole cross-section can cause high stresses on the rivet, leading to its failure [41] . Several hole machining processes, including drilling, milling, laser-beam and abrasive water-jet, etc., have been proposed for a variety of economic and quality reasons. In order

to describe the machining results a qualitative assessment is necessary of those features, which define the machining quality.

6.1 Effect of the Predicted Parameters on the Cut Quality and Dimensional Accuracy in Drilling and Milling Cutting Processes

It can be noticed from the table 5 that minimum thrust force which is equal to 57.8 N and minimum surface roughness which is 1.208 μm is obtained by using high level of cutting speed and low level of feed rate. Minimum thrust force will lead to minimum delamination damage around the hole surface [83], The presence of delamination around the cut hole surface in the GFRP will reduce the strength against fatigue, results in a poor assembly tolerance and affects the composites structures integrity [84]. Therefore, minimizing the thrust force will increase the composite performance on the count of life of the joints such as bolts and rivets [63]. The surface roughness was improved by increasing the cutting speed. This behavior was due to the decreasing of thrust force with increasing cutting speed [41]. The improvements in the surface roughness of the hole wall result in improve the dimensions and accuracy of the holes. The decreasing in thrust force with increasing cutting speed was due to the increase of the generated heat that assisted by the low coefficient of thermal conduction and low transition temperature of plastics. The accumulated heat stagnates around tool edge and destroys the matrix stability behind tool edge. The destroyed matrix reduces the resistance forces developed on the lips and the moment of the resistance force. Also the accumulated heat around tool edge leads to softening the polymer matrix, where the softener materials make as a lubricant material, which reduces the friction forces, moment of friction force on the margins and moment of the forces of friction of the chip on the drill and on the

machined surface, the reduction of thrust force causes improve in the surface roughness [6]. When the feed rises, the cutting resistance grows as well. From the practical point of view, smaller values of feed are better as far as tool life is concerned. On the other hand, this causes the process to be more time consuming (minimum production) and the process becomes expensive (high cost) [24]. Table 6 shows the same observation concerning the machining force, surface roughness, cost per hole and productivity in using milling process. The effect of changing feed rate on R_a has been more significant than that of the spindle speed and depth of cut as indicated in the statistical analyses, since feed rate influences mechanisms of chip formation, which will largely determine the value of R_a. Furthermore, deterioration in surface roughness at higher feed rate could be attributed to the increase strain rate on the composite material, which promotes excessive fractures on glass fibers and epoxy matrix [77]. A sample of microscopic pictures for the holes cut by drilling and milling processes can be seen in figures 43 and 44, respectively. Graphs a and b of the figure 43, represent the upper and lower surfaces optical picture of exp. no.16 (table no. 5) cut by drilling process. It can be shown from this figure that, BC1 represents the cut hole diameter while BC2 represents the diameter that includes the defects in upper and lower surfaces, respectively. The difference between BC1 (graph a) and BC1 (graph b) which represents the difference between upper and lower hole diameter is equal to 0.131 mm, while the difference between upper and lower hole diameter, which was cut by milling process as shown in graphs a and b of figure 44, is equal to 0.027 mm.This observation is clear with all comparison between the drilling and milling experiments. It means that the difference between upper and lower hole diameter in the case of milling process is lesser than that in the case of drilling process. This is because; in milling process, the increase in tool wear

is minimal due to reducing the spindle speed [77] and the resulting process forces will be directed toward the center of the work piece at both the entry and the exit side-using standard milling tool [48]. The milling cutter is made of cemented carbide, which has high strength and wear resistance.

6.2 Effect of the Predicted Variables on the Surface Roughness in AWJM and LBM Processes

It is obvious from tables 7 and 8 that in AWJM process, the minimum value of the hole surface roughness which is equal to 0.402 μm, is obtained by using the low settings of water jet pressure and the standoff distance. Tables 9 and 10 indicate that in LBM process, the minimum value of hole surface roughness which is equal to 2.730 μm was obtained by using the low settings of cutting speed, laser power and standoff distance. This means that using high setting values of machining parameters in LBM process will give a higher value of surface roughness rather than using AWJM process. During LBM process, the GFRP composite will be burned through cut. By increasing the cutting speed and laser power, there is not enough time available for an adequate melt and flow of molten plastic, this phenomenon causes generation of a rough cut hole surface [75].

6.3 Effect of the Predicted Variables on the Difference Between Upper and Lower Diameters in AWJM and LBM Processes

For all the holes which have been cut by AWJM and LBM processes, a microscopic analysis was used to measure the dimensional accuracy including the difference between upper and lower diameters and the out of roundness in the hole diameter. The microscopic analysis was also used to measure the difference between upper and

lower hole diameter. A sample of microscopic pictures for the holes cutting by AWJM and LBM processes can be shown in figures 45 and 46, respectively. Graphs a and b of figure 45 represent the upper and lower surfaces optical picture of experiment no.32 (table no.7) cut by AWJM process. It can be seen from the figure that BC1 represents the cut hole diameter while BC2 represents the diameter that includes the defects in both upper and lower surfaces respectively. The difference between BC1 (graph a) and BC1 (graph b) which represents the difference between upper and lower hole diameters is equal to 0.237 mm, while the difference between upper and lower hole diameters, which was cut by LBM process as shown in graphs a and b of Figure46, is equal to 0.048 mm. It means that the difference between upper and lower hole diameter in the case of LBM process is lesser than that in the case of AWJM process. This observation is clear with all comparison between the AWJM and LBM experiments. This is due to inertia experience by AWJM nozzle, as the nozzle is unable to maintain a true curved path that causes the jet to decrease in energy resulting in a very narrow cut at the bottom. This is in agreement with the phenomenon studied by Shanmugam et al. [20].

6.4 Effect of the Predicted Variables on the Out of Roundness in AWJM and LBM Processes

A microscopic analysis was used to determine the value of the deviation (out- of-roundness). To determine the deviation in the cut hole diameter (out- of-roundness),the deviation distances (L_1, L_2 and L_3) at three different points were measured from the optical microscope picture for each cut hole as shown in Figs.45 and 46, the values of L_1, L_2 and L_3 is substitute in equation 1 to find the deviation in the hole diameter. It was found that the measured value of the deviation by AWJM

process is equal to 0.196 mm while that for LBM process is 0.333mm. The high value of the out of roundness in the diameter of the cut hole by CO_2 laser is due to the high laser power action. As the power is increased, the heat gets intensified and thermal effects on the surface of the hole are increased causing thermal damage. From figure 46 (a, b), delamination is observable as a result of inadequate heat dissipation in the laser beam cutting process. A composite material is one, which contains two chemically distinct phases that are not in thermodynamic equilibrium. The properties of the two phases used in the material are usually significantly different, which makes the machining of them difficult. The laser beam has a certain power and, thus, has a defined heat input into the material. However, because of the different properties of the fiber and matrix, the two components react very differently to the thermal input. In general, the energy needed for the vaporization of the fibers is higher than that required for the matrix. When a CO2 laser is employed to cut these composites, a large volume of resin is vaporized in the process, this causes delamination and matrix recession of the composite [85]. On the other hand, some degree of delamination can also be observed (from figure 45) for GFRP cut by AWJM process but it was of very low magnitude as compared to the LBM process.

6.5 Effect of the Predicted Variables on the Tensile Strength in AWJM and LBM Processes

It is obvious from the experimental results tables (7 - 10), that the holes cut by AWJM process result in less reduction in tensile strength of GFRP as compared to LBM process. This is because AWJM technology is less influential on the material properties as it does not cause chatter, has no thermal effects, and impose minimal stresses on the work piece. In addition, the results also show that less operational cost

and high productivity are achieved by AWJM process in comparison with LBM process.

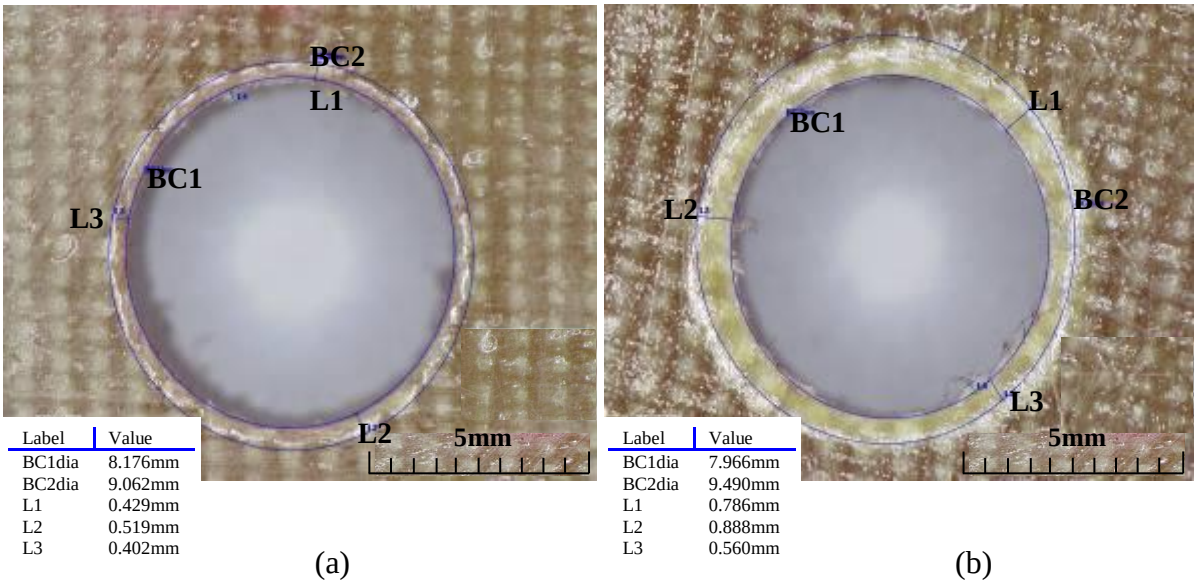

(a) (b)

Figure 43: Optical microscope pictures for hole no.16, of drilling process (a) upper hole surface (b) lower hole surface

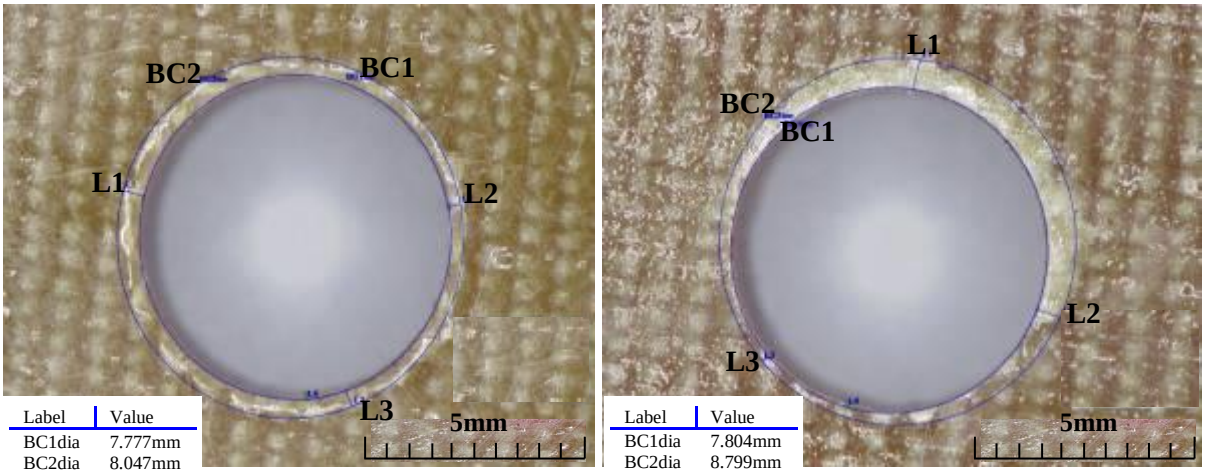

(a) (b)

Figure 44: Optical microscope pictures for hole no.16, of milling process (a) upper hole surface (b) lower hole surface

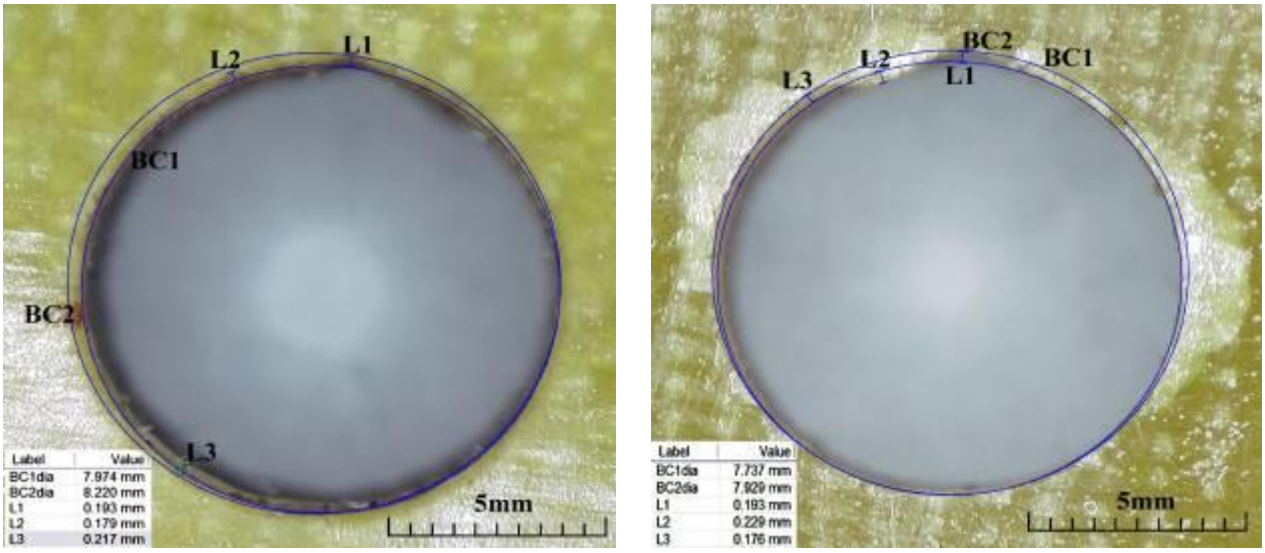

(a) **(b)**

Figure 45: Optical microscope pictures for hole no.32, group 2 of AWJM process (a) upper hole surface (b) lower hole surface

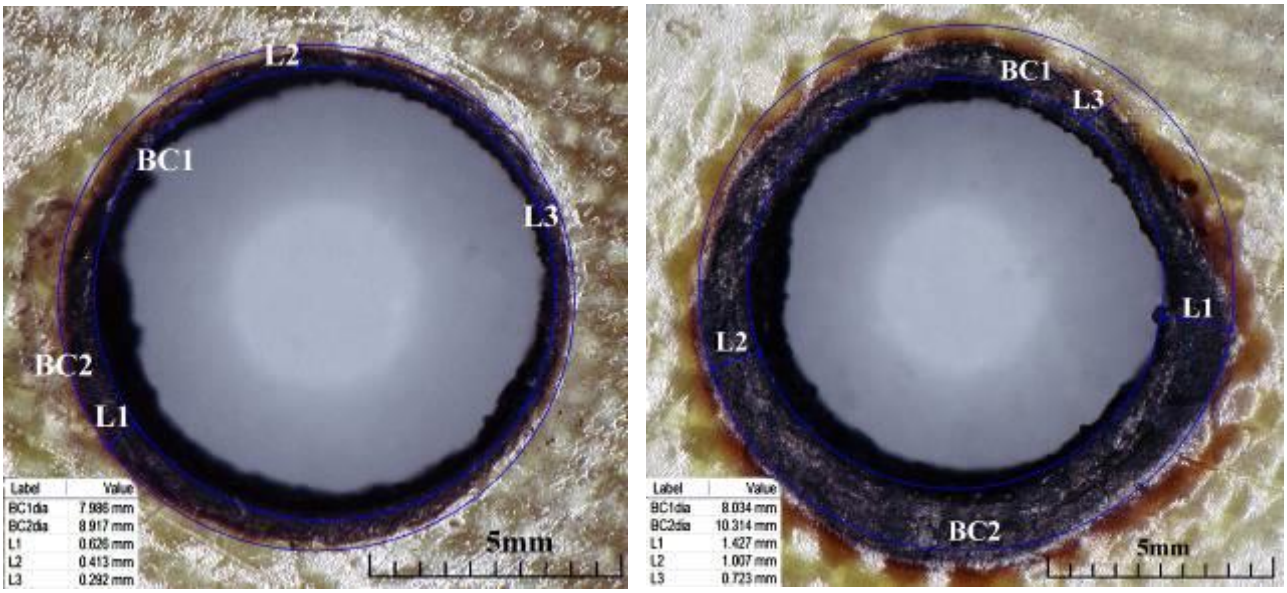

(a) **(b)**

Figure 46: Optical microscope pictures for hole no.32, group 2 of LBM process (a) upper hole surface (b) lower hole surface.

6.6 Conclusions

The present study is intended to provide a technical information related to the cut quality (surface roughness, deviation in hole cut profile or out of roundness and difference between upper and lower hole diameter), strength, cost and the productivity of hole making in GFRP using drilling, milling, AWJM, and LBM processes. Comprehensive statistical analyses were performed to investigate the effects of the major input cutting parameters upon the selected response parameters mentioned in previous chapters. The following conclusions can be drawn in this regard:

6.6.1 Drilling and Milling:

- In both the processes, surface roughness along the hole depth can be reduced by reducing feed rate and increasing cutting speed.
- In both the processes, delamination factor at upper and lower surfaces can be reduced by reducing the feed rate and cutting speed. In general lower spindle speed and lower feed rate can be effectively employed to have holes without delamination.
- In drilling process, the average thrust force can be reduced by reducing the cutting speed while in milling; the machining force can be reduced by reducing the feed rate.
- In drilling process, difference between upper and lower diameters can be reduced by reducing material thickness and hole diameter, while in milling, it can be reduced by reducing cutting speed and feed rate.

6.6.2 AWJM Process:

- Reducing the surface roughness of the hole can be achieved by reducing the abrasive mass flow rate and the standoff distance.

- Improving the dimensional accuracy (reducing out of roundness, difference between upper and lower diameter of the cutting hole) can be done by reducing the standoff distance
- Reducing the cost of operation and increasing the productivity can be achieved by increasing the cutting feed, standoff distance and reducing the jet pressure and abrasive mass flow rate.

6.6.3 LBM Process:

- Improvement in surface roughness of the hole can be achieved by reducing the cutting feed, laser power and standoff distance and increasing the assist. gas flow rate.
- Improving dimensional accuracy (reducing out- of- roundness) can be done by reducing cutting feed, stand- off distance and increasing laser power whereas reducing the difference in the upper & lower diameter of the cutting hole can be done by increasing cutting feed, stand of distance and decreasing laser power.
- Reducing the loss in the strength of the cutting material can be achieved by reducing the laser power, cutting feed and standoff distance.
- Reducing the cost of operation and increasing the productivity can be achieved by increasing the cutting feed, assist gas flow rate and reducing the laser beam power and standoff distance.
- Abrasive flow rate and standoff distance are more influential machining parameters in AWJM process while cutting feed, laser power, standoff distance and assist gas flow rate are more influential machining parameters in LBM process.
- The experimental results show that:

  1. Better quality of final cutting wall (minimum Ra and O.O.R)

2. Higher difference between upper and lower diameter,
3. Minimum cost operation per hole and higher productivity (No. of holes/min.)
4. Higher tensile strength. Can be obtained by the use of AWJ technology over LBM and drilling processes while better cut quality, higher tensile strength, close operation cost and less difference between upper and lower diameters can be obtained by the use of AWJM over milling process for comparable working conditions. It was concluded that AWJM cutting process is more suitable than LBM ,drilling and milling cutting processes at high level of cutting speed and low level of feed rate, when the cutting quality (minimum surface roughness and out of roundness), tensile strength , cost and productivity is of critical importance in the manufacturing industry, especially for precision assembly operation. It was shown also that experimental values are fairly close to the predicted values of the objectives and thus optimization method is valuable.

- The detailed analyses reveal that CO_2 laser beam cutting is not a viable method for cutting this type of composite material as compared to AWJM process, drilling and milling processes. This is because of the conductive nature of the composites, which increases the heat transfer to the body causing increase in the size of the HAZ. This reflects the quality of laser cutting on composite materials.
- This work is likely to prove beneficial for generating superior quality holes by drilling, milling, AWJM and LBM in GFRP composites used in different manufacturing applications.

References

[1] R. Komanduri. (1997). Machining of fiber-reinforced composites, Machining science and technology, 1(1), 113-152.

[2] Mazumdar.SK. (2002).Composites Manufacturing –Materials, Product and Process Engineering, CRC Press

[3] E. Lemma, L. Chen and E. Siores. (2002). Study of Cutting Fiber-Reinforced Composites by Using Abrasive Water-Jet with Cutting Head Oscillation. Composite Structures. 57(1-4): 297-303.

[4] Presentation by HEXCEL regarding composites and their utilizes, accessed at library.corporate-ir.net/library/75/755/75598/items/182188/hxl-020606.pdf.

[5] D. Liu, Y. Tang, W.L. Cong. (2012). A review of mechanical drilling for composite laminates. Composite Structures, 94: 1265–1279

[6] El-Sonbaty, U. Khashaba, T. Machaly. (2004). Factors affecting the machinability of GFR/epoxy composites, Composite Structures 63: 329–338

[7] Teti R. Machining of composite materials. CIRP Annals–J Man. Tech. (2002), 51:611-6 34

[8] Abrao AM, Faria PE, Campos Rubio JC, Reis P, Davim JP. (2007) Drilling of fiber reinforced plastics: a review. J Mater Process Techno, 186:1–7.

[9] A.K.Bhargava. (2005). Engineering materials polymers, ceramic and composites, 226-235.

[10] D.Hull, T.W.Clyne. (1996). An introduction to composite material. Second edition Cambridge University Press, New York, 14-47.

[11] R. K. Verma. (2011).Fuzzy rule based optimization in machining of glass fiber reinforced polymer (GFRP) composites, M.SC. Thesis.

[12] Davim JP, Reis P, Antonio CC. (2004). Experimental study of drilling glass fiber reinforced plastics (GFRP) manufactured by hand lay-up. Compos Sci Techno, 64:289–97.

[13] S. Gordon and M. T. Hillery. (2003). A review of the cutting of composite materials, Proc. Inst. Mech. Eng, J. Materials: Design and Applications, Vol. 217 Part L.

[14] E. Kilickap. (2010). Optimization of cutting parameters on delamination based on Taguchi method during drilling of GFRP composite, Expert Systems with Applications, 37: 6116–6122

[15] J. George, D.Shah, R. G. Jivani, D. Gupta. (2011). Abrasive water jet machining – a review, National Conference on Recent Trends in Engineering & Technology.

[16] DeFu Liu, YongJun Tang, W.L. Cong. (2012). A review of mechanical drilling for composite laminates, Composite Structures, 94: 1265–1279.

[17] http://www.efunda.com/processes/machining/drill.cfm.

[18] K. Palanikumar. (2011). Experimental investigation and optimization in drilling of GFRP composites, Measurement 44: 2138–2148.

[19] http://en.wikipedia.org/wiki/Drilling

[20] J. P. Davim , P. Reis , C. C. Antonio. (2004). A study on milling of glass fiber reinforced plastics manufactured by hand-lay up using statistical analysis (ANOVA), Composite Structures 64:493–500

[21] http://classes.engr.oregonstate.edu/mime/winter(2010)/ie337001/Laboratories/4a.Milling%20lab.df

[22] http://www.efunda.com/processes/machining/mill.cfm

[23] S. Jahanmir, M. Ramulu, P. Koshy. (2000). Machining of Ceramics and Composites, Marcel Dekker, Inc., New York, 267–293.

[24] Rafal Rusinek. (2010). Cutting process of composite materials: An experimental study, International Journal of Non-Linear Mechanics, 45: 458–462.

[25] J. George, D. Shah, R. G. Jivani, D. Gupta. (2011). Abrasive water jet - A review. National Conference on Recent Trends in Engineering & Technology, India

[26] V.K. Jain. (2002). Advanced (Non-traditional) Machining Processes, Allied, New Delhi.

[27] 11/304-306.

[28] M. Palleda. (2007). A study of taper angles and material removal rates of drilled holes in the abrasive water jet machining process, Journal of Materials Processing Technology189:292-

[29] D.K. Shanmugam, S.H. Masood. (2009). An investigation on kerf characteristics in abrasive waterjet cutting of layered composites, journal of materials processing technology,209: 3887–3893.

[30] J. P. M. R. Dias. (2011).The effect of velocity in abrasive water jet. Thesis, Dept.of Mechanical Engineering, Coimbra University, Setembro,

[31] Shanmugam, D. K., Wang, J., Liu, H. (2008), Minimization of kerf tapers in abrasive waterjet machining of alumina ceramics using a compensation technique, International Journal of Machine Tools & Manufacture, 48 :1527–1534.

[32] Chen F. L., Siores E., Morsi Y. and Yang W. (1997). A study of surface striation formation mechanisms applied to abrasive waterjet process, Proceedings of the CIRP, 570–575.

[33] Chao, J. and Geskin E.S. (2003). Experimental study of the striation formation and spectral analysis of the abrasive water jet generated surfaces, J of Mat. Proc. Tech, 141: 213–218.

[34] Sergej H., Stanislav F., Miroslav R.(2008).Design of experiments applied on abrasive water jet factors sensitivity identification, Nonconventional Technologies Review – no. 2

[35] http://www.nitc.ac.in/dept/me/jagadeesha/mev303/overview_of_NTM_process.pdf

[36] Fenoughty, A. Jawaid and I, R. Pashby. (1994). Machining of advanced engineering materials using traditional and laser techniques, Journal of Materials Processing 42: 391-400.

[37] A. A. Cenna, P.Mathew. (1997). Evaluation of Cut Quality of Fiber reinforced plastic, A review, Int.J.Mach.Tools Manufact, 723-736.

[38] W. Zhang, Y. Lawrence Yao. (2004). Manufacturing engineering handbook. Chapter 34, Laser materials processing. New York, 11-13.

[39] I.A.Choudhury, S.Shirley. (2010). Laser cutting of polymeric materials: An experimental investigation, Optics & Laser Technology, 42: 503–508.

[40] E. Kilickap. (2010). Optimization of cutting parameters on delamination based on Taguchi method during drilling of GFRP composite. Expert Systems with Applications, 37: 6116–6122

[41] I. El-Sonbaty, U.A. Khashaba, T. Machaly. (2004). Factors affecting the machinability of GFR/epoxy composites, Compos. Struct. , 63: 329–338.

[42] N.S. Mohana, S.M. Kulkarni, A. Ramachandra. (2007). Delamination analysis in drilling process of glass fiber reinforced plastic (GFRP) composite materials, Journal of Materials Processing Technology, 186: 265–271.

[43] M.B. Lazar, P. Xirouchakis. (2011). Experimental analysis of drilling fiber reinforced composites. International Journal of Machine Tools & Manufacture, 51: 937–946.

[44] M. Adam Khan, A. Senthil Kumar. (2011). Machinability of glass fiber reinforced plastic (GFRP) composite using alumina-based ceramic cutting tools, Journal of Manufacturing Processes, 13: 67–73.

[45] V. Krishnaraj, S. Vijayarangan, A. Ramesh Kumar. (2007). Effect of drilling parameters on mechanical strength in drilling glass fiber reinforced plastic**,** International Journal of Computer Applications in Technology, 28: 87-93.

[46] Lee E-S. (2001). Precision machining of glass fiber reinforced plastics with respect to tool characteristics. Int J Adv Manuf Techno, 17:791–798.

[47] S.A. Hussain, V. Pandurangadu, K. Palanikumar. (2010). Surface Roughness Analysis in Machining of GFRP Composites by Carbide Tool (K20), European Journal of Scientific Research, 41: 84-98.

[48] V. Schulze, C. Becke, K. Weidenmann, S. Dietrich. (2011). Machining strategies for hole making in composites with minimal work piece damage by directing the process forces inwards. Journal of Materials Processing Technology, 211: 329–338.

[49] R. Rusinek. (2010). Cutting process of composite materials: An experimental study. International Journal of Non-Linear Mechanics, 45: 458–462.

[50] M. A. Azmir, A.K. Ahsan, A. Rahmah. (2007). Investigation on abrasive water jet machining of Kevlar reinforced phenloic composite using taguchi approach, Proceedings of the International Conference on Mechanical Engineering, Dhaka, Bangladesh.

[51] D.A.Axinte, D.S.Srinivasu, M.C.Kong, P.W.Butler-Smith. (2009). Abrasive water jet cutting of polycrystalline diamond: A preliminary investigation. International Journal of Machine Tools & Manufacture, 49: 797–803.

[52] A. A. E1-Domiaty, M. A. Shabara, A. A. Abdel-Rahman, A. K. AI-Sabeeh. (1996). On the Modeling of Abrasive Water jet Cutting, Int. J. Adv. Manuf. Techno, 12: 255-265.

[53] L.M. Hlavaˇc, I.M. Hlavacˇova, L. Gembalova, J. Kalicˇinsky, S. Fabian,

J. Mˇeˇst'anek, J. Kmec, V. Madr. (2009). Experimental method for the investigation of the abrasive water jet cutting quality. Journal of Materials Processing Technology, 209: 6190–6195.

[54] J.Wang. (1999). A machinability study of polymer matrix composites using abrasive water jet cutting technology. Journal of Materials Processing Technology, 94: 30–35.

[55] A.A. Cenna, P. Mathew. (2002). Analysis and prediction of laser cutting parameters of fiber reinforced plastics (FRP) composite materials. International Journal of Machine Tools & Manufacture 42: 105–113.

[56] Z.L. Li, H.Y. Zheng, G.C. Lim, P.L. Chu, L. Li. (2010). Study on UV laser machining quality of carbon fiber reinforced composites. Composites, Part A, 41: 1403–1408.

[57] F. Caiazzo, F. Curcio, G. Daurelio, F. Minutolo. (2005). Laser cutting of different polymeric plastics (PE, PP and PC) by a CO2 laser beam, Journal of Materials Processing Technology, 159: 279–285.

[58] Ming-Fei Chen, Yu-SenHo, Wen-TseHsiao, Tse-HungWu, Shih-FengTseng, Kuo-ChengHuang. (2011). Optimized laser cutting on light guide plates using grey relational analysis, Optics and Lasers in Engineering, 49: 222–228.

[59] H.A. Eltawahni, A.G.Olabi, K.Y.Benyounis. (2011). Investigating the CO2 laser cutting parameters of MDF wood composite material, Optics & Laser Technology, 43: 648–659.

[60] D.K. Shanmugam, F.L. Chen, E. Siores, M. Brandt. (2002). Comparative study of jetting machining technologies over laser machining technology for cutting composite materials, Composite Structures, 57: 289–296.

[61] Abrao AM, Faria PE, Campos Rubio JC, Reis P, Davim JP. (2007). Drilling of fiber reinforced plastics: a review, J Mater Process Techno, 186:1–7.

[62] Mishra R, Malik J, Singh I, Davim JP. (2010). Neural network approach for estimate the residual tensile strength after drilling in uni-directional glass fiber reinforced plastic laminates, Material Design, 31:2790–5.

[63] R. Raja**,** G. Chandramohan, S. Jannet, and D. Alexander. (2012). Delamination Analysis in Drilling of Glass Fiber Reinforced Plastics (GFRP) by Special Drill Bits, European Journal of Scientific Research, 83:121-128.

[64] D. Abdul B, S. Basavarajappa, M. Prasanna Kumar, Ajith G. J. (2011). Influence of fiber volume reinforcement in drilling GFRP laminates, Journal of Engineering Science and Technology, 6:733 – 744.

[65] www.devileye.net/laser cutting composite materials. Laser cutting of composite materials.

[66] Hashish M. (1991). Characteristics of surfaces machined with abrasive water jets. J.Eng Mater Techno, 113:354–362.

[67] Hashish M. (1992). On the modeling of surface waviness produced by abrasive-water jets. In: Proceedings of the 11th International Symposium on Jet Cutting Technology, Kent, Washington, 17–34.

[68] Hashish M. (1991). Characteristics of surfaces machined with abrasive water jets. JEng Mater Techno, 113:354–62.

[69] Hashish M. (1984). A modeling study of metal cutting with abrasive water jets. J.Eng. Mater Techno, 106:88–100.

[70] El-Domiaty AA, Abdel-Rahman AA. (1997). Fracture mechanics-based model of abrasive water jet cutting for brittle materials, J.Advance Manufact Techno, 13:172–81

[71] Janet Folkes. (2009). Water jet—An innovative tool for manufacturing. Journal of Materials Processing Technology, 209: 6181–6189

[72] M.A. Azmir, A.K. Ahsan. (2009). A study of abrasive water jet machining process on glass/epoxy composite laminate, Journal of Materials Processing Technology, 209: 6168–6173.

[73] M.A. Azmir, A.K. Ahsan. (2008). Investigation on glass/epoxy composite surfaces machined by abrasive water jet machining, journal of materials processing technology, 198:122–128

[74] Khan, A.A., Haque, M.M. (2007). Performance of different abrasive materials during abrasive water jet machining of glass, J. Mater. Process. Techno, 191: 404–407.

[75] Davim JP, Oliveira C, Barricas N, Conceicão M. (2008). Evaluation of cutting quality of PMMA using CO2 lasers, Int. J. Advance Manuf Techno, 35:875–879.

[76] G. Derringer, R. Suich. (1980). Simultaneous optimization of several response variables, Journal of Quality Technology, 12: 214–219

[77] A. I. Azmi & R. J. T. Lin & D. Bhattacharyya. (2012). Machinability study of glass fiber reinforced polymer composites during end milling, Int. J. Adv. Manuf Technol.

[78] A. Iqbal, N. Udar, G. Hussain. (2011). Optimization of Abrasive Water Jet Cutting of Ductile Materials, Journal of Wuhan University of Technology-Mater. Sci. Ed. Vol.26 No.1

[79] P.Praven Raj, A. Elaya Perumal and P.Ramu. (2012). Prediction of Surface roughness and Delamination in End Milling of GFRP Using Mathematical Model and ANN, Indian Journal of Engineering and Material Sciences, 19:107-120

[80] K.Chen, Y.Lawrence and V.Modi. (2000). Gas Jet Workpiece Interaction in Laser Machining, J. of Manufacturing and Engineering, 122:429.

[81] Hassan Abdel Gawad EL-Hofy. Advanced Machining Processes, McGraw-Hills, Digital Engineering Library

[82] M. Zeleňák, J. Valíček, J. Klich, P. Židková. (2012). Comparison of Surface Roughness Quality Created By Abrasive Water Jet and CO2 Laser Beam Cutting, Tehnički vjesnik, 19:481-485

[83] H. Hocheng, C.C. Tsao. (2003). Comprehensive analysis of delamination in drilling of composite materials with various drill bits, Journal of Materials Processing Technology, 140: 335–339.

[84] V. Krishnaraj, S. Vijayarangan, G.Suresh. (2005). An Investigation on high speed drilling of glass fiber reinforced plastic (GFRP), Indian J.of Engineering and Sciences,12: 189-195

[85] A.A. Cenna, P. Mathew. (1997). Evaluation of Cut Quality of Fiber – Reinforced Plastics- A Review, Int. J. Much. Tools Manfact.37: 723-736.

[86] H.A. Eltawahni, A.G.Olabi, K.Y.Benyounis. (2010). Effect of process parameters and optimization of CO2 laser cutting of ultra high-performance polyethylene, Materials and Design 31: 4029–4038.

APPENDICES

Appendix A: Hole Distributions on the GFRP Work Pieces

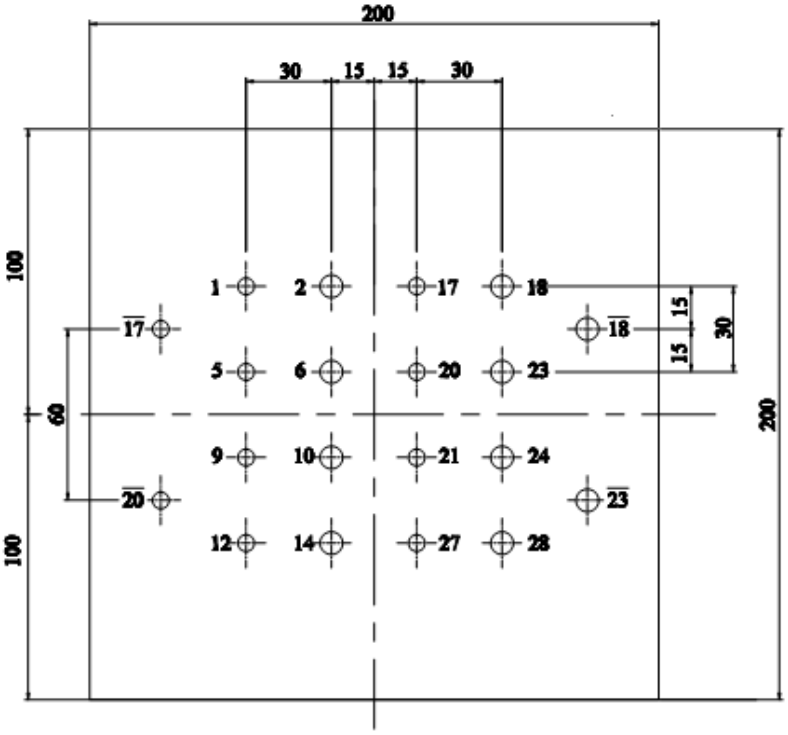

All Units in mm

Hole Distributions on the GFRP (0.82g/cm^3) of thickness 8mm for AWJ and LBM

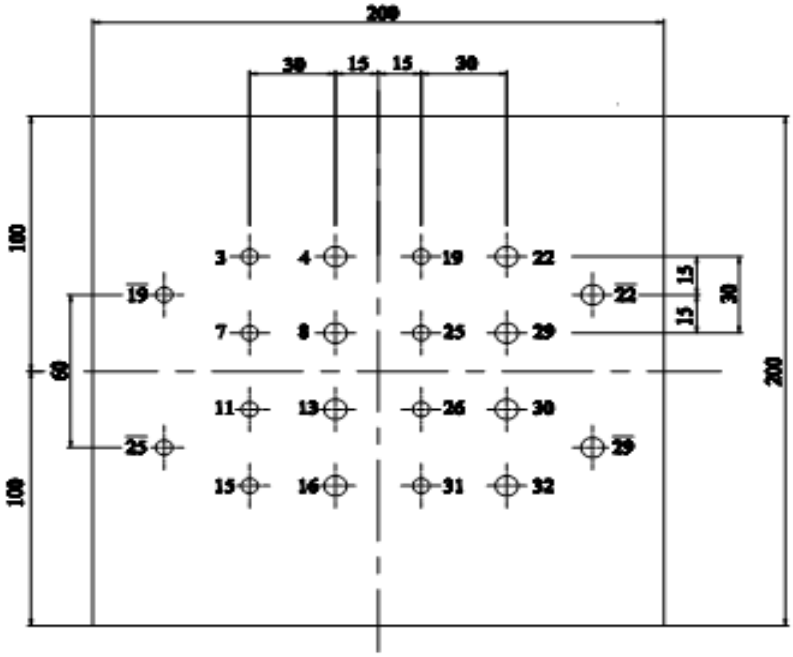

Hole Distributions on the GFRP (0.82g/cm3) of thickness 16mm for AWJ and LBM

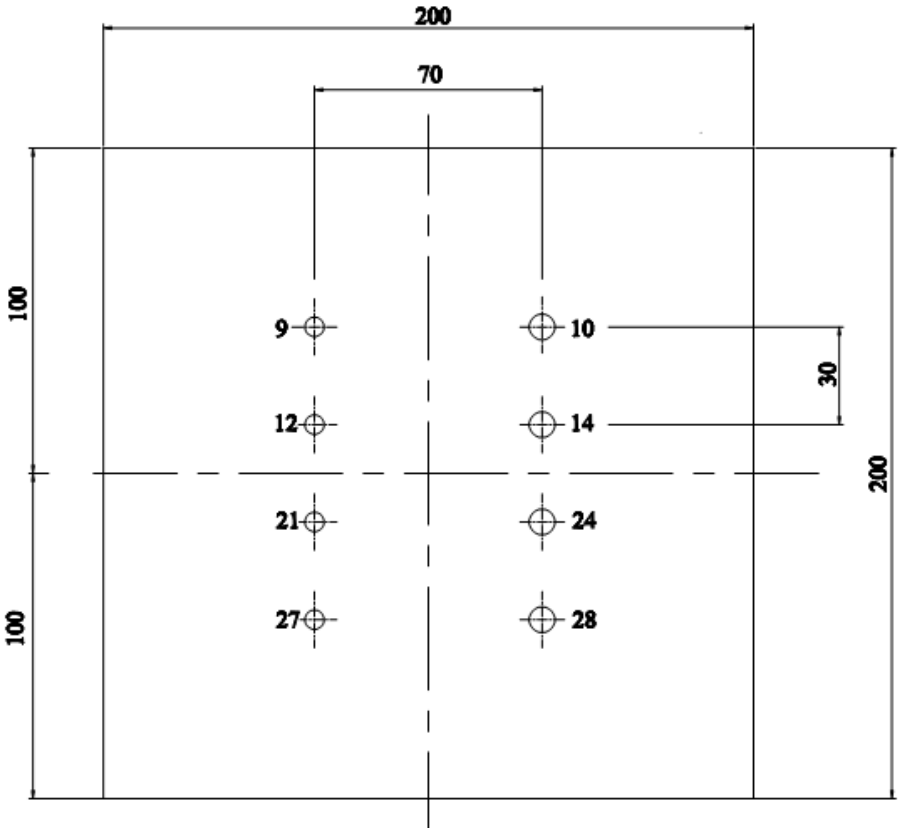

Hole Distributions on the GFRP (1.32g/cm3) of thickness 8mm for AWJ and LBM

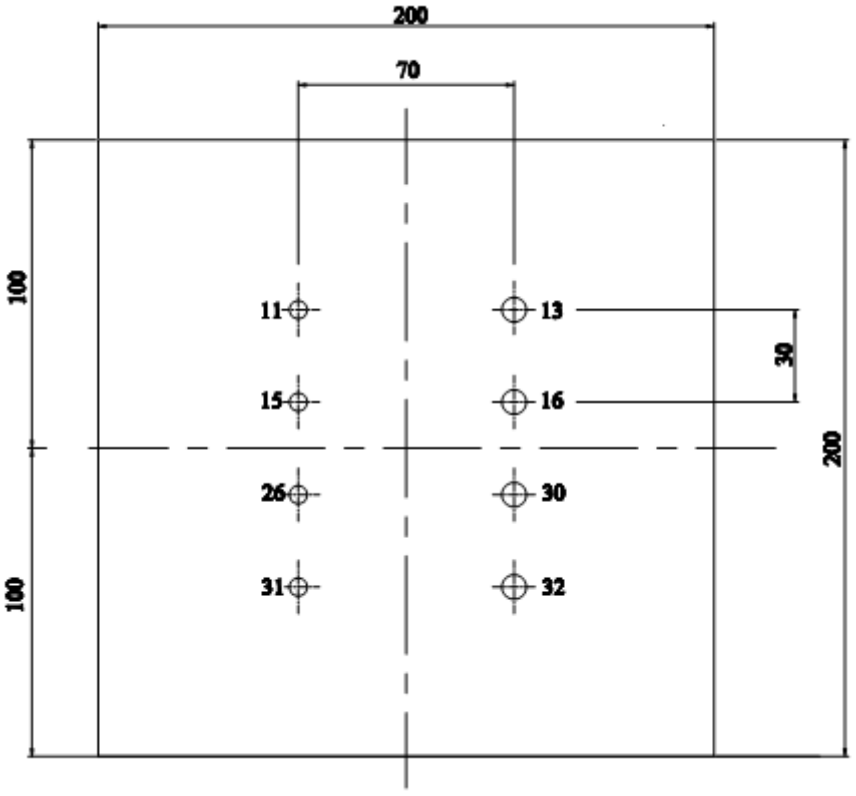

Hole Distributions on the GFRP (1.32g/cm3) of thickness 16mm for AWJ and LBM

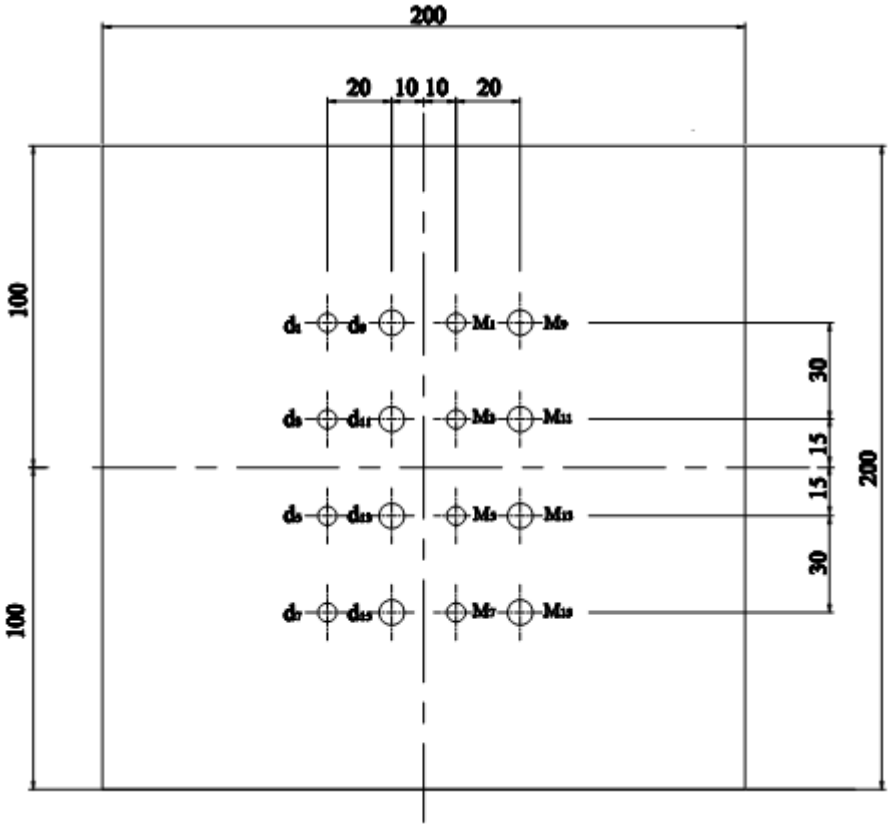

Hole Distributions on the GFRP (0.82g/cm3) of thickness 8mm for Drilling & Milling

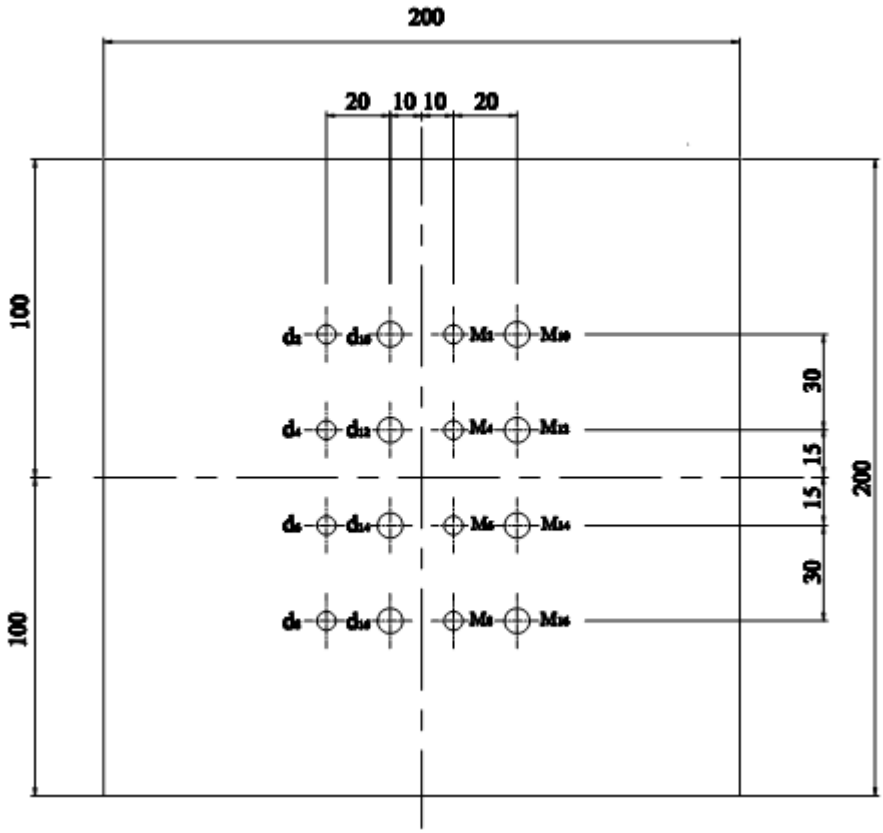

Hole Distributions on the GFRP (0.82g/cm3) of thickness 16mm for Drilling & Milling

Appendix B: Cutting Forces Measurements for Drilling and Milling

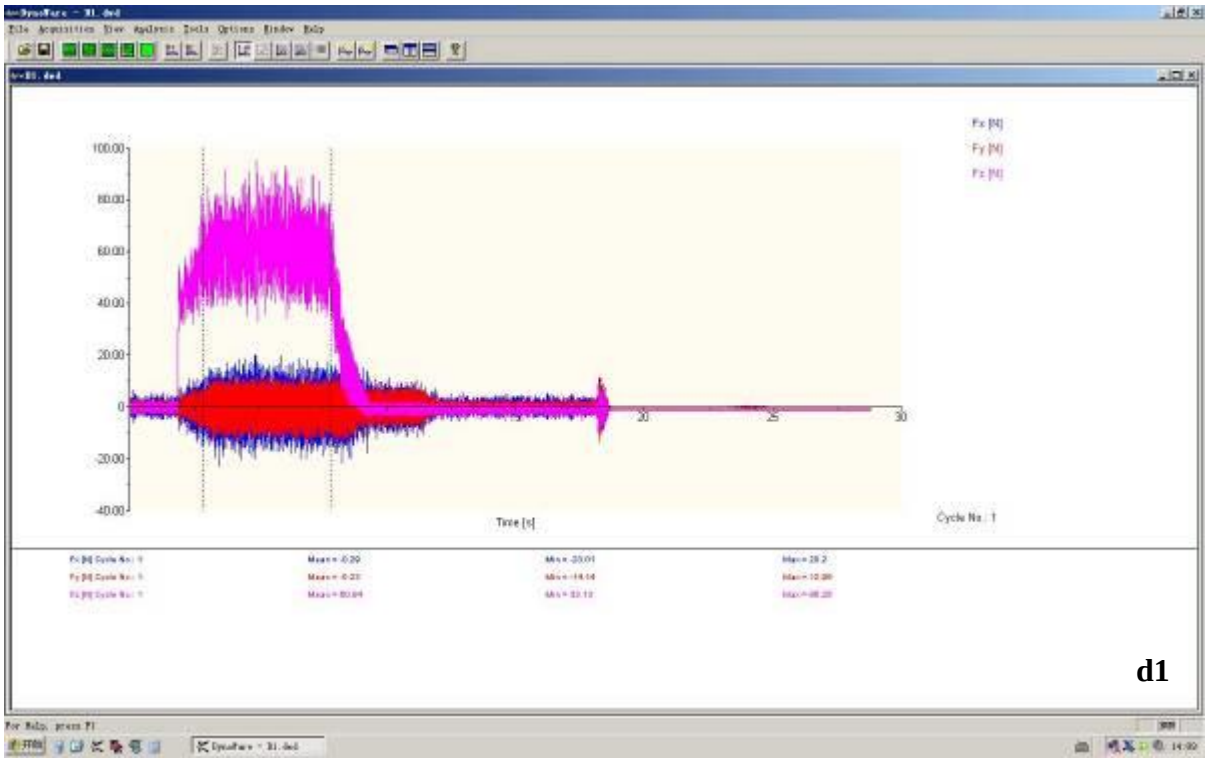

d1

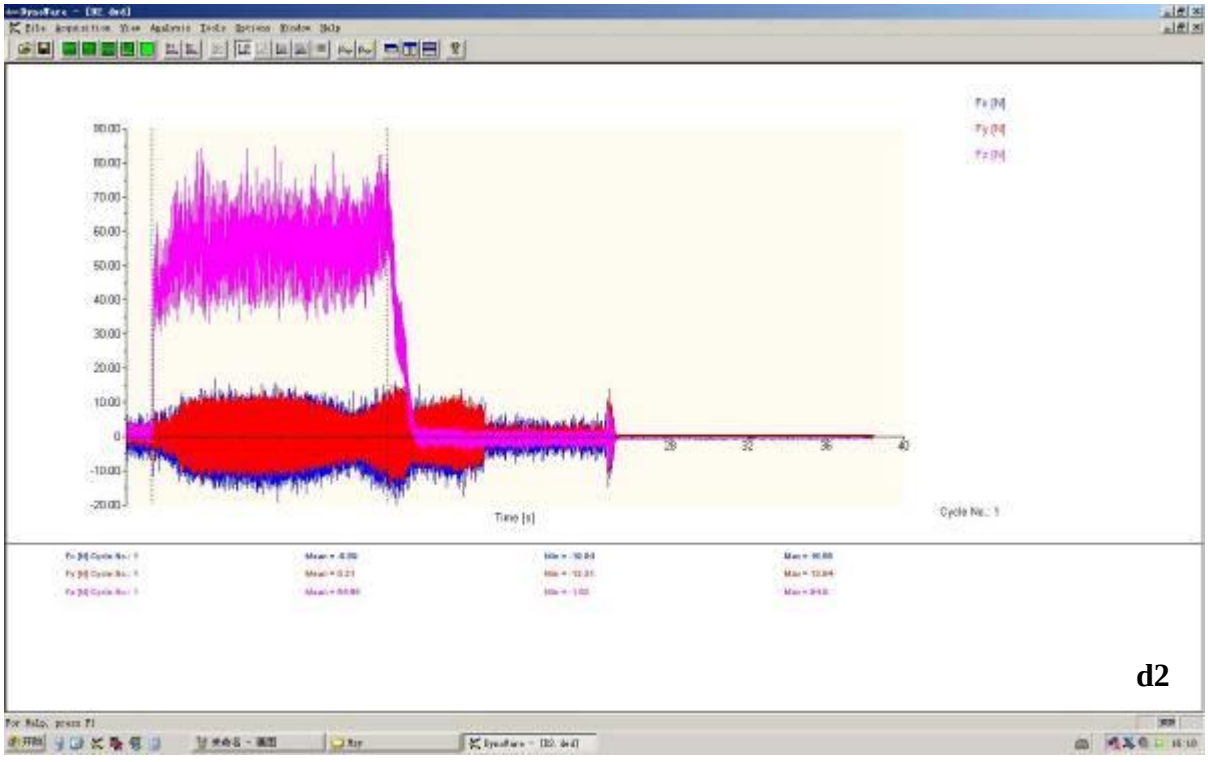

d2

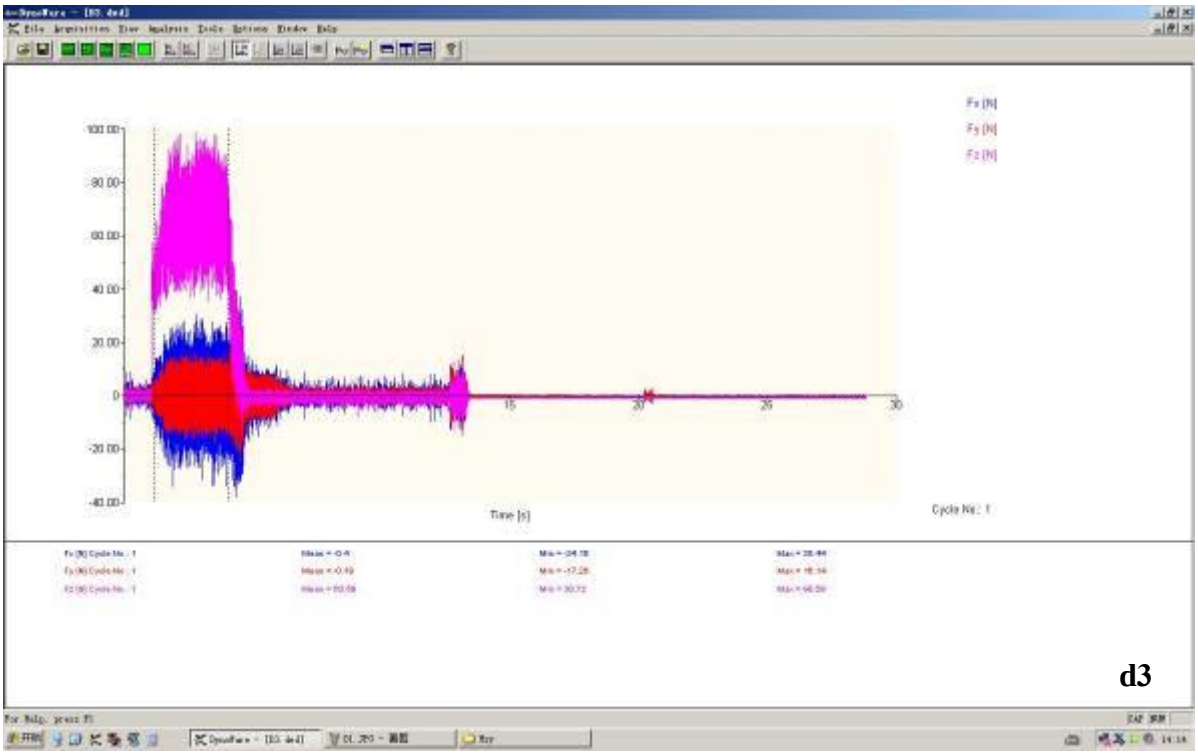

d3

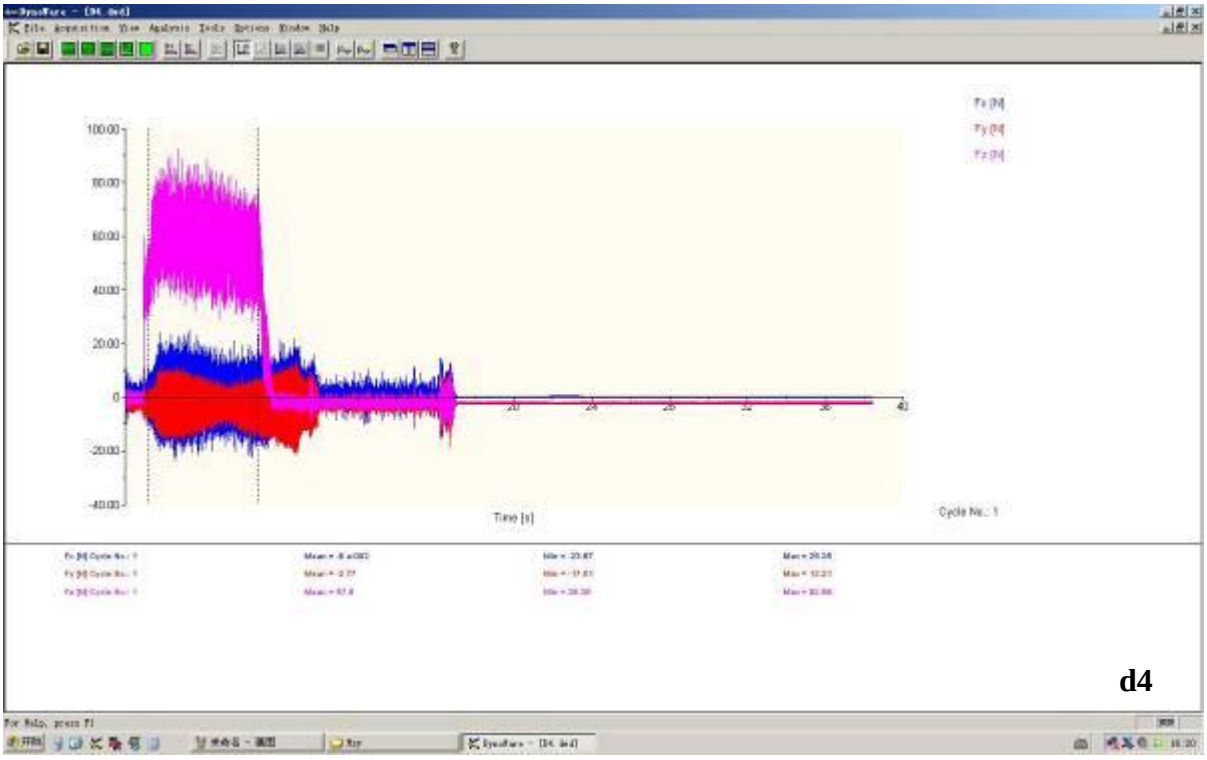

d4

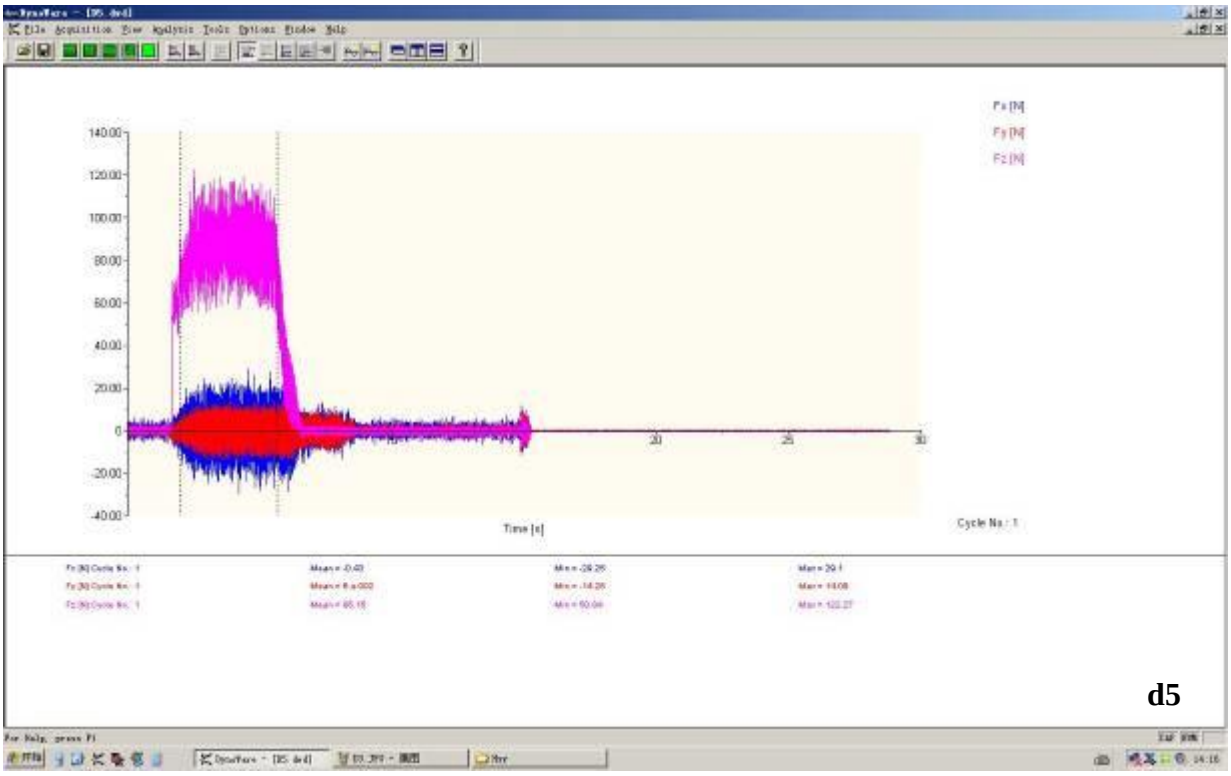
Fx [N]
Fy [N]
Fz [N]
140.00
120.00
100.00
80.00
60.00
40.00
20.00
0
-20.00
-40.00
20
25
30
Time [s]
Cycle No.: 1

d5

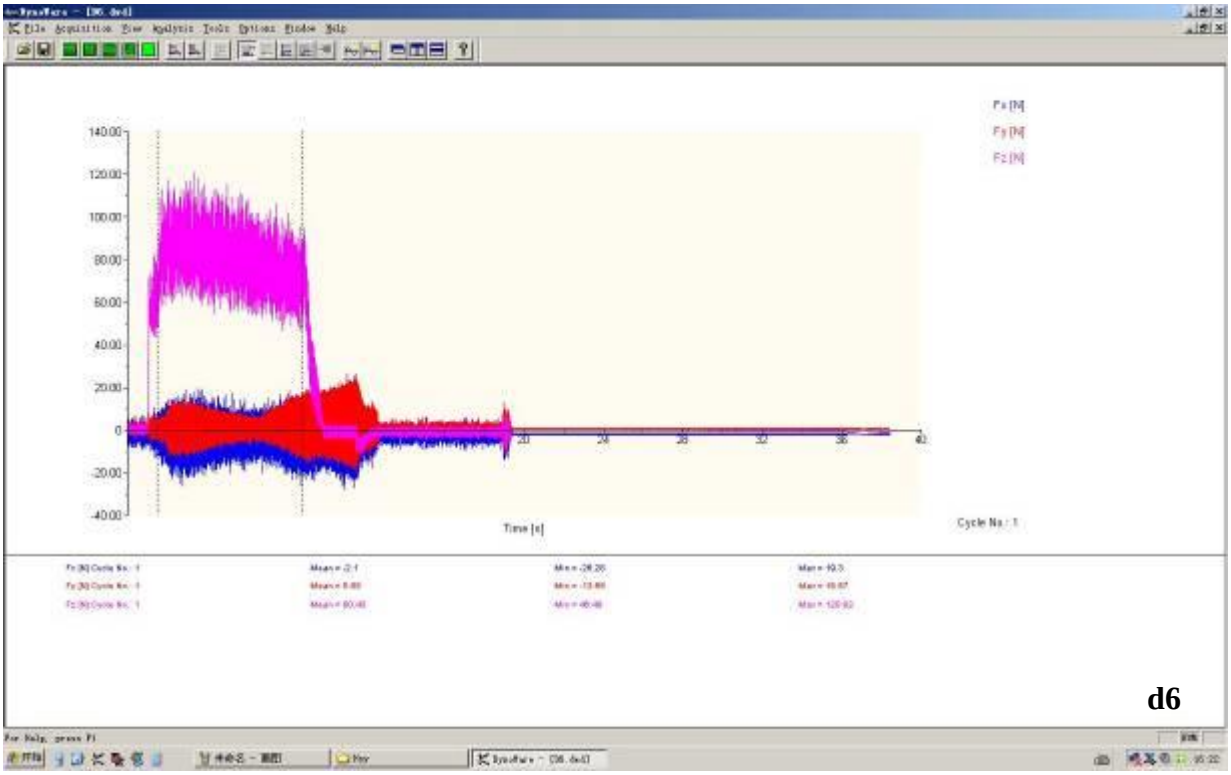
Fx [N]
Fy [N]
Fz [N]
140.00
120.00
100.00
80.00
60.00
40.00
20.00
0
-20.00
-40.00
20
28
36
32
40
Time [s]
Cycle No.: 1

d6

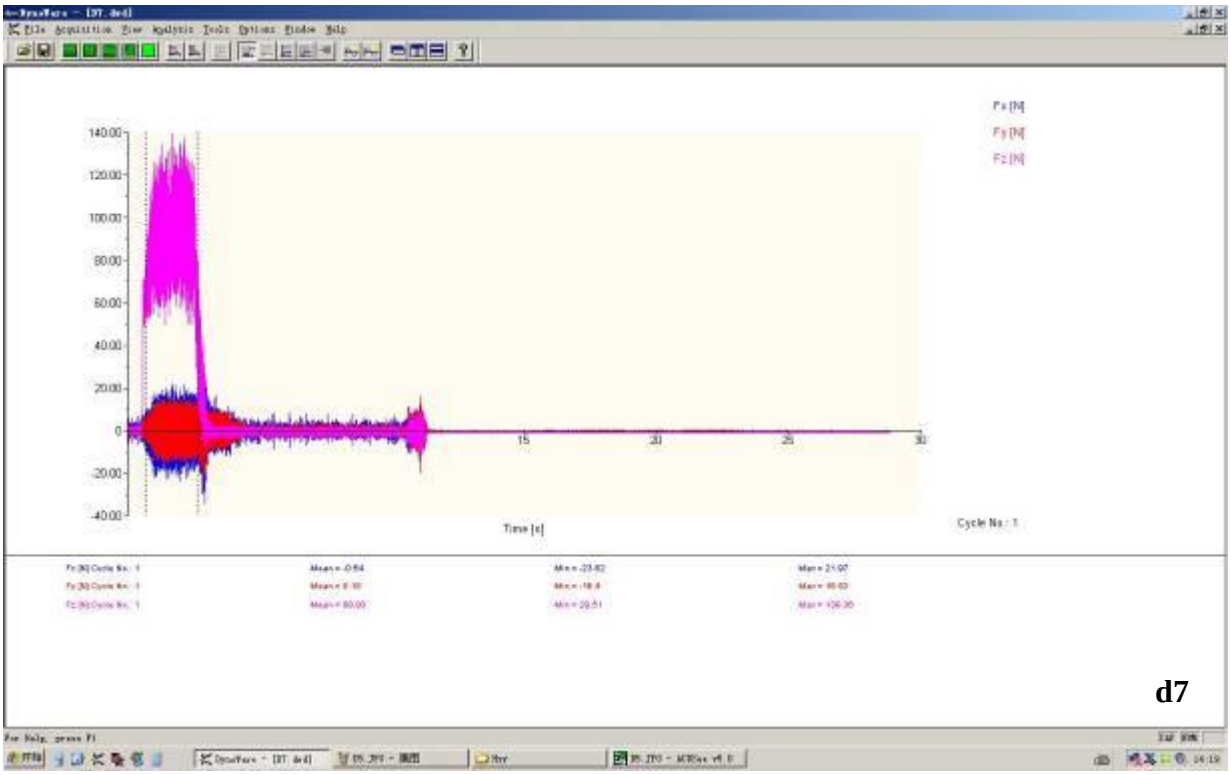

d7

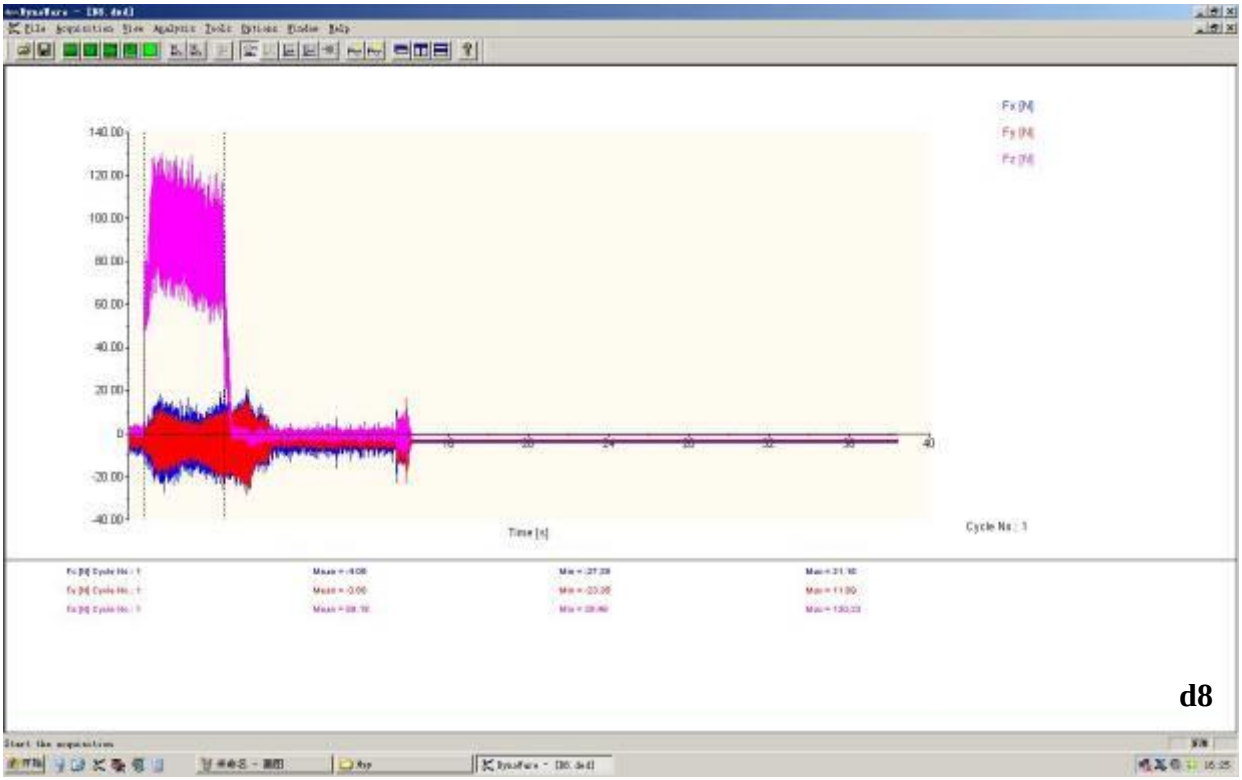

d8

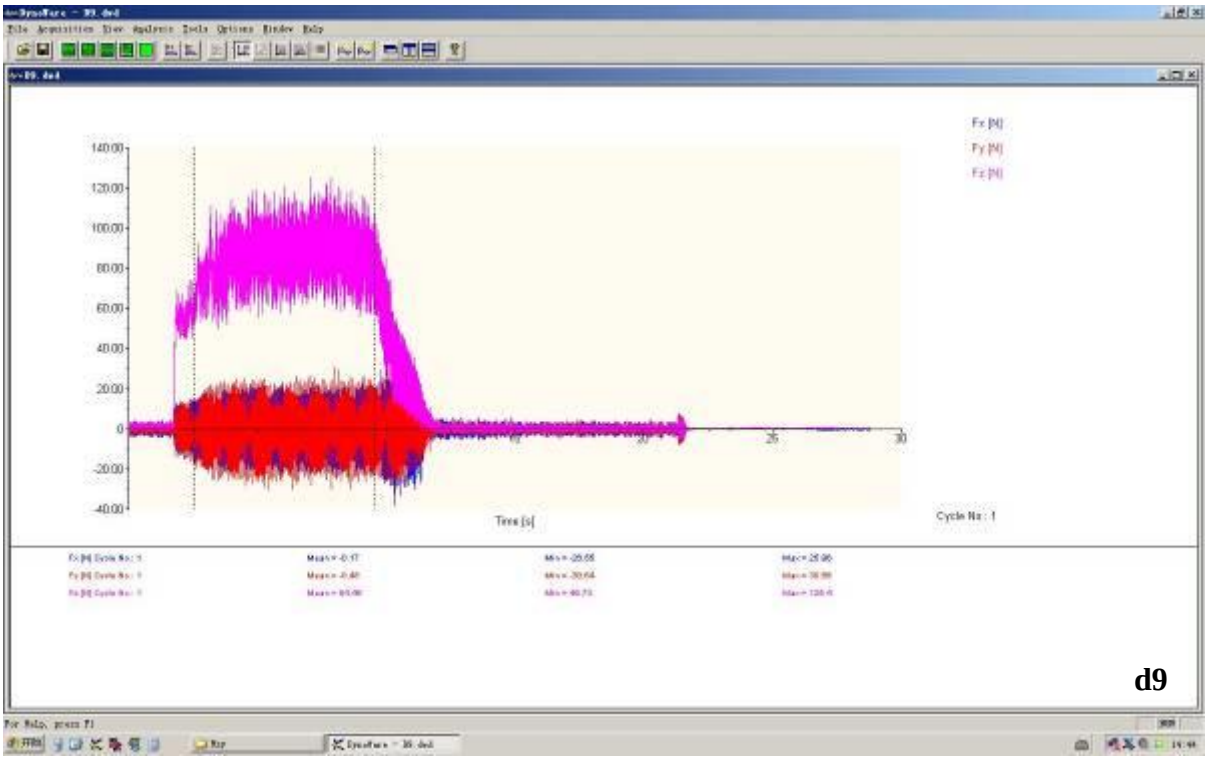

d9

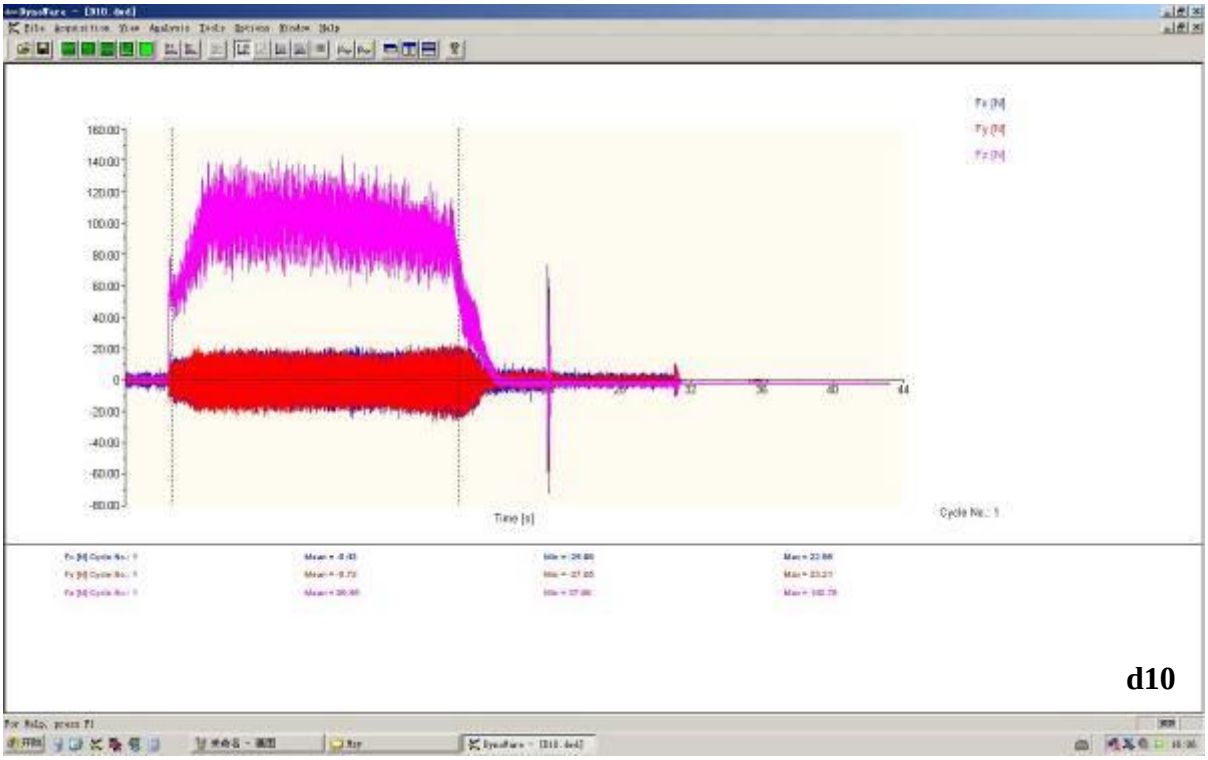

d10

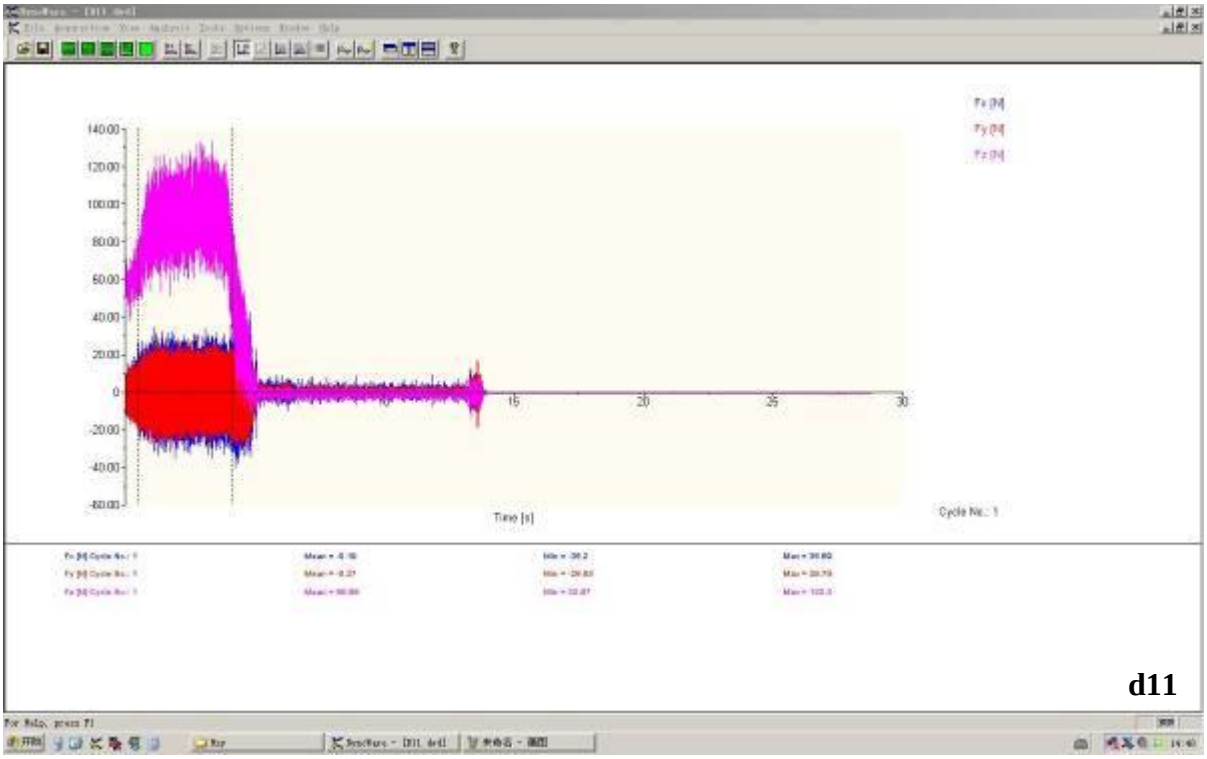

d11

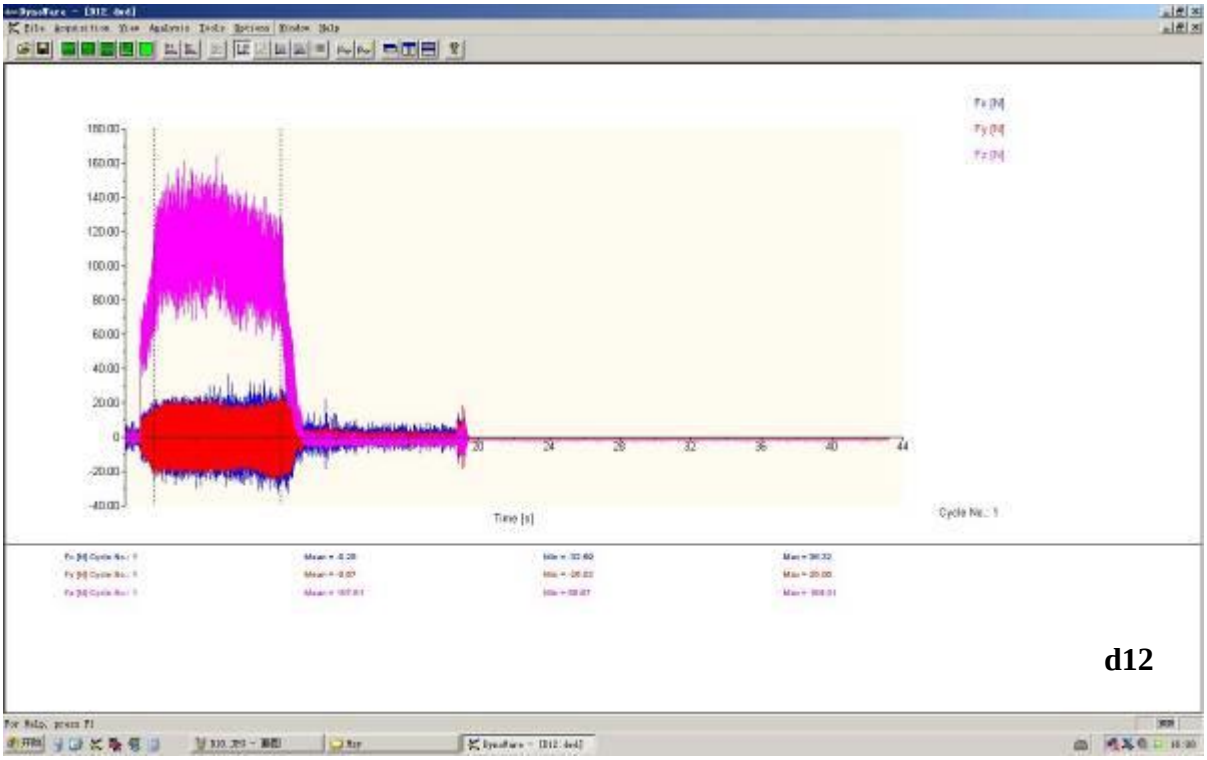

d12

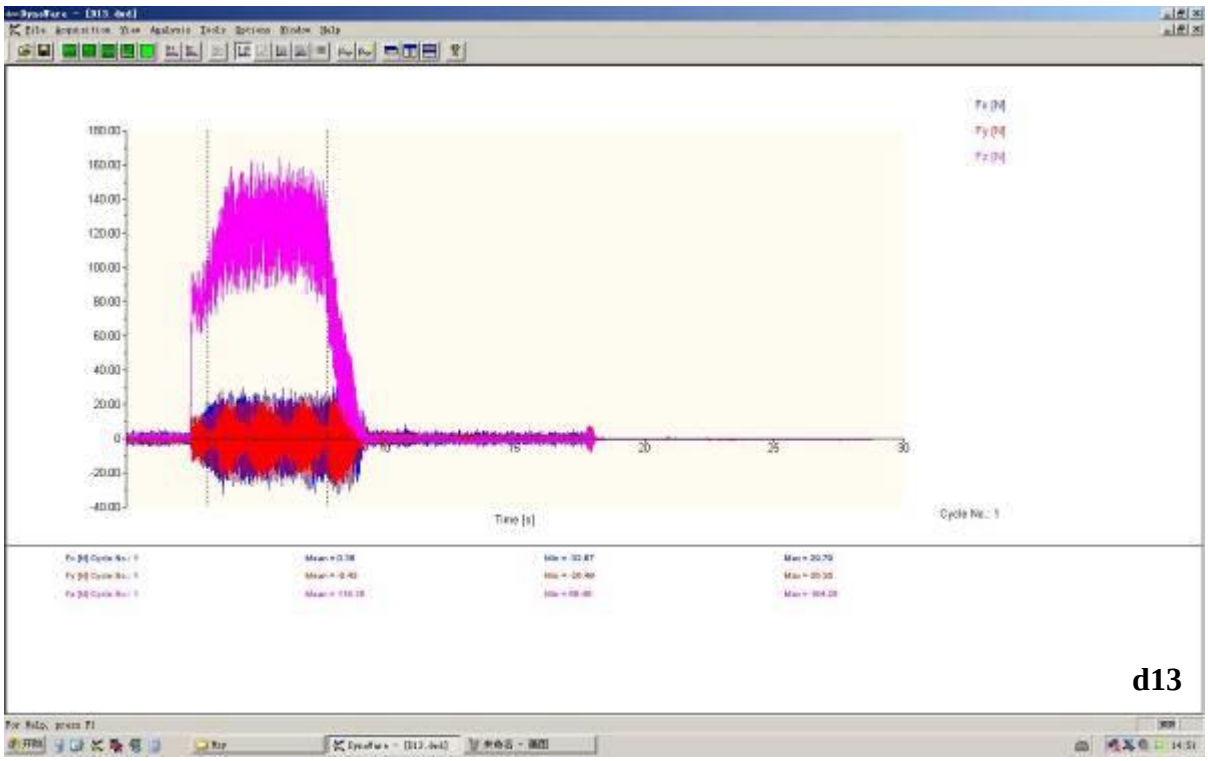

d13

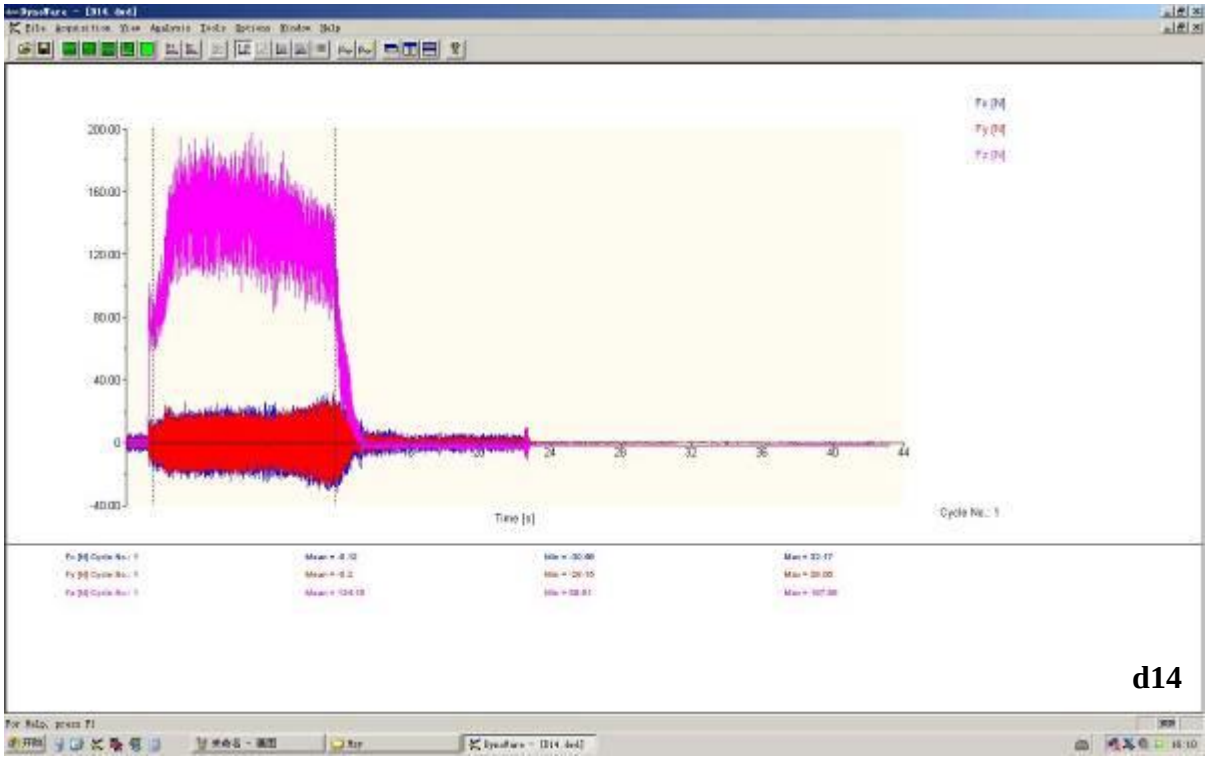

d14

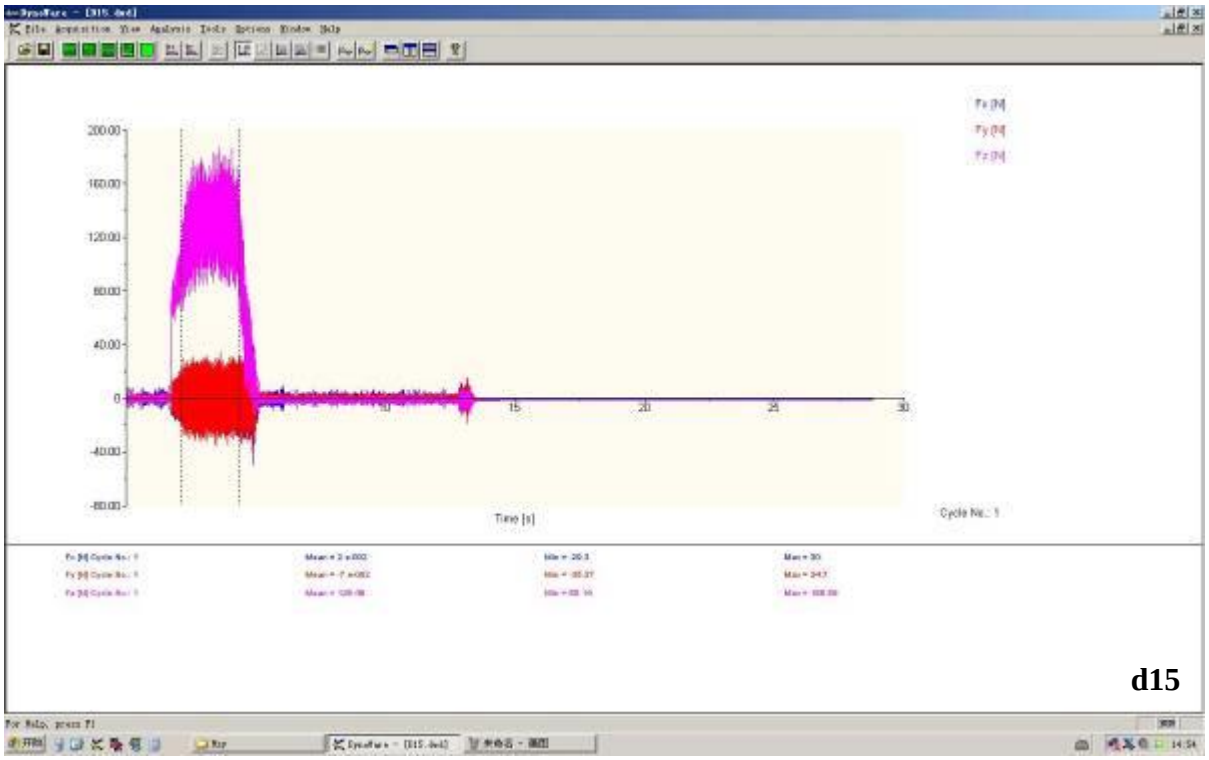
Fx [N]
Fy [N]
Fz [N]
200.00
160.00
120.00
80.00
40.00
0
-40.00
-80.00
5
10
15
20
25
30
Time [s]
Cycle No.: 1

d15

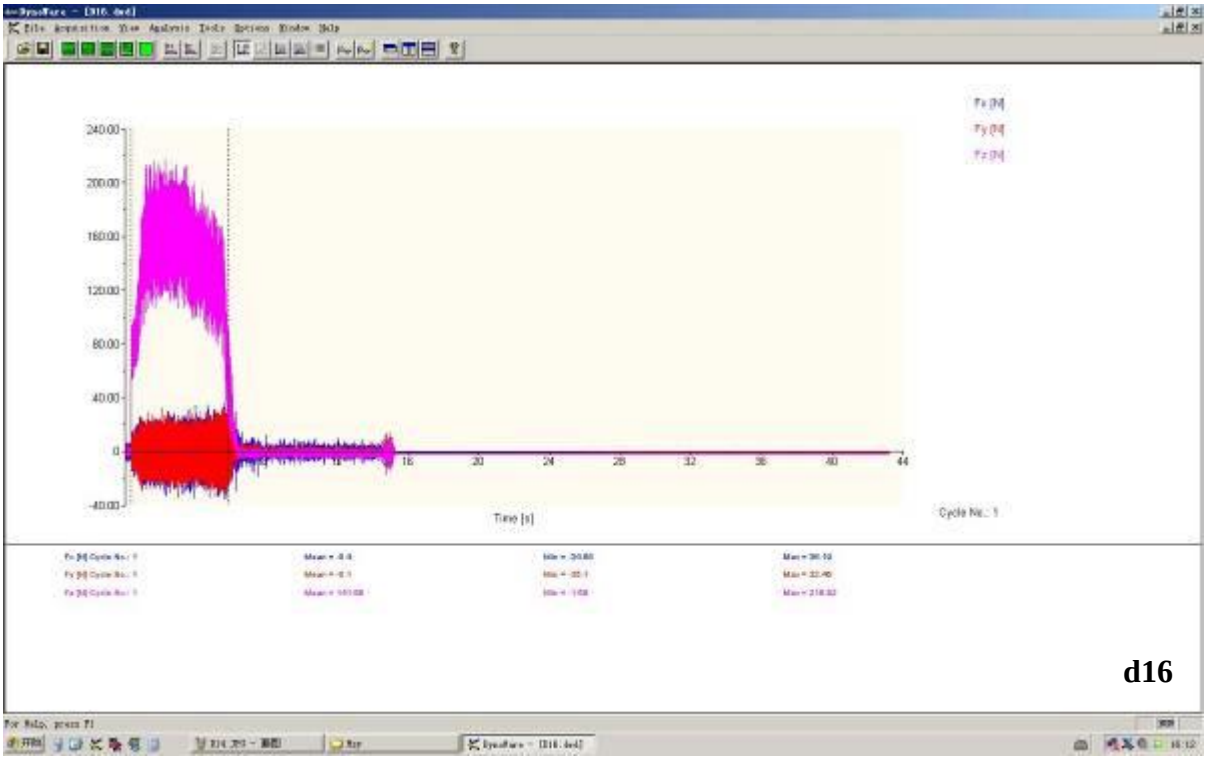
Fx [N]
Fy [N]
Fz [N]
240.00
200.00
160.00
120.00
80.00
40.00
0
-40.00
16
20
24
28
32
36
40
44
Time [s]
Cycle No.: 1

d16

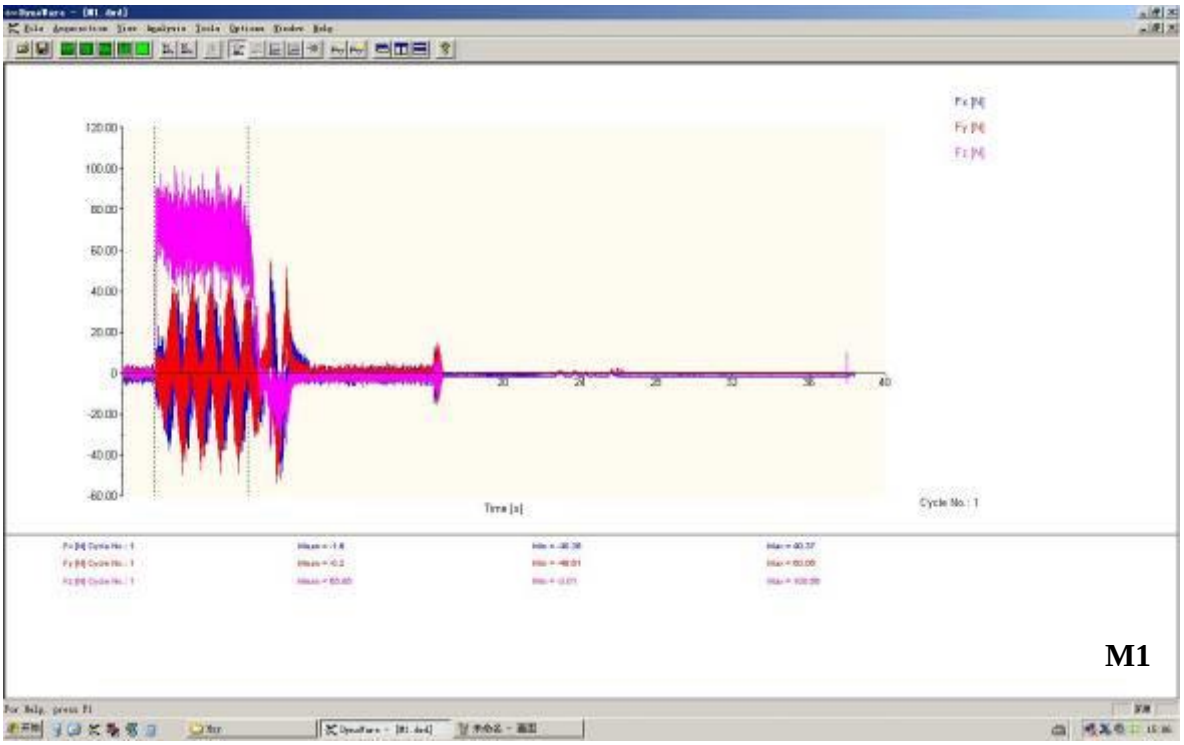

M1

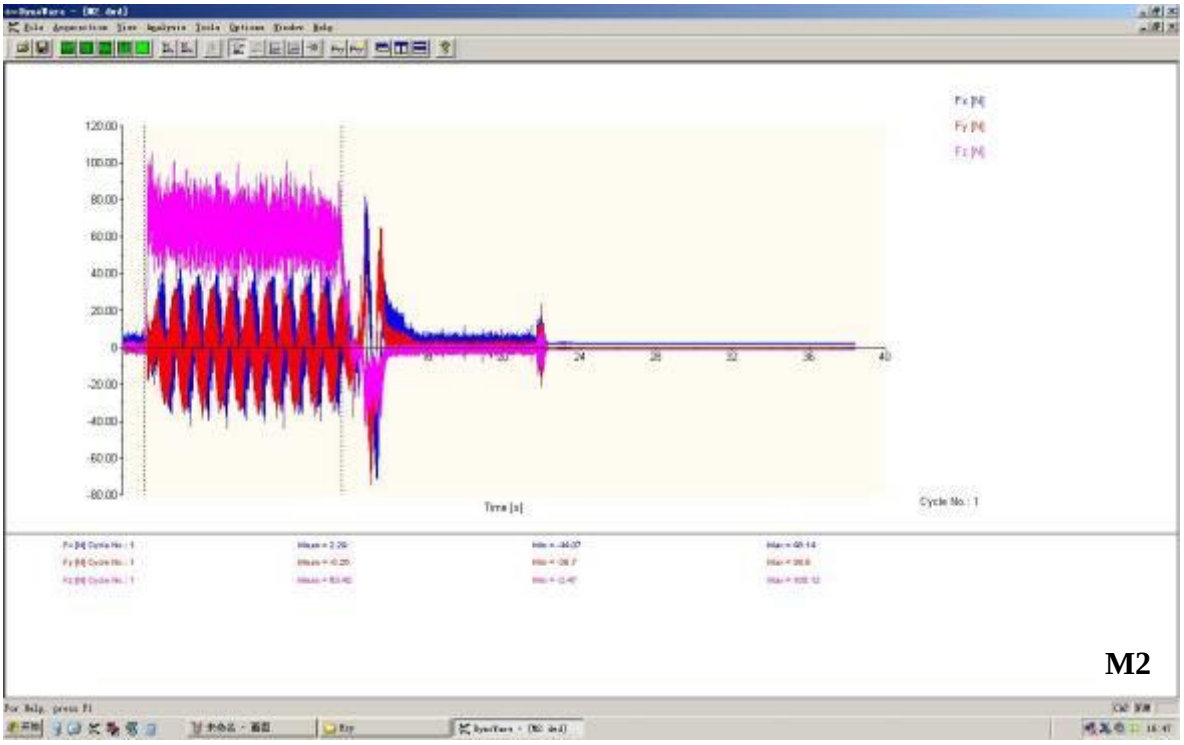

M2

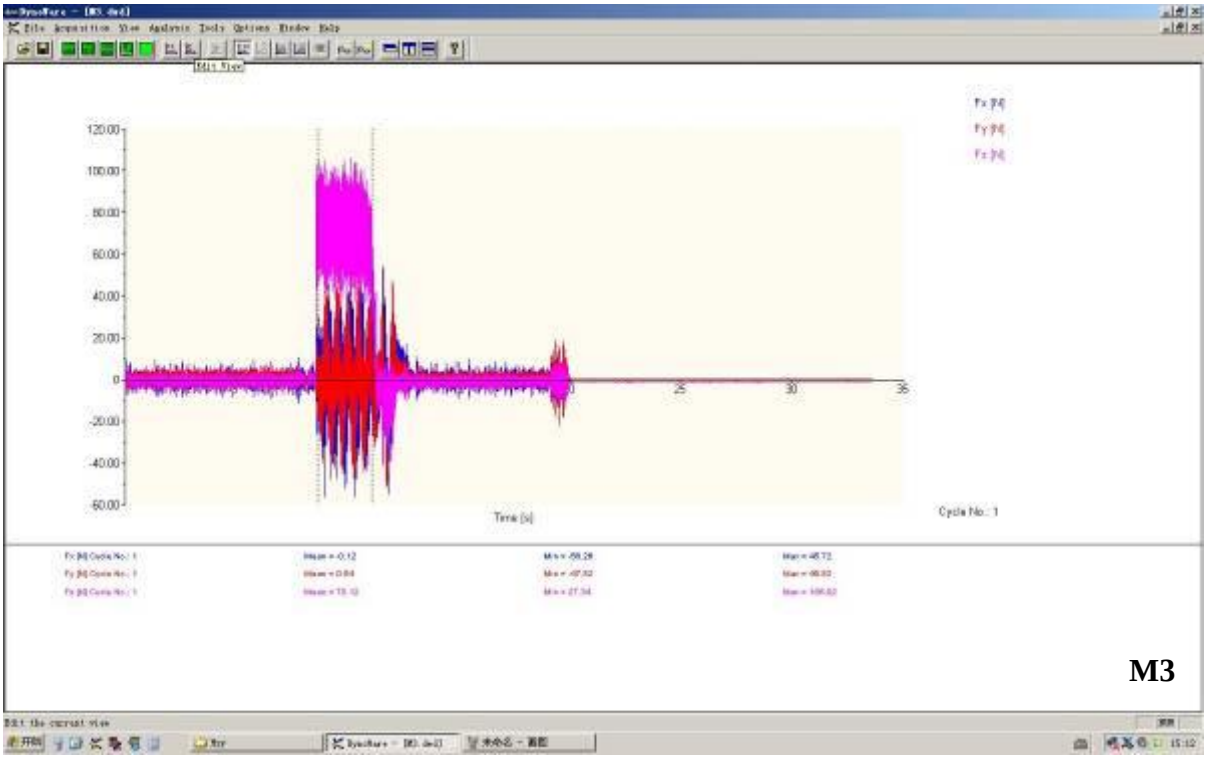

M3

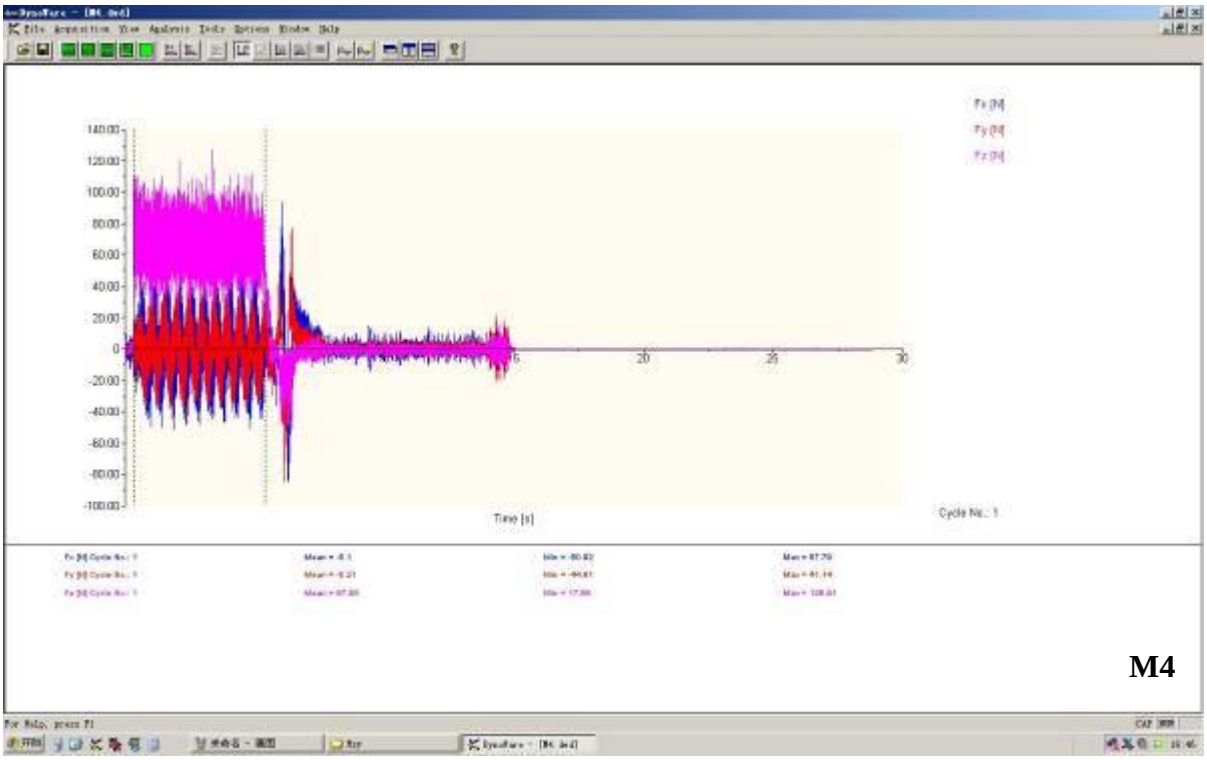

M4

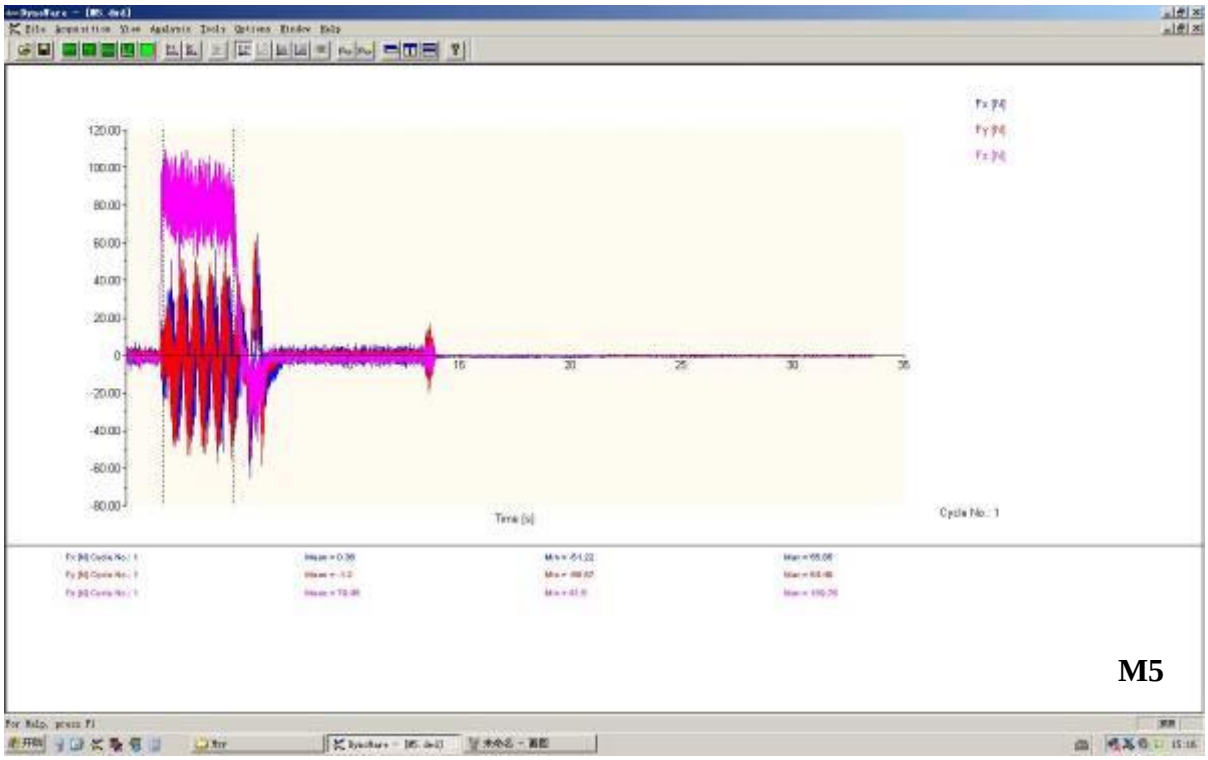

M5

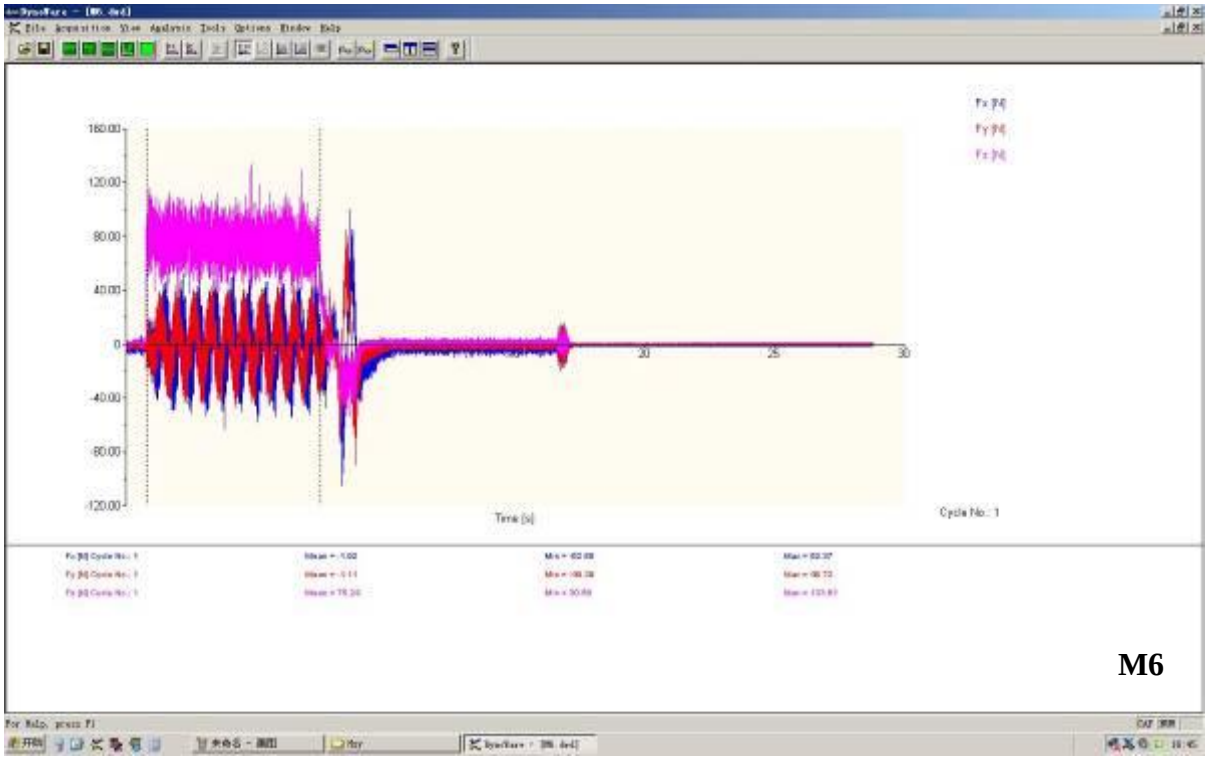

M6

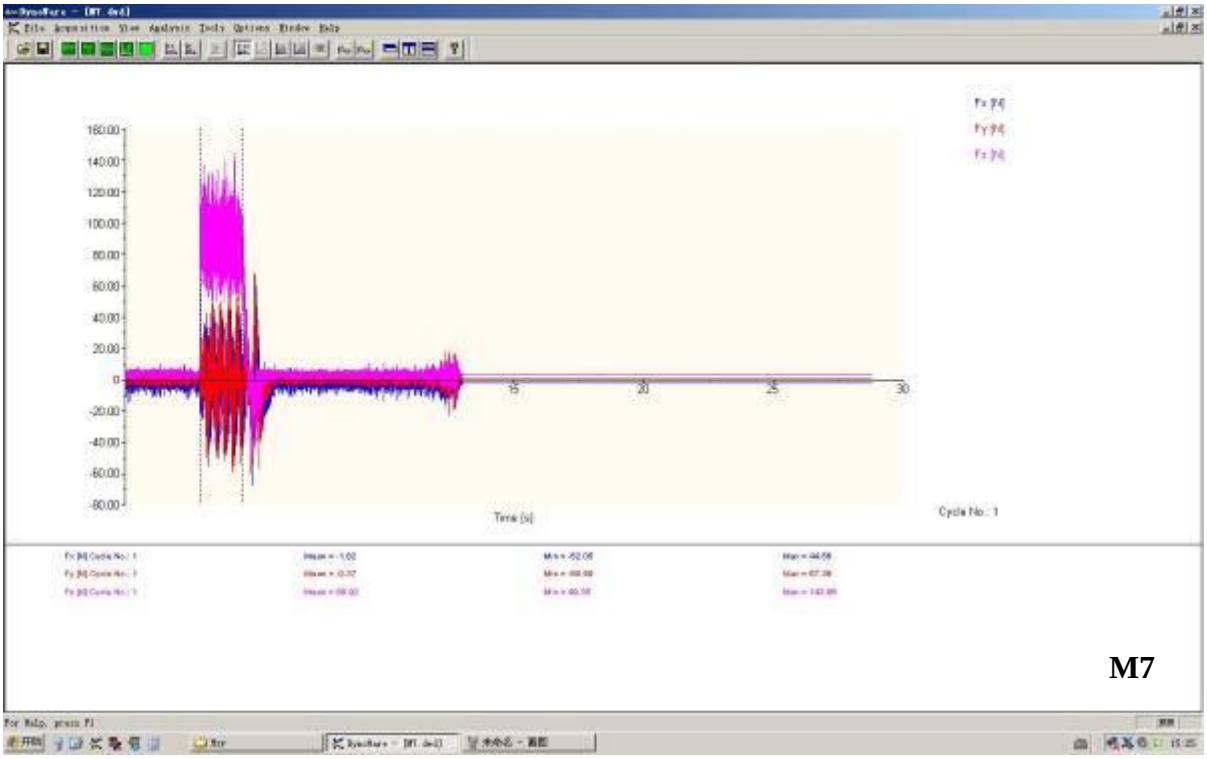

M7

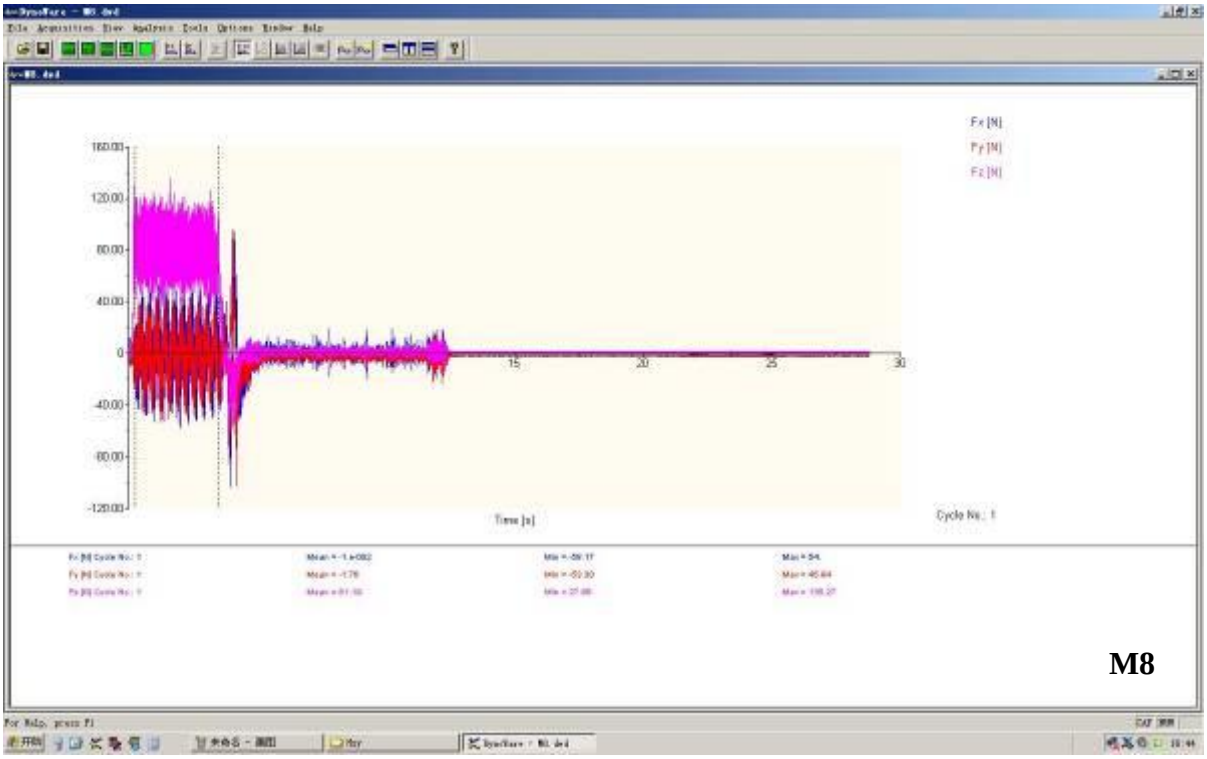

M8

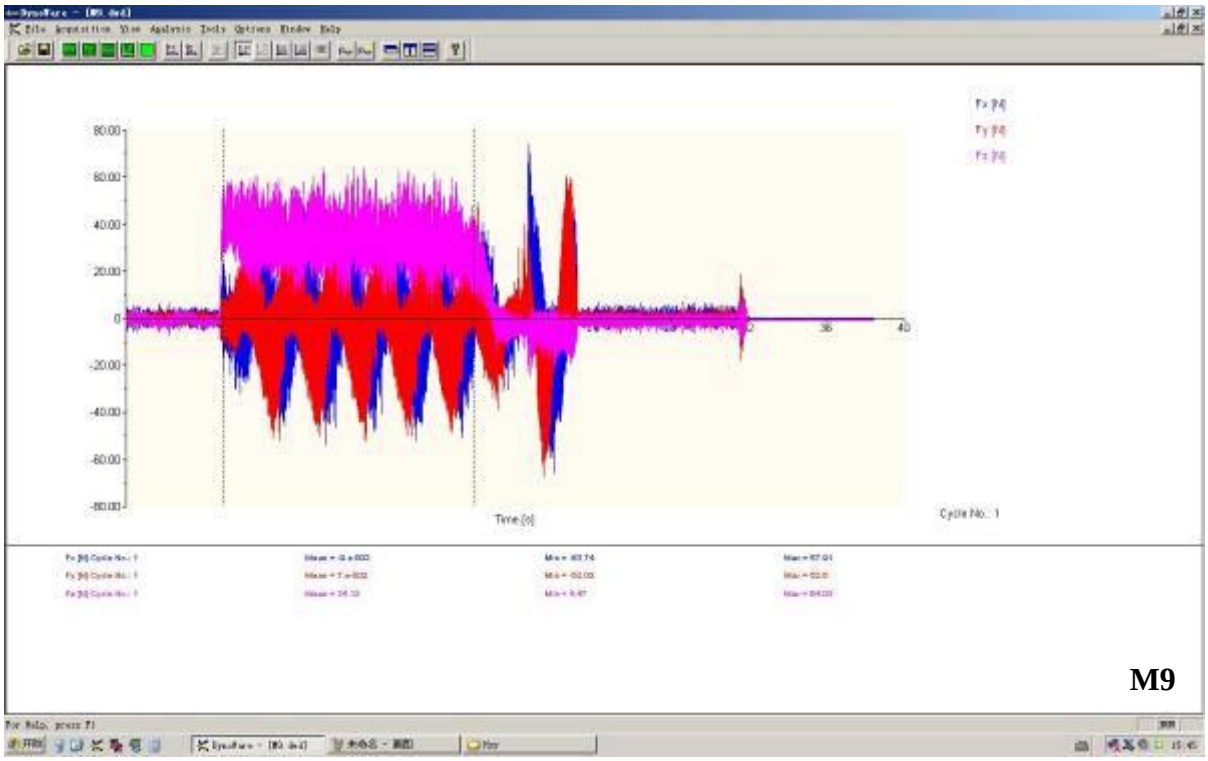
Fx [N]
Fy [N]
Fz [N]
80.00
60.00
40.00
20.00
0
-20.00
-40.00
-60.00
-80.00
Time [s]
Cycle No.: 1

M9

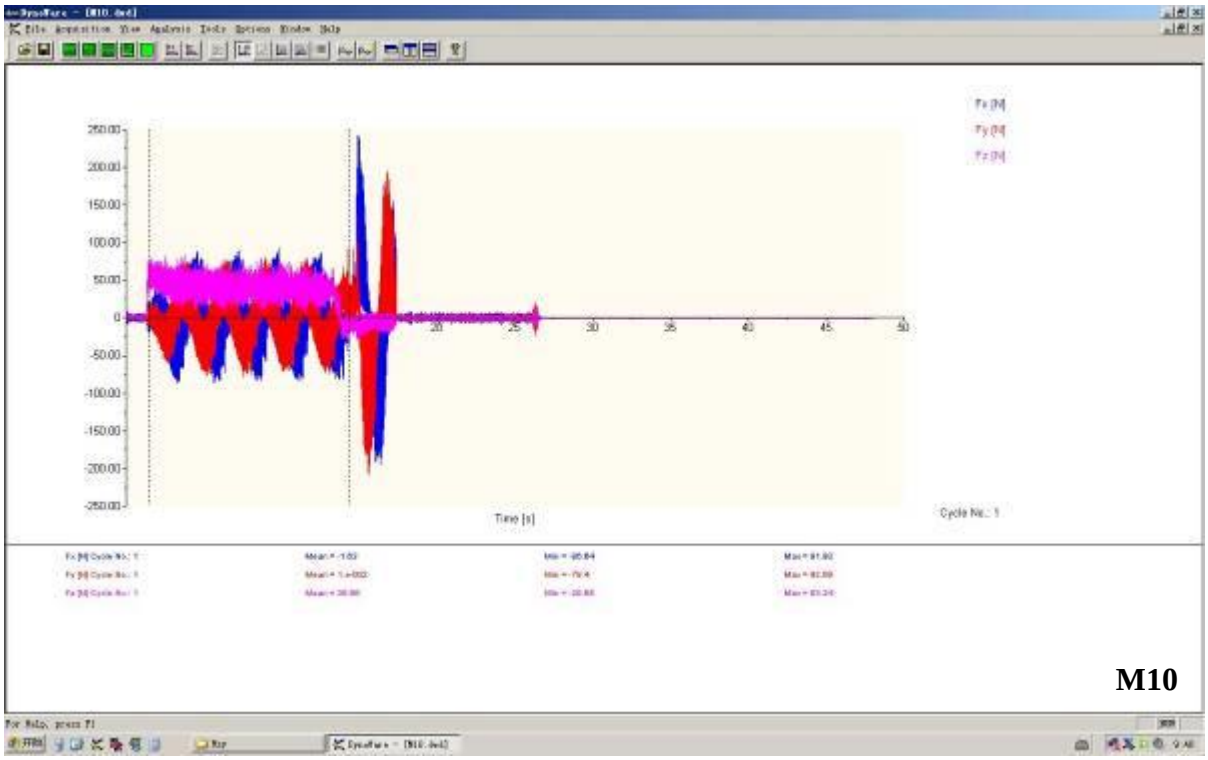
Fx [N]
Fy [N]
Fz [N]
250.00
200.00
150.00
100.00
50.00
0
-50.00
-100.00
-150.00
-200.00
-250.00
Time [s]
Cycle No.: 1

M10

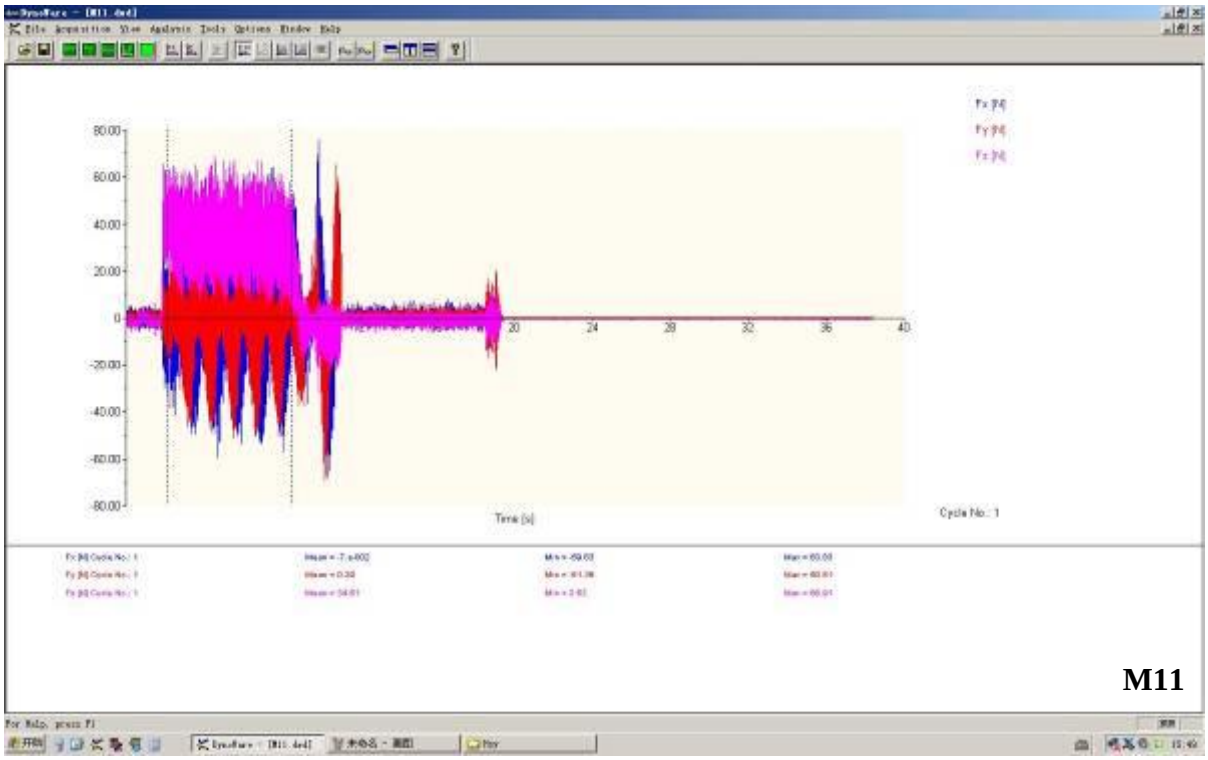
Fx [N]
Fy [N]
Fz [N]
80.00
60.00
40.00
20.00
0
-20.00
-40.00
-60.00
-80.00
20
24
28
32
36
40
Time [s]
Cycle No.: 1

M11

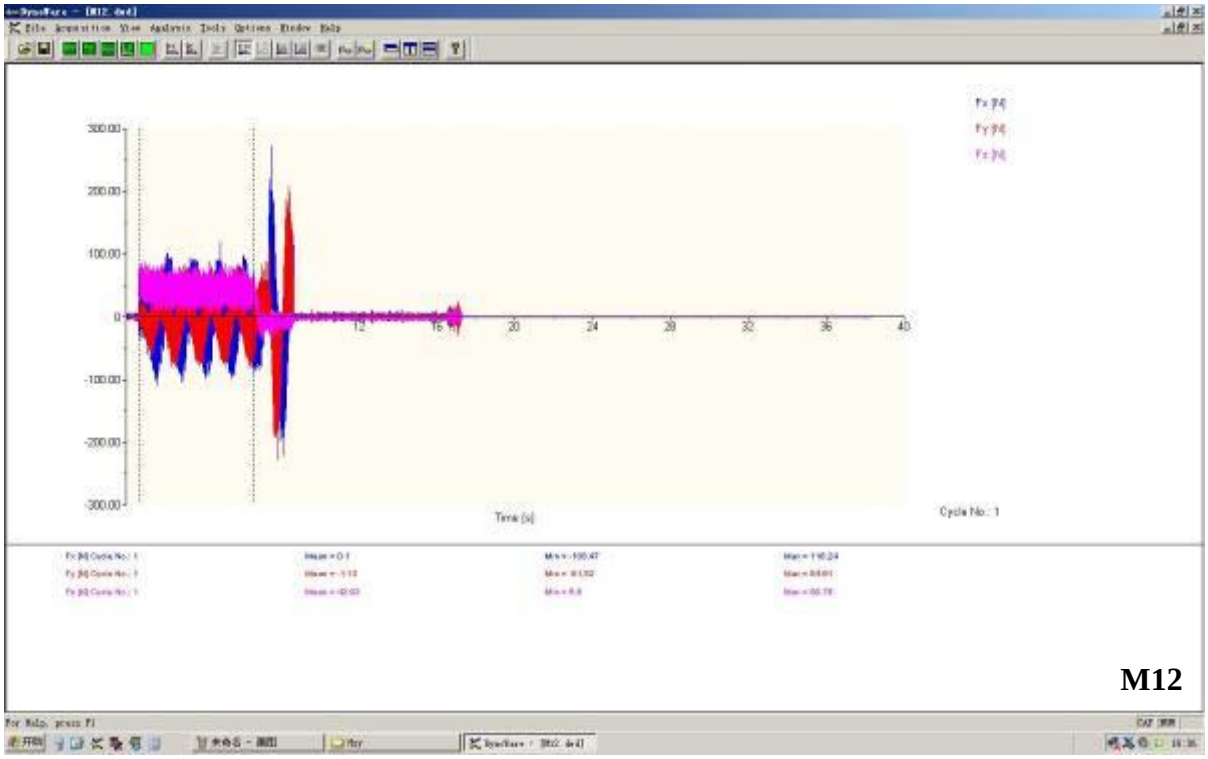
Fx [N]
Fy [N]
Fz [N]
300.00
200.00
100.00
0
-100.00
-200.00
-300.00
12
16
20
24
28
32
36
40
Time [s]
Cycle No.: 1

M12

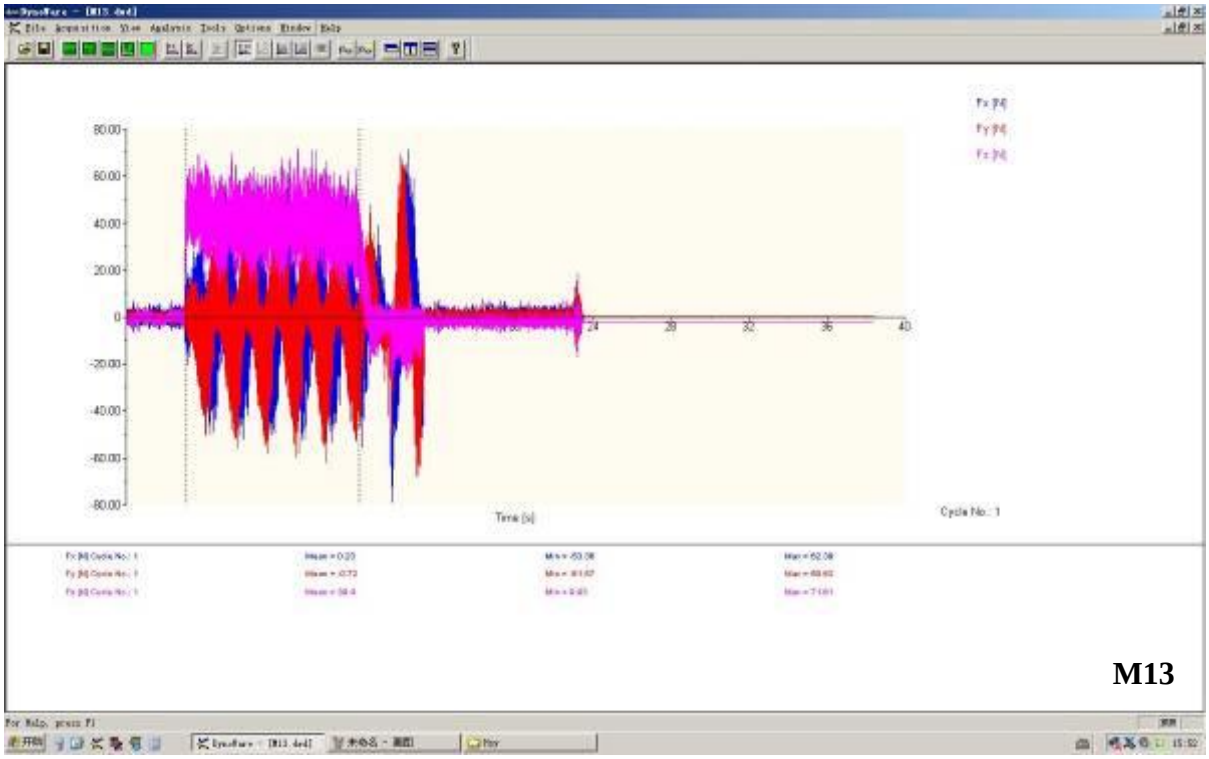
Fx [N]
Fy [N]
Fz [N]
80.00
60.00
40.00
20.00
0
-20.00
-40.00
-60.00
-80.00
24
28
32
36
40
Time [s]
Cycle No.: 1

M13

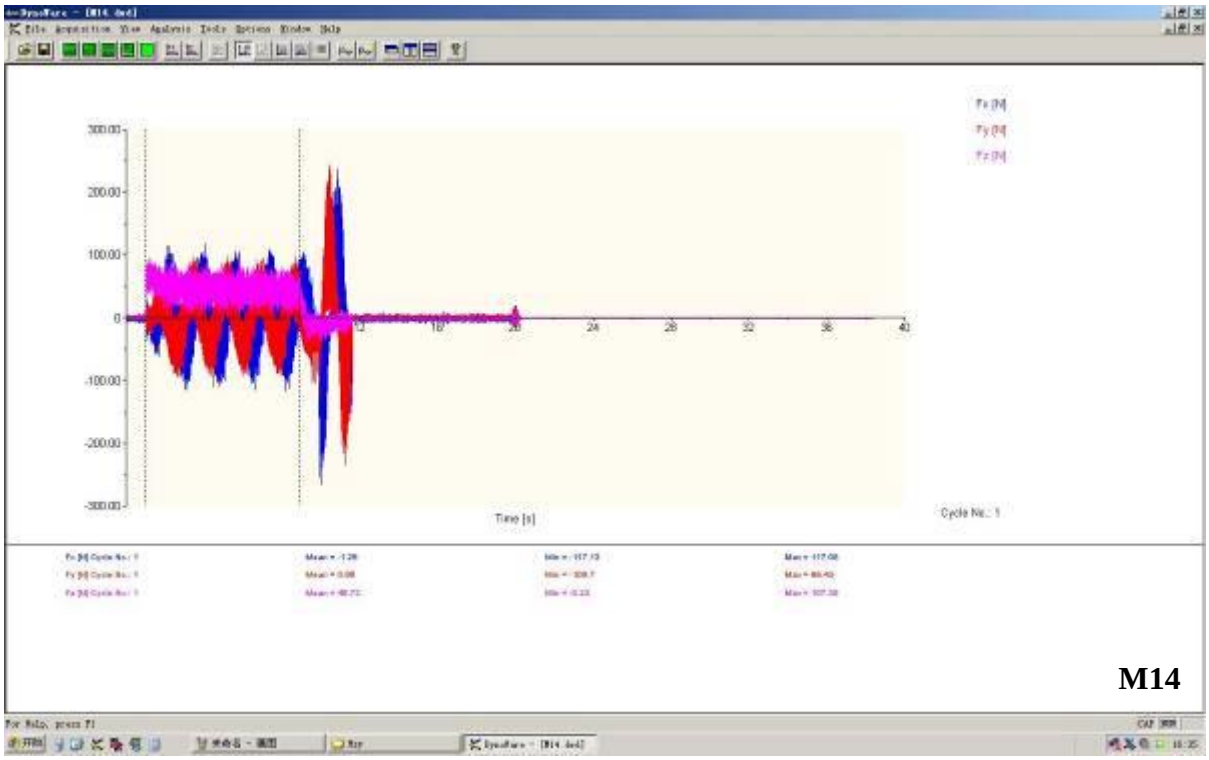
Fx [N]
Fy [N]
Fz [N]
300.00
200.00
100.00
0
-100.00
-200.00
-300.00
16
20
24
28
32
36
40
Time [s]
Cycle No.: 1

M14

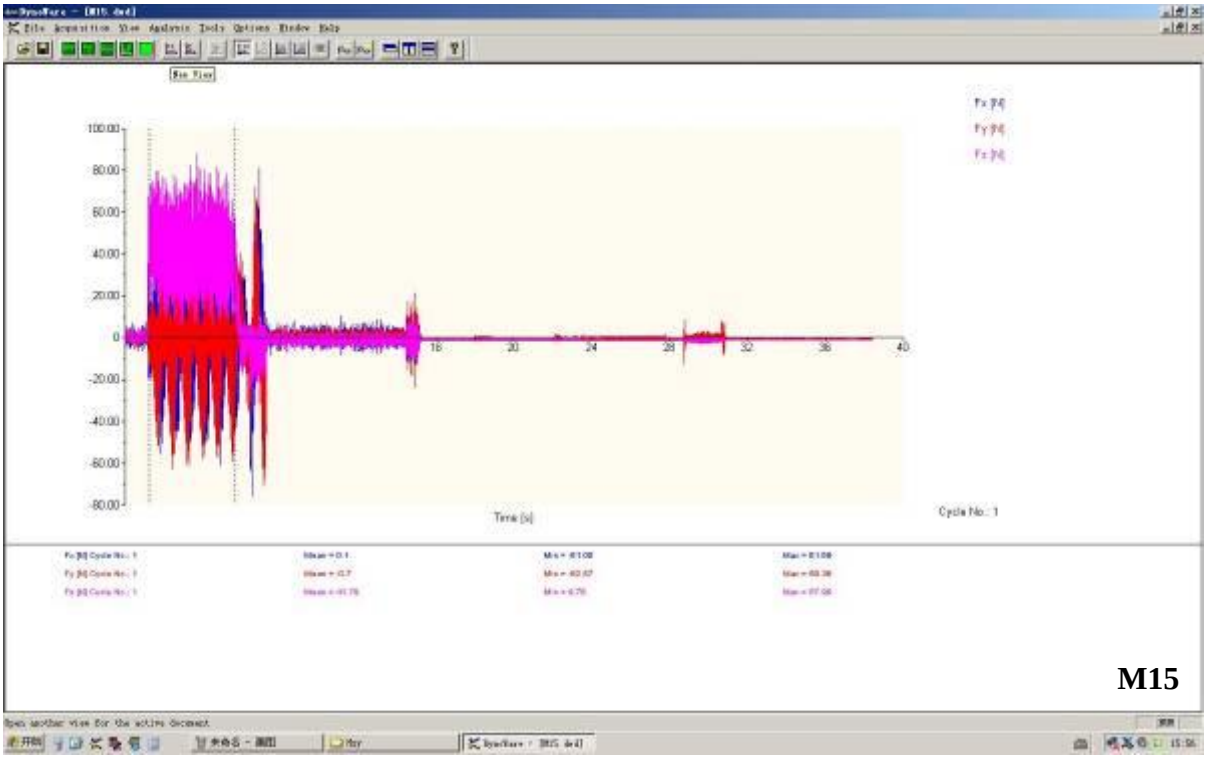
M15

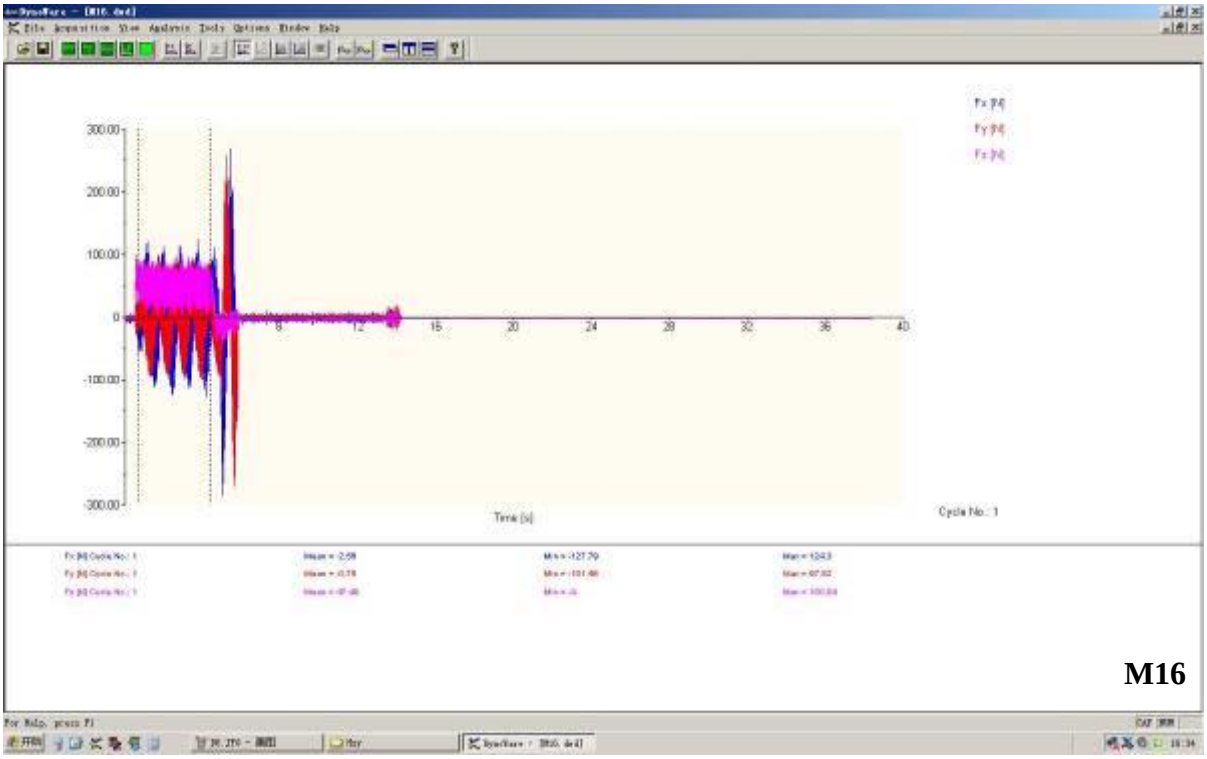
M16

Appendix C: Optical Microscopic Pictures for Drilling and Milling

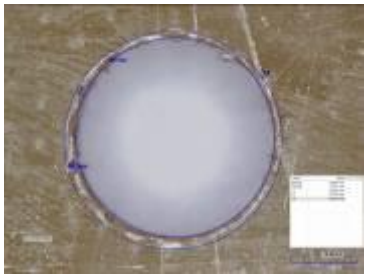

d1L

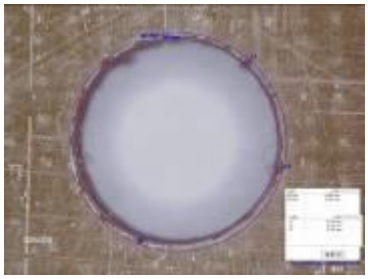

d1u

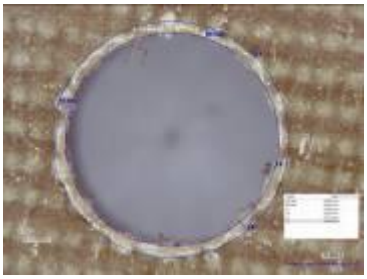

d2L

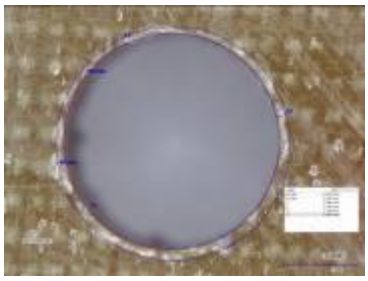

d2u

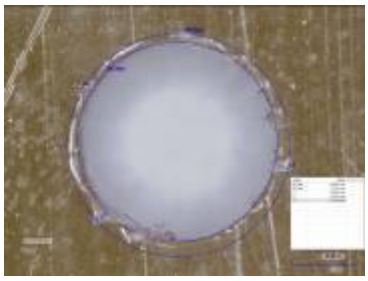

d3L

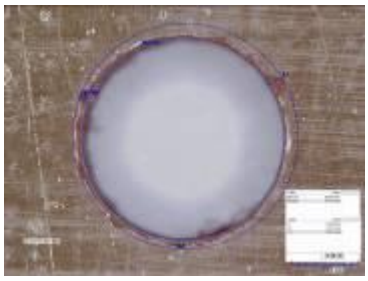

d3u

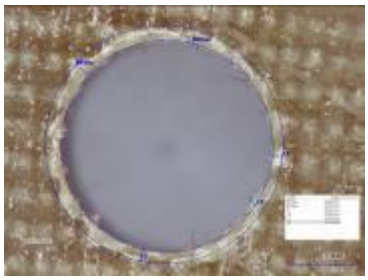

d4L

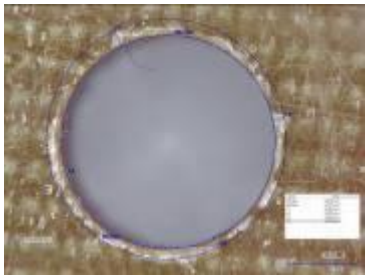

d4u

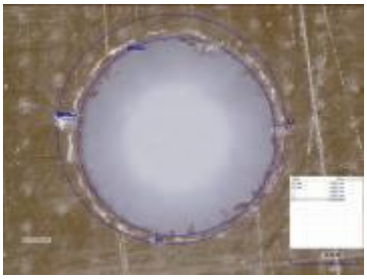

d5L

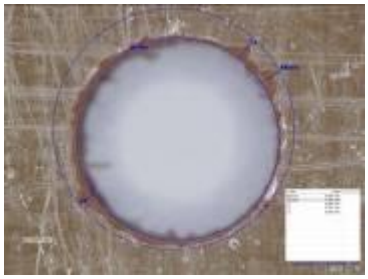

d5u

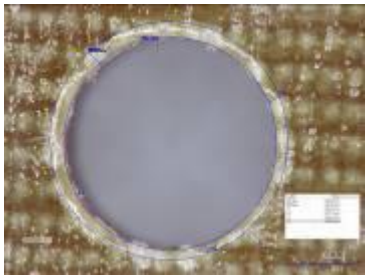

d6L

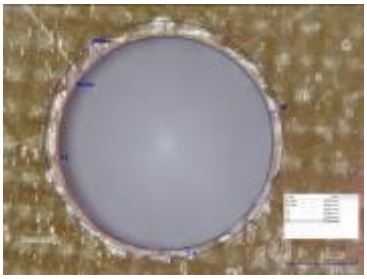

d6u

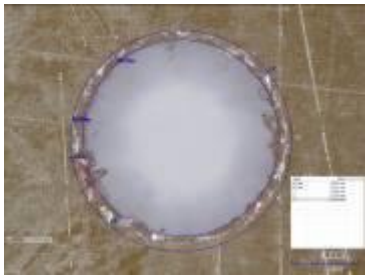

d7L

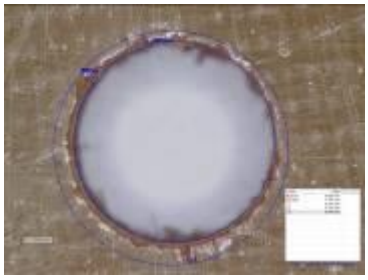

d7u

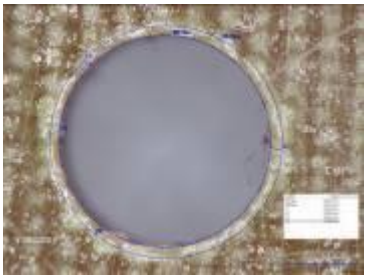

d8L

d8u

d9L

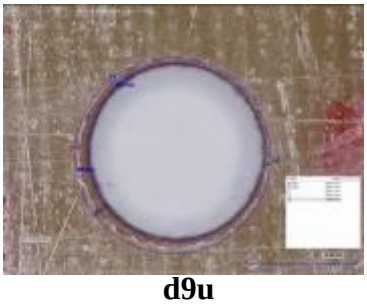

d9u

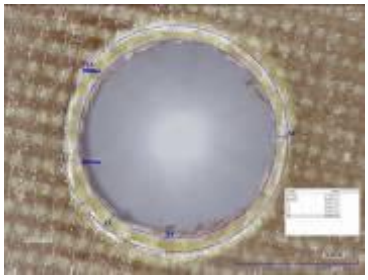

d10L

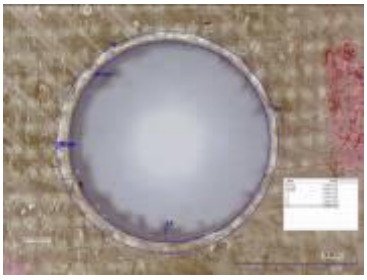

d10u

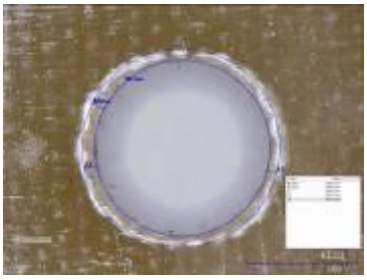

d11L

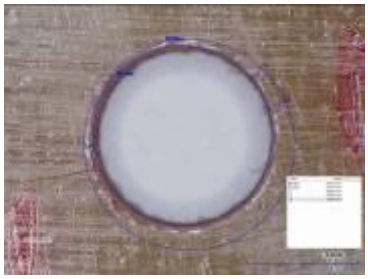

d11u

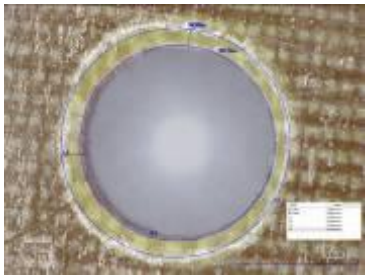

d12L

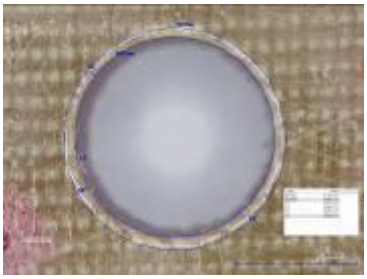

d12u

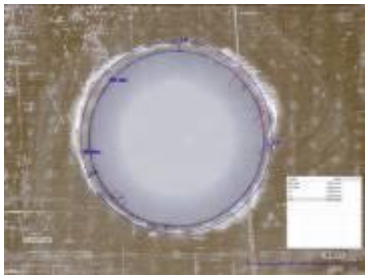

d13L

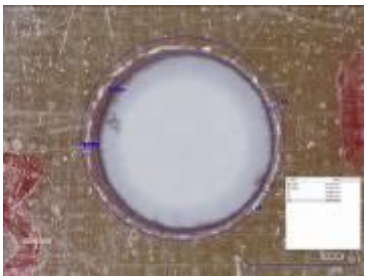

d13u

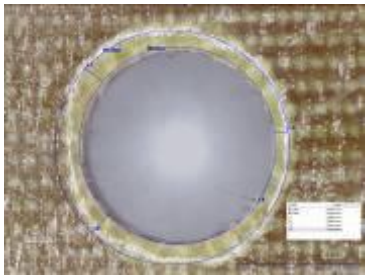

d14L

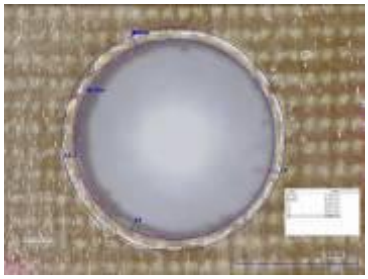

d14u

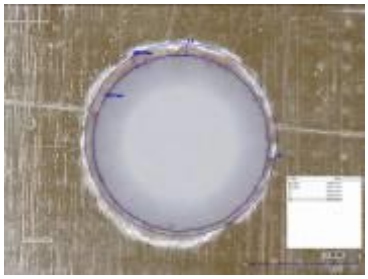

d15L

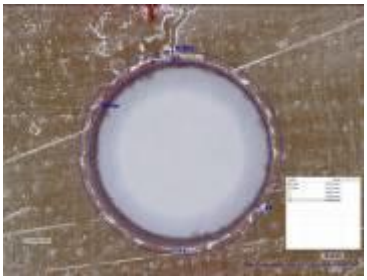

d15u

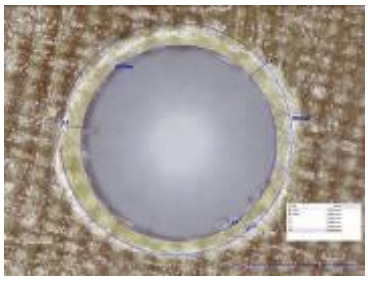

d16L

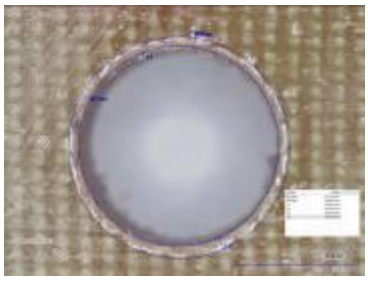

d16u

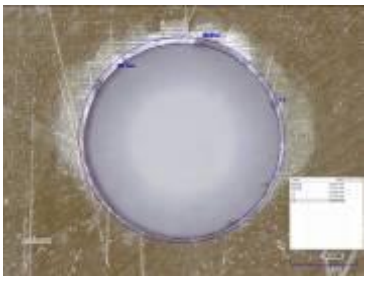

M1L

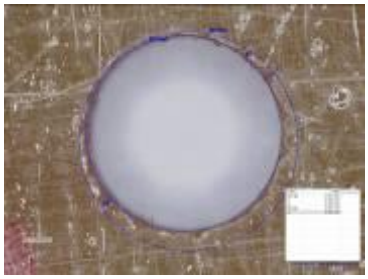

M1u

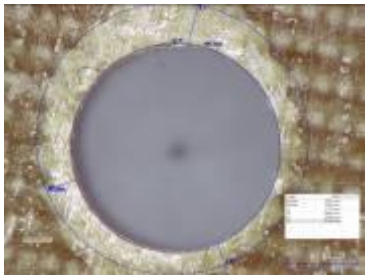

M2L

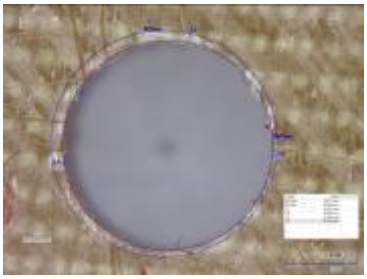

M2u

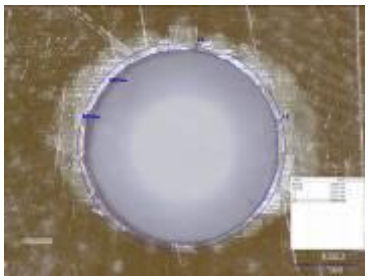

M3L

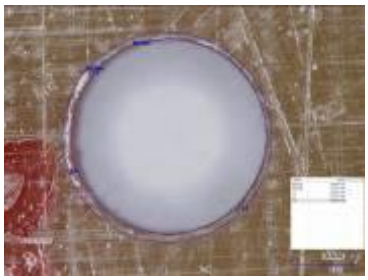

M3u

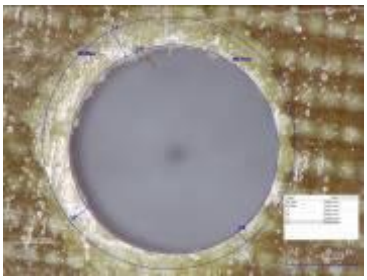

M4L

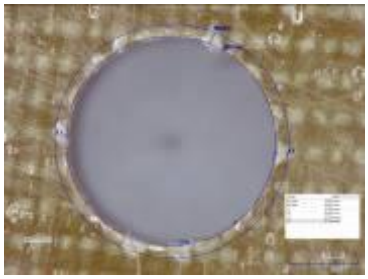

M4u

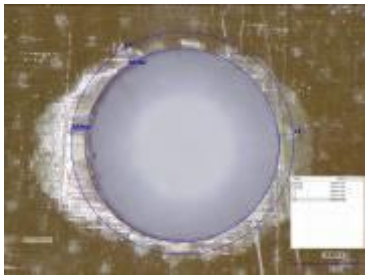

M5L

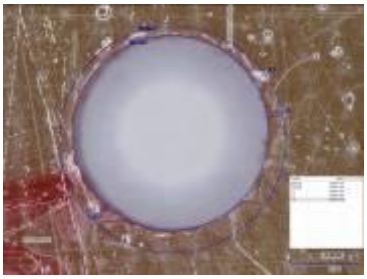

M5u

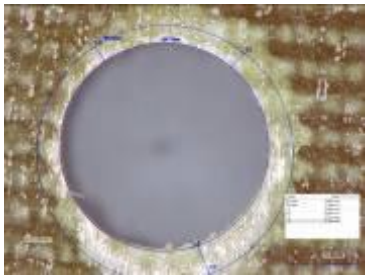

M6L

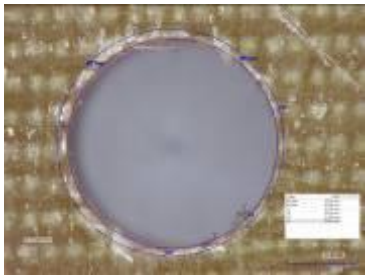

M6u

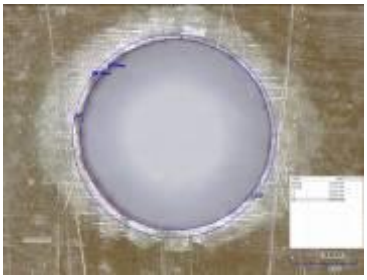

M7L

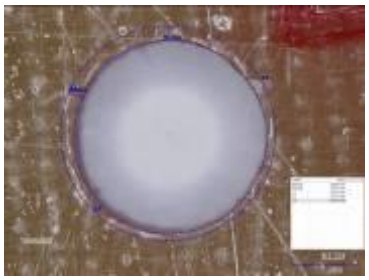

M7u

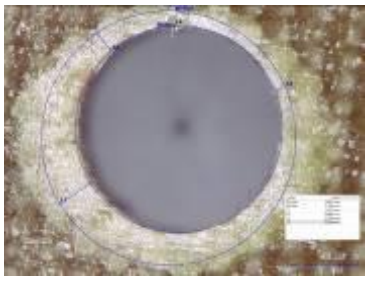

M8L

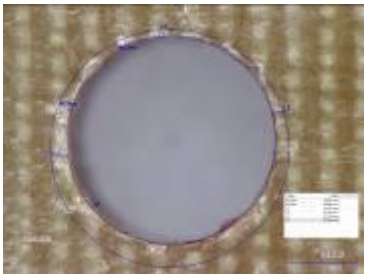

M8u

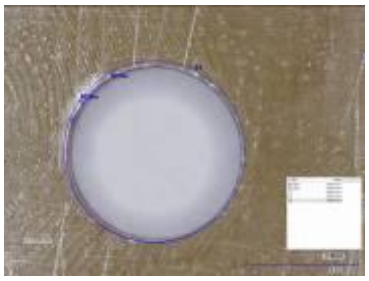

M9L

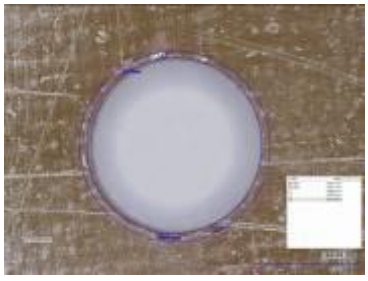

M9u

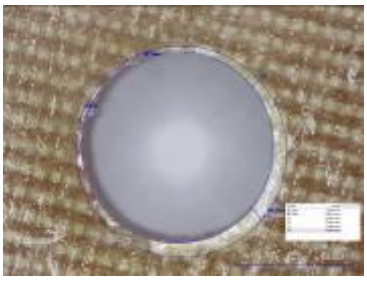

M10L

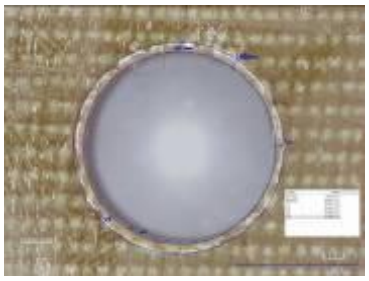

M10u

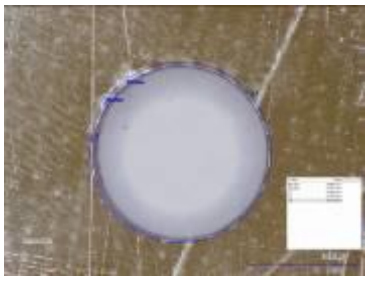

M11L

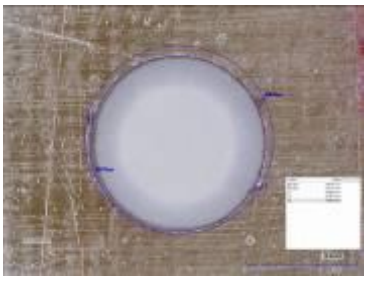

M11u

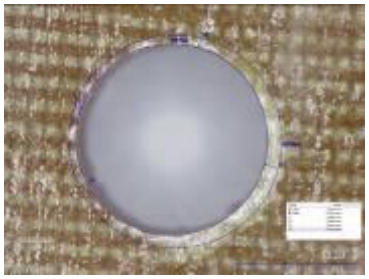

M12L

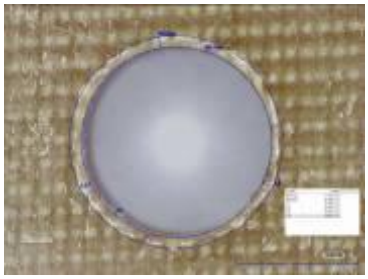

M12u

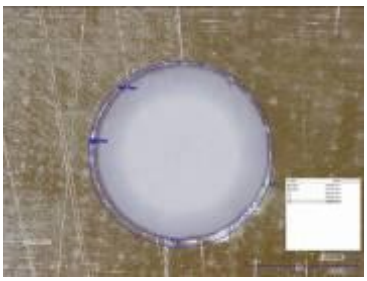

M13L

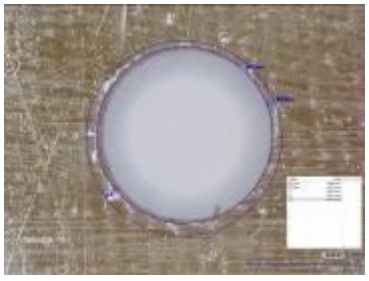

M13u

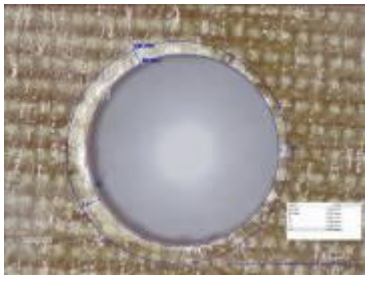

M14L

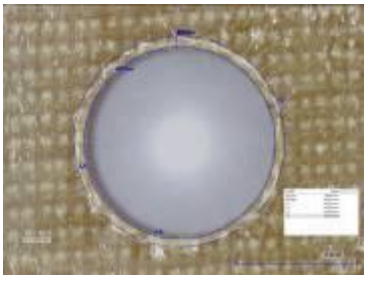

M14u

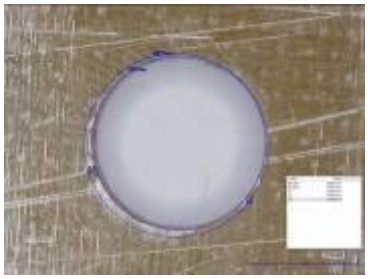

M15L

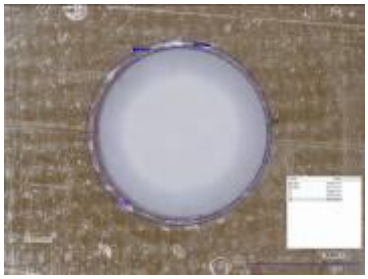

M15u

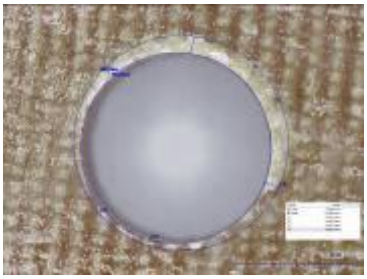

M16L

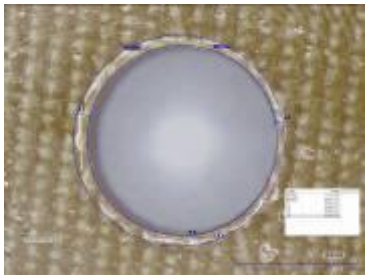

M16u

Appendix D: Optical Microscopic Pictures for Group (1) of AWJM Process

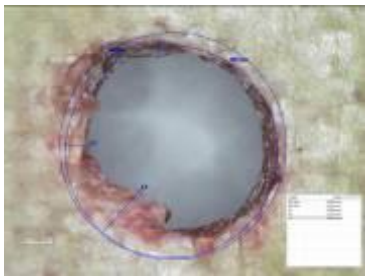

ad1L1

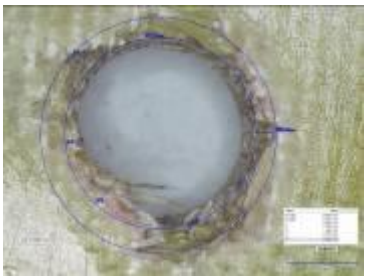

ad1L2

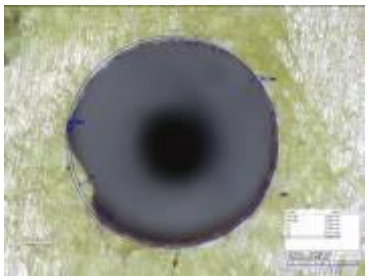

ad1L3

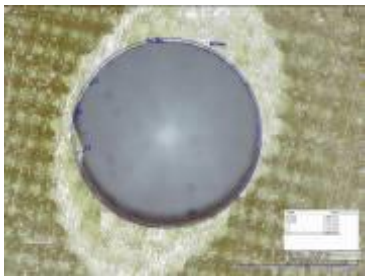

ad1L4

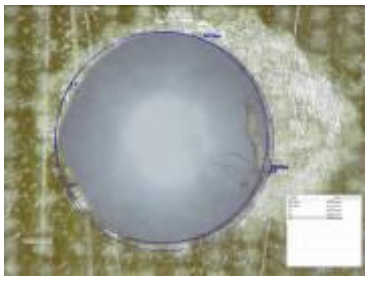

ad1L5

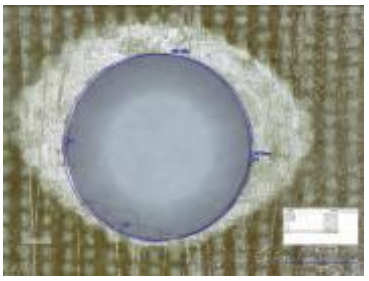

ad1L6

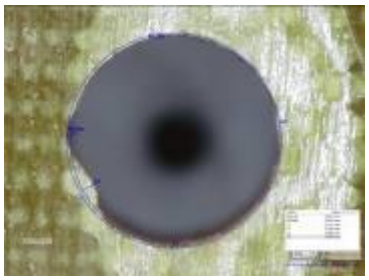

ad1L7

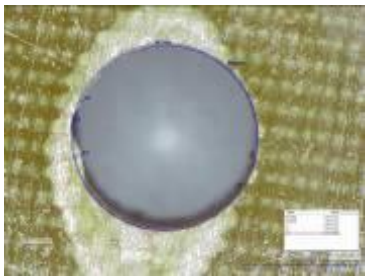

ad1L8

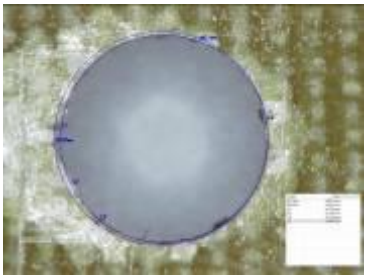

ad1L9

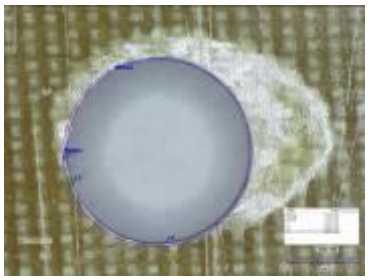

ad1L10

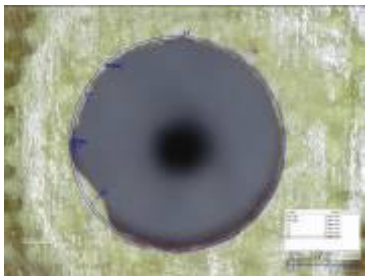

ad1L11

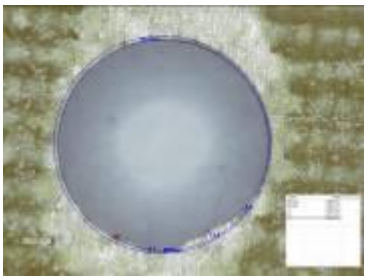

ad1L12

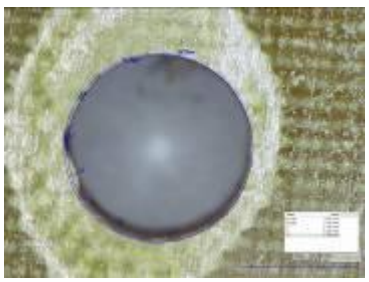

ad1L13

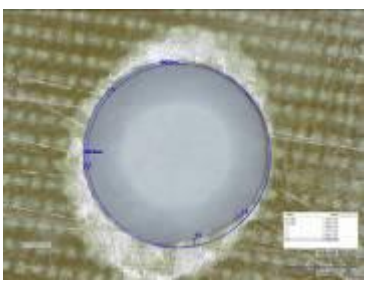

ad1L14

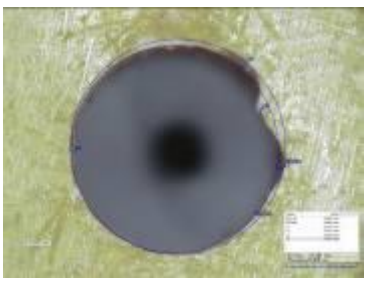

ad1L15

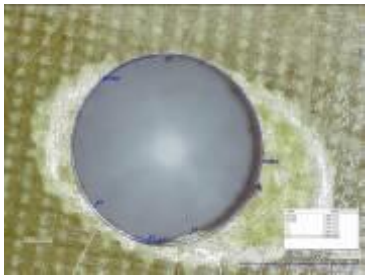

ad1L16

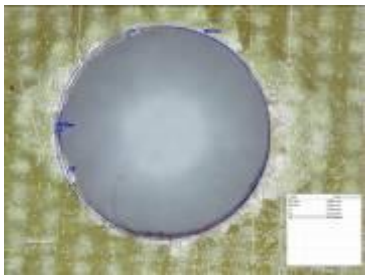

ad1L17

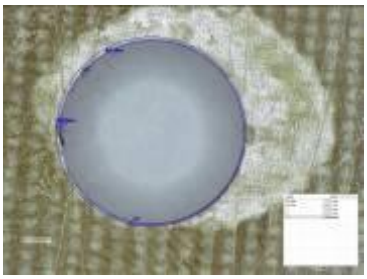

ad1L18

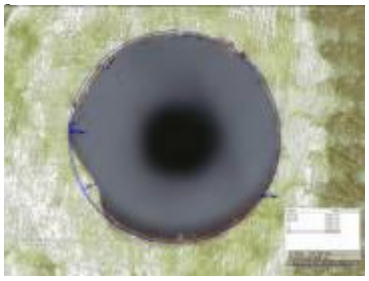

ad1L19

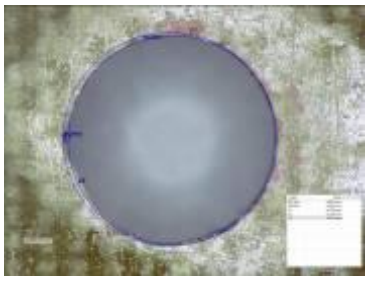

ad1L20

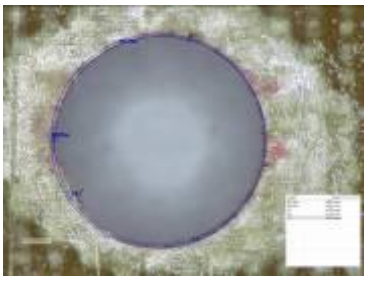

ad1L21

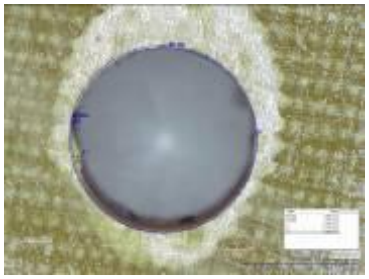

ad1L22

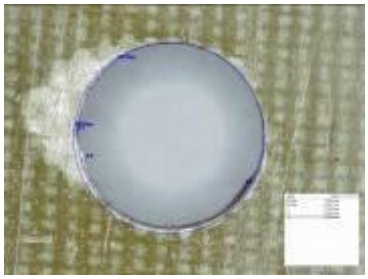

ad1L23

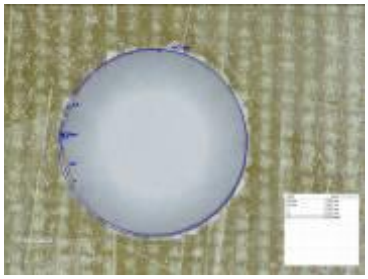

ad1L24

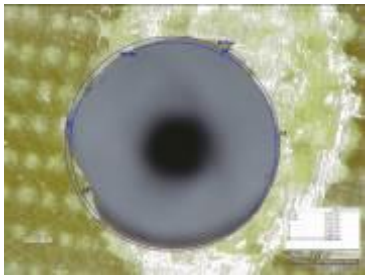

ad1L25

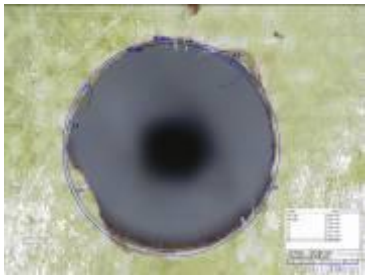

ad1L26

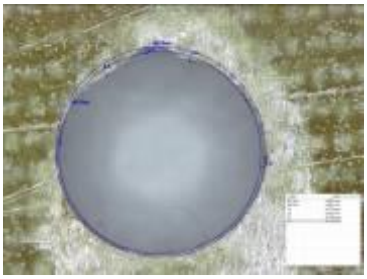

ad1L27

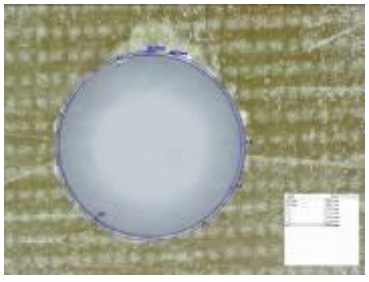

ad1L28

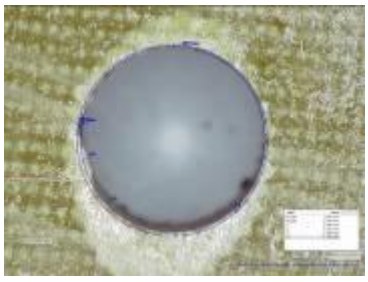

ad1L29

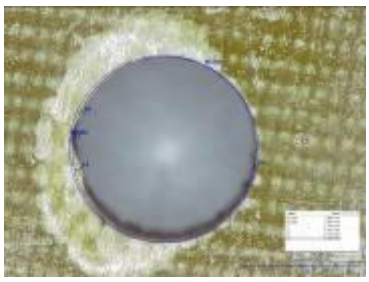

ad1L30

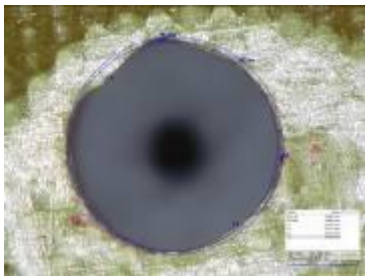

ad1L31

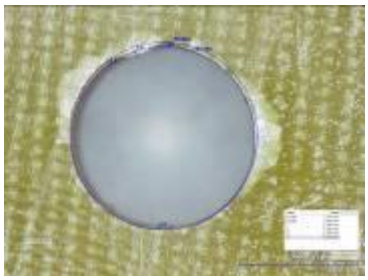

ad1L32

ad1u1

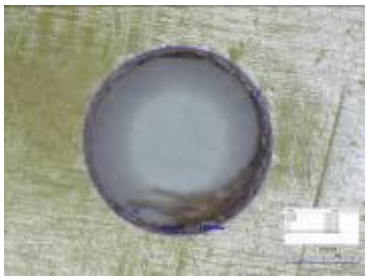

ad1u2

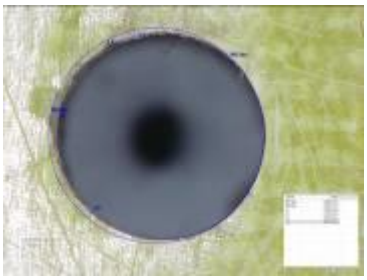

ad1u3

ad1u4

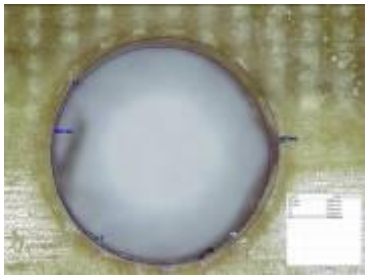

ad1u5

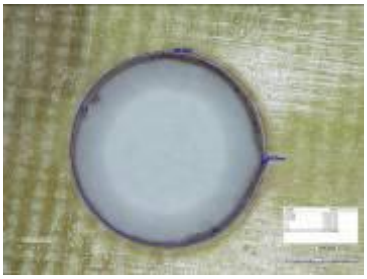

ad1u6

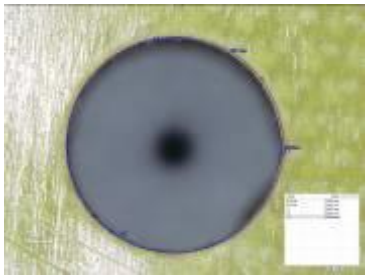

ad1u7

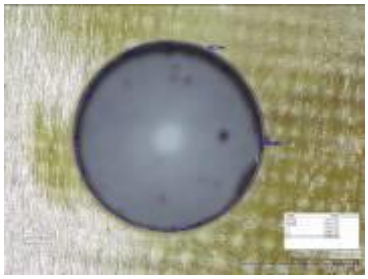

ad1u8

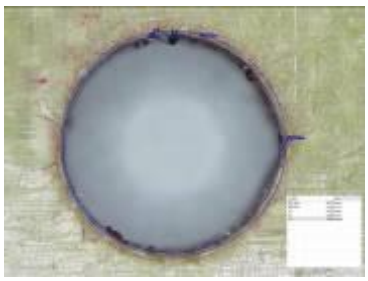

ad1u9

ad1u10

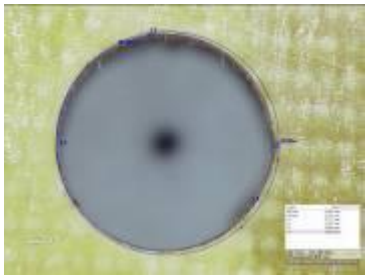

ad1u11

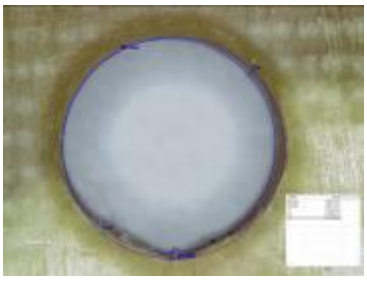

ad1u12

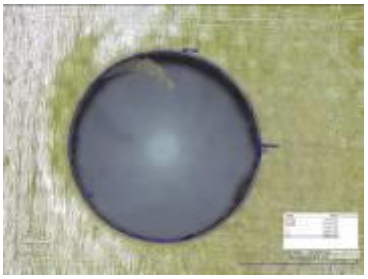

ad1u13

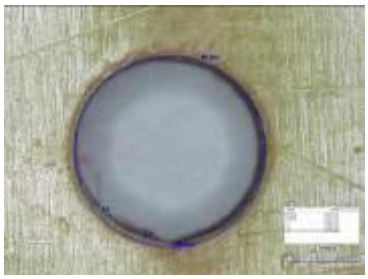

ad1u14

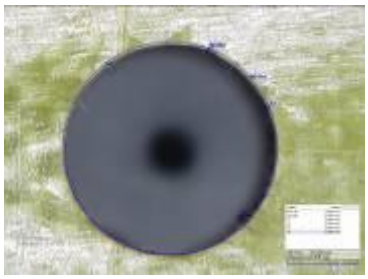

ad1u15

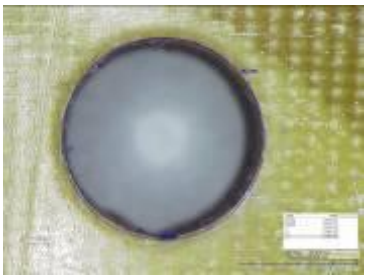

ad1u16

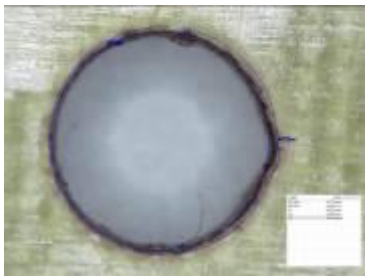

ad1u17

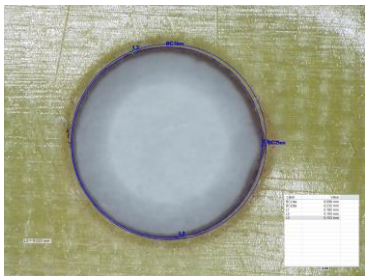

ad1u18

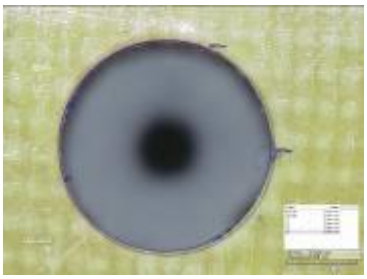

ad1u19

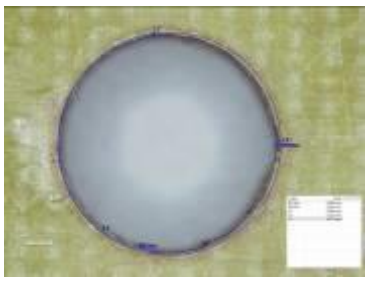

ad1u20

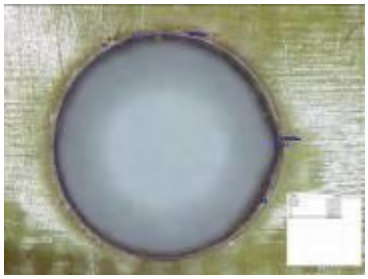

ad1u21

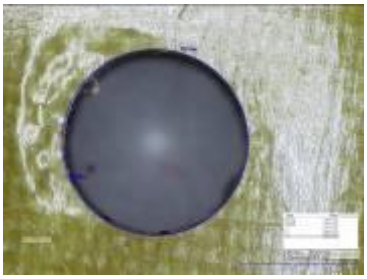

ad1u22

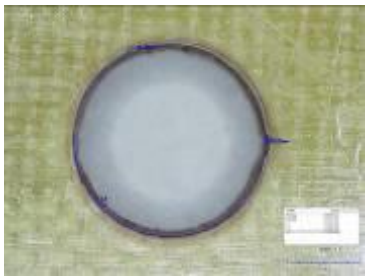

ad1u23

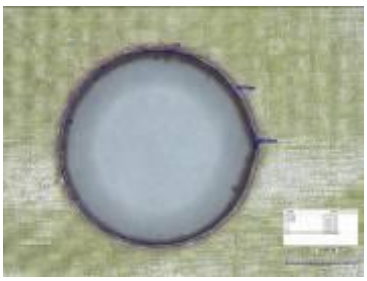

ad1u24

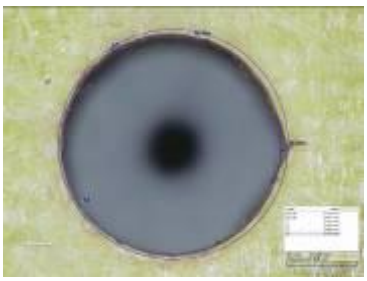

ad1u25

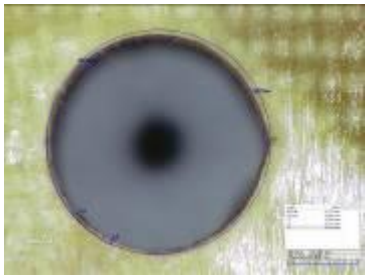

ad1u26

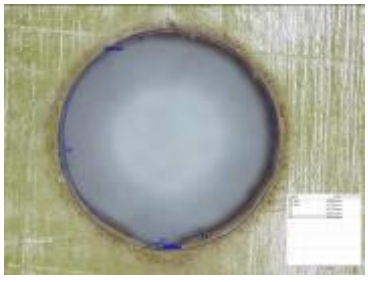

ad1u27

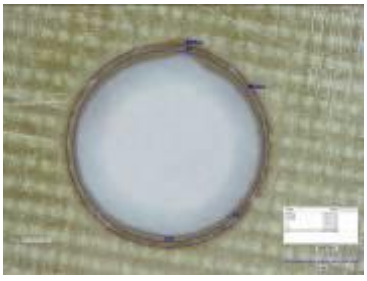

ad1u28

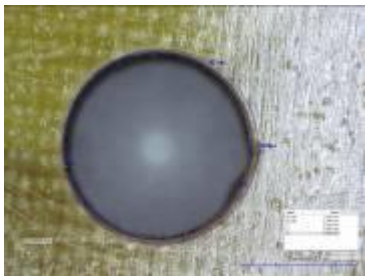

ad1u29

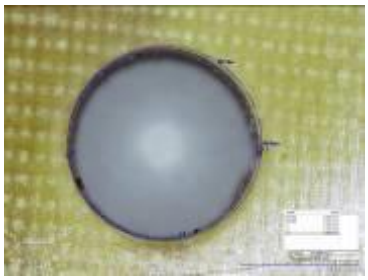

ad1u30

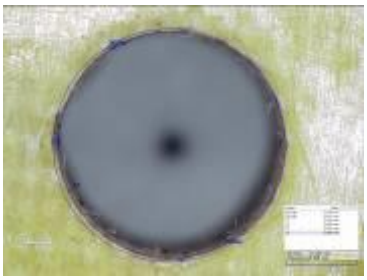

ad1u31

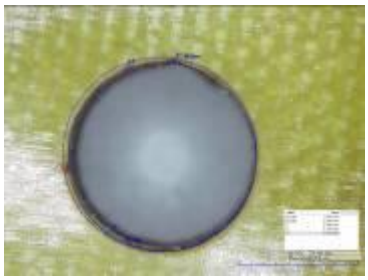

ad1u32

Appendix E: Optical Microscopic Pictures for Group (2) of AWJM Process

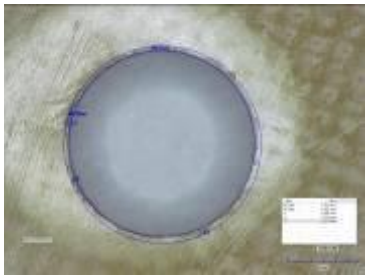

ad2L9

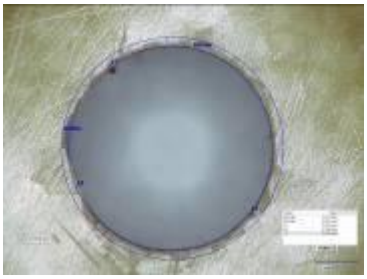

ad2L10

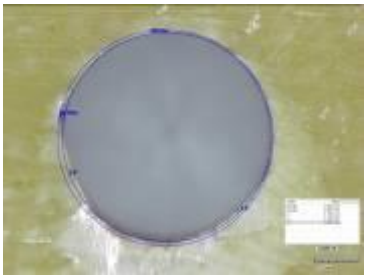

ad2L11

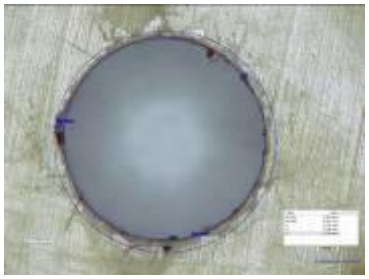

ad2L12

ad2L13

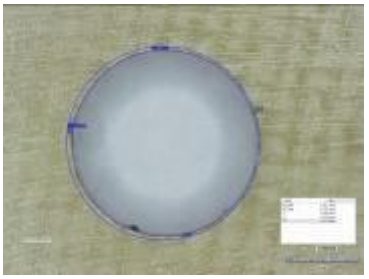

ad2L14

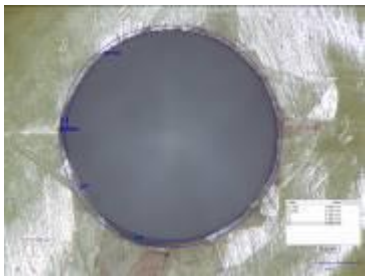

ad2L15

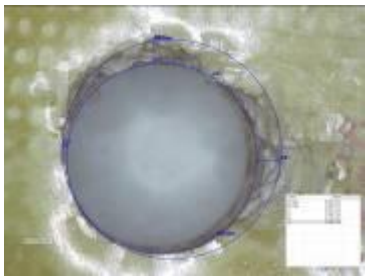

ad2L16

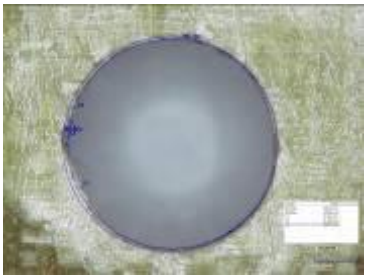

ad1L17~

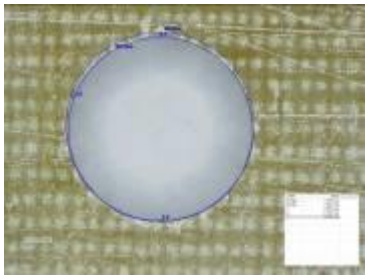

ad1L18~

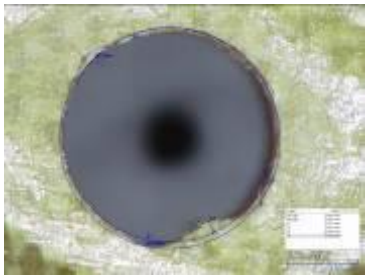

ad1L19~

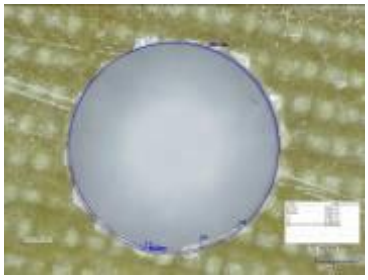

ad1L20~

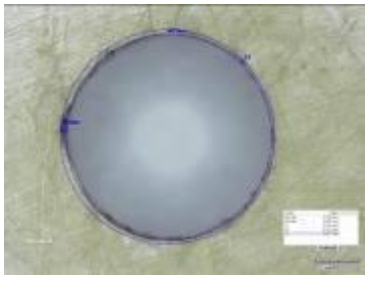

ad2L21

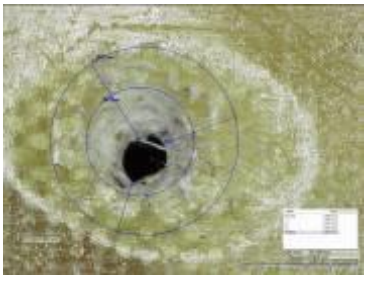

ad1L22~

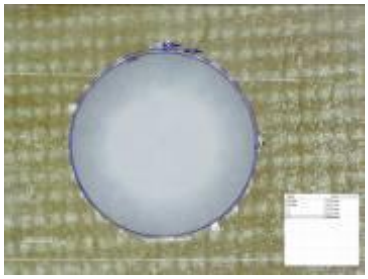

ad1L23~

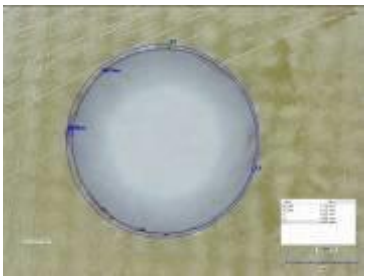

ad2L24

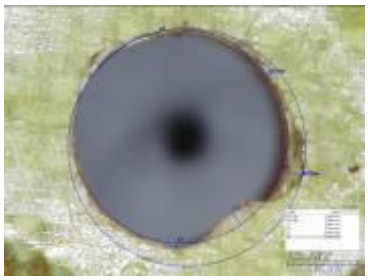

ad1L25~

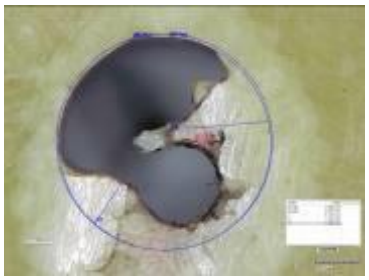

ad2L26

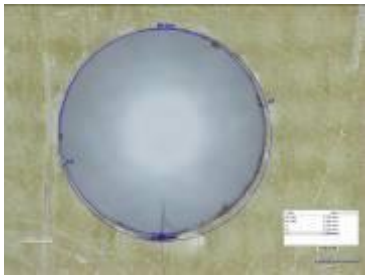

ad2L27

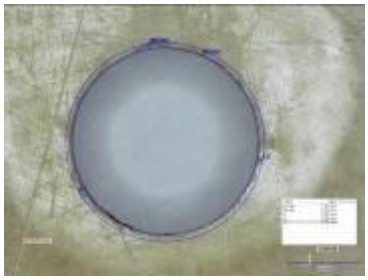

ad2L28

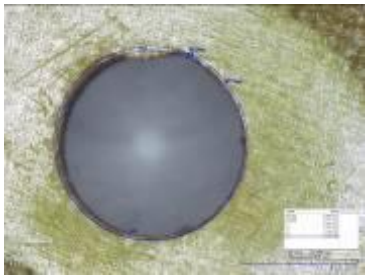

ad1L29~

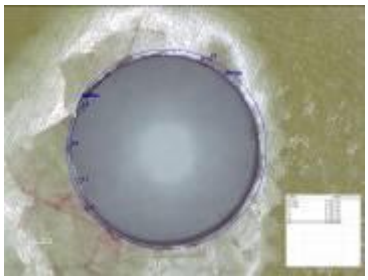

ad2L30

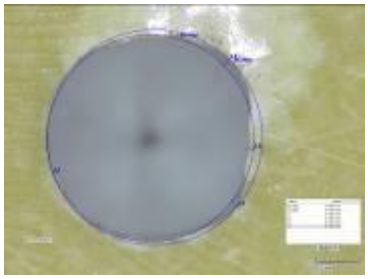

ad2L31

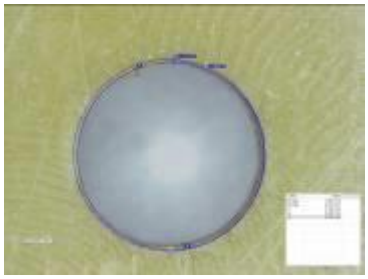

ad2L32

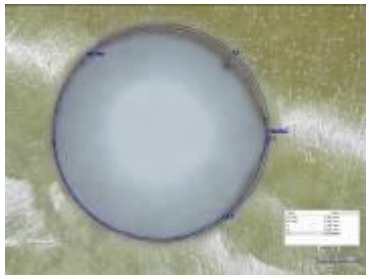

ad2u9

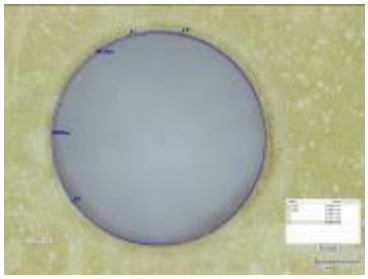

ad2u10

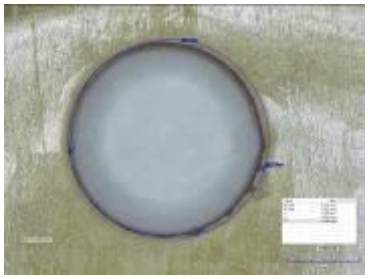

ad2u11

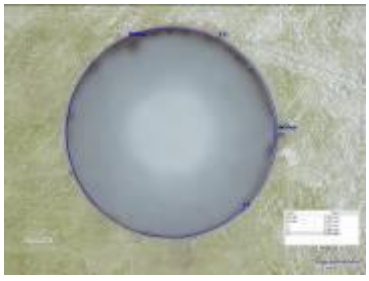

ad2u12

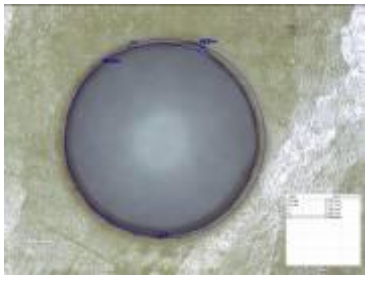

ad2u13

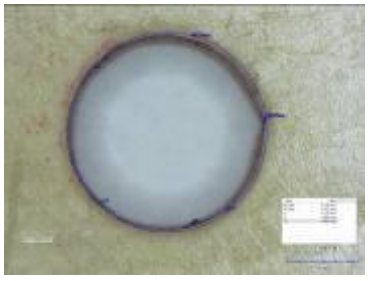

ad2u14

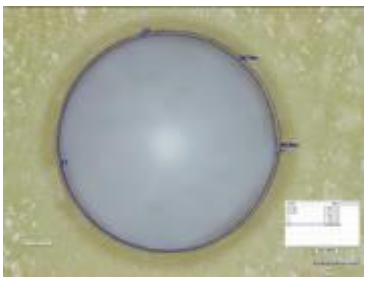

ad2u15

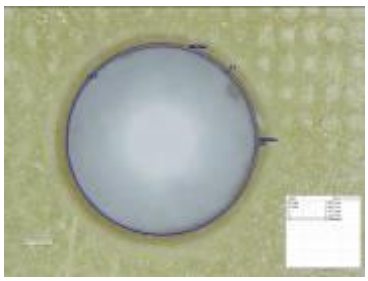

ad2u16

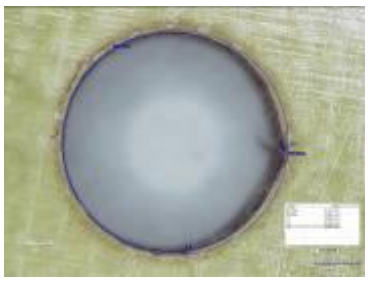

ad1u17~

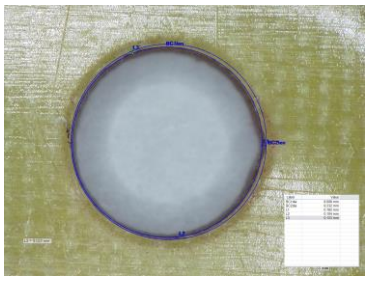

ad1u18~

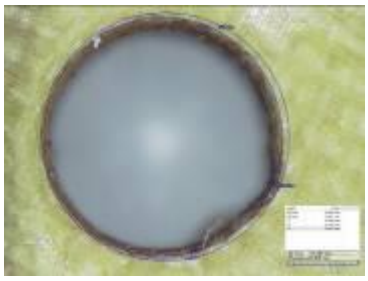

ad1u19~

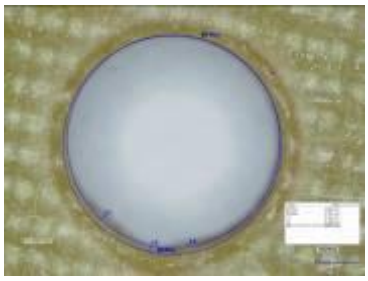

ad1u20~

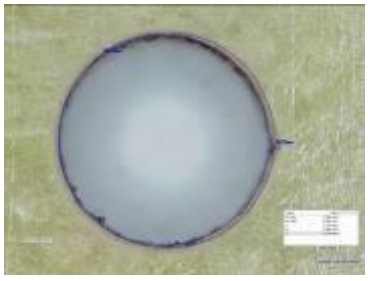

ad2u21

ad1u22~

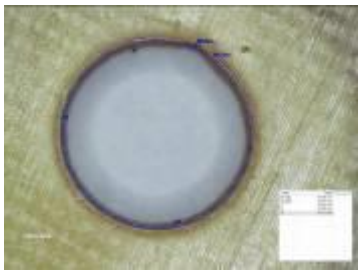

ad1u23~

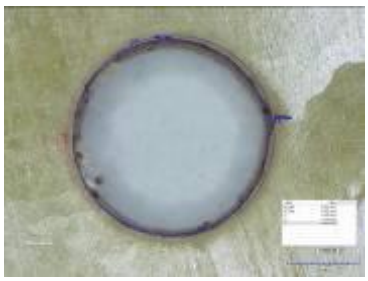

ad2u24

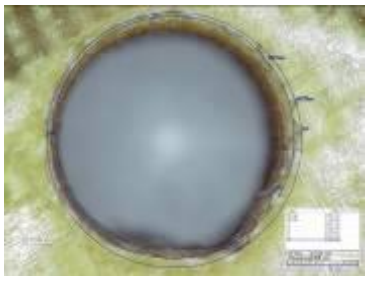

ad1u25~

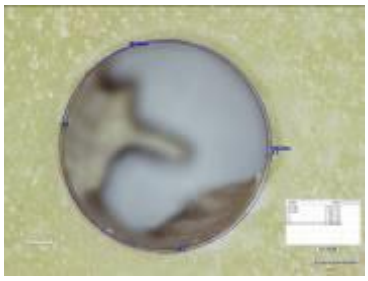

ad2u26

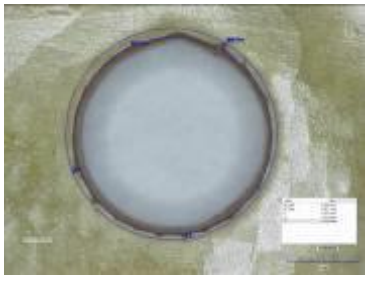

ad2u27

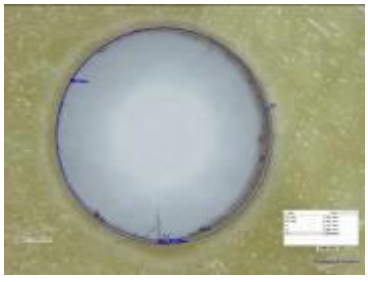

ad2u28

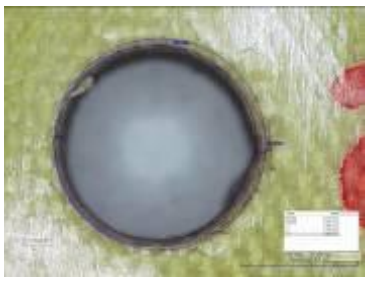

ad1u29~

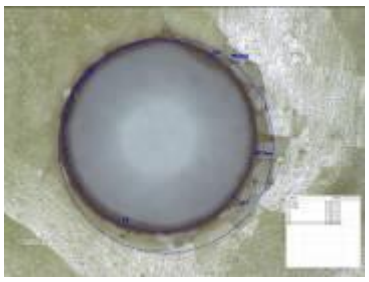

ad2u30

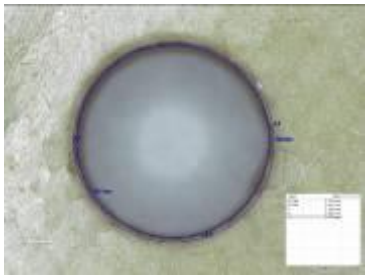

ad2u31

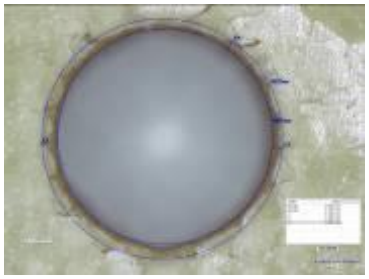

ad2u32

Appendix F: Optical Microscopic Pictures for Group (1) of LBM process

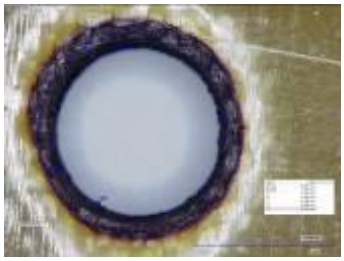

1L

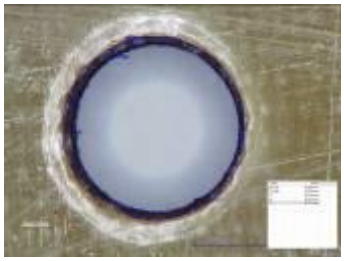

1u

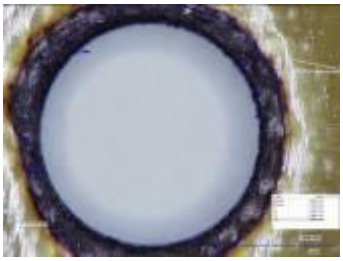

2L

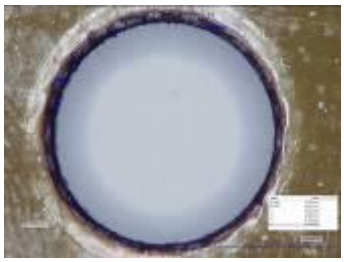

2u

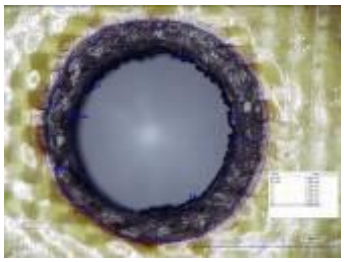

3L

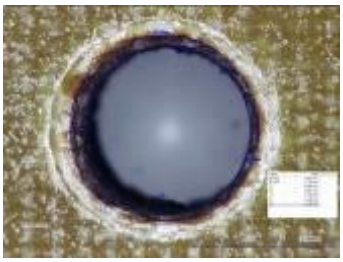

3u

4L

4u

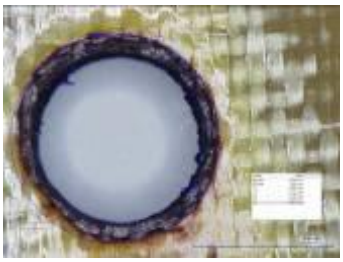

5L

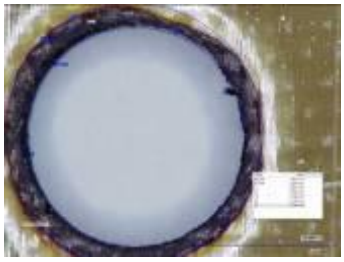

5u

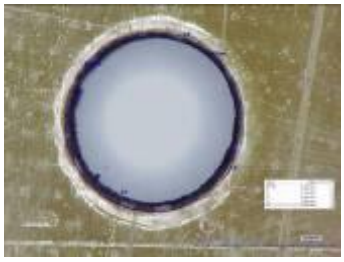

6L

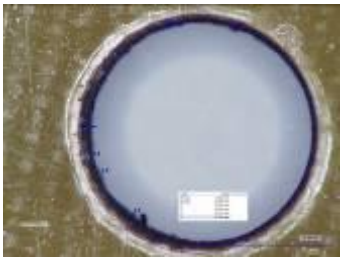

6u

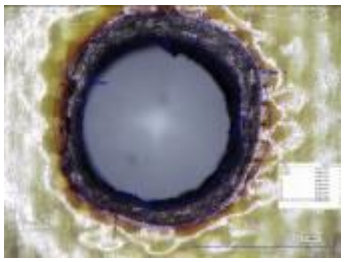

7L

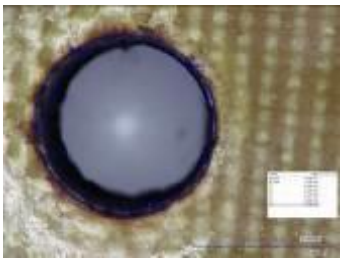

7u

8L

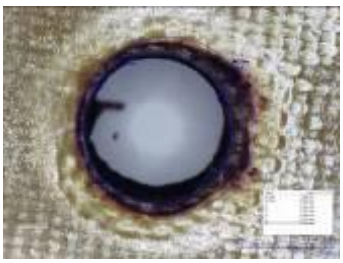

8u

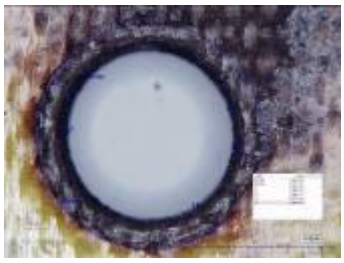

9L

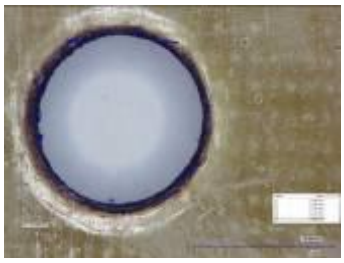

9u

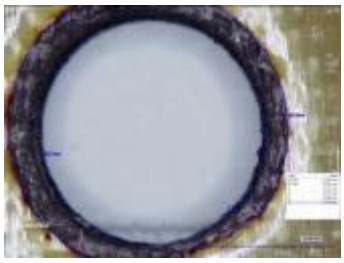

10L

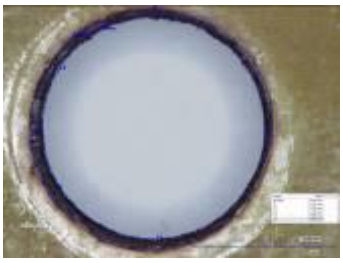

10u

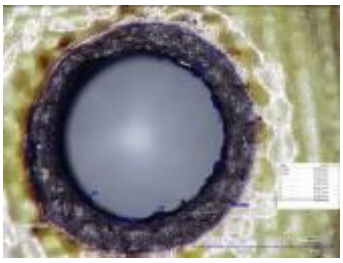

11L

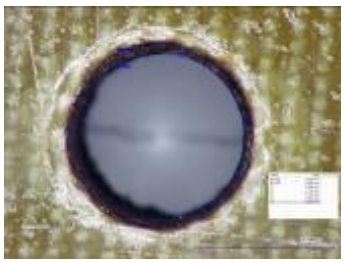

11u

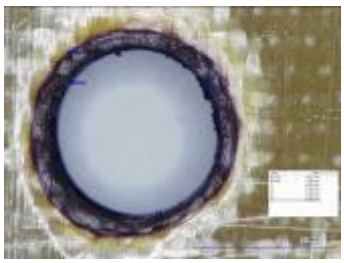

12L

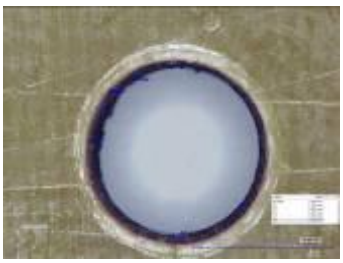

12u

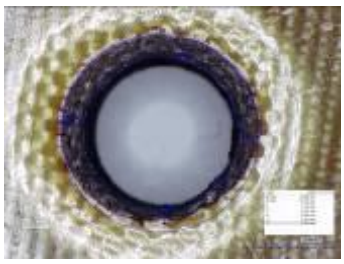

13L

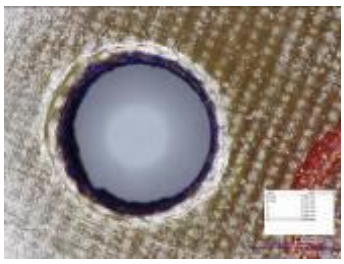

13u

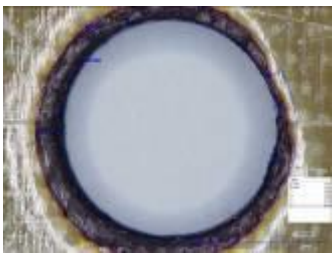

14L

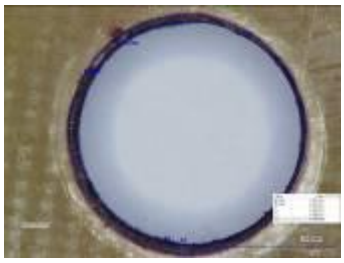

14u

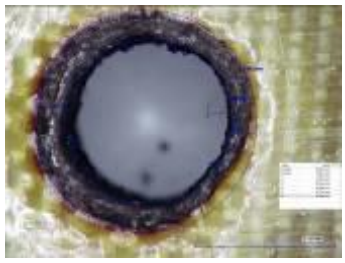

15L

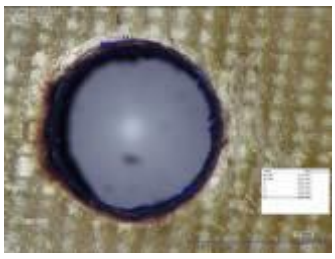

15u

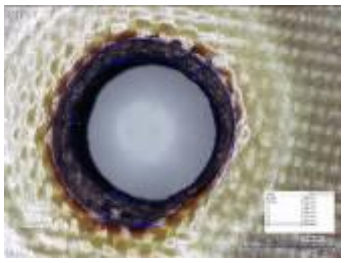

16L

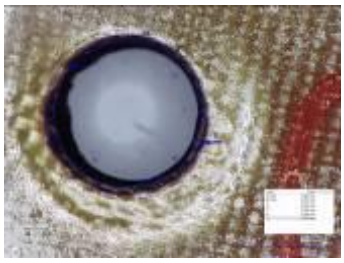

16u

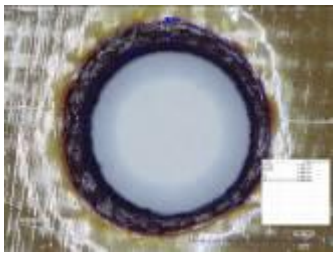

17L

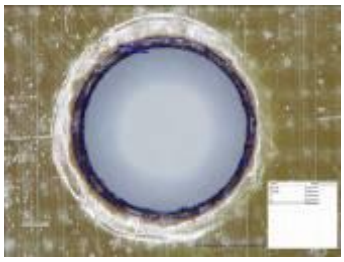

17u

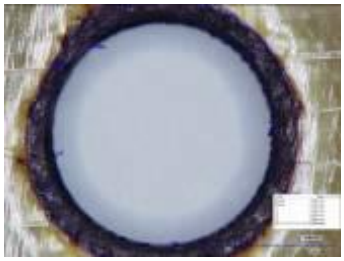

18L

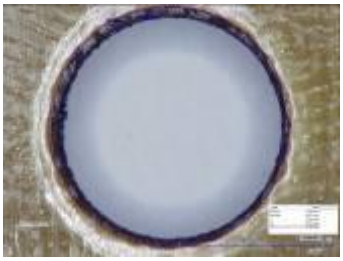

18u

19L

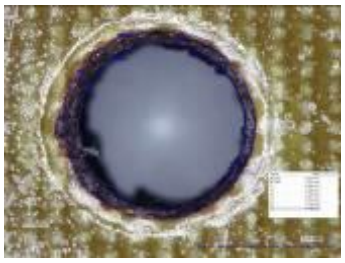

19u

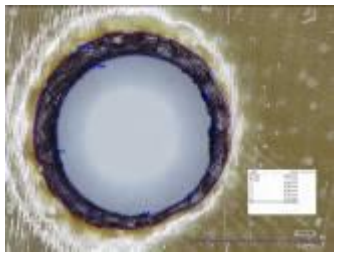

20L

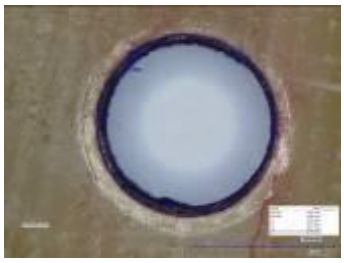

20u

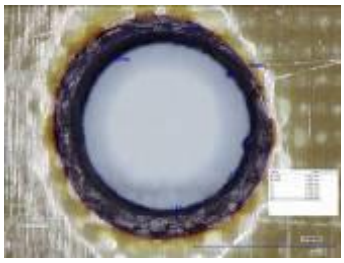

21L

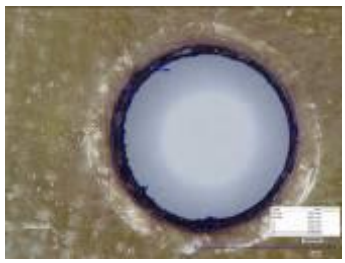

21u

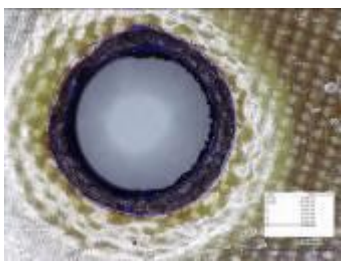

22L

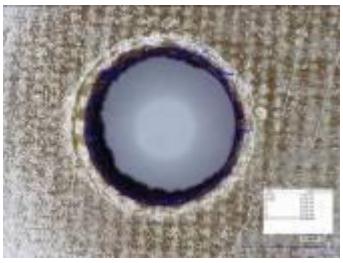

22u

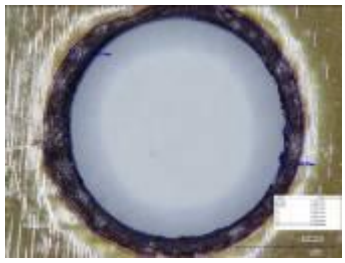

23L

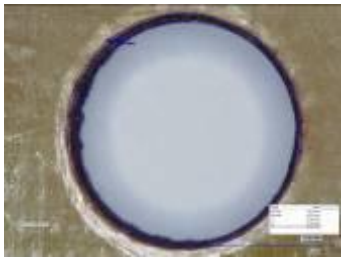

23u

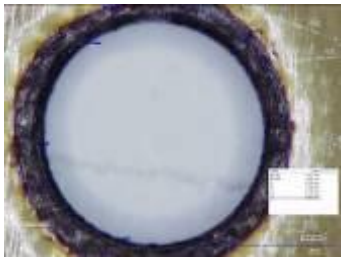

24L

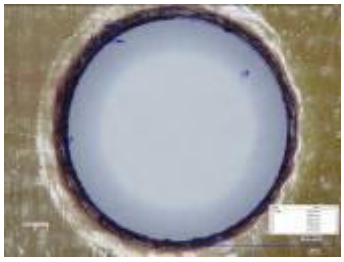

24u

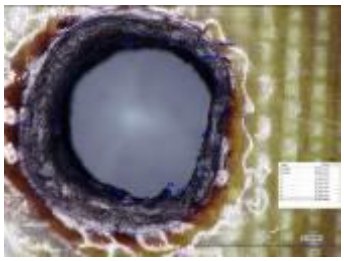

25L

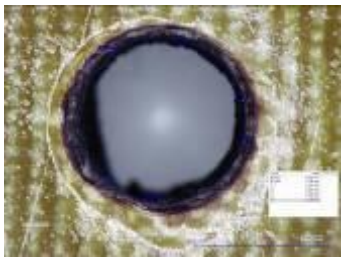

25u

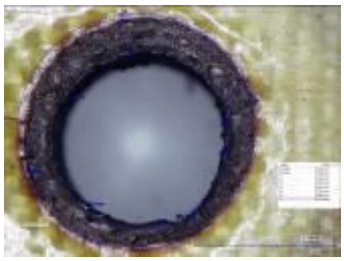

26L

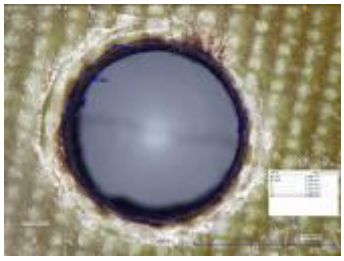

26u

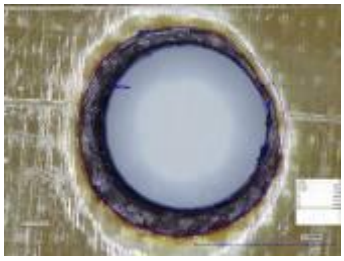

27L

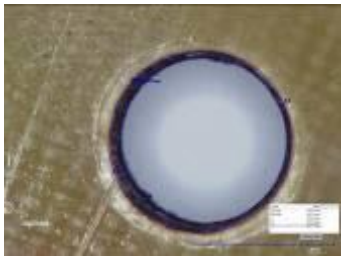

27u

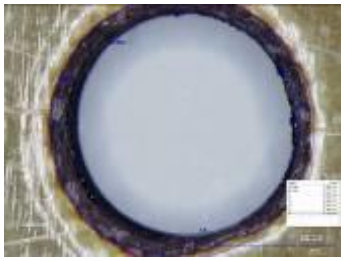

28L

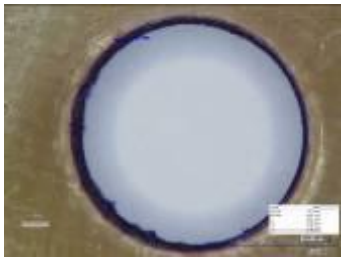

28u

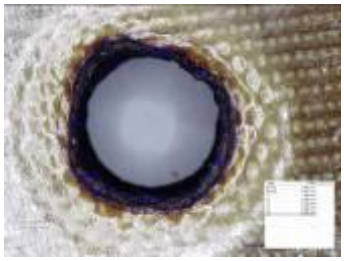

29L

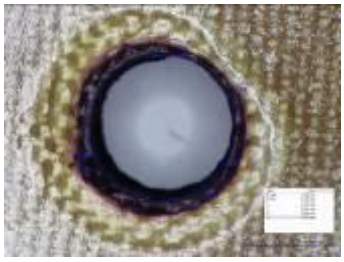

29u

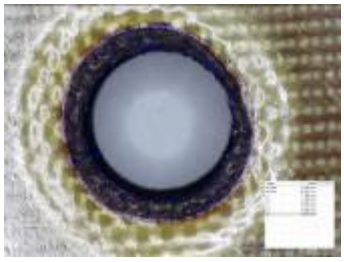

30L

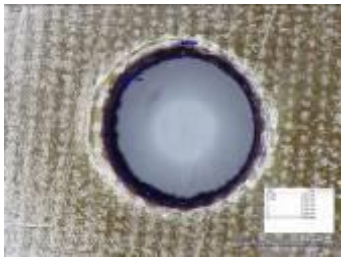

30u

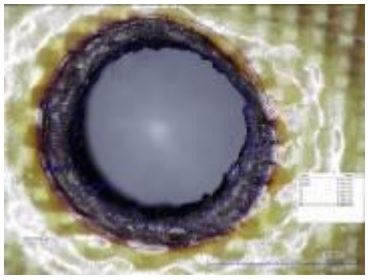

31L

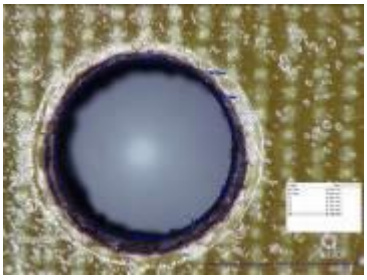

31u

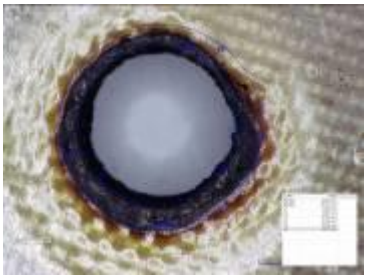

32L

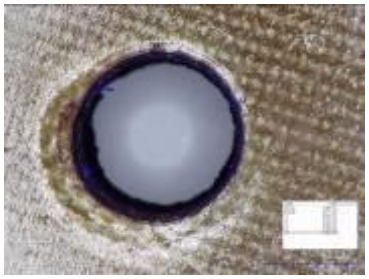

32u

Appendix G: Optical Microscopic Pictures for Group (2) of LBM Process

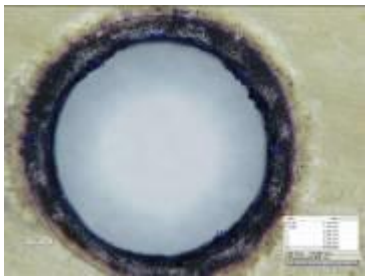

Ld2l 9

Ld2l10

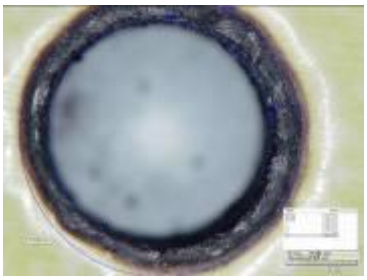

Ld2l11

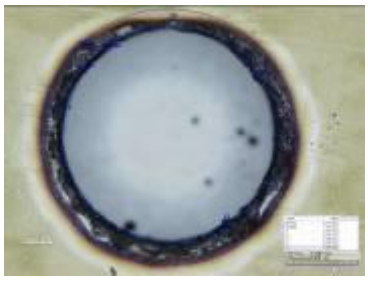

Ld2l 12

Ld2l13

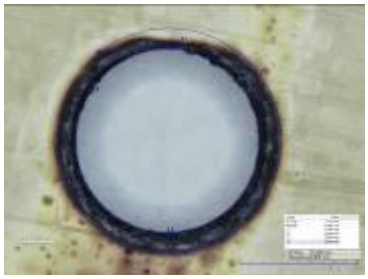

Ld2l14

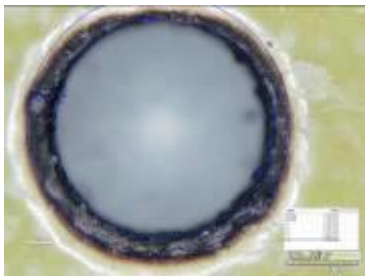

Ld2ll 5

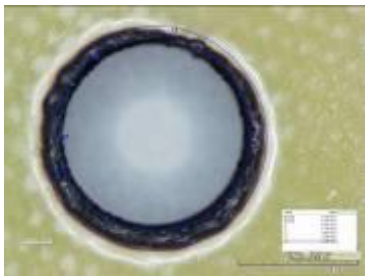

Ld2l16

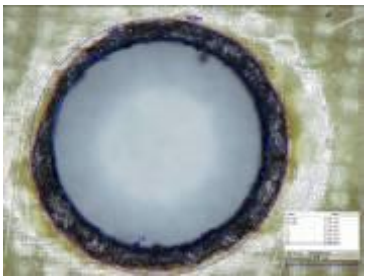

Ld1l17~

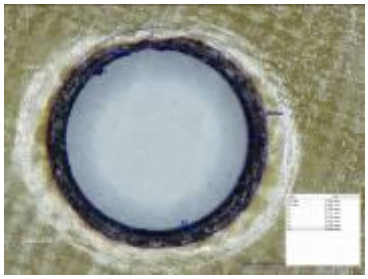

Ld1l 8~

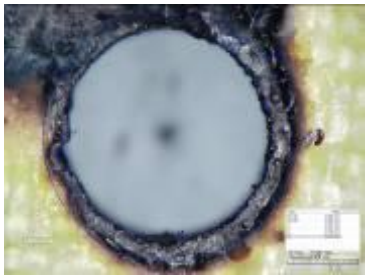

Ld1l19~

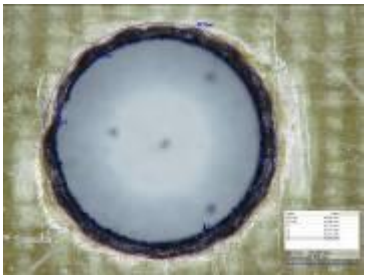

Ld1l20~

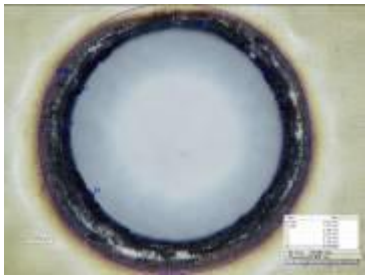

Ld2l21

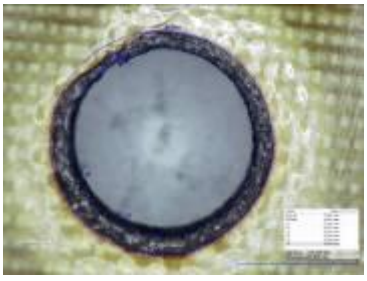

Ld1l22~

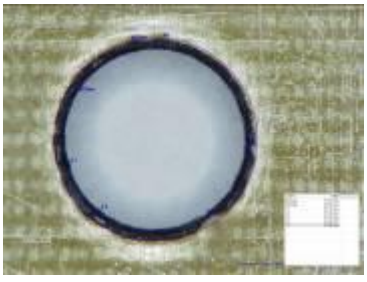

Ld1l23~

Ld2l24

Ld1l25~

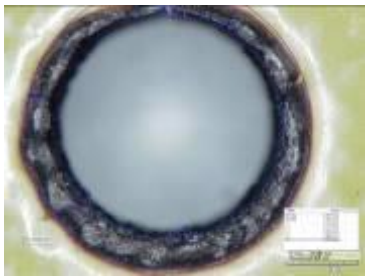

Ld2l26

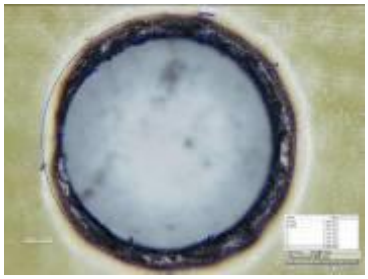

Ld2l27

Ld2l28

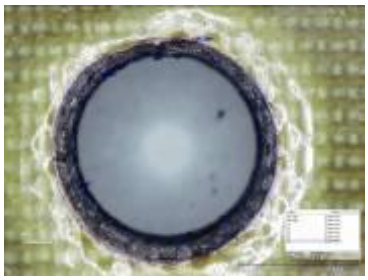

Ld1l29~

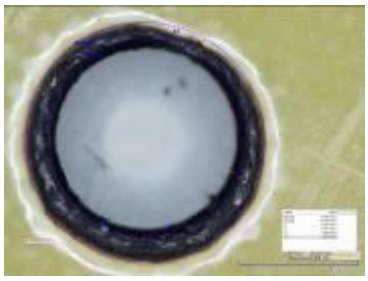

Ld2l30

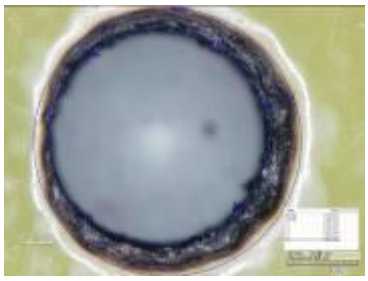

Ld2l31

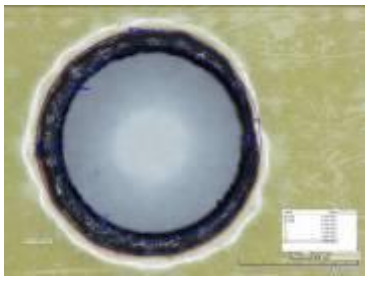

Ld2l32

Ld2u 9

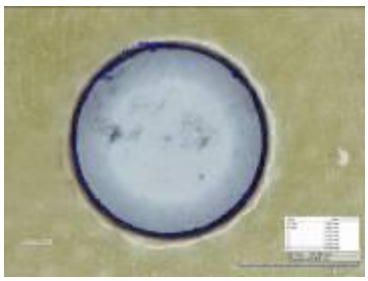

Ld2u10

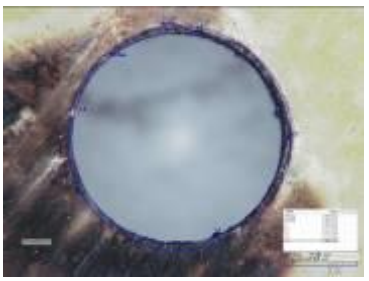

Ld2u11

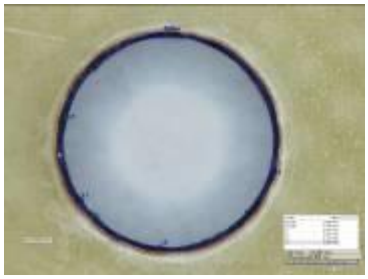

Ld2u12

Ld2u13

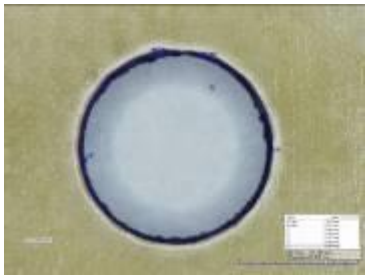

Ld2u14

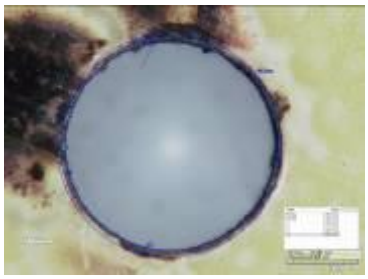

Ld2u15

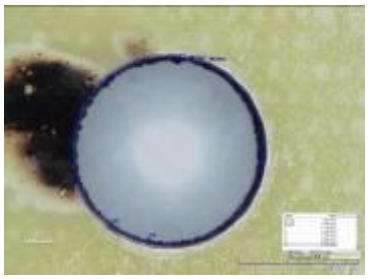

Ld2u16

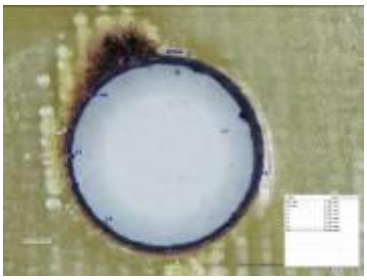

Ld1u17~

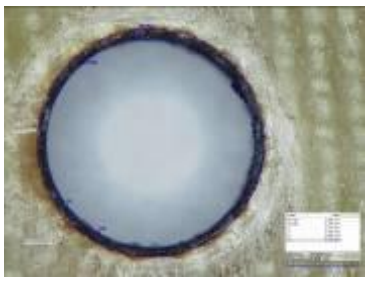

Ld1u18~

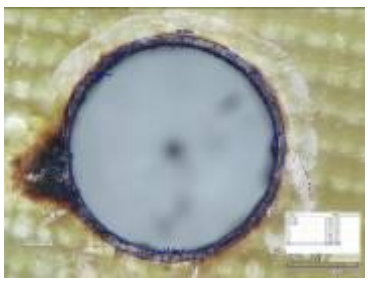

Ld1u19~

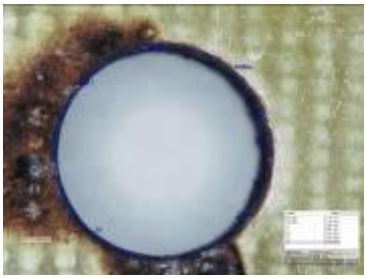

Ld1u20~

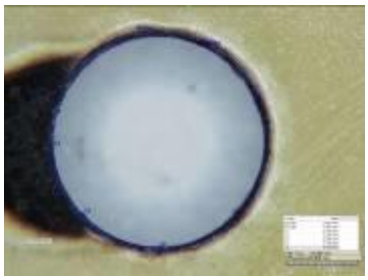

Ld2u21

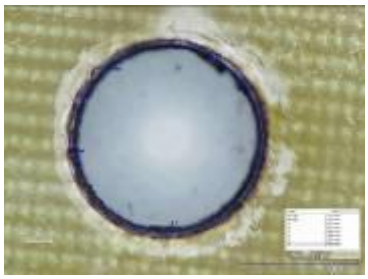

Ld1u22~

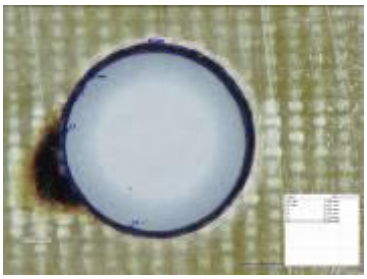

Ld1u23~

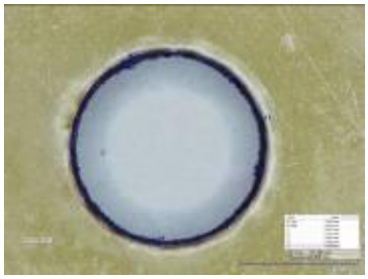

Ld2u24

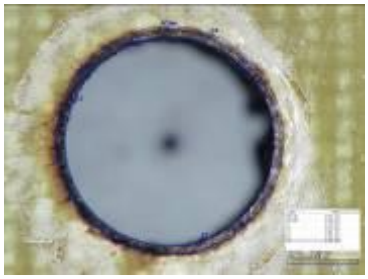

Ld1u25~

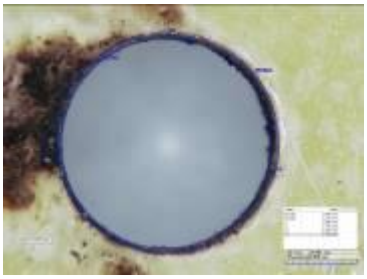

Ld2u26

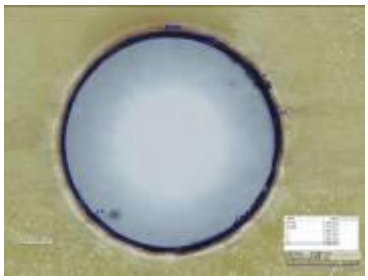

Ld2u27

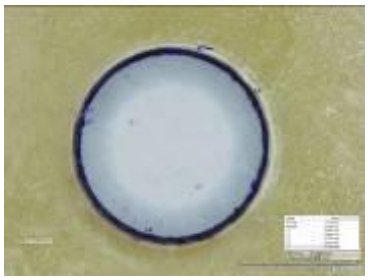

Ld2u28

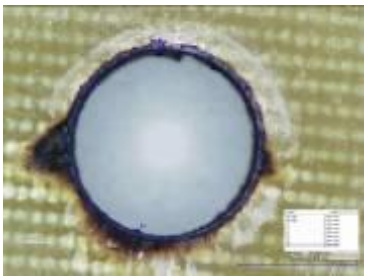

Ld1u29~

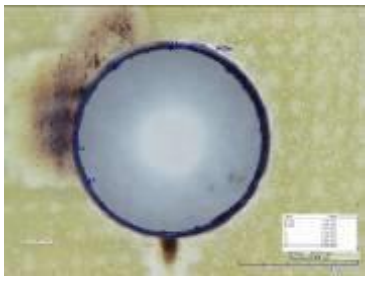

Ld2u30

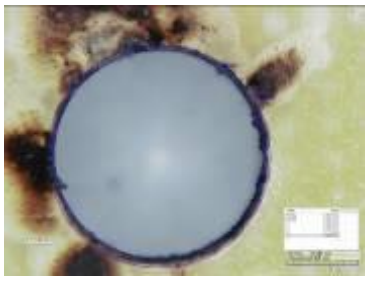

Ld2u31

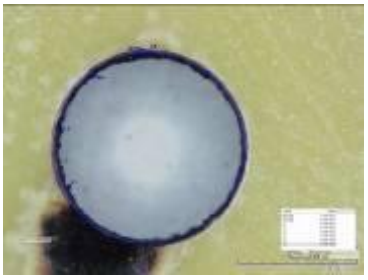

Ld2u32

Appendix H: Tensile Strength Calculations

Tensile strength = Max. load / (width of the specimen – hole diameter) × thickness of the specimen

Tensile strength for drilling cutting

Hole No.	Max. load (KN)	Width of specimen (mm)	Thickness of specimen (mm)	Hole diameter (mm)	Cross sectional area (mm^2)	Tensile strength (MPa)
d1	40.35	25	8	6	152	265.46
d2	49.52	25	16	6	304	162.89
d3	40.43	25	8	6	152	265.99
d4	45.7	25	16	6	304	150.33
d5	19.99	25	8	6	152	131.51
d6	47.67	25	16	6	304	156.81
d7	40.48	25	8	6	152	266.32
d8	46.8	25	16	6	304	153.95
d9	35.49	25	8	8	136	260.96
d10	40.93	25	16	8	272	150.48
d11	17.6	25	8	8	136	129.41
d12	41.06	25	16	8	272	150.96
d13	18.81	25	8	8	136	138.31
d14	41.71	25	16	8	272	153.35
d15	18.09	25	8	8	136	133.01
d16	40.79	25	16	8	272	149.96

Tensile strength for milling cutting

Hole No.	Max. load (KN)	Width of specimen (mm)	Thickness of specimen (mm)	Hole diameter (mm)	Cross sectional area (mm^2)	Tensile strength (Mpa)
M1	40.7	25	8	6	152	267.76
M2	58.71	25	16	6	304	193.13
M3	39.31	25	8	6	152	258.62
M4	48.4	25	16	6	304	159.21
M5	19.4	25	8	6	152	128.16
M6	48.14	25	16	6	304	158.36
M7	19.37	25	8	6	152	127.43
M8	45.04	25	16	6	304	148.16
M9	17.33	25	8	8	136	127.43
M10	58.39	25	16	8	272	214.67
M11	36.69	25	8	8	136	269.78
M12	41.34	25	16	8	272	151.99
M13	18.25	25	8	8	136	134.19
M14	42.28	25	16	8	272	155.44
M15	35.54	25	8	8	136	261.32
M16	44.4	25	16	8	272	163.24

Tensile strength for group 1 of AWJM

Hole No.	Max. load (KN)	Width of specimen (mm)	Thickness of specimen (mm)	Hole diameter (mm)	Cross sectional area (mm^2)	Tensile strength (MPa)
1	43.16	25	8	6	152	283.95
2	38.56	25	8	8	136	283.53
3	86.71	25	16	6	304	285.23
4	67.12	25	16	8	272	246.76
5	44.80	25	8	6	152	294.74
6	36.60	25	8	8	136	269.12
7	75.90	25	16	6	304	249.67
8	79.24	25	16	8	272	291.32
9	51.92	25	8	6	152	341.57
10	47.09	25	8	8	136	346.27
11	105.49	25	16	6	304	347.02
12	54.75	25	8	6	152	360.17
13	92.01	25	16	8	272	338.29
14	50.56	25	8	8	136	371.74
15	106.49	25	16	6	304	350.31
16	94.68	25	16	8	272	348.10
17	14.81	25	8	6	152	97.43
18	16.70	25	8	8	136	122.79
19	71.55	25	16	6	304	235.36
20	13.87	25	8	6	152	91.25
21	53.08	25	8	6	152	349.23
22	77.43	25	16	8	272	284.67
23	38.11	25	8	8	136	280.22
24	43.60	25	8	8	136	320.56
25	91.64	25	16	6	304	301.45
26	109.66	25	16	6	304	360.71
27	54.58	25	8	6	152	359.09
28	47.26	25	8	8	136	347.48
29	76.57	25	16	8	272	281.51
30	94.02	25	16	8	272	345.65
31	108.98	25	16	6	304	358.50
32	97.67	25	16	8	272	359.09

Tensile strength for group 2 of AWJM

Hole No.	Max. load (KN)	Width of specimen (mm)	Thickness of specimen (mm)	Hole diameter (mm)	Cross sectional area (mm^2)	Tensile strength (MPa)
1	43.16	25	8	6	152	283.95
2	38.56	25	8	8	136	283.53
3	86.71	25	16	6	304	285.23
4	67.12	25	16	8	272	246.76
5	44.80	25	8	6	152	294.74
6	36.60	25	8	8	136	269.12
7	75.90	25	16	6	304	249.67
8	79.24	25	16	8	272	291.32
9	17.51	25	8	6	152	115.20
10	15.71	25	8	8	136	115.51
11	91.08	25	16	6	304	299.6
12	41.74	25	8	6	152	274.61
13	74.69	25	16	8	272	274.60
14	13.33	25	8	8	136	98.01
15	88.70	25	16	6	304	291.78
16	61.12	25	16	8	272	224.71
17	42.62	25	8	6	152	280.39
18	35.90	25	8	8	136	263.97
19	71.55	25	16	6	304	235.36
20	15.04	25	8	6	152	98.95
21	42.82	25	8	6	152	281.71
22	77.43	25	16	8	272	284.67
23	15.61	25	8	8	136	114.78
24	16.23	25	8	8	136	119.34
25	89.62	25	16	6	304	294.8
26	88.60	25	16	6	304	291.45
27	10.94	25	8	6	152	71.97
28	16.26	25	8	8	136	119.56
29	75.98	25	16	8	272	279.34
30	78.12	25	16	8	272	287.21
31	87.62	25	16	6	304	288.22
32	76.63	25	16	6	272	281.73

Tensile strength for group 1 of LBM

Hole No.	Max.Load (KN)	Width of the specimen (mm)	Thickness of the specimen (mm)	Hole diameter (mm)	Cross sectional area $(mm)^2$	Tensile strength (Mpa)
1	24.18	25	8	6	152	159.08
2	33.59	25	8	8	136	246.99
3	48.80	25	16	6	304	160.53
4	46.22	25	16	8	272	169.93
5	16.48	25	8	6	152	108.42
6	14.20	25	8	8	136	104.41
7	48.50	25	16	6	304	159.54
8	37.61	25	16	8	272	138.27
9	27.73	25	8	6	152	182.41
10	20.71	25	8	8	136	152.252
11	70.55	25	16	6	304	232.067
12	28.22	25	8	6	152	185.657
13	60.37	25	16	8	272	221.935
14	21.11	25	8	8	136	155.244
15	87.80	25	16	6	304	288.83
16	62.78	25	16	8	272	230.809
17	13.50	25	8	6	152	88.82
18	31.13	25	8	8	136	228.90
19	53.36	25	16	6	304	175.53
20	40.59	25	8	6	152	267.04
21	23.31	25	8	6	152	153.34
22	44.82	25	16	8	272	164.78
23	12.40	25	8	8	136	91.18
24	51.05	25	8	8	136	375.4
25	55.88	25	16	6	304	183.82
26	71.47	25	16	6	304	235.093
27	28.12	25	8	6	152	184.994
28	20.32	25	8	8	136	149.379
29	47.86	25	16	8	272	175.96
30	70.64	25	16	8	272	259.692
31	70.09	25	16	6	304	230.571
32	67.30	25	16	8	272	247.435

Tensile strength for group 2 of LBM

Hole No.	Max.Load (KN)	Width of the specimen (mm)	Thickness of the specimen (mm)	Hole diameter (mm)	Cross sectional area (mm)	Tensile strength (Mpa)
1	24.18	25	8	6	152	59.08
2	33.59	25	8	8	136	246.99
3	48.80	25	16	6	304	160.53
4	46.22	25	16	8	272	169.93
5	16.48	25	8	6	152	108.42
6	14.20	25	8	8	136	104.41
7	48.50	25	16	6	304	159.54
8	37.61	25	16	8	272	138.27
9	10.87	25	8	6	152	71.51
10	9.57	25	8	8	136	70.37
11	20.03	25	16	6	304	65.89
12	11.72	25	8	6	152	77.11
13	17.88	25	16	8	272	65.73
14	10.78	25	8	8	136	79.26
15	21.30	25	16	6	304	70.07
16	18.96	25	16	8	272	69.69
17	13.45	25	8	6	152	88.49
18	11.45	25	8	8	136	84.19
19	41.50	25	16	6	304	136.51
20	39.86	25	8	6	152	262.24
21	10.41	25	8	6	152	68.49
22	35.41	25	16	8	272	130.18
23	12.86	25	8	8	136	94.56
24	10.03	25	8	8	136	73.75
25	52.29	25	16	6	304	172.01
26	19.02	25	16	6	304	62.56
27	11.55	25	8	6	152	75.99
28	10.62	25	8	8	136	78.09
29	35.72	25	16	8	272	131.32
30	17.91	25	16	8	272	65.84
31	21.33	25	16	6	304	70.18
32	19.01	25	16	8	272	69.88

Appendix K: Cost calculations

Cost calculation details for drilling process

Hole No.	Cutting time (sec)	Cost of tool (USD)	Cost of tool per hole (USD)	Machining cost (USD)/hour	Machining cost(USD)	Total cost (USD)
d1	22	1.92	0.019	11.2	0.068	0.087
d2	29	1.92	0.019	11.2	0.090	0.109
d3	15	1.92	0.019	11.2	0.046	0.065
d4	19	1.92	0.019	11.2	0.059	0.078
d5	17	1.92	0.019	11.2	0.052	0.071
d6	22	1.92	0.019	11.2	0.068	0.087
d7	14	1.92	0.019	11.2	0.043	0.062
d8	17	1.92	0.019	11.2	0.052	0.071
d9	26	2.56	0.025	11.2	0.080	0.105
d10	35	2.56	0.025	11.2	0.108	0.133
d11	16	2.56	0.025	11.2	0.049	0.074
d12	21	2.56	0.025	11.2	0.065	0.09
d13	19	2.56	0.025	11.2	0.059	0.084
d14	25	2.56	0.025	11.2	0.077	0.102
d15	15	2.56	0.025	11.2	0.046	0.071
d16	18	2.56	0.025	11.2	0.056	0.081

Cost calculation details for milling process

Hole No.	Cutting time (sec)	Price of mill cutter (USD)	Cost of tool per hole (USD)	Machining cost (USD)/hour	Machining cost(USD)	Total cost (USD)
M1	20	8.01	0.013	11.2	0.062	0.075
M2	25	8.01	0.013	11.2	0.077	0.09
M3	13	8.01	0.013	11.2	0.040	0.053
M4	16	8.01	0.013	11.2	0.049	0.062
M5	15	8.01	0.013	11.2	0.046	0.059
M6	19	8.01	0.013	11.2	0.059	0.072
M7	13	8.01	0.013	11.2	0.040	0.053
M8	15	8.01	0.013	11.2	0.046	0.059
M9	35	9.61	0.016	11.2	0.108	0.124
M10	31	9.61	0.016	11.2	0.096	0.112
M11	22	9.61	0.016	11.2	0.068	0.084
M12	19	9.61	0.016	11.2	0.059	0.075
M13	26	9.61	0.016	11.2	0.080	0.096
M14	23	9.61	0.016	11.2	0.071	0.087
M15	19	9.61	0.016	11.2	0.059	0.075
M16	17	9.61	0.016	11.2	0.052	0.068

Cost calculation for group 1 of AWJ

Hole No.	Cutting time (sec)	Machining cost USD/hr	Cost of consumables + Cost of maintenance &service (USD/hr	Total cost USD
1	14	8.012	8.012	0.062
2	12	8.012	8.012	0.053
3	14	8.012	8.012	0.062
4	17	8.012	8.012	0.075
5	12	8.012	8.012	0.053
6	14	8.012	8.012	0.062
7	12	8.012	8.012	0.053
8	14	8.012	8.012	0.062
9	14	8.012	8.012	0.062
10	17	8.012	8.012	0.075
11	14	8.012	8.012	0.062
12	12	8.012	8.012	0.053
13	17	8.012	8.012	0.075
14	12	8.012	8.012	0.053
15	12	8.012	8.012	0.053
16	14	8.012	8.012	0.062
17	11	8.012	8.012	0.048
18	16	8.012	8.012	0.071
19	14	8.012	8.012	0.062
20	15	8.012	8.012	0.066
21	14	8.012	8.012	0.062
22	14	8.012	8.012	0.062
23	13	8.012	8.012	0.057
24	17	8.012	8.012	0.075
25	12	8.012	8.012	0.053
26	15	8.012	8.012	0.066
27	12	8.012	8.012	0.053
28	17	8.012	8.012	0.075
29	12	8.012	8.012	0.053
30	17	8.012	8.012	0.075
31	12	8.012	8.012	0.053
32	14	8.012	8.012	0.062

Cost calculation for group 2 of AWJ

Hole No.	Cutting time (sec)	Machining cost USD/hr	Cost of consumables + Cost of maintenance &service (USD/hr)	Total cost USD
1	14	8.012	8.012	0.062
2	12	8.012	8.012	0.053
3	14	8.012	8.012	0.062
4	17	8.012	8.012	0.075
5	12	8.012	8.012	0.053
6	14	8.012	8.012	0.062
7	12	8.012	8.012	0.053
8	14	8.012	8.012	0.062
9	14	8.012	8.012	0.062
10	17	8.012	8.012	0.075
11	13	8.012	8.012	0.057
12	12	8.012	8.012	0.053
13	17	8.012	8.012	0.075
14	12	8.012	8.012	0.053
15	14	8.012	8.012	0.062
16	12	8.012	8.012	0.053
17	18	8.012	8.012	0.080
18	17	8.012	8.012	0.075
19	16	8.012	8.012	0.071
20	13	8.012	8.012	0.057
21	14	8.012	8.012	0.062
22	17	8.012	8.012	0.075
23	14	8.012	8.012	0.062
24	17	8.012	8.012	0.075
25	13	8.012	8.012	0.057
26	13	8.012	8.012	0.057
27	12	8.012	8.012	0.053
28	14	8.012	8.012	0.062
29	13	8.012	8.012	0.057
30	17	8.012	8.012	0.075
31	14	8.012	8.012	0.062
32	17	8.012	8.012	0.075

Cost calculation table for group 1 of LBM

Hole No.	Cutting time (sec)	Machining cost USD/hr	Total cost USD
1	12	48.076	0.160
2	14	48.076	0.186
3	14	48.076	0.186
4	17	48.076	0.227
5	8	48.076	0.106
6	10	48.076	0.133
7	10	48.076	0.133
8	11	48.076	0.146
9	12	48.076	0.160
10	14	48.076	0.186
11	13	48.076	0.173
12	8	48.076	0.106
13	17	48.076	0.227
14	10	48.076	0.133
15	8	48.076	0.106
16	10	48.076	0.133
17	14	48.076	0.186
18	17	48.076	0.227
19	13	48.076	0.173
20	8	48.076	0.106
21	12	48.076	0.160
22	17	48.076	0.227
23	10	48.076	0.133
24	17	48.076	0.227
25	8	48.076	0.106
26	12	48.076	0.160
27	8	48.076	0.106
28	10	48.076	0.133
29	10	48.076	0.133
30	16	48.076	0.213
31	8	48.076	0.106
32	10	48.076	0.133

Cost calculation table for group 2 of LBM

Hole No.	Cutting time (sec)	Machining cost USD/hr	Total cost per part USD
1	12	48.076	0.160
2	14	48.076	0.186
3	14	48.076	0.186
4	17	48.076	0.227
5	8	48.076	0.106
6	10	48.076	0.133
7	10	48.076	0.133
8	11	48.076	0.146
9	15	48.076	0.200
10	17	48.076	0.227
11	13	48.076	0.173
12	12	48.076	0.160
13	17	48.076	0.227
14	10	48.076	0.133
15	11	48.076	0.146
16	12	48.076	0.160
17	14	48.076	0.186
18	17	48.076	0.227
19	14	48.076	0.186
20	8	48.076	0.106
21	12	48.076	0.160
22	16	48.076	0.213
23	10	48.076	0.133
24	17	48.076	0.227
25	10	48.076	0.133
26	13	48.076	0.173
27	14	48.076	0.186
28	10	48.076	0.133
29	16	48.076	0.213
30	17	48.076	0.227
31	10	48.076	0.133
32	17	48.076	0.227

Appendix L: Productivity Calculations

Productivity Calculations of Drilling Process

Hole No.	Material thickness (mm)	Cutting Feed (mm/min)	Tool positioning &Retraction time (sec)	Productivity (No. of holes/min)
d1	8	76.39443721	2	9.54
d2	16	76.39443721	2	4.77
d3	8	152.7888744	2	19.09
d4	16	152.7888744	2	9.54
d5	8	114.5916558	2	14.32
d6	16	114.5916558	2	7.16
d7	8	229.1833116	2	28.64
d8	16	229.1833116	2	14.32
d9	8	57.29582791	2	7.16
d10	16	57.29582791	2	3.58
d11	8	114.5916558	2	14.32
d12	16	114.5916558	2	7.16
d13	8	85.94374186	2	10.74
d14	16	85.94374186	2	5.37
d15	8	171.8874837	2	21.48
d16	16	171.8874837	2	10.74

Productivity calculation of milling

Hole No.	Material thickness (mm)	Cutting Feed (mm/min)	hole diam. (D)	Tool diam. (D_m)	Tool positioning &Retraction time (sec)	Productivity (No. of holes/min)
M1	8	183.346649	6	5	2	10.04
M2	16	183.346649	6	5	2	6.98
M3	8	366.693299	6	5	2	15.05
M4	16	366.693299	6	5	2	11.33
M5	8	275.019974	6	5	2	12.90
M6	16	275.019974	6	5	2	9.38
M7	8	550.039948	6	5	2	18.04
M8	16	550.039948	6	5	2	14.29
M9	8	183.346649	8	6	2	6.90
M10	16	183.346649	8	6	2	5.30
M11	8	366.693299	8	6	2	11.23
M12	16	366.693299	8	6	2	9.02
M13	8	275.019974	8	6	2	9.29
M14	16	275.019974	8	6	2	7.31
M15	8	550.039948	8	6	2	14.19
M16	16	550.039948	8	6	2	11.76

Productivity calculation for group 1 of AWJM

Hole No.	Hole diam. (mm)	Diam. of water jet (mm)	Cutting feed (mm/min)	Retraction & positioning time (sec)	Piercing Time (sec)	Productivity (No. of holes/min)
1	6	1	200	2	1	7.51
2	8	1	200	2	1	5.90
3	6	1	200	2	1	7.51
4	8	1	200	2	1	5.90
5	6	1	300	2	1	9.74
6	8	1	300	2	1	7.87
7	6	1	300	2	1	9.74
8	8	1	300	2	1	7.87
9	6	1	200	2	1	9.74
10	8	1	200	2	1	7.87
11	6	1	200	2	1	7.51
12	6	1	300	2	1	9.74
13	8	1	200	2	1	5.90
14	8	1	300	2	1	7.87
15	6	1	300	2	1	9.74
16	8	1	300	2	1	7.87
17	6	1	200	2	1	7.51
18	8	1	200	2	1	5.90
19	6	1	200	2	1	7.51
20	6	1	300	2	1	9.74
21	6	1	200	2	1	7.51
22	8	1	200	2	1	5.90
23	8	1	300	2	1	7.87
24	8	1	200	2	1	5.90
25	6	1	300	2	1	9.74
26	6	1	200	2	1	7.51
27	6	1	300	2	1	9.74
28	8	1	300	2	1	7.87
29	8	1	300	2	1	7.87
30	8	1	200	2	1	5.90
31	6	1	300	2	1	9.74
32	8	1	300	2	1	7.87

Productivity calculation for group 2 of AWJM

Hole No.	Hole diam. (mm)	Diam. of water jet (mm)	Cutting feed (mm/min)	Retraction & positioning time (sec)	Piercing Time (sec)	Productivity (No. of holes/min)
1	6	1	200	2	1	7.51
2	8	1	200	2	1	5.90
3	6	1	200	2	1	7.51
4	8	1	200	2	1	5.90
5	6	1	300	2	1	9.74
6	8	1	300	2	1	7.87
7	6	1	300	2	1	9.74
8	8	1	300	2	1	7.87
9	6	1	200	2	1	7.51
10	8	1	200	2	1	5.90
11	6	1	200	2	1	7.51
12	6	1	300	2	1	9.74
13	8	1	200	2	1	5.90
14	8	1	300	2	1	7.87
15	6	1	300	2	1	9.74
16	8	1	300	2	1	7.87
17	6	1	200	2	1	7.51
18	8	1	200	2	1	5.90
19	6	1	200	2	1	7.51
20	6	1	300	2	1	9.74
21	6	1	200	2	1	7.51
22	8	1	200	2	1	5.90
23	8	1	300	2	1	7.87
24	8	1	200	2	1	5.90
25	6	1	300	2	1	9.74
26	6	1	200	2	1	7.51
27	6	1	300	2	1	9.74
28	8	1	300	2	1	7.87
29	8	1	300	2	1	7.87
30	8	1	200	2	1	5.90
31	6	1	300	2	1	9.74
32	8	1	300	2	1	7.87

Productivity for group 1 of LBM

Hole No.	Hole diam. (mm)	Diam. of laser beam (mm)	Cutting feed (mm/min)	Retraction & positioning time (sec)	Piercing Time (sec)	Productivity (No. of holes/min)
1	6	1	100	1.5	1.5	4.31
2	8	1	100	1.5	1.5	3.28
3	6	1	100	1.5	1.5	4.31
4	8	1	100	1.5	1.5	3.28
5	6	1	200	1.5	1.5	7.09
6	8	1	200	1.5	1.5	5.63
7	6	1	200	1.5	1.5	7.09
8	8	1	200	1.5	1.5	5.63
9	6	1	100	1.5	1.5	4.31
10	8	1	100	1.5	1.5	3.28
11	6	1	100	1.5	1.5	4.31
12	6	1	200	1.5	1.5	7.09
13	8	1	100	1.5	1.5	3.28
14	8	1	200	1.5	1.5	5.63
15	6	1	200	1.5	1.5	7.09
16	8	1	200	1.5	1.5	5.63
17	6	1	100	1.5	1.5	4.31
18	8	1	100	1.5	1.5	3.28
19	6	1	100	1.5	1.5	4.31
20	6	1	200	1.5	1.5	7.09
21	6	1	100	1.5	1.5	4.31
22	8	1	100	1.5	1.5	3.28
23	8	1	200	1.5	1.5	5.63
24	8	1	100	1.5	1.5	3.28
25	6	1	200	1.5	1.5	7.09
26	6	1	100	1.5	1.5	4.31
27	6	1	200	1.5	1.5	7.09
28	8	1	200	1.5	1.5	5.63
29	8	1	200	1.5	1.5	5.63
30	8	1	100	1.5	1.5	3.28
31	6	1	200	1.5	1.5	7.09
32	8	1	200	1.5	1.5	5.63

Productivity for group 2 of LBM

Hole No.	Hole diam. (mm)	Diam. of laser beam (mm)	Cutting feed (mm/min)	Retraction & positioning time (sec)	Piercing Time (sec)	Productivity (No. of holes/min)
1	6	1	100	1.5	1.5	4.31
2	8	1	100	1.5	1.5	3.28
3	6	1	100	1.5	1.5	4.31
4	8	1	100	1.5	1.5	3.28
5	6	1	200	1.5	1.5	7.09
6	8	1	200	1.5	1.5	5.63
7	6	1	200	1.5	1.5	7.09
8	8	1	200	1.5	1.5	5.63
9	6	1	100	1.5	1.5	4.31
10	8	1	100	1.5	1.5	3.28
11	6	1	100	1.5	1.5	4.31
12	6	1	200	1.5	1.5	7.09
13	8	1	100	1.5	1.5	3.28
14	8	1	200	1.5	1.5	5.63
15	6	1	200	1.5	1.5	7.09
16	8	1	200	1.5	1.5	5.63
17	6	1	100	1.5	1.5	4.31
18	8	1	100	1.5	1.5	3.28
19	6	1	100	1.5	1.5	4.31
20	6	1	200	1.5	1.5	7.09
21	6	1	100	1.5	1.5	4.31
22	8	1	100	1.5	1.5	3.28
23	8	1	200	1.5	1.5	5.63
24	8	1	100	1.5	1.5	3.28
25	6	1	200	1.5	1.5	7.09
26	6	1	100	1.5	1.5	4.31
27	6	1	200	1.5	1.5	7.09
28	8	1	200	1.5	1.5	5.63
29	8	1	200	1.5	1.5	5.63
30	8	1	100	1.5	1.5	3.28
31	6	1	200	1.5	1.5	7.09
32	8	1	200	1.5	1.5	5.63